Faculty of Health Sciences

Department of Psychology

Neural mechanisms of the wandering mind

Josephine Maria Groot

A dissertation for the degree of Philosophiae Doctor   April 2023

Cover page art

'The Wondermind'

Noui

Slovenia, 09/2019

Acknowledgements

They say that everybody reads the acknowledgments first – and for many, it may be the only part of the thesis they will ever read. Ironically, this is the part I probably thought about the least in these last couple of months. Yet, as I sit here reflecting, I realize how much I have to be grateful for and how many people have contributed to this journey. So, with a mix of humility and pride, I want to take this opportunity to offer my sincerest appreciation to all those who have helped me along the way.

First and foremost, I want to express my deepest gratitude to my supervisory team, Matthias, Birte, Gabor, and Pilou. Completing this PhD would have been an impossible task without you. I have learned so much from you, and your investment, both professionally and personally, has been invaluable to me. Gabor and Pilou, thank you for your unwavering support, encouragement, and always keeping an open (digital) door throughout these years. Birte, thank you for giving me this opportunity and guiding me throughout. I can only hope to pursue academia with the same level of passion and determination as you. Matthias, I can not stress how easy you have made this journey for me. Your mentoring has been inspiring, on point, and a lot of fun. With your never-ending patience, expertise, and commitment, you went above and beyond what I could expect from a supervisor, and it has made me feel incredibly lucky.

To my dear friends and colleagues, you are the best. I am happy that my office sofa has become such a social hub. Whether it was to complain, to cry, to celebrate, or just to casually chat, I gladly kept my door open to you all. Nobody understands PhD-life better than fellow PhD's. Patty, Mette, Kasper, Malin, Linda, and Kristoffer, thank you for the moral support, friendship, imposter syndrome-inducing pubquiz nights, and the many, many coffee breaks. You have made me feel at home in a foreign country and provided a much needed outlet during hard times. Patty, you are one of the smartest and funniest people I know. I can honestly say that living and working in Tromsø would not have been half as great without you. Together with Olivia and Kirsten, thank you for the fun and sometimes weird adventures – from camping trips to knitting nights to drinking prosecco in a canoe. Mette, you are the life of the party, and you have a way of bringing people together and creating unforgettable moments – mixing akevitt and julebrus in tubes outside the wet lab during the Christmas party comes to mind. Special thanks to Kasper and Yevhen for being wonderful office buddies. Thank you for putting up with me, for being a sounding board, and for making frustrating days so much more bearable.

I feel fortunate to have so many wonderful colleagues to thank here. Jaime for keeping us caffeinated, Marta for hosting the vinlotteri (even though to this day, I never won a single bottle), Eelke for sharing your love of playing piano, and Roy for being a great listener and providing me with life-saving advice countless of times. Nya, you are one of the nicest people I know and you were incredibly helpful when I first started my PhD, thank you. Benedicte, I am grateful that our PhD's partially overlapped, and I got to admire your dedication to work and your positive take on life.

I am also thankful for all the fantastic colleagues at the IMCN research unit. In particular, I want to thank Sarah, Steven, Scott, Anne, Reilly, Niek, Ettore, Pilou, and Anneke for making Amsterdam such a welcoming and enjoyable place to work, and I hope I get to share many more good times with you in the future.

To the people back home, mom, dad, Sander, Lisette, and Ayla. Despite long periods of absence, missing out as an aunt, and being unable to attend important moments, you always expressed your support and understanding. I am forever grateful for your encouragement and patience, and I hope that I can make up for all the lost time.

To those I may have forgotton; blame it on the head, not the heart. I hope that you know that I am truly grateful to have (had) your support, friendship, or mentorship.

Jonathan, this final paragraph is for you. I feel so blessed that I get to share this milestone with you. Thank you for inspiring me and reminding me of what is truly important. You told me not to strive for a thesis that is perfect, but to write about what excites and drives me. Whenever we talk, you fill my head with new ideas, and you remind me that science thrives when challenging convention and pursuing wild possibilities. I admire your creativity and playfulness, and for always chasing your heart. Thank you for being my home, my love.

Abstract

The human mind wanders spontaneously and pervasively throughout daily life, pursuing trains of thought that are untethered to the world around us. Although mapping the many facets of mind wandering has become a compelling objective in the cognitive neurosciences, researchers have yet to achieve a congruous mechanistic account of its neurobiological underpinnings. In this thesis, a multidisciplinary strategy was implemented to illuminate the various aspects of mind wandering during passive rest and cognitive task performance. To more confidently detect changes in attention, we combined spatially localized and temporally precise features from different neural modalities, subjective experience, and changes in moment-to-moment behavior. Furthermore, we leveraged recent advances in subcortical imaging and atlasing to lay the groundwork for exploring the contributions of understudied regions in the subcortex. Mind wandering is a complex and heterogeneous phenomenon that interacts with situational factors and defies a unitary neural representation. While singular systems, such as the default mode network (DMN), were not unambiguously related to mind wandering, the dynamic coupling between the DMN and its antagonistic network was identified as essential feature. The integration of information processes in these networks during mind wandering was especially enabled by functional connections of the posterior cingulate cortex (PCC), substantiating its role for regulating internal attention. More subtle connections were also spontaneously echoed in the subcortex, demonstrating functional properties analogous to the PCC. Disentangling the interactions between neuromodulatory influences, behavior, and the functional synergy in cortical and subcortical networks, may reveal qualitatively distinct types off-task thought that remain elusive with experience sampling. These findings emphasize that a comprehensive understanding of how the brain orchestrates mind wandering resides in the harmonics between diverse neural systems.

List of Papers

Paper I   Groot JM, Boayue NM, Csifcsák G, Boekel W, Huster R, Forstmann BU, Mittner M (2021) Probing the neural signature of mind wandering with simultaneous fMRI-EEG and pupillometry. *NeuroImage, 224*:117412. doi:10.1016/j.neuroimage.2020.117412

Paper II   Groot JM, Csifcsák G, Wientjes S, Forstmann BU, Mittner M (2022) Catching wandering minds with tapping fingers: Neural and behavioral insights into task-unrelated cognition. *Cerebral Cortex, 00*:1-17. doi:10.1093/cercor/bhab494

Paper III   Groot JM, Miletić S, Isherwood SJS, Tse DHY, Habli S, Håberg AK, Forstmann BU, Bazin P-L, Mittner M (*preprint*) Echoes from intrinsic connectivity networks in the subcortex. doi:10.31234/osf.io./xr25q

Relevant coauthored work

Alexandersen A, Csifcsák G, **Groot J**, Mittner M (2022) The effect of transcranial direct current stimulation on the interplay between executive control, behavioral variability and mind wandering: A registered report. *Neuroimage: Reports, 2:*100109. doi:10.1016/j.ynirp.2022.100109

Keuken MC, Liebrand LC, Bazin P-L, Alkemade A, Van Berendonk N, **Groot JM**, Isherwood SJS, Kemp S, Lute N, Mulder MJ, Trutti AC, Caan MWA, Forstmann BU (2022) A high-resolution multi-shell 3T diffusion magnetic resonance imaging dataset as part of the Amsterdam Ultra-high field adult lifespan database (AHEAD). *Data in Brief, 42:*108086. doi:10.1016/j.dib.2022.108086

Isaacs BR, Mulder MJ, **Groot JM**, Van Berendonk N, Lute N, Bazin P-L, Forstmann BU, Alkemade A (2020) 3 versus 7 Tesla magnetic resonance imaging for parcellations of subcortical brain structures in clinical settings. *PLoS One, 15:*0236208. doi:10.1371/journal.pone.0236208

Alkemade A, Mulder MJ, **Groot JM**, Isaacs BR, Van Berendonk N, Lute N, Isherwood SJS, Bazin P-L, Forstmann BU (2020) The Amsterdam Ultra-high field adult lifespan database (AHEAD): A freely available multimodal 7 Tesla submillimeter magnetic resonance imaging database. *NeuroImage, 221:*117200. doi:10.1016/j.neuroimage.2020.117200

Alkemade A, Pine KJ, Kirilina E, Keuken MC, Mulder M, Balesar R, **Groot JM**, Bleys RL, Trampel R, Weiskopf N, Herrler A, Möller H, Bazin P-L, Forstmann B (2020) 7 Telsa MRI followed by histological 3D reconstructions in whole-brain specimens. *Frontiers in Neuroanatomy, 14:*536838. doi:10.3389/fnana.2020.536838

Boayue NM, Csifcsák G, Aslaksen P, Turi Z, Antal A, **Groot J**, Hawkins GE, Forstmann B, Opitz A, Thielscher A, Mittner M (2020) Increasing propensity to mind-wander by transcranial direct current stimulation? A registered report. *European Journal of Neuroscience, 51:*755-780. doi:10.1111/ejn.14347

Csifcsák G, Boayue NM, Aslaksen PM, Turi Z, Antal A, **Groot J**, Hawkins GE, Forstmann BU, Opitz A, Thielscher A, Mittner M (2019) Commentary: Transcranial stimulation of the frontal lobes increases propensity of mind-wandering without changing meta-awareness. *Frontiers in Psychology, 10*:130. doi:10.3389/fpsyg.2019.00130

Turi Z, Csifcsak G, Boayue NM, Aslaksen P, Antal A, Paulus W, **Groot J**, Hawkins GE, Forstmann B, Opitz A, Thielscher A, Mittner M (2019) Blinding is compromised for transcranial direct current stimulation at 1 mA for 20 minutes in young healthy adults. *European Journal of Neuroscience, 50:*3261-3268. doi:10.1111/ejn.14403

Alkemade A, **Groot JM**, Forstmann BU (2018) Do we need a human *post mortem* whole-brain anatomical ground truth in *in vivo* magnetic resonance imaging? *Frontiers in Neuroanatomy, 12:*110. doi:10.3389/fnana.2018.00110

Abbreviations

ACN	anticorrelated network
ADHD	attention-deficit/hyperactivity disorder
AE	approximate entropy
AGT	adaptive gain theory
BOLD	blood oxygen level dependent
BV	behavioral variability
DAN	dorsal attention network
dlPFC	dorsolateral prefrontal cortex
DMN	default mode network
ECN	executive control network
EEG	electroencephalography
ERP	event-related potential
FC	functional connectivity
fMRI	functional magnetic resonance imaging
FPN	frontoparietal network
FT-RSGT	finger-tapping random sequence generation task
GLM	general linear model
HPC	hippocampus
ICA-DR	independent component analysis-dual regression
ICN	intrinsic connectivity network
a/pIPL	anterior/posterior inferior parietal lobule
LC/NE	locus coeruleus/norepinephrine
MASSP	multi-contrast anatomical subcortical parcellation
mPFC	medial prefrontal cortex
MTL	medial temporal lobe
PCC	posterior cingulate cortex
PD	pupil diameter
RFE	recursive feature elimination
ROI	region of interest
RT	reaction time
SART	sustained attention to response task
SN	salience network
SVM-RBF	support vector machine-radial basis functions
tDCS	transcranial direct current stimulation

Figures and Tables

Table of contents

Chapter 1
General Introduction

Despite being faced with constant demands and potential threats in our environment, humans find themselves frequently lost in thought, unaware of their surroundings or the passage of time. The work presented here is dedicated to deepening our understanding of how the phenomenon of *mind wandering* is orchestrated by the brain and interacts with our subjective internal experience and behavior. In this opening chapter, I summarize the evidence from well-studied behavioral paradigms and functional brain networks, as well as from a less explored perspective that concerns the contribution of subcortical structures and neuromodulation.

1.1 Delimiting the concept of mind wandering

This background review starts with a deceptively simple question: how do we define mind wandering? The term 'mind wandering' was first adopted in scientific context by Smallwood and Schooler (2006) as a form of attention that is neither directed nor related to the immediate environment, making it qualitatively distinct from types of attention that encompass the selection of external information. Rather, the phenomenon of mind wandering is described as the internally oriented stream of consciousness comprising thoughts and feelings that do not pertain to the here and now, but are instead often related to personal goals and concerns (Klinger 2013; Smallwood & Schooler 2015; Shepard 2019). In this sense, mind wandering is untethered to constraints from the outside world and can embody a broad range of thought, including retrospective and prospective thinking and self-referential mentation (Smallwood & Schooler 2015). Although 'stream of consciousness' might imply that mind wandering is a feature of volitional cognition, it can conduct itself in a manner that is unintentional and unaware (Smallwood & Schooler 2006; Schooler et al 2011).

The scientific interest in internal attention dates back to William James' famous writings on the '*flights and perchings*' of the mind in 1890, followed by the rise of behaviorism which nourished the criticism toward introspective psychology. Only more recently, research focus returned to undirected forms of thought such as daydreaming (e.g., Klinger 1971). The past few decades witnessed an explosive growth in publications on mind wandering studied under a varied terminology (Callard et al 2013), among which stimulus-independent thought, task-unrelated thought, attentional lapse, undirected thought, and 'zoning-out'. This heterogeneity was furthermore expressed in the study of various dimensions of conscious experience, such as temporal focus, self-relevance, emotional valence, and the level of detail of internal trains of thought (e.g., Stawarczyk et al 2011a; Banks et al 2016; Maillet et al 2017; Bocharov et al 2019; Turnbull et al 2019a; Liefgreen et al 2020).

In an attempt to structure the field toward a more unified ontology of mind wandering, several influential frameworks were proposed. Smallwood and Schooler (2015) characterized mind wandering as thoughts that are both *self-generated* and *task-unrelated*, thereby placing emphasis on aspects of formation and content. This definition makes an important distinction between mind wandering and external distractions (i.e., task-unrelated thought that is perceptually guided) and spontaneous thoughts that are not independent from the task (e.g., metacognition regarding one's performance). In contrast, Christoff et al (2016) prioritized the transitory, dynamic properties of mind wandering over its content. Their model consists of a continuum of spontaneous thoughts that can be discerned based on their position amidst two dimensions: deliberate and automatic constraints. Deliberate constraints on thought flow are under control of top-down systems and are stronger for mind wandering compared to dreaming, but weaker compared to creative thinking. Automatic constraints, which arise from bottom-up mechanisms such as saliency, are most pronounced in thought with excessive stability (e.g., ruminating,

obsessing) and are expected to be low to intermediate for mind wandering. Finally, Seli et al (2018a) criticize previous definitions such as 'task-unrelated' and 'stimulus-independent' thought by arguing that mind wandering can take place in a task-free manner (e.g., daydreaming on the bus) or be directly induced by a perception (e.g., rethinking a past conflict upon seeing that person). These various nuances and facets of mind wandering may therefore be more appropriately described in terms of a graded membership to a larger family. However, a lack of classification by defining, universal features has been argued to hamper empirical progress because it allows disparate internal experiences to be conflated with mind wandering (Christoff et al 2018).

Intriguingly, episodes of mind wandering seem strikingly frequent across different settings, both in daily life and during experimental tasks (Klinger & Cox 1987; Kane et al 2007; Killingsworth & Gilbert 2010; Seli et al 2018b), indicating that our natural ability to generate mental experiences without sensory guidance constitutes a substantial and important part of human brain function. Nonetheless, mind wandering can be maladaptive as it pervasively interferes with tasks that require sustained external attention, such as driving and reading (Smallwood 2011; Baldwin et al 2017), and has been negatively associated with mental health (Smallwood et al 2007; Killingsworth & Gilbert 2010; Deng et al 2014). Understanding the neural mechanisms of mind wandering can thus provide imperative insights into cognitive functioning in general and facilitate the development of tools that reduce its negative impact on performance and psychological well-being. Although research on the function of mind wandering is advancing (e.g., Schooler et al 2011; Smallwood 2013; Shepard 2019), explanatory accounts remain limited by the methodological barriers to reliably detect the onset and cessation of covert, internal phenomena. In the next section, the experimental evidence on mind wandering and its relationship with other cognitive functions are discussed in more detail.

1.2   Interactions with other cognitive functions and behavior

Lapses in externally focused attention were initially detected as performance errors on vigilance tasks, of which the most widely used is the Sustained Attention to Response Task (SART; Robertson et al 1997). The SART was developed to measure failures in sustained attention, or '*slips of action*', operationalized as the inability to withhold a motor response to rare target among frequent non-target visual stimuli. In the original study, the occurrence of such commission errors was preceded by shorter reaction times (RTs), suggesting '*a drift from controlled to automatic processing*', and was correlated with the severity of frontal lobe damage and daily-life attention failures in patients with traumatic brain injury (Robertson et al 1997). Early work combining the SART with experience sampling – i.e., periodically probing individuals to report their current focus of attention – demonstrated that periods of task-unrelated thoughts also coincided with shortened RTs, a relationship that was most pronounced when target stimuli were less frequent (Smallwood et al 2004). Henceforth, the SART became a popular paradigm to study mind wandering, followed by reports of robust associations between suboptimal task performance, including response errors and increases in RT variability, and shifts from external to internal attention (e.g., Mooneyham & Schooler 2013; Bastian & Sackur 2013; Hawkins et al 2019; Zanesco et al 2020a).

Such performance decrements due to mind wandering were primarily regarded as the result of ineffective goal monitoring and control, a characterization that was corroborated by the negative relationship between an individual's working memory capacity and a tendency to disengage from a cognitively demanding task (Kane et al 2007; McVay & Kane 2009). These observations led to the *executive failure hypothesis*, which states that mind wandering results from an inability to maintain current task goals (McVay & Kane 2010). However, individuals exhibited the reversed relationship between working memory capacity and mind wandering in situations with low cognitive demand (Levinson et al 2012; Rummel & Boywitt 2014), suggesting a degree of flexible regulation rather than a temporary breakdown of top-down control. The capacity to adaptively adjust the inner train of thought according to environmental demands was formulated in the *context-regulation theory* of mind wandering (Smallwood & Andrews-Hanna 2013). It was hypothesized by Smallwood & Schooler (2006) that this capacity is associated with goal pertinence, in which salient personal goals can outweigh the incentive of an external task and eventually lead to mind wandering. This opposing view, the *executive control hypothesis*, thus characterizes mind wandering not as a result of executive failure but of an adaptive redirection of resources away from the task, which could be enabled by top-down 'decoupling' mechanisms that impair the processing of external information (Schooler et al 2011).

Direct empirical evidence for decoupling emerged from the analysis of cortical event-related potentials (ERPs) derived from electroencephalography (EEG). Specifically, reductions in the poststimulus amplitudes of early sensory ERPs, including N1 and P1 (Kam et al 2011), as well as P300

– a positive component at later latency reflecting cognitive processes – were associated with task errors and probe-caught mind wandering (Smallwood et al 2008; O'Connell et al 2009; Kam et al 2013), even for stimuli that were task-irrelevant distractors (Barron et al 2011). Similarly, mind wandering was related to smaller stimulus-evoked pupil dilations (Smallwood et al 2011) and decoupling attention from perceiving painful sensations (Kucyi et al 2013). Together, these findings were interpreted as evidence for a domain-general mechanism that actively inhibits the selection and processing of sensory information in favor of mind wandering (Smallwood 2013). If the function of perceptual decoupling is indeed to protect the integrity and maintenance of task-unrelated thoughts from external interference, it can be considered a hallmark of mind wandering conceptualized as goal-directed cognition (Smallwood & Schooler 2006; Schooler et al 2011; Kam & Handy 2013; Smallwood et al 2021). The preferential selection of internal information is not implausible given the nature of vigilance tasks employed in most studies, which are dull and low in extrinsic motivation. Hence, performance on such tasks likely competes with internally guided thoughts that are more engaging because they better align with personal concerns and goals (Smallwood & Schooler 2006; Shepard 2019).

The precise interplay between mind wandering and executive control remains, however, unresolved. For example, Franklin et al (2013a) argued that the observation of perceptual decoupling should not be mistaken for its functional significance in perpetuating the internal train of thought, as the phenomenon may simply reflect a depletion of attentional resources. Rather than being a process that is purposefully shielding from distractions, mind wandering could likewise be the result of enduring failures to redirect attention back to the external task. Furthermore, the SART was criticized for inducing speed-accuracy tradeoffs, where strategies that prioritize being fast over being accurate are conflated with mind wandering (Seli et al 2013). The Metronome Response Task (MRT) was subsequently developed to circumvent this issue by requiring individuals to respond in tune with a rhythmic tone, which allows researchers to derive mind wandering from gradual changes in response variability rather than a dichotomy based on the presence or absence of errors (Seli et al 2013). It was argued that consistent responding on the MRT requires executive resources to be focused on the task, and that the observed increases in RT variability preceding self-reports of mind wandering indicate the withdrawal of such resources (Seli et al 2013; Anderson et al 2020). Importantly, the temporally coarse measurement of both mind wandering and behavior in previous studies has set limitations for tracking interactions between attentional focus and executive control (Franklin et al 2013a; Boayue et al 2020a). Despite pivotal efforts toward developing paradigms that enable continuous monitoring of executive resource use at high temporal resolution (Boayue et al 2020a), a consensus regarding the validity of either executive hypotheses has not been established.

1.3 Interplay between default mode, executive, and attention networks

The human brain is naturally organized into stable or recurrent patterns of synchronized activity in distributed regions, often described as intrinsic connectivity networks (ICNs). Using functional magnetic resonance imaging (fMRI), these networks have been robustly observed during both spontaneous mentation and cognitive demand (e.g., Yeo et al 2011; Cole et al 2016; Smitha et al 2017). Particularly, a set of regions that was found to consistently deactivate in the presence of an external task – collectively termed the default mode network (DMN, Figure 1) – became a spotlight for neuroscientific investigation (Raichle et al 2001). Activity in these regions, including the medial prefrontal cortex (mPFC), posterior cingulate cortex (PCC), posterior inferior parietal lobule (pIPL), temporoparietal junction (TPJ), medial temporal lobe (MTL) including the hippocampal formation (HF) and tentatively the lateral temporal/temporopolar cortex (LTC), was subsequently associated with the mental operations that are solicited during passive states, such as episodic memory retrieval, future simulations, and theory of mind (Buckner et al 2008; Spreng et al 2009). Not surprisingly, the DMN quickly became synonymous to the spontaneous thought processes that take place during mind wandering (e.g., Andrews-Hanna 2012; Smallwood & Schooler 2015).

The notion of the DMN as the predominantly implicated functional network, however, contradicts the behavioral evidence that typifies mind wandering as a dynamic cognitive process that interacts with executive control and competes for attentional resources. Several important findings from fMRI research favor this latter depiction. First, the majority of evidence for a link between mind wandering and the DMN traces back to studies in which changes in attention were not directly probed but inferred from behavioral performance, experimental manipulations, or retrospective reports (Weissman et al 2006; McKiernan et al 2006; Mason et al 2007; Andrews-Hanna et al 2010). In contrast, the first study that combined task-based fMRI with online experience sampling observed increased neural activity in the DMN as well as in nodes of the executive control network (ECN), including the dorsal anterior cingulate cortex (dACC) and dorsolateral prefrontal cortex (dlPFC), preceding self-reports of mind wandering (Christoff et al 2009). Similarly, Stawarczyk et al (2011b) reported activity in the DMN as well as the inferior frontal gyrus (IFG) relating to periods of stimulus-independent thought. Together, these results provided strong initial evidence that mind wandering partially relies on brain regions associated with executive functions and therefore likely shares functional processes with externally directed, higher-level cognition (Smallwood 2013). Indeed, significant meta-analytic clusters of neural activity associated with spontaneous and task-unrelated thoughts were most often confined to the DMN and ECN, including the (rostral) mPFC, PCC, precuneus (PCUN), IPL, left parahippocampal cortex, right (rostral) dlPFC, left ventrolateral PFC, dACC, and left temporopolar cortex (Fox et al 2015).

Furthermore, consistent with the perceptual decoupling theory, Christoff et al (2012) observed that activity in the PCC was negatively correlated with sensorimotor and visual cortices during mind

wandering. In another study, Greicius and Menon (2004) found that individuals with more persisting DMN recruitment throughout a passive task demonstrated attenuated responses to sensory stimuli. The DMN is intrinsically anticorrelated with the dorsal attention network (DAN; Figure 1), which is associated with top-down attentional control of external information selection and includes the intraparietal sulcus (IPS), middle temporal/visual motion area (MT/V5), and frontal eye field (FEF) in the inferior precentral sulcus (Fox et al 2005). In an experimental study, Spreng et al (2010) showed that autobiographical and visuospatial planning tasks strongly discriminated regional brain recruitment, where the former engaged the DMN and the latter the DAN. Crucially, ECN nodes including the dACC, rostrolateral PFC (rlPFC), middle frontal gyrus (MFG), and anterior IPL (aIPL) – also referred to as the frontoparietal network (FPN; Figure 1) – were coactivated during both tasks, presumably to supply the executive resources needed for external as well as internal planning performance. Together, these findings led to the proposal of a 'global workspace' model, in which the FPN adaptively couples with either the DMN or DAN in order to amplify the processing of internally or externally focused information, respectively (Smallwood et al 2012a). Specifically, by reinforcing the winner of these competing attentional foci, the FPN is proposed to govern the integrity of the stream of consciousness, whether it being fueled by self-referential, autobiographical content (i.e., DMN) or perceptual input (i.e., DAN).
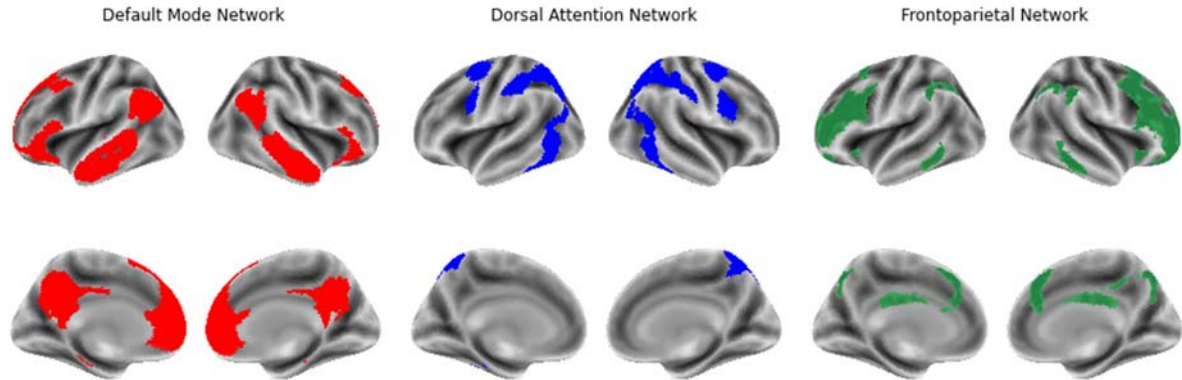
Figure 1. Coarse topography of functional brain networks. Parcellation is taken from the 7-network cortical parcellation by Yeo et al (2011) and based on clustering of 1000 resting-state datasets. The default mode network (red) generally constitutes the pIPL and LTC laterally (top row) and the PCC, mPFC, and HF medially (bottom row). The dorsal attention network (blue) often includes the IPS, MT/V5, and FEF. The frontoparietal network (green) consists of lateral frontoparietal regions including the dlPFC, MFG, and aIPL, and the dACC medially.

The parallel activation of these seemingly functionally opposite networks during mind wandering could indicate that their cooperation is necessary for enabling a cohesive train of thought, for example by guiding and evaluating the pursuit of internal goals (Christoff et al 2016; Fox et al 2015). Although it could be similarly argued that their co-recruitment simply reflects the metacognitive awareness of failing task goals followed by the exertion of cognitive control to restore attention to the external task,

the executive failure view falls short in explaining several key observations, among which the relative increase in dACC and dlPFC activity when individuals were unaware of their thoughts wandering away from the task (Christoff et al 2009).

Nonetheless, not all neural evidence converges on support for executive control during mind wandering. For example, Mittner et al (2014) employed a sophisticated approach in which neuroimaging data were integrated with a cognitive process model on a Stop-Signal task, which requires individuals to periodically inhibit a habitual motor response to stimuli that are followed by a stopping cue. Based on the modeled behavior, the authors characterized mind wandering as deficient task monitoring and executive failure. At the neural level, this was preceded by stronger recruitment of the DMN and deactivation of its data-driven anticorrelated network (ACN), consisting of the IPS, supplementary motor area (SMA), dlPFC, and insula. Additionally, both the positive connectivity within either network and the negative connectivity between them were stronger prior to self-reported mind wandering compared to task-focused attention. Although expected for the IPS which is typically considered part of the DAN (Fox et al 2005; Buckner et al 2008), the decoupling of the other ACN nodes from the DMN during mind wandering – including the dlPFC as a key region of the FPN – contradicts previous findings (Christoff et al 2009; Spreng et al 2010). In another study, Kucyi et al (2017a) measured ongoing behavioral performance as an indicator for attentional focus by quantifying the variability in rhythmic finger-tapping. Interestingly, they similarly observed that the dynamic connectivity among nodes of the DMN was increased during periods of 'out-the-zone' attention – i.e., tapping with greater variability – but contrary to the finding of Mittner et al (2014), they also reported stronger coupling (or weaker anticorrelation) between the mPFC and the right anterior insula. Such a reduction in anticorrelation during periods of mind wandering was supported by several other studies (Kelly et al 2008; Esterman et al 2013; Thompson et al 2013) and suggests that the persistent antagonism between these two networks is likely required for maintaining optimal, less variable task performance. Kucyi et al (2017a) also reported a surprising pattern of general network activity, as 'out-the-zone' attention was correlated with regional activation of the DAN and salience network (SN), including the anterior insula, mid cingulate cortex (MCC), FEF, superior parietal lobule (SPL), SMA, middle temporal gyrus (MTG), and cerebellum (lobule V/VI, left lobule VII/VIII), whereas regions predominantly in the DMN, including the mPFC, PCC, right dlPFC, and cerebellum crus I/II, were more active during stable, 'in-the-zone' tapping behavior. Similarly, Kucyi et al (2016) found that higher levels of response variability on a gradual-onset Continuous Performance Task (CPT) were significantly correlated with the DAN/SN, but not with the DMN or FPN. Instead, the DMN was most strongly associated with stable response behavior combined with self-reported mind wandering, even though those measures themselves were negatively correlated. Contrary to expectations of DMN and FPN coactivation, their findings thus describe an opposite pattern of elevated DAN/SN activity during periods of variable response behavior that are strongly linked to mind wandering. As neither response variability nor mind wandering reports predicted

DMN activity on their own as well as they did jointly, the authors argued that recruitment of the DMN may reflect separate neural processes associated with fluctuations in attention.

Chiefly, these studies dispute the unequivocal role of the DMN in mind wandering and appeal to its potential function beyond internally driven cognition. Intriguingly, they may conform to a recently proposed model by Mittner et al (2016), in which a tentative, subconscious 'off-focus' state is discerned from an 'active mind wandering' state, each characterized by distinct behavioral and neural signatures. Csifcsák & Mittner (2017) asserted that the overrepresentation of off-focus attention rather than mind wandering could reconcile the initial counterintuitive pattern of increased DMN activity without impaired behavioral performance, and also explain the absence of MTL recruitment that is thought to provide the necessary content for the active mind wandering state. Their model hence suggests that different components of the DMN may support different facets of mind wandering, and that distinct types of mind wandering may be more recurring in certain settings. However, given that self-reports are unlikely to capture completely unaware, off-focus episodes and that both self-reports and behavior independently predicted DMN recruitment, Kucyi et al (2017b) argued that alternative explanations should be considered.

The notion that the DMN has functionally heterogeneous characteristics is corroborated by evidence that it can be partitioned into multiple, interacting subsystems that play distinct roles in spontaneous cognition. For example, Stawarczyk et al (2011b) observed that midline DMN regions (i.e., mPFC and PCC) were involved in different kinds of thought unhelpful to task performance, such as task-related interference (e.g., performance appraisal), mind wandering, and external distractions, whereas the LTC was only associated with the two former (stimulus-independent) and the pIPL only with the two latter (task-unrelated) types. Among the different types of thought they measured in their study, mind wandering elicited the strongest neural activation, which was unique to the mPFC and PCC, indicating their particular involvement in self-referential thinking, while other parts of the DMN also supported unfocused monitoring of the external environment. Buckner et al (2008) argued that regions situated in the MTL provide associative content from episodic memory, the dorsomedial PFC facilitates the formation of self-relevant material, and both systems are strongly connected to the ventromedial PFC (vmPFC), PCC and IPL, that together form a cohesive core. Christoff et al (2016) further shaped this model by proposing that the MTL subsystem in particular is recruited under circumstances of weak deliberate constraints to enable memory-based simulations and promote variability and diversification of thought flow. While the FPN – predominantly the dlPFC – is a source of deliberate constraints, the DMN-core system together with the DAN and regions responsible for saliency detection exercise automatic constraints on MTL output, thereby facilitating more stability in salient thought patterns. Furthermore, the DMN-MTL subsystem, in particular the hippocampus (HPC), has been proposed to play a crucial role in generating mind wandering episodes by initiating a switch toward internally

focused attention whenever a memory reaches a given threshold of saliency (Buckner 2010; Smallwood 2013).

Finally, the DMN-core system has received considerable scientific attention, both in relation to mind wandering and regarding its role as a specialized convergence zone for ICNs involved in cognition and attention (e.g., Braga et al 2013; Mittner et al 2016). In particular, the PCC may possess 'hub-like' properties by integrating functional processes from the DMN and other distributed regions, making it a likely site to coordinate switches in attentional focus (Leech et al 2011; Leech et al 2012; Kucyi & Davis 2014). For example, Leech et al (2011) showed that at rest, the PCC is strongly interconnected with other DMN nodes, including the vmPFC and medial and lateral parietal cortex, as well as with frontoparietal regions involved in cognitive control. Although the entire PCC deactivated as difficulty on an *n*-back working memory task increased, a more posteroventral part became less connected to the rest of the DMN and more connected (less anticorrelated) to cognitive control regions, whereas a more anterodorsal part behaved in the opposite way. The ventral PCC's cooperation with the DMN during low demand and the dorsal PCC's cooperation with the FPN during high demand was thought to represent distinct roles in thought that is either directed internally or externally, respectively. Similarly, Leech et al (2012) reported a high degree of functional heterogeneity within the PCC. Using a data-driven 'echo' analysis, the authors found that multiple independent signals from separate – yet somewhat overlapping – spatial subregions correlated with the pattern of activity in different ICNs during rest and performance on a simple Choice Reaction Time (CRT) task. Interestingly, only the ventral PCC was connected to other DMN nodes and was unaffected by changes in external demands. Instead, dorsal subregions that correlated with left and right lateralized frontoparietal areas showed significant deactivation during the CRT compared to rest, suggesting that dorsal PCC-FPN functional connectivity reflects the monitoring of environmental changes and ceases when attentional focus is sustained on a specific task. Although the result of Leech et al (2012) do not substantiate the precise ventral-dorsal functional roles of the PCC as interpreted previously (Leech et al 2011), they support the finding that the PCC can adjust its connectivity profile depending on the demands from the outside world.

In summary, previous work has yielded inconsistent results regarding the pattern of activity and connectivity of ICNs, behavior, and mind wandering, likely highlighting the multifaceted nature of mind wandering as well as that of the DMN. Although originally regarded as the 'task-negative' network, the DMN has a heterogeneous functional architecture that may support highly integrated information processing and is involved in task-related cognitive functions (e.g., Crittenden et al 2015; Margulies et al 2016; Smith et al 2018; Sormaz et al 2018). Given the contemporary neural evidence, the precise role of the DMN in mind wandering therefore remains debatable. Moreover, there exists a large diversity across studies regarding the patterns of neural recruitment attributed to spontaneous forms of thought indicating that activity in neither the DMN nor FPN alone is sufficient to explain its neural basis (Fox et al 2015).

1.4   Neuromodulation of mind wandering

As becomes clear from the previous section, research into mind wandering has focused heavily on the activity and connectivity of regions confined to large-scale cortical networks. The dynamics of these networks, however, are influenced by neuromodulatory systems ascending from subcortical nuclei deep in the brain. In a separate line of research, it has been shown that neuromodulators such as norepinephrine (NE), dopamine, and acetylcholine govern brain states by altering the sensitivity, or *gain*, of receptive neuronal populations (e.g., Lee & Dan 2012; Ferguson & Cardin 2020). Concentrations of cortical, hippocampal, and cerebellar NE are almost exclusively supplied by the locus coeruleus (LC), a thin and elongated structure situated in the dorsal pons. The diffuse release of NE across the cortex is thought to adaptively regulate task (dis)engagement in terms of exploration-exploitation tradeoffs by modulating the gain of computational processes across the cortex (Aston-Jones et al 1999; Aston-Jones & Cohen 2005). In their adaptive gain theory (AGT), Aston-Jones & Cohen (2005) propose that NE modulates behavior through two distinct modes of neuronal firing in the LC: a phasic mode that facilitates *exploitation* by coupling strong, transient bursts of activity to relevant external events that selectively enhance task performance, and a tonic mode that facilitates *exploration* through general, uncoupled increases in firing rate that deprioritize task-relevant information and promote competing representations.

In line with the hypothesis that mind wandering transpires in a functional manner as a consequence of cognitive control processes (Shepard 2019), the AGT states that transitions between the LC/NE modes occur adaptively based on top-down evaluations of the goal utility – likely rendered by the ACC and orbitofrontal cortices (Aston-Jones & Cohen 2005). In other words, when pursuing a task is considered no longer sufficiently rewarding, reconfiguring the system toward a state of exploration allows a search for alternative and potentially more rewarding goals. Mittner et al (2016) hypothesized that exploration characterizes a high-gain, off-focus mode of mind wandering that intersects two more stable states with external and internal foci of attention, both of which instead rely on optimal tonic NE levels to sustain the ongoing conscious experience. Given evidence for increased clustering of established network connections during tonic NE modes (Eldar et al 2013) and a high degree of amalgamated network signals within the PCC and mPFC (Leech et al 2012; Braga et al 2013), it was proposed by Mittner et al (2016) that the off-focus state is neurally reflected in the converging network activity in the DMN-core hubs. In contrast, episodes of mind wandering are expected to recruit functionally specific networks, such as the DMN-MTL, whilst suppressing widely distributed connectivity, and hence should theoretically not be reflected in increased DMN-core activity (Figure 2).

Like other neuromodulators, LC/NE dynamics follow a Yerkes-Dodson curve, such that both low and high levels of tonic NE generate a suboptimal milieu for selective phasic responses, resulting in the demotion of task-related information processing and subsequently impaired behavioral performance

(Aston-Jones et al 1999; Aston-Jones & Cohen 2005). Evidence indicates that changes in pupil size covary with LC firing patterns in non-human primates (Rajkowski et al 1993; Joshi et al 2016) and show the expected Yerkes-Dodson relationship with task performance in humans (e.g., Gilzenrat et al 2010; Jepma & Nieuwenhuis 2011; Murphy et al 2011; Van den Brink et al 2016). Since the LC is challenging to visualize with standard fMRI methods due to its high neuromelanin content and location deep within the brain (Liu et al 2017; Tona et al 2017), researchers have accordingly utilized baseline and evoked changes in pupil diameter (PD) as a proxy for LC/NE-driven tonic and phasic states, respectively (Mathôt 2018). However, the neurobiological pathways underlying the relationship between LC firing rates and pupil size are unidentified, and there is substantial inconsistency in findings that link changes in PD to episodes of mind wandering (e.g., Smallwood et al 2011; Smallwood et al 2012b; Franklin et al 2013b; Grandchamp et al 2014; Mittner et al 2014; Konishi et al 2017; Pelagatti et al 2018; Unsworth & Robison 2018; Robison & Unsworth 2019; Jubera-Garcia et al 2019).
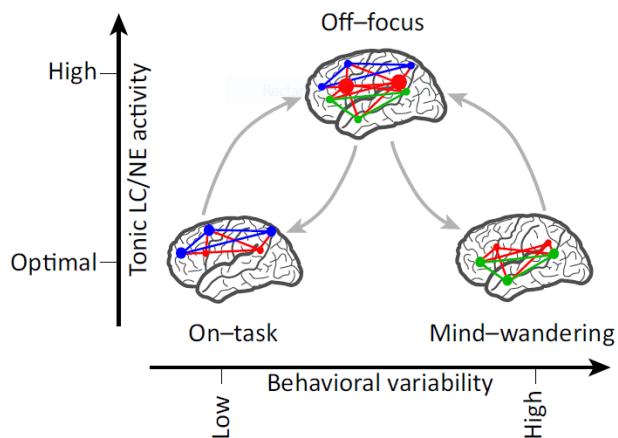

Figure 2. Neural model of mind wandering. Mittner et al (2016) proposed three distinct states through which an individual cycles during a cognitive task. The on-task state is featured by strong task-engagement, optimal performance, strong stimulus-locked bursts of NE, and recruitment of attention networks (blue). As the task progresses, an off-focus state emerges periodically that is characterized by stronger functional connectivity that converges on the DMN-core (red). When internal representations are prioritized over task-relevant information, the brain enters an active mind wandering state during which network configurations depend heavily on mental content (e.g., the DMN-MTL subsystem for autobiographical retrieval, green). Similar to the on-task state, tonic NE is at optimal levels to facilitate phasic responses that are linked to salient internal events but decoupled from task-relevant information, resulting in poor task performance. *(Copied from Mittner et al 2016)*

Eldar et al (2013) demonstrated with a simple but elegant neural simulation that *globally* elevated (tonic) gain resulted in more focused attention selection that enhanced task performance for stimuli with specific features to which the system was predisposed. Instead, low global gain weakened this bias by reinforcing broader information processing. While the former was associated with stronger clustered brain activity, the latter was represented in more distributed, equally competitive neural connections. These results contradict the AGT, which poses that *selective* increases in (phasic) gain through temporally coupled NE release enhance the system's signal-to-noise ratio by driving neurons more

toward binary function, whereas global, non-specific increases in NE amplify neuronal responsivity indiscriminantly, thereby making the system more sensitive to distracting events (Aston-Jones & Cohen 2005). Although the findings from Eldar et al (2013) could perhaps be interpreted as resulting from the selective, phasic influences on gain, the authors additionally reported smaller phasic pupil responses to task events for individuals whose task performance strongly matched their predisposition.

Whereas Eldar et al (2013) argue that increases in tonic gain support a narrow focus of attention, Mittner et al (2016) instead propose that high tonic gain and the associated increase in clustered brain activity represent an expansion of attentional focus during which different functional networks compete for dominance. Indeed, stronger within-network connectivity of the DMN and ACN as well as attenuated phasic pupil responses to task-events were associated with mind wandering but not task-focused attention (Mittner et al 2014). However, a conflicting observation of simultaneously reduced baseline PD instead suggests that task disengagement was associated with the lower end of the Yerkes-Dodson curve, theoretically indicating a hypoaroused state leading to inattentiveness or mind blanking (Murphy et al 2011; Unsworth & Robison 2016, 2018). Thus, although measures of PD provide opportunities to more objectively gauge internal and covert processes in humans, the previously observed discrepancies question the exact nature of the relationship between mind wandering and LC/NE-dependent neuromodulation of gain as derived from pupillometry, or at least emphasize a level of heterogeneity that complicates one-to-one mappings.

1.5 The role of the subcortex

Besides deep neuromodulatory nuclei, there is an abundance of subcortical structures situated in the fore- and midbrain that are anatomically and functionally embedded in extensive cortico-subcortical circuitry (e.g., Forstmann et al 2017; Ji et al 2019). Although subcortical structures have been relatively neglected in human fMRI studies compared to the cortex, they are asserted to play numerous and diverse roles in cognition (Keuken et al 2018a; Janacsek et al 2022). Furthermore, subcortical dysfunction is implicated in a range of neuropsychiatric disorders – e.g., attention-deficit/hyperactivity disorder (ADHD), obsessive-compulsive disorder (OCD), major depressive disorder (MDD), and Alzheimer's disease (AD) – that are also associated with deviations in mind wandering (Bonelli & Cummings 2007; Seli et al 2015; Marchetti et al 2016; Seli et al 2017; Bozhilova et al 2018; El Haj et al 2019). Recent findings have revealed widespread functional connectivity between subcortical areas on the one hand, including the basal ganglia, thalamus, and midbrain, and cortical networks including the DMN on the other (Bär et al 2016; Zhang et al 2016; Alves et al 2019; Li et al 2021), and some studies even reported specialized subcortical integration zones that facilitate the dynamic communication between distributed regions to support higher-level cognition (Jarbo & Verstynen 2015; Bell and Shine 2016; Greene et al 2020; Marek et al 2021). Recent studies show that basal forebrain and thalamic nuclei are especially integrated with DMN functioning (Alves et al 2019; Harrison et al 2022) and may be prominent subcortical drivers of the dynamic organization of complex and self-guided mental representations during internally focused states.

Few studies have reported recruitment of subcortical structures during periods associated with self-generated mental experience. Particularly the striatum (i.e., caudate nucleus and putamen dorsally and nucleus accumbens ventrally), together with the ACC, has been argued to support the maintenance of the ongoing brain state and hence sustain episodes of mind wandering (Tang et al 2012). Indeed, during performance of the SART, significant activation of the caudate nucleus and thalamus was found, among other regions, in relation to self-reports of mind wandering and unawareness of mind wandering, respectively (Christoff et al 2009). Furthermore, Chou et al (2017) observed that functional decoupling of the caudate nuclei from the left insula was related to the continuity of mind wandering, possibly indicating a reward-related inhibitory connection that suppresses switches in attentional focus governed by the insular cortex (Tang et al 2012). In a study using resting-state connectivity clustering, it was demonstrated that increased variability in network participation of the caudate nucleus was correlated with retrospective reports of more intrusive, past-oriented mind wandering (Schaefer et al 2014). Speculatively, the recruitment of the caudate nucleus as part of cortico-striatal-thalamic circuitry could reflect the regulation of bottom-up ('automatic') constraints on the train of thought that, when too strong, results in repetitious, inflexible patterns (Christoff et al 2016). Contrarily, Hasenkamp et al (2012) reported recruitment of the caudate body, thalamus, and frontoparietal cortex (dlPFC and IPL) directly after practiced meditators became consciously aware of their mind wandering during focused breathing,

indicating a goal-directed shift in attention back to the task, whereas the period directly prior to self-caught mind wandering sollicited the anterior insula together with the dACC, midbrain regions, and motor cortex. Instead, in another study, predisposed (i.e., trait-level) mindfulness – a construct described as attentiveness to experiencing the present moment and arguably opposite of mind wandering – was correlated with weaker functional coupling between the thalamus and PCC (Wang et al 2014). Although the precise functional roles of striatal and thalamic activity and connectivity are unidentified, these findings together provide preliminary evidence for their involvement in mind wandering. Since prior efforts have mostly focused on these larger structures, the potential contributions of the majority of subcortical nuclei remain, however, largely obscured.

1.6 Aims of the thesis

The wide range of identified neural and behavioral correlates of self-generated, 'off-task' types of thought have provided important clues into how the brain orchestrates episodes of mind wandering. More or less independent lines of research have implicated the DMN, attention and executive control networks, and neuromodulatory systems as established partakers, but empirical evidence for their interactions and relative importance in giving rise to mind wandering is at present incomplete. The divergent findings on the role of functional networks are especially emblematic for the, at best, modest understanding of the complex neural dynamics that underlie changes in attentional focus. Importantly, the contemporary literature reveals a poverty of approaches that combine fMRI with other neurophysiological methods such as EEG and pupillometry, subcortical imaging, and the application of more temporally refined and cognitively demanding behavioral paradigms. Although descriptive accounts have been proposed, these shortcomings likely underlie the absence of contemporary explanatory accounts of mind wandering.

To uncover new mechanistic insights into the neural underpinnings of mind wandering, a triangulation strategy was employed by integrating behavioral and neurophysiological evidence obtained during external tasks as well as wakeful rest. Through this multidisciplinary approach, this thesis aimed to disentangle the complex interplay between the various implicated neural systems and more closely delineate the multifaceted architecture of the wandering mind and its impact on behavior. Firstly, Paper I (*'Probing the neural signature of mind wandering with simultaneous fMRI-EEG and pupillometry'*) focused on assessment of the spatiotemporal signature of mind wandering during a sustained attention task by identifying informative features from simultaneously acquired multimodal data using supervised classification learning. In Paper II (*'Catching wandering minds with tapping fingers: Neural and behavioral insights into task-unrelated cognition'*), the neural substrates of direct and indirect markers of mind wandering were investigated with a finger-tapping paradigm that requires highly controlled executive functions for generating random response sequences. Lastly, we aimed to chart the presence of amalgamated signals from diverse functional networks associated with spontaneous cognition within a varied set of subcortical nuclei in Paper III (*'Echoes from intrinsic connectivity networks in the subcortex'*). In the final chapter, the findings from these three independent studies are integrated with the aim to foster new mechanistic knowledge on how large-scale network dynamics, subcortical contributions to the whole-brain functional landscape, and neuromodulatory influences together shape the human wandering mind.

Chapter 2
Methods

To advance our knowledge of the neurobiological basis of mind wandering, a multidisciplinary strategy was adopted involving a wide range of techniques. Three independent reseach works utilized both established and innovative methodologies, among which experience sampling, functional neuroimaging, pupillometric modeling, and supervised machine learning. In the following sections, I will describe these aspects in detail.

2.1 Participants and ethics

An overview of the three separately conducted experiments is presented in Table 1. The studies were approved by the local Ethics Review Board of the Faculty of Social and Behavioral Sciences at the University of Amsterdam (Paper I, II, III) and the Regional Committees for Medical and Health Research Ethics in Norway (Paper III). Data were collected from healthy volunteers between the ages of 19 and 45 years recruited from the general population in The Netherlands and Norway for Paper I and III, respectively, and from the Amsterdam ultra-high field adult lifespan database (AHEAD; Alkemade et al 2020) for Paper II. All participants met the following general inclusion criteria by self-report: normal or corrected-to-normal vision and no (history of) psychiatric or neurological illness. Due to the rhythmic finger-tapping task employed in Paper II, experienced or professional musicians were excluded to avoid individual biases in tapping performance. It should be noted that the participants in all three studies were predominantly Caucasian, thereby underrepresenting other ethnic groups. To ensure the safety of participants, careful screening for MRI-related contraindications took place prior to any experimental procedure. All participants signed written informed consent forms and were compensated for their time with a monetary reward (Paper I, II) or gift card (Paper III). The collected data for this thesis are stored on secure university-based servers and shared with other researchers through open access platforms following thorough anonymization procedures to guarantee the privacy of all those who participated.

Table 1. Overview of participant demographics, study design, and neuroimaging methods.

	Paper I	**Paper II**	**Paper III**
Sample	N=30 (25 female) age: M=21, SD=2.51	N=27 (12 female) age: M=27.5, SD=7.20	N=40 (21 female) age: M=26.5, SD=5.50
Data acquisition	3T fMRI, EEG, pupillometry	3T fMRI, pupillometry	7T fMRI
Paradigm	Sustained Attention to Response Task (SART)	Finger-Tapping Random Sequence Generation Task (FT-RSGT)	Resting-state (eyes open, fixation cross)
Mind wandering	Probe-caught	Probe-caught	No explicit measure
Main analysis*	SVM-RBF	Whole-brain GLM	ICA-DR

Support vector machine with radial basis functions (SVM-RBF), general linear models (GLM), independent component analysis - dual regression (ICA-DR).

2.2   Measuring mind wandering and behavior

2.2.1 Experience sampling

In Paper I and II, mind wandering was periodically sampled by interrupting the experimental task with a thought probe that prompted participants to report their current focus of attention (Figure 3a). This experience sampling technique is to date considered the most direct way to measure periods of task disengagement and is ubiquitously used in mind wandering research (e.g., Klinger & Cox 1987; Kane et al 2007; Killingsworth & Gilbert 2010; Seli et al 2018b). In contrast to the 'self-caught' method, which depends on individuals' ability to consciously report episodes of mind wandering as they arise, the probe-caught method allowed us to capture ongoing mind wandering that transpired either with or without awareness, which has been argued to provide more reliable estimates of the amount of mind wandering throughout a task (Smallwood & Schooler 2006). Participants were given instructions to report 'off-task' thoughts when they introspected content that was not related to the primary task, performance appraisals, or external distractions. Consequently, we assume that at least the majority of self-reports classified as mind wandering in this thesis consisted of both self-generated and task-unrelated mental processes, such as self-referential, episodic, and prospective thoughts (Smallwood & Schooler 2015).

In Paper I, thought probes were formulated as the following question: '*Where was your attention during the previous trials*?', to which participants answered using a four-point Likert scale ranging from 'off-task' to 'on-task'. To maximize the probability of capturing ongoing episodes of mind wandering, probe onsets were manipulated by an online algorithm that continuously monitored changes in behavioral performance. That is, when trial-by-trial RT variability dropped below or exceeded a certain threshold, the algorithm initiated the onset of a thought probe. A similar, previous approach demonstrated that thought probes whose onsets were controlled by task performance were more successful in catching mind wandering than did randomly occurring thought probes (Franklin et al 2011). However, to achieve a sampling frequency comparable to other studies, the online algorithm was constrained to produce a thought probe at most every 21s and at least every 63s, resulting in an average of 44 probes presented to each participant. In Paper II, we reproduced the method from Boayue et al (2020a) by probing for mind wandering with the question: '*Where was your attention (i.e. your thoughts) focused just before this question?*', accompanied by a six-point Likert scale annotated with: 'clearly on-task', 'partly on-task', 'slightly on-task', 'slightly off-task', 'partly off-task', 'clearly off-task'. Thought probes appeared once every 55-65s, independently of task performance, with a fixed number of 27 probes per participant.

Although there are numerous ways of thought probing, the common use of Likert scales offers several methodological advantages. For example, dichotomization of probe responses into separate categories for contrast analyses (e.g., Christoff et al 2009) is less complicated compared to continuous

response scales. Additionally, a wide range of response options may make it more difficult for individuals to select the appropriate choice and may be more sensitive to biases such a primacy effects and satisficing (Weinstein 2018). Following previous studies, we used a simple split-the-middle approach to separate the four options in Paper I into off-task and on-task categories, which were subsequently used as labels to train a supervised classification algorithm. To account for possible biases arising from individual variation in introspective judgments and response tendencies, some studies employed modifications to this dichotomization. For example, Mittner et al (2014) incorporated subject-specific minimum and maximum responses only, resulting in exclusion of almost half the thought probes on average. In Paper II, we implemented a similar approach while avoiding such loss of data by determining subject-specific split-points that resulted in approximately equal proportions of off-task and on-task responses for each subject. Both traditional and custom dichotomies were subsequently contrasted in a whole-brain fMRI analysis to investigate the difference in neural activity prior to self-reported attentional states.

2.2.2 Experimental paradigms

A fast-paced version of the SART with thought probes was employed in Paper I. Stimuli were presented as digits (1 to 9) that briefly replaced a centered fixation cross at the start of each trial (Figure 3b). Participants were instructed to respond to every digit as fast and accurate as possible by pressing a button with their right index finger, except when that digit was the target '3'. Digits were presented every 1400 ms with an average 9:1 ratio of non-targets to targets, inducing a monotonous yet attention-demanding environment suitable for eliciting mind wandering (Smallwood & Andrews-Hanna 2013). Although the utility of the SART in mind wandering research is undisputable, it has several drawbacks. First, the majority of the task can be performed without recruiting executive functions, and the temporal resolution at which decrements in executive control can be measured is limited to incidental target trials. Second, performance on target trials is quantified into a dichotomous decision (error versus correct), preventing a gradual expression of the underlying attentional state. Hence, it has been argued that more complex paradigms are necessary to investigate the interaction between mind wandering, other cognitive functions, and behavior (e.g., Mittner et al 2014; Boayue et al 2020a). Driven by this need, Boayue et al (2020a) developed the Finger-Tapping Random Sequence Generation Task (FT-RSGT) by combining simple, metronome-cued finger tapping (Seli et al 2013; Kucyi et al 2017a) with random number generation (Teasdale et al 1995; Baddeley et al 1998) and probe-caught experience sampling. Participants are tasked with using left and right index fingers to tap in a rhythm that is synchronized with an auditory cue (metronome paced at 750 ms) whilst generating a sequence of left and right taps that is as random, or unpredictable, as possible (Figure 3c). Whereas the degree of response variability is regarded a particularly sensitive marker for mind wandering (e.g., Seli et al 2013; Bastian & Sackur

2013), the aspect of response randomization is known to reflect strategic and goal-directed behavior that requires self-monitoring, planning, and suppression of habitual responses (e.g., Teasdale et al 1995; Miyake et al 2000; Jahanshahi et al 2000; Peters et al 2007). Crucially, changes in both indices can be continuously monitored throughout the course of the experiment at subsecond temporal resolution and related to self-reported attentional state. The repetitive character of the FT-RSGT was shown to elicit comparable levels of task-unrelated thought as the SART (Boayue et al 2020a), making it a suitable new paradigm to study the interplay between mind wandering and executive control. In Paper II, the FT-RSGT was supplemented with pseudo-random interspersed blocks of alternating finger-tapping to provide a control condition identical in terms of stimulus pacing, motor responses, and probe frequency but without the randomization criterion and hence demand on executive functioning.
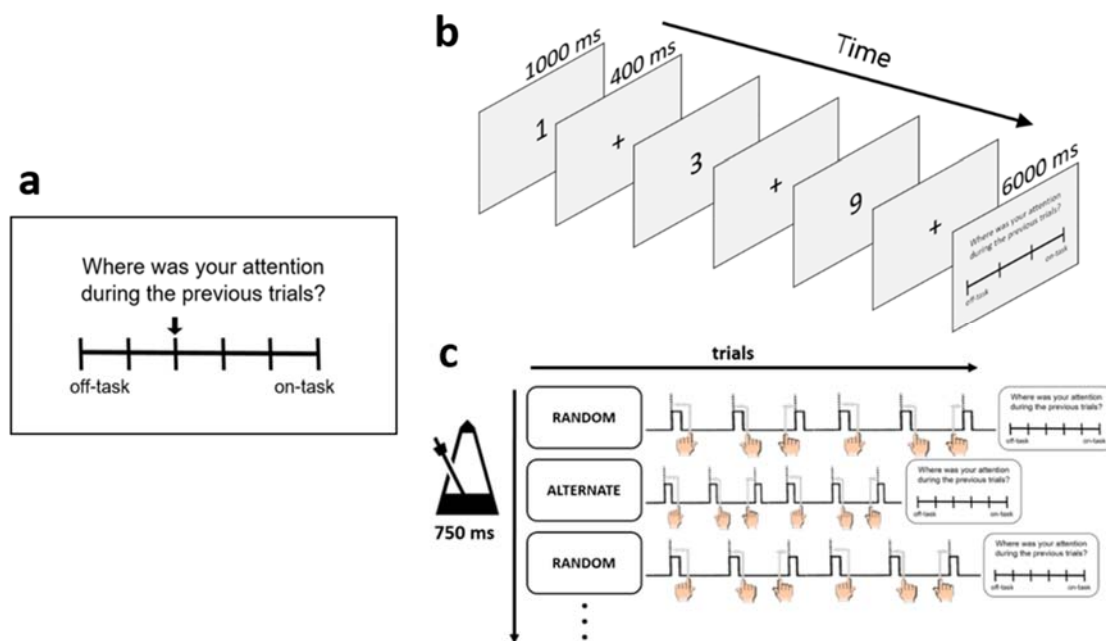

Figure 3. Methods for measuring mind wandering and behavior during cognitive task performance. **a)** Experience sampling probes were interspersed thoughout the cognitive task, asking participants to self-report their current focus of attention by moving an arrow above a slidebar ranging from 'off-task' to 'on-task'. The question and response scales were slightly different for Paper I and II. **b)** Flowchart of the Sustained Attention to Response Task (SART), showing the presentation of target (digit 3) and non-target (digits 1-9 except 3) stimuli that was occassionally interrupted by a thought probe. **c)** Overview of the Finger-Tapping Random Sequence Generation Task (FT-RSGT) and Alternating finger-tapping task. Participants were instructed at the start of each one-minute block whether they should tap their left and right index fingers in synchrony with the metronome in an alternating order (ALTERNATE) or in a random order (RANDOM), followed by a thought probe.

No cognitive task was administered in Paper III. Instead, participants were instructed to stay awake and keep their eyes fixated on a crosshair presented centrally on the screen for two resting-state sessions of 15 minutes each. Resting-state fMRI is a widely used technique to map the intrinsic activity of the human brain that is undetermined by changes in the environment (e.g., Smitha et al 2017). Intriguingly, descriptions of ICNs – i.e., endogeneous patterns of statically correlated voxel timeseries – show a strong spatial similarity to networks that are activated in a task-dependent manner, suggesting that during rest, the brain cycles through states that relate to cognitive and perceptual processes recruited during external demands (Ingvar 1979; Smith et al 2009; Spreng et al 2010; Kristo et al 2014). More directly, a growing body of work demonstrates that the brain dynamics during wakeful rest can be translated to – both retrospective and online – measures of mind wandering (Schaefer et al 2014; Van Calster et al 2017; Chou et al 2017; Karapanagiotidis et al 2020). Together, these findings strongly indicate that unfolding self-generated experiences explain a large portion of the variability in the spontaneous brain signal observed during resting-state fMRI. Consequently, the task-free paradigm in Paper III permitted the investigation of how stable patterns of intrinsic functional connectivity are represented, or echoed, in a varied set of subcortical regions, thereby generating data on the synergy between cortical networks and the subcortex during periods that are dominated by mind wandering.

2.2.3 Behavioral analysis

For the SART, four aspects of behavioral performance were assessed based on the trials preceding thought probes, including mean RT, RT variability, proportion of errors of omission (not responding to a non-target), and commission (responding to a target). For each of these indices, the difference in behavior leading up to on-task versus off-task self-reports was statistically tested by means of paired *T*-tests to investigate the impact of mind wandering on task performance. For the FT-RSGT, two features of task performance features were extracted: behavioral variability (BV) was calculated as the standard deviation of inter-tap intervals and (ii) approximate entropy (AE) was based on the formula developed by Pincus and Kalman (1997). While descriptive or rank order statistics do not discriminate between a binary sequence whose pattern is predictable (e.g., 0-1-0-1-0-1-0) and one whose pattern is more random (e.g., 0-1-1-1-0-1-0), AE instead quantifies the degree of irregularity in the tapping series by calculating the average of the logarithms of the frequency with which subsequences remain identical when moved up by one position in the sequence. Higher values of AE indicate a higher degree of randomness and imply greater executive control over the self-determination of complex response sequences. Similar to Paper I, the relationships between task performance and self-reports of mind wandering were assessed by statistically testing the difference in BV and AE values based on the trials prior to the thought probes for the different probe responses. Rather than imposing a dichotomy on the six-point Likert scale, we followed a previous approach by using the ordinal scale as dependent variable in a more statistically

appropriate Bayesian hierarchical ordered probit regression model (Boayue et al 2020a, 2020b). This modal is particularly useful for experience sampling data as the hierarchical implementation (i.e., random intercepts at subject level) accounts for interindividual variation in mind wandering propensity and self-report tendencies. The resulting Bayesian model coefficients are expressed as posterior means (b) with corresponding 95% highest-density intervals (HDI) and evidence ratios favoring a positive (ER_+) or negative (ER_-) relationship with the outcome variable.

2.3 Functional neuroimaging

There are numerous contemporary functional neuroimaging techniques that provide exciting ways to study the human central nervous system non-invasively, of which EEG and fMRI are the most widely used. Particularly fMRI has proven an extremely useful tool in the cognitive neurosciences with an overwhelming amount of studies capitalizing on the finding that changes in neuronal firing relate to regional changes in blood supply (Logothetis 2008). While EEG directly records the summed electrical activity of postsynaptic potentials from neuronal populations in the cortex, fMRI generates images based on the difference in magnetic properties between oxygenated and deoxygenated hemoglobin in the blood, called the blood oxygen level-dependent (BOLD) contrast. Both methods have advantages and limitations, but their relative strengths are mostly expressed in terms of spatiotemporal detail. Given that EEG samples real-time yet averaged neuronal activity through electrodes attached to the scalp and fMRI measures a delayed but local increase in oxygenated blood, the former provides a superior temporal resolution (i.e., order of milliseconds) whereas the latter has a higher spatial resolution (i.e., up to submillimeter depending on field strength and pulse sequence). Two fMRI techniques were utilized in this thesis: task-based (Paper I, II) and resting-state (Paper III). Whereas task-based fMRI allows investigation of activity patterns during specific experimental conditions, resting-state fMRI contributes to a better understanding of the endogenous neural rhythms that underlie intrinsic brain organization. Interestingly, task-induced changes in brain activity reflect only a fraction of the metabolic energy that is consumed during quiescent, task-free states, emphasizing the behavioral relevance of studying neural dynamics with resting-state fMRI (Raichle 2010).

2.3.1 Defining intrinsic connectivity networks

The identification of synchronized patterns of neural activity from the fMRI voxel timeseries across the brain can be statistically achieved with functional connectivity (FC) analysis. Two commonly used static FC methods, seed-based correlation and independent component analysis (ICA), were employed in Paper I and III, respectively. Data in Paper I were first subjected to a preprocessing step to regress out all systematic, task-evoked BOLD signal (e.g., motor responses, visual stimuli) and obtain the residual signal presumed to capture underlying, spontaneous fluctuations in brain activity. Subsequently, voxel-wise seed-based correlation analysis was used to define the spatial boundaries of the DMN (5% most positive correlations) and its ACN (5% most negative correlations) based on the temporal pattern of the averaged signal in the PCC as a predefined seed-region. Whole-brain spatial maps of the DMN and ACN were then automatically parcellated into seven and six regions of interest (ROIs), respectively, to investigate their relationship with self-reported mind wandering during the SART. The ROIs were labeled manually as PCC/PCUN, mPFC, bilateral pIPL (angular gyri), bilateral SFG, and left MTG for the DMN, and SMA, bilateral insula, bilateral dlPFC, and right pIPL (supramarginal gyrus) for the ACN.

Although seed-based correlation analysis is widely used and easy to implement, it has several limitations, among which the requirement of an *a priori* seed region and the relatively large impact of exact seed location on the resulting spatial map (Cole et al 2010). Following ROI definition, single-trial activity as well as dynamic FC based on sliding window correlations were extracted for every node and node pair, respectively.

In Paper III, we utilized a fully data-driven approach by determining ICNs at group level using ICA, which is a multivariate, exploratory technique that decomposes the fMRI timeseries by finding maximum independence in its constituent components. It does so by assuming that the data represents a Gaussian mixture of separate 'hidden' signals that are themselves non-Gaussian. Although the purpose of ICA is conceptually similar to, for example, principal component analysis (PCA) and factor analysis (FA), it uses higher-order statistics to reveal independence instead of variance and does not enforce orthogonality of components. Consequently, ICA tends to produce more reliable results for datasets with multiple and correlated sources of variability (Cole et al 2010). To find group-level independent components, individual datasets are often concatenated along the time dimension and treated as a single, extended dataset. However, it has been argued that temporal concatenation, especially for data with a high degree of interindividual variability and when using higher model order, can lead to artifacts such as spatial fragmentation of the DMN (Hu & Yang 2021). Given this potential drawback, we chose to implement a hierarchical approach, in which individual datasets were decomposed prior to a canonical correlation analysis that identified commonalities at group level (Varoquaux et al 2010). The resulting network components demonstrated satisfactory spatial overlap with an established cortical network parcellation (Yeo et al 2011) and generally greater correlations with subcortical connectivity profiles, further validating our approach.

2.3.2 Exploring network echoes in the subcortex

Compared to the cortex, the subcortex has been relatively neglected in human connectome mapping and atlasing efforts (Johansen-Berg 2013; Alkemade et al 2013; Forstmann et al 2017) and only a small proportion of subcortical structures are systematically investigated in relation to cognitive functions (Keuken et al 2018a). Likely, this gap is due to the challenges associated with subcortical imaging. The subcortex consists of hundreds of individual structures with highly variable magnetic susceptibilities (i.e., differences in iron, myelin, and neuromelanin content) and has a larger distance from the radiofrequency coil that results in generally lower signal-to-noise ratio (SNR) compared to the cortex (De Hollander et al 2017; Keuken et al 2018b; Miletić et al 2020; Miletić et al 2022). Consequently, MR protocols that optimize BOLD sensitivity in the cortex do not necessarily generalize to the subcortex. Given that increases in magnetic field strength produce gains in SNR without considerably increasing acquisition time, the use of ultra-high field MRI (i.e., 7 Tesla) poses strong benefits for

achieving the fine-grained spatial resolution needed to resolve small structures deep in the brain and elucidate subcortical structure-function relationships (e.g., Forstmann et al 2017; Keuken et al 2018b; Tian et al 2020).

In Paper III, we exploited a subcortical-tailored functional imaging protocol at 7 Tesla to optimize the BOLD signal in a varied set of 14 subcortical ROIs generated by the Multi-contrast Anatomical Subcortical Structures Parcellation algorithm (MASSP; Bazin et al 2020), among which basal ganglia, midbrain, and brainstem nuclei – including those rarely considered in human fMRI research (Keuken et al 2018a). MASSP takes advantage of quantitative MRI to determine priors for subcortical delineation, providing a strategy that could ultimately abolish the need for time-consuming and laborious manual work (Bazin et al 2020). We simultaneously studied the intrinsic functional architecture of 12 MASSP-derived ROIs in addition to parcellations of the hippocampus (Yeo et al 2011) and locus coeruleus (Ye et al 2021). To further boost the subcortical signal, we implemented retrospective image-based correction for removing the prominent effects of physiological noise (Glover et al 2000) as well as minimal spatial smoothing for reducing the risk of signal blurring among adjacent structures (De Hollander et al 2015).

Following preprocessing, canonical ICAs were performed on the whole-brain timeseries to extract a set of data-driven networks as well as within each subcortical ROI to identify spatiotemporal independent subregions, followed by a dual regression (DR) analysis to assess the spatial overlap between the whole-brain FC pattern of each subregion and every network component. Critically, ICA-DR is a multivariate technique that allows estimation of the subject-specific subregional timecourses and corresponding voxel-wise FC patterns while accounting for the variance in the remaining timecourses within each ROI, thereby revealing a connectivity profile that is more unique to that subregion. This approach was previously successful in identifying heterogeneous patterns of network signal repetitions within transmodal cortical regions, which has been argued to reflect evidence for multi-network information integration (Leech et al 2012; Braga et al 2013). The objective of Paper III was to establish the presence of such 'echoes' – i.e., a mixture of dissociable signals from multiple intrinsic networks – within often understudied subcortical regions, which could provide a compelling future approach for charting the functional significance of network topology and its convergence in the subcortex for orchestrating spontaneous cognitive processes such as mind wandering. Echoes of ICNs were quantified by calculating the spatial correlations between subregional FC maps and data-driven reference networks derived from a whole-brain canonical ICA. The number of above-threshold spatial correlations in each ROI was counted to provide a comparative summary measure, taking the 97th percentile of all spatial correlations as arbitrary threshold.

2.3.3 Modeling the neural correlates of mind wandering

General linear models (GLMs) are commonly used for the preprocessing and statistical analysis of fMRI data and were implemented in Papers I, II, and III for various purposes. Denoising of fMRI data is a necessary step to remove the influence of numerous sources of nuisance, including artifacts due to head motion, tissue movement related to physiological dynamics, and low-frequency signal drifts caused by the scanner hardware. In voxel-wise, whole-brain GLMs, a design matrix is fitted to the measured BOLD signal in every voxel, consisting of the weighted sum of a set of explanatory variables that represent nuisance or that model the expected timeseries under a certain experimental condition. Consequently, voxels whose measured timeseries correlates with a given explanatory event produce large regression coefficients that can be statistically tested in a second-level analysis.

In Paper I and III, GLMs were implemented for denoising purposes and included nuisance parameters (e.g., average signal from white matter, head rotation and translation) so that the residual, unexplained variance would reflect fluctuations in neural activity rather than noise. In Paper II, GLMs were used in the primary analysis to model the neural correlates of task performance, pupillary dynamics, and periods of probe-caught mind wandering. Specifically, statistical contrast images were generated to assess: (i) the difference in neural activity between random and alternating finger-tapping tasks and between self-reported mind wandering and task-focused attention, and (ii) the voxel-wise correlations with ongoing task performance and pupillary dynamics. To create regressor functions for behavior, BV and AE were calculated with sliding windows, such that each individual trial was assigned a value for BV and AE based on the preceding 25 tapping responses (approximately 18-19s). This procedure led to smoothed and time-lagged regressor functions that, after resampling to the resolution of the fMRI timeseries, mimicked the distribution of a hemodynamic response function (HRF)-convolved event.

2.3.4 Simultaneous fMRI-EEG

One of the research questions in Paper I concerned the influence of combining sources of data rich in spatial (i.e., fMRI) or temporal (i.e., EEG) information on classification of mind wandering episodes with supervised machine learning. Given that periods of task-disengagement are thought to occur transiently and frequently throughout a task, temporally resolved methods such as EEG and pupillometry are theoretically well-suited to complement fMRI in tracking ongoing changes in attention. Fast recurrent oscillatory dynamics in the EEG signal have been shown to underlie the slower fluctuating activity that gives rise to brain networks observed with resting-state fMRI (Britz et al 2010; Hunyadi et al 2019) and specific EEG signatures are consistently associated with mind wandering, such as increases in alpha band frequency power and reductions in ERP magnitude (Compton et al 2019; Jin et al 2019; Kam et al 2022). In accordance with these findings, we supplemented the SVM in Paper I with single-

trial features for prestimulus oscillatory power in delta, theta, alpha, and beta frequency bands across electrodes positioned over frontal, bilateral parietal, and occipital cortices, as well as event-related amplitudes at midline occipital (relating to P1 topography), occipitotemporal (N1), midline parietal (P300), and midline frontal electrodes.

Concurrent imaging techniques are vitally important for facilitating investigations in the interactions between modalities that are temporally refined and precisely localized (e.g., Scheeringa et al 2008; Neuner et al 2014; Marino et al 2019) as well as their relative potency for detecting non-stationary internal states. However, fMRI components introduce strong artifacts that obscure the EEG signal and in turn, electromagnetic inference from EEG can lead to image distortions (Krakow et al 2000; Bullock et al 2021), emphasizing pronounced disadvantages of simultaneous fMRI-EEG acquisition. Particularly, cardioballistic artifacts arising from subtle movements within the magnetic field (i.e., blood pulsation and heartbeat-related whole-body motion) are prominently present in EEG. To negate some of these effects and achieve data quality comparable to that outside of the fMRI environment, we utilized carbon-wire loops (CWL) integrated within the EEG equipment for providing a motion reference signal that can be used for efficient, offline regression-based correction (Van der Meer et al 2016).

2.4 Estimating neuromodulation with pupillometry

Investigating pupillary dynamics in relation to mind wandering is theoretically attractive because (i) patterns of pupil dilation are a presumed correlate of LC/NE-modulated exploration-exploitation tradeoffs (e.g., Gilzenrat et al 2010) and (ii) reduced pupil responses to external stimuli are thought to reflect a perceptual decoupling mechanism during mind wandering (e.g., Smallwood et al 2011). In addition, pupillometry has several appealing methodological aspects. For example, eye-tracking can be performed at both high spatial and temporal resolution (~0.25-0.50 degrees of visual angle, submillimeter pixel resolution, 2000 Hz sampling rate) and the hardware set-up allows easy combination with other techniques, including fMRI and EEG. Importantly, previous studies reported evidence that variations in pupil diameter (PD) relate to changes in the underlying attentional state (e.g., Mittner et al 2014; Grandchamp et al 2014; Unsworth & Robison 2016), indicating that pupillometry can provide a useful tool to objectively gauge processes that have little behavioral manifestations or are difficult to self-report.

Standard approaches for PD analysis often consist of signal averaging in fixed prestimulus (baseline) and poststimulus (evoked) intervals. However, it has been argued that the buildup of stimulus-evoked increases in PD can resemble slower baseline fluctuations, especially in fast-paced paradigms where visual or auditory stimuli are presented in quick succession (Mittner 2020). Consequently, spillover of evoked pupil responses can contaminate subsequent trials' baseline measures, hampering estimations of the underlying tonic state. To circumvent this issue, a novel modeling method was developed to separate tonic and phasic components (Mittner 2020). With this technique, high-prominent negative peaks in the ongoing pupil signal were identified and enveloped by means of cubic spline interpolation (Paper I) or two iterations of B-spline basis functions (Paper II). This resulted in a smooth delineation consistently positioned underneath the raw pupil signal, thereby providing an estimate of tonic fluctuations that is relatively unaffected by the accumulation of phasic responses. To measure the magnitude of task-evoked pupillary dilations, single-trial GLMs with regressors for both stimuli and response onsets convolved with a canonical pupil response function (Hoeks & Levelt 1993) were fitted after subtraction of the modeled tonic signal. This approach allowed us to more reliably index the different behavioral states associated with LC firing rates: the phasic mode that prioritizes task-relevant information and supports optimal performance, and the tonic mode that facilitates task-disengagement and exploration of alternative behavioral goals (Aston-Jones & Cohen 2005).

31

2.5   Machine learning of multimodal data

Machine learning-based identification of patterns in neural and behavioral data is frequently leveraged to better understand the mechanisms of latent cognitive processes such as mind wandering (e.g., Bastian & Sackur 2013; Dhindsa et al 2019; Jin et al 2020; Zanesco et al 2020b). Rather than being restricted to data that are temporally linked to a self-reported state (i.e., the trials directly preceding a thought probe), a supervised learning algorithm trained on probe responses can generalize to periods uninterrupted by experience sampling and therefore provides a powerful instrument to analyze the full extent of a dataset. Researchers have implemented non-linear support vector machines (SVM) for this purpose, demonstrating successful detection of mind wandering episodes based on self-report in various task settings (Grandchamp et al 2014; Mittner et al 2014; Faber et al 2018; Jin et al 2019). Essentially, SVMs create a hyperplane to separate two classes by maximizing the distance between observations from the opposite class, called support vectors. To model non-linear relationships, SVMs are augmented with a kernel trick that transforms the data into a higher-dimensional space. Without altering the algorithm, a linear hyperplane can be fitted through the kernelized landscape, generating a non-linear decision boundary when the data are projected back to original space. Gaussian radial basis functions (RBF) are commonly used and parameterized by kernel parameter gamma, which determines kernel shape and hence influences model fit: a too small gamma can cause underfitting because kernels with a large variance might not match the complexity of the data, and a too large gamma can result in overfitting because kernels with a small variance may only capture the support vectors and thus poorly generalize to out-of-sample data.

In Paper I, we trained an SVM-RBF on a large set of neurophysiological features obtained from simultaneous fMRI-EEG and pupillometry, using the dichotomized thought probe responses as training labels. Parameters were optimized by means of grid search and leave-one-out (LOO) cross-validation (CV), during which the SVM-RBF was trained on all datasets but one and tested on the one left out. This was repeated for all possible permutations (i.e., every individual dataset was left out once), generating a mean CV accuracy at every step of the search to identify the parameters that yielded the best classification performance. Subsequently, recursive feature elimination (RFE) was performed to eliminate redundant features, thereby reducing data dimensionality and risk of overfitting. At every iteration of the RFE, mean CV accuracy was determined for every combination of sets leaving one feature out, such that the highest performing set could continue to the next round and one feature was permanently dropped. In a second RFE procedure, different combinations of feature sets depending on modality (e.g., dynamic FC, pupil diameter, oscillatory power) were evaluated with separate SVM-RBFs to assess the performance of modalities collectively and individually, as well as in all possible pairs, triples, and quadruples. This procedure generated an 'importance score' for every feature depending on its pattern of elimination across the classifiers, providing an indication of the utility for differentiating between the two self-reported attentional states. Thus, this RFE procedure was instrumental in assessing

the relative importance of both domain-specific and feature-specific information for detecting mind wandering during the SART.

2.6   Open Science practices

Open Science refers to the practice of sharing materials, code, and data through channels that are freely available to other researchers, students, clinicians, and the general public with the purpose of making scientific progress more accessible and increase its use for society. To adhere to this principle, all three research works in this thesis were published as preprints and linked to an Open Science Framework (OSF) repository (Table 2). Besides facilitating transparency, collaboration, and replication, Open Science can provide researchers with access to costly neuroimaging data and state-of-the-art analytical tools. For example, the work in this thesis strongly took advantage of publicly available databases (AHEAD; Alkemade et al 2020), cortical and subcortical parcellations (e.g., Yeo et al 2011; Bazin et al 2020), and pupil modeling software (Mittner 2020).

Table 2. Overview of data sharing and repositories.

Paper	Data	Code	Materials	Preprint	Repository
Groot et al *preprint*		✓	✓	✓	osf.io/wt3uc
Groot et al 2022, *Cereb Cortex*	✓	✓	✓	✓	osf.io/56fcx
Groot et al 2021, *NeuroImage*	✓	✓	✓	✓	osf.io/43dp5

Chapter 3
Summary of Results

Three empirical studies were conducted with the objective to contribute new knowledge to the field by examining mind wandering signatures across a broad spectrum of neurophysiological features, its interaction with the organization of complex behavior, and how the intrinsic architecture of task-free states within functional networks is echoed throughout the subcortex. This chapter serves to provide a summary that focuses on the key findings and outcomes for each study.

3.1 Probing the neural signature of mind wandering with simultaneous fMRI-EEG and pupillometry

In this study, we sought to obtain a more comprehensive understanding of the spatiotemporal signature of mind wandering by identifying robust neurophysiological features from fMRI, EEG, and pupillometry. We expected that the different modalities provide complementary information for detecting changes in attentional focus by means of supervised machine learning. An SVM-RBF was trained on the probe responses using preceding single-trial data features that were grouped in five domains: activity in DMN and ACN nodes, dynamic FC of node pairs within and between networks, prestimulus oscillatory power, magnitude of event-related components, and tonic and phasic PD.

In accordance with the expected decrements in SART performance during mind wandering, we found significantly higher RT variability and error rates prior to off-task reports. The SVM-RBF achieved a mean CV accuracy of 65% with 74 surviving features representing all five domains, indicating above chance-level ability to detect episodes of mind wandering. As hypothesized, each modality contributed unique information that improved classification accuracy (Figure 4, left). Notably, all classifiers that excluded dynamic FC features performed worse on average, thereby demonstrating that time-varying connectivity within and between the DMN and ACN best captured transient changes in attentional focus.

The off-task classified trials were contrasted with on-task trials for every feature (i.e., the average difference in standardized single-trial feature activity) to summarize the spatiotemporal signature of probe-caught mind wandering during the SART across the various domains (Figure 4, right). Relative to sustained external attention, off-task probes were on average preceded by deactivation of DMN nodes, activation of ACN nodes, and stronger functional coupling between them. Since coherence within either network was also weaker, mind wandering was represented by widespread functional integration rather than clustering. Several nodes were eliminated, including the PCC, right SFG, and right dlPFC, indicating that their general activity was not perceived as helpful for tracking either attentional state over and above the other features. However, dynamic FC between nodes from both networks and the PCC was more often positively associated with mind wandering, suggesting that the PCC coupled with both the DMN and ACN to coordinates switches from external to internal attention. Except for the beta band, prestimulus oscillatory power was generally increased and was most pronounced for frequencies within the alpha range. While poststimulus amplitudes reflecting early perceptual processes (i.e., P1, N1) were relatively unaffected by mind wandering, midline frontal and parietal components at later latencies (>250 ms) were predominantly reduced, indicating a degree of decoupling from the task at deeper stages of information processing. Despite PD contributing least to classification performance, tonic dilatory patterns survived feature elimination and showed a relative increase preceding off-task reports, theoretically indicating elevated levels of tonic NE to facilitate task-disengagment.
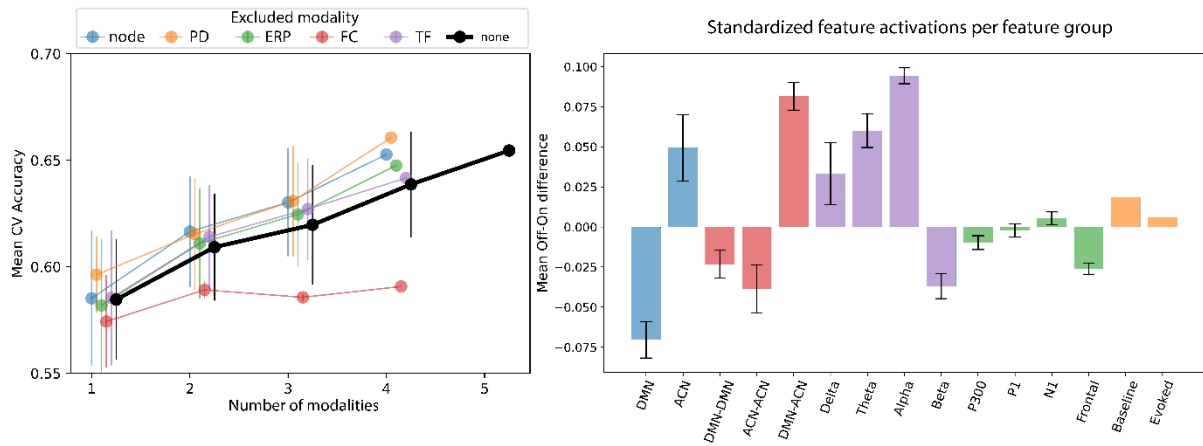
Figure 4. Supervised classification learning of multimodal signatures of probe-caught mind wandering.
Left) Means and standard errors of SVM-RBF mean CV accuracy as a function of number of included modalities, plotted separately for network activity (blue), dynamic FC (red), oscillatory power (purple), event-related amplitudes (green), and pupil diameter (yellow) features as excluded modality. The black line represents the performance across the all-inclusive permutations, i.e., five singles, 10 doubles, 10 triples, five quadruples, one quintuple. **Right)** Means and standard errors of the difference between off-task and on-task single-trial standardized feature activations, illustrating on average relatively stronger activation in off-task trials if above zero and relatively stronger activation in on-task trials if below zero.

3.2   Catching wandering minds with tapping fingers: Neural and behavioral insights into task-unrelated cognition

Previous experiments demonstrated suitability of the FT-RSGT for investigating the interplay between mind wandering, behavior, and executive functioning at high temporal resolution. Here, the FT-RSGT was combined with concurrent fMRI and pupillometry in order to identify the neural correlates of task performance and PD as indirect markers for mind wandering as well as their relationship with direct self-reports.

First, neural recruitment during the FT-RSGT was contrasted with an alternating finger-tapping task to confirm the hypothesis that random-sequence generation requires strategic, goal-directed cognitive processes that rely on frontoparietal brain regions associated with attention and executive control, among which the dlPFC, SPL, and IPS in the right hemisphere and bilateral anterior insula and SMA (Figure 5, top left). Although the marked increase in task difficulty resulted in a significant deterioration of rhythmic stability as indexed by BV, it did not amount to significant differences in the frequency of probe-caught mind wandering. Yet, a Bayesian probit model revealed consistent increases in BV and decreases in the degree of sequence randomness as indexed by AE as Likert scale ratings indicated stronger engagement in off-task thought, although the HDI of the AE effect did not exclude zero. While neither single-trial tonic nor phasic PD significantly related to off-task reports on their own in a second Bayesian probit regression, they showed an interaction that indicated that the expected relationship between mind wandering and reduced phasic responses was dependent on relatively larger tonic PD.

As expected, the neural regions that covaried with increases in AE resembled the general pattern of the FT-RSGT but to a lesser extent, including the right posterior MFG, right IPS, and SMA, while the right dlPFC and bilateral anterior insula did not significantly covary with this aspect of task performance. Both periods of behavioral stability and alternating finger-tapping in general, but not probe-caught mind wandering, were associated with the DMN. Specifically, the left SFG, vACC, and vmPFC correlated with low BV, whereas the PCC/PCUN and left pIPL were more active during alternating finger-tapping compared to the FT-RSGT. Instead, increases in BV – which were robustly related to self-reported mind wandering – recruited bilateral dorsal attention and salience network regions, including the SPL, pIPL, MT/V5 (posterior MTG), anterior insula, MCC, lingual gyri, and cerebellum (Figure 5, top right).

Prior to self-reports of off-task contrasting to on-task attention, significant neural activity was detected in the left inferior occipital gyrus (IOG) and cerebellar regions during the easier, alternating task, and the right striatum during the FT-RSGT (Figure 5, bottom). These patterns demonstrate a strong dissociation from the correlates of behavioral performance, indicating a clear divergence between direct and indirect markers of mind wandering.
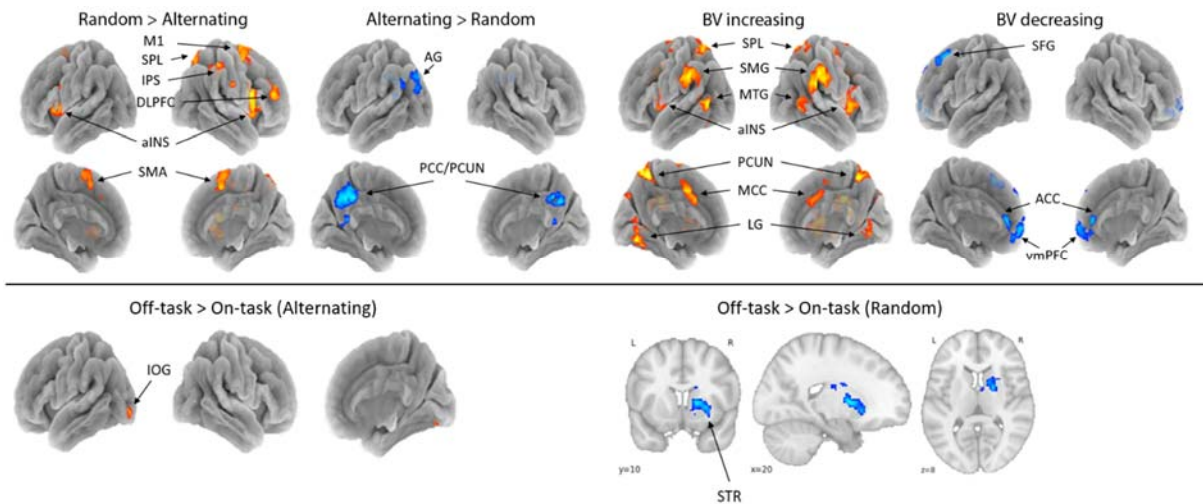
Figure 5. Neural correlates for task performance and self-reported mind wandering. Top left) Significant brain activity during the FT-RSGT when contrasted with alternating finger-tapping (red) and vice versa (blue), demonstrating recruitment of frontoparietal and default mode networks, respectively. **Top right)** Brain regions significantly correlating with increases (red) and decreases (blue) in tapping variability as indexed by BV, indicating activation in dorsal attention and default mode networks, respectively. **Bottom)** Significant clusters preceding probe-caught mind wandering compared to task-focused attention during alternating finger-tapping (red) and the FT-RSGT (blue). *Labels: M1 (primary motor cortex), SPL (superior parietal lobule), IPS (intraparietal sulcus), DLPFC (dorsolateral prefrontal cortex), aINS (anterior insula), SMA (supplementary motor area), AG (angular gyrus/posterior inferior parietal lobule; pIPL), PCC/PCUN (posterior cingulate cortex/precuneus), SMG (supramarginal gyrus/anterior inferior parietal lobule; aIPL), MTG (middle temporal gyrus/visual motion area; MT/V5), MCC (mid cingulate cortex), LG (lingual gyrus), SFG (superior frontal gyrus), ACC (anterior cingulate cortex), vmPFC (ventromedial prefrontal cortex).*

3.3 Echoes from intrinsic connectivity networks in the subcortex

The efficient integration of information from distributed brain regions is necessary for orchestrating higher-level cognition. Despite the subcortex being well-positioned to support network convergence, these dynamics are seldomly explored beyond the cortex. To investigate the largely uncharted substrates of multi-network integration in the human subcortex, we leveraged recent advances in deep brain imaging and atlasing to extend an established multivariate connectivity analysis to 14 subcortical structures. Similar to previous findings in transmodal cortex, we expected that the subcortex would exhibit a composite of dissociable neural signals from different ICNs during rest, including those implicated in spontaneous cognition.

ICNs that were most often represented, or echoed, included the data-driven counterparts of Salience B, Default A, Control A, and Visual Peripheral networks. Varying degrees of functional heterogeneity were detected, with the strongest diversification in connectivity profiles being observed in subdivisions of the thalamus, striatum, hippocampus, and claustrum (Figure 6, left). Coarse topographical maps for these structures broadly concurred with prior work. For example, ventral thalamic subregions echoed somatomotor and salience networks, while dorsomedial subregions were more strongly connected to the DMN. Within the striatum, DMN, control, and salience networks converged mostly on subregions within the caudate head and tail. The connectivity profile of the dorsomedial head of the caudate nucleus overlapped with both DMN and control network regions, whereas the nucleus accumbens echoed DMN and salience network regions. In the hippocampus, topography was more lateralized, with a left posterior area demonstrating a functional connection with the DMN and a right posterior area with the DAN and visual cortex (Figure 6, right).

While the globus pallidus externa, subsantia nigra, and ventral tegmental area each echoed more than one ICN – although the signals were localized to only one subregion – the amygdala and pedunculopontine nucleus demonstrated singular network affiliations (i.e., Default A and Salience B, respectively) and were thus less compatible with integrative capabilities. The remaining structures, including the LC, subthalamic nucleus, globus pallidus interna, red nucleus, and periaqueductal grey, did not show evidence of cortical network echoes. Based on these findings, we can speculate that while the aforementioned subcortical structures are more equipped to converge and propagate transmodal information, others are more embedded in local circuitry and likely support segregated functional processing.

In summary, features indicative of multi-network convergence were most prominent in centrally located subcortical structures contiguous to the cortex, suggesting that these are more likely to participate in large-scale functional integration compared to remote, deep brain structures. Together, these findings underscore the rich functional architecture of the subcortex and potentially provide a mechanism through which subcortical structures engage in dynamic cognitive processes during rest.
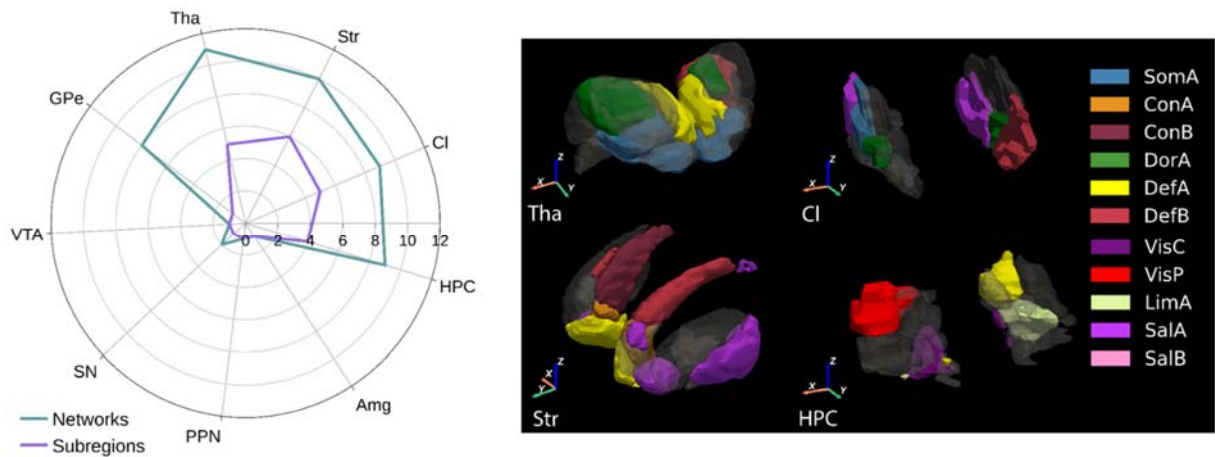
Figure 6. Intrinsic cortical network echoes in the subcortex. Left) The number of subregions (purple) that exhibited at least one network echo and the total number of networks (green) that were represented among the subregions in subcortical ROIs, counting only above-threshold spatial correlations ($r \geq .16$). **Right)** The topographical pattern of network echoes for the thalamus, striatum, claustrum, and hippocampus, color coded according to the strongest echo at subregional level or made translucent if the maximum spatial correlation did not exceed threshold. *Labels: thalamus (Tha), striatum (Str), claustrum (Cl), hippocampus (HPC), amygdala (Amg), pedunculopontine nucleus (PPN), substantia nigra (SN), ventral tegmental area (VTA), globus pallidus externa (GPe), Somatomotor A (SomA), Control A/B (ConA/B), Dorsal Attention A (DorA), Default A/B (DefA/B), Visual Central (VisC), Visual Peripheral (VisPer), Limbic A (LimA), Salience A/B (SalA/B).*

Chapter 4

General Discussion

In this final chapter, I aim to bring together the various findings from each study and synthesize new mechanistic insights into the neurobiological underpinnings of mind wandering. Particular emphasis is placed on exploring the interplay between the diverse neural and behavioral features that characterize this complex phenomenon. Moreover, the methodological strengths of the studies and the limitations of my findings are reviewed along with relevant implications for future research.

4.1 From neural and behavioral correlates to underlying mechanisms

This thesis aimed to achieve a more profound understanding of the neural mechanisms of mind wandering, a dynamic and multifaceted construct that dominates a substantial part of our mental experience. The underlying neurobiology of this fleeting phenomenon continues to be a compelling question for neuroscientists, and its solution has undoubtedly been hindered by methodological limitations regarding the reliable detection of cognitive states when attention is directed inward. Three empirical studies were conducted that elucidated the diverse aspects of self-generated, 'off-task' trains of thought, focusing on its neurophysiological signatures, interactions with behavior and executive functions, and the intrinsic functional synergy between the cortex and subcortex. The overarching key findings are elaborated upon in the following paragraphs.

4.1.1 Mind wandering signatures across task contexts

In Paper I, we combined multiple sources of information by means of simultaneous fMRI-EEG and pupillometry that together produced a comprehensive description of the spatiotemporal signature of mind wandering during the SART. We found that mind wandering as opposed to task-focused attention was associated with poor task performance, relatively increased tonic PD, greater oscillatory power in predominantly alpha and delta frequencies, reduced event-related cortical components at later latencies, stronger activity within frontal and salience regions (i.e., dlPFC, SMA, insula) and increased dynamic FC between these regions and the DMN-core (i.e., PCC, mPFC, pIPL). Collectively, this signature describes mind wandering as a state that involves the attenuation of task-relevant information processing in favor of mental explorations, possibly guided by top-down control. In contrast, in Paper II, while the difference in executive task demand on a rhythmic finger-tapping task strongly differentiated between regional recruitment of the DMN-core versus frontoparietal and salience networks, mind wandering reports were not preceded by similar cortical patterns of brain activity. Instead, mind wandering was associated with decrements in both rhythmic and executive task performance, reduced phasic PD when tonic PD was relatively high, and recruitment of cerebellar, visual, and subcortical regions depending on task demand.

Together, these findings are in stark contrast with several prior studies describing clear patterns of DMN activity preceding probe-caught mind wandering (e.g., Christoff et al 2009; Mittner et al 2014). The inevitable question arises as to how it is possible that a similarly operationalized construct that produces comparable decrements in task performance across studies yields such inconsistent neural correlates. Given that the literature reveals interacting relationships between mind wandering and task contexts, one explanation could be that different types of internal experiences and their neural correlates are dependent on task-specific factors. For example, experimental manipulations were shown to influence the temporal orientation of mind wandering (Liefgreen et al 2020) and the extent to which it

was independent from task-stimuli (Maillet et al 2017). In turn, the emotional valence of task-unrelated thoughts differentially effected task performance (Banks et al 2016). Thinking along these lines, it seems plausible that the marked difference between the cognitive processes required for performing the SART and FT-RSGT – the former involving visual target detection and response inhibition and the latter requiring sensorimotor coordination while evaluating and planning complex response sequences – partially resolves the observed disparity. Speculatively, the SART may have permitted the adaptive redistribution of executive and attentional resources for guiding cognition toward exploring goals alternative to the task, whereas the higher cognitive load and faster pace of the FT-RSGT may have prevented prolonged deprioritization of task-relevant information processing, merely allowing transient 'breaks' from self-monitoring sequence-generation performance. As a consequence of such contextual demands, mind wandering during the SART could have been dominated by thought that is more deliberate, for example by preparing scenarios that help anticipate the future (Stawarczyk et al 2011a). Instead, departures from task-focused states during the FT-RSGT could have been mainly reflected in the reduced suppression of external distractions and task-related interferences, such as perceiving the metronome sound. This would explain why self-reported mind wandering was associated with striatal and cerebellar activation, both regions that have been implicated in beat perception (Merchant et al 2015; Paquette et al 2017), and why increases in tapping variability throughout the task were correlated with regions associated with external attention and salience detection (i.e., SPL, MT/V5, anterior insula, MCC). If external processing was indeed temporarily enhanced, we would expect concurrent increases in the modeled pupillary responses to task events prior to mind wandering reports. There was indeed some evidence for this relationship, but it was dependent on periods of generally reduced tonic PD. Instead, when pupil measures indicated relatively higher tonic gain, we observed the reversed pattern consistent with perceptual decoupling. Although preliminary, disentangling these interactions may thus allow the critical separation between active mind wandering and external distraction on a scale that is more temporally refined than what can be achieved with experience sampling.

A primary outcome in mind wandering research frequently concerns experience sampling data, and robust relationships between mind wandering and behavioral outcomes were replicated in Paper I and II. Mind wandering as captured by experience sampling thus seems to converge well at the behavioral but not the neural level, and contrasting brain activity directly preceding thought probes has led to neural patterns that diverge from those correlating with behavioral performance (e.g., Paper II; Kucyi et al 2016). These effects are not likely attributed to sampling frequency, as thought probes were presented at a rate similar to prior research, for example 44-60 s (Kucyi et al 2016), ~60 s (Christoff et al 2009), and 40-80 s (Boayue et al 2020a), compared to 21-63 s (Paper I) and 55-65 s (Paper II). Similarly, we observed levels of mind wandering comparable to other work using various paradigms (e.g., 42%, Paper I; 36%, Paper II; 43%, Christoff et al 2009; 30.2%, Boayue et al 2020a; 37%, Boayue et al 2020b; 35%, Dhindsa et al 2019; 12-60%, Seli et al 2018b). Given that mind wandering propensity does not seem

significantly different across studies, an intriguing conclusion would be that the aforementioned contextual factors do not necessarily alter the amount of time engaged in self-generated thought or its impact on task performance, but rather its phenomenological and dynamic aspects, such as the depth of the experience or extent to which fleeting thoughts develop into a cohesive stream. For example, they might influence the proportion of off-focus cognition versus deep mind wandering, which are theoretically reflected different neural correlates (Mittner et al 2016; Csifcsák & Mittner 2017). Additionally, there is evidence that thought probe responses are generated from underlying states that are gradual and varied rather than distinctly off-task or on-task (Zanesco et al 2020b). Perhaps, these dimensions of variance constitute the reason why correlates of probe-caught mind wandering fail to focalize into replicable neural patterns.

In summary, the results in this thesis strongly support mind wandering as a heterogeneous construct that – while debilitating behavior in relatively uniform ways – corresponds to neural correlates that are influenced by external factors. Alternatively, some of the discrepancies could be rooted in attempts to directly contrast functional processes based on the assumption that mind wandering and on-task attention are mutually exclusive, while in reality they might exhibit partially overlapping neural signatures. For example, in paradigms where performance relies less on continuous processing of perceptual input and more on internal monitoring and planning (e.g., the FT-RSGT), the neural representations of task-related cognition could display similar spatiotemporal properties as those transpiring during self-generated thoughts that are not related or helpful to the task. As a consequence, contrast analyses do not produce a strongly differentiating neural pattern (Paper II). Moreover, the positive contrast for brain regions involved in executive control could be a direct consequence of a cognitive task with a weak reliance on those regions (e.g., the SART). Hence, comparative neurobiological descriptions of mind wandering across paradigms should be balanced against potential task-dependent effects of both phenomenological and methodological origin.

4.1.2 The intricate relationship with the default mode network

The precise role of the DMN in mind wandering remains elusive, with studies reporting diverging, if not contradictory, findings regarding the patterns of DMN activity and connectivity during periods associated with spontaneous, task-unrelated cognition. In neither of the task-based fMRI studies in this thesis was the DMN directly associated with periods of mind wandering. Instead, part of the DMN-core was significantly more active during periods of simple, alternating finger-tapping compared to a more demanding task with response randomization (i.e., PCC and left pIPL). While the alternating task can be performed without explicit evaluation of past and upcoming responses in the longer sequence, random sequence generation requires ongoing monitoring of the immediate tapping history in order to achieve the most optimal entropy with the next choice. Markedly, this difference in more automated

versus deliberate behavior strongly dissociated DMN-core and frontoparietal/salience network recruitment, which is consistent with earlier work that inferred a relationship between mind wandering and the DMN by comparing easy and difficult task conditions (e.g., Mason et al 2007). Two other regions associated with the DMN (i.e., mPFC and left SFG) were correlated with periods of stabilized finger-tapping that were robustly introspected as attending to the external task. Interestingly, activity in these four DMN nodes was also relatively increased in Paper I during SART trials that were classified as on-task attention. Very similar to the monotonous alternating finger-tapping task, the low target frequency of the SART meant that optimal performance predominantly consisted of repetitive motor responses at stable intervals.

Together with previous observations, these findings suggest that the DMN is recruited under circumstances of automated, effortless behavior (Esterman et al 2013; Shamloo & Helie 2016; Kucyi et al 2017). Specifically, the DMN may govern cognitive states that involve a weaker engagement of goal-directed processing and top-down control, such as during repetitive button pressing in a predictable environment. Since perseverative, entrained motor responses produce little ongoing decrements in performance on rhythmic tasks such as the SART and FT-RSGT, these periods may be less likely introspected as mind wandering, resulting in the link between DMN recruitment and on-task attention as observed in Paper I. When the demands on deliberate processing increase, behavior is no longer effortless and the DMN deactivates, as was observed in Paper II during a more difficult, random finger-tapping task. Besides its tentative role in behavioral automatization, a provoking speculation would be that the DMN is analogously involved in 'cognitive' automatization – i.e., undirected thought without conscious effort. For example, Christoff et al (2016) hypothesized that the DMN-core emerges when automatic constraints on the flow of thought are strong while deliberate constraints are weak. Highly automatically constraint thoughts, mostly driven by salient features, are presumed stable or even 'stuck' in the same routine. Following this idea, transitions from trains of thought that are more rigid to those more free-flowing could then be reflected in transient increases in response variability and deactivation of the DMN-core, as found in Paper II.

Earlier work argues for a role of the DMN in self-referential and prospective thinking, and more recent studies demonstrate its involvement in conscious experiences that are highly detailed and immersive (e.g., Sormaz et al 2018; Turnbull et al 2019a). Accordingly, the DMN could have reflected, at least partially, a preoccupation with active mind wandering, assuming that task demands were sufficient low to allow ample available resources to mind wander while preserving rudimentary elements of behavioral performance. However, this account crucially fails to explain why such deeply engaging experiences were not reflected in the responses to regular experience sampling in either Paper I and II. Perhaps a more plausible alternative is the DMN's presumed involvement in conscious monitoring and unspecific information gathering when external demands are low (i.e., the 'sentinel hypothesis', Raichle 2001), *without* necessarily reflecting an absorption with self-generated experiences. In theory, this could

align with the proposed idea that the DMN-core manifests when there is a high degree of converging network activity to support a transient broadening of attentional focus (Mittner et al 2016). The assumed low incentive of the SART and periods of alternating finger-tapping could have elicited this 'off-focus' cognitive mode in order to adaptively drive a global state of unfocused exploration. Given that attentional states in off-focus mode are hypothetically subconscious and thus inaccessible to introspection, it would explain why its pattern of neural recruitment is mostly independent from self-report and why blocks of easier, alternating finger-tapping in Paper II did not elicit significantly more mind wandering reports. Furthermore, Mittner et al (2016) propose that off-focus states relatively preserve behavioral performance as attention is not completely decoupled from the external environment compared to active mind wandering, permitting the observed correlation between ventromedial DMN recruitment (i.e., vmPFC, vACC) and stabilized, rhythmic finger-tapping.

Although the off-focus account resolves the correlation between adequate task performance and the DMN, it does not explain why increases in tapping variability correlate with DAN and SN regions, including the SPL, IPL, MT/V5, MCC, PCUN, anterior insula, lingual gyrus, and cerebellum. These regions far extend the somatomotor cortex, which has been interpreted as evidence that response variability sensitively monitors moment-to-moment fluctuations in the underlying attentional state rather than motor performance (Kucyi et al 2017). For example, the DAN/SN have been implicated in the self-regulation and perceived attentional control over self-generated thought, both during rest and cognitive performance (Van Calster et al 2017; Turnbull et al 2019a). However, these correlates strongly diverge from the observed neural recruitment preceding probe-caught mind wandering. This could indicate that changes in response variability represent attentional fluctuations that are not invariably caught by experience sampling, possibly because they are too short-lived to be reflected in the probe responses. It is conceivable that metronome-cued finger-tapping tasks require individuals to flexibly switch between internal and external modes of attention in order to achieve sensorimotor synchronization of responses to the metronome cue. Consequently, the timing of tapping responses may subtly track the diverting focus from self-monitoring one's rhythmic performance to orienting toward salient features of the external environment – e.g., to correct for response deviations or focus on external distractions – to ultimately more severe disengagements such as mind wandering. Such transient attentional variations are problematic to diagnose with experience sampling, not only because they rely on unbiased introspection but also because thought probes are interspersed at a temporal resolution that is incompatible with such moment-to-moment changes.

Finally, recent work advocates a role for the DMN at the top of the brain's functional hierarchy (e.g., Margulies et al 2016). The DMN-core has a heterogeneous organization that contains a mixture of dissociable signals from distributed cortical networks (Leech et al 2012; Braga et al 2013), a finding that we replicated in Paper III and that likely reflects its role in integrating transmodal information for regulating switches in attentional focus. Furthermore, we observed that intrinsic fluctuations within

DMN regions were abundantly repeated, or echoed, in various subcortical structures, underscoring its extensive interconnectedness with other cortical as well as subcortical areas. Together with observations that DMN functioning may support aspects of task-relevant processing (Sormaz et al 2018), these findings further weaken a homogeneous functional characterization of the DMN and its specificity as a diagnostic for mind wandering. Perhaps, the DMN has been previously conflated with mind wandering due its diverse involvement in information gathering and integration, off-focus cognition, automatic constraints on thought flow, and automatization of behavior. The results in this thesis suggest that mind wandering transpires largely independent from the DMN, but the DMN's domain-general operations may allow interactions with mind wandering that are contingent on situational factors. As Csifcsák and Mittner (2017) proposed, a 'many-to-many' scheme that takes into account the non-unitary nature of both the DMN and mind wandering is therefore likely necessary to accurately map their equally multifaceted relationship.

4.1.3 Dynamic functional connectivity sensitively tracks changes in attention

Catching internal trains of thought with minimal external manifestations poses a significant methodological challenge. Such detection, however, is crucial to address the current knowledge gap on the neurobiological mechanisms of mind wandering. While experience sampling is the most commonly used technique to probe individuals' inner conscious experience, it is subject to several confounds. In addition to the necessity to interrupt the task and the uncertainty of introspection, thought probing itself can introduce framing and satisficing effects (Weinstein 2018). One approach that minimizes the need for experience sampling is supervised machine learning, which can extrapolate self-reported states to uninterrupted data such that the analysis is no longer restricted to the periods directly preceding thought probes. In Paper I, we employed an SVM-RBF to investigate the unique contributions of different neurophysiological measures for detecting mind wandering among periods of sustained external attention based on periodical thought probing. The results indicated that while each neurophysiological modality contributed to optimizing classification performance, the most determining information was derived from changes in dynamic FC among nodes of the DMN and its ACN.

Considering mind wandering as a collection of transient experiences that evolve from one thought to another, it is not surprising that relatively rapid alterations in interregional synchronization of brain activity serve as a suitable neural marker (Kucyi & Davis 2014; Kucyi 2018). Specifically, probe-caught mind wandering in Paper I was represented by relatively strengthened dynamic FC between the DMN-core, particularly the PCC, and other cortical regions in the DMN and the ACN. Although some within-DMN connections were also strengthened, mind wandering was overall associated with stronger coupling between the networks. In other words, while activity in the PCC was anticorrelated with these regions over the course of minutes, recurring periods of synchronized activity (i.e., in the order of

seconds) were indicative of mind wandering throughout the task. This heterogeneous pattern is consistent with the hypothesis that the PCC integrates transmodal information to regulate changes in attentional focus. The results of Paper III corroborate this by demonstrating separate functional subdivisions within the PCC that selectively connect with different functional networks, which may indicate a mechanism through which it expresses its prominent functional property as a network hub (Leech et al 2012; Braga et al 2013). Remarkably, comparable characteristics were discovered within several subcortical structures in Paper III, which aligns with proposed functions for the subcortex in network convergence and cross-network information integration (Bell & Shine 2015, 2016) and raises the exciting possibility that these structures contribute to the spontaneous functional architecture that gives rise to mind wandering. Especially the thalamus, striatum, claustrum, and hippocampus exhibited multiple, dissociable signals from functional networks within a specialized, subregional topography, potentially highlighting their role as subcortical analogues to integrative hubs in the cortex such as the PCC and mPFC.

The dynamic FC pattern of the PCC in concert with other cortical, and possibly subcortical, structures holds promise for monitoring transitory episodes of internal and external attention without the need for task interruptions with experience sampling. This also emphasizes the limitations of studying individual systems in isolation (e.g., average activity in the DMN) in relation to mind wandering. While quantifying connectivity patterns in terms of time-varying FC or multivariate echoes may yield sensitive neural markers of mind wandering, contemporary research has yet to determine the precise configurations that pertain to qualitatively distinct internal states. For example, prior studies have reported divergent functional profiles in both cortical and subcortical regions, revealing discrepancies among the preferential network connections at the subregional level (Paper III; Leech et al 2011; Leech et al 2012; Choi et al 2012; Seitzman et al 2020). Such variance may relate to individual differences in the functional connectome or dynamic reorganizations representing ongoing spontaneous cognitive processes or changes in external demand (e.g., Leech et al 2013; Chou et al 2017; Tian et al 2020; Gonzales-Castillo et al 2021). Sources of variability that are challenging to control experimentally contribute to the difficulty to reproduce findings across studies and identify the specific patterns that are consistently attributed to various facets of mind wandering.

4.1.4 Mind wandering and executive functioning

An ongoing discussion within the field of mind wandering concerns its interaction with executive functions. Two opposing hypotheses have been proposed: the executive failure hypothesis states that mind wandering arises as a result of failures in the executive system to maintain attention directed to the external task, whereas the executive control hypothesis states that mind wandering operates cooperatively with the same system to synthesize and sustain self-generated trains of thought (McVay

& Kane 2009; Smallwood & Andrews-Hanna 2013; Smallwood 2013). Although both hypotheses predict that periods of mind wandering negatively impact external task performance, previous observations of perceptual decoupling and context-regulation have been regarded as evidence in favor of executive involvement in mind wandering.

In the first fMRI study with probe-caught mind wandering, Christoff et al (2009) observed parallel recruitment of DMN and ECN nodes preceding mind wandering reports, which was speculated to reflect the engagement of executive control processes in mind wandering. In Paper I, we found additional evidence that these two systems flexibly cooperate to support episodes of mind wandering, which was expressed in increased dynamic FC between the DMN-core and ACN nodes among which the dlPFC, insula, and SMA. Simultaneously, we observed reduced amplitudes of midline frontal and parietal EEG components, indicating attenuated cortical responses to external stimuli. Although more superficial sensory processing was relatively unaffected (i.e., N1, P1, evoked pupillary dilation), reductions that reflected impairments at later, cognitive stages of processing (i.e., P300 and frontal) are consistent with prior work (Handy & Kam 2015; Kam et al 2022) and may reflect the deprioritization of task-related cognitive processes when individuals are occupied with mind wandering. Together with relatively increased recruitment of frontal and salience regions, these results are consistent with the involvement of top-down regulation and insulation of task-unrelated thoughts, perhaps because they are regarded as more salient or rewarding relative to pursuing the primary task.

Such top-down control, particularly from the dlPFC, may entail specific contextual modulation of mind wandering, for example depending on task difficulty (Turnbull et al 2019b). Interestingly, we found in Paper II that the right dlPFC and anterior insula were recruited together with the IPS and SMA during the FT-RSGT compared to a non-demanding alternating finger-tapping task, but did not significantly covary with the performance index of executive resource use (i.e., sequence randomness as quantified with AE), nor was their recruitment apparent prior to self-reports of mind wandering. This could indicate that while the IPS and SMA are more important for self-determined complex motor action, the right dlPFC and insula were activated in a manner that was not strictly dependent on either optimizing sequence randomness or mind wandering. Correspondingly, the RFE procedure in Paper I revealed that average activity in the right dlPFC and insula were not perceived by the classifier as predictive for mind wandering among periods of task-focused attention on the SART. Together, these results imply that the right dlPFC and insula – like the PCC – surpass functionally specific roles in governing either internal or external foci of attention during cognitive performance, but rather act in a more a general fashion, i.e., by evaluating task utility and tuning mind wandering in line with environmental demands. Given that mind wandering was present at comparable levels across the different tasks (i.e., SART, FT-RSGT, alternating finger-tapping), it could be speculated that such adaptive tuning pertains to thought dimensions other than frequency, for example the degree of self-relevance or coherence of the train of thought. Alternatively, the amount of time spend mind wandering

during a task is significantly altered depending on contextual demands but was not adequately captured by the periodical experience sampling in Paper I or II.

Flexible context-dependent regulation has been argued to feature an aspect of higher-level, controlled cognition. Nonetheless, engagement of an executive system that decides when it is more appropriate (or less detrimental) to mind wander does not necessarily imply that mind wandering itself involves goal-directed processes. Conclusive remarks on this relationship may rely on our ability to experimentally manipulate extent of available executive resources and assess its effect on mind wandering. That is, if the executive failure hypothesis were true, increasing the amount of resources would lead to improved task performance and reduced mind wandering. Several studies have attempted to investigate this premise by means of transcranial direct current stimulation (tDCS), but have produced contradictory results on mind wandering propensity (Axelrod et al 2015; Filmer et al 2019; Boayue et al 2020a, 2020b). For example, Boayue et al (2020a) observed slightly reduced mind wandering during the FT-RSGT with anodal tDCS over the left dlPFC. However, as executive functioning (i.e., AE) was not modulated by tDCS, the difference in mind wandering could not be confidently related to changes in available executive resources. An important point to consider is that if mind wandering is indeed adaptively regulated according to contextual factors signaled by the dlPFC, we would not expect a one-sided change in mind wandering upon dlPFC stimulation but rather more effective tuning based on external demands or perceived task utility. The evidence presented here suggests that the dlPFC is not unambiguously associated with sustaining either mind wandering or task-related attention, but stimulation of the (right) dlPFC might be fruitful for calibrating episodes of mind wandering depending on situational factors.

4.1.5 Gain modulation and subcortical mechanisms

An unambiguous outcome of Paper I is that episodes of mind wandering among task-focused attention are best described by dynamic changes in the coordinated activity of large-scale functional networks. Previous studies have produced inconsistent results regarding the exact patterns of connectivity and it remains unclear how naturally anticorrelated networks are driven into a cooperative architecture to enable self-generated trains of thought. One prominent candidate system for orchestrating dynamic reconfigurations that facilitate mind wandering during external cognitive demand is LC/NE-dependent neuromodulation of cortical gain (Aston-Jones & Cohen 2005; Mittner et al 2016).

In Paper I, we observed on average weaker coherence *within* and stronger *between* the DMN and its ACN during mind wandering compared to task-focused attention. Concurrent pupillometric measures indicated relatively larger tonic PD, indexing globally elevated levels of NE. This finding contradicts the simulated influences of temporally uncoupled increases in neural gain, which showed enhanced binary function that resulted in the strengthening of strong connections while weakening weak

connections (Eldar et al 2013). In rather opposing perspectives, it was argued that such heightened clustering in FC patterns support more narrowly focused attention (Eldar et al 2013), versus expanding the scope of attention in order to promote the exploration of competing internal representations (Mittner et al 2016). Although Mittner et al (2014) indeed found increased dynamic coupling among nodes within the DMN and ACN in relation to mind wandering, this observation was not simultaneously associated with increases in neural gain. Together with the findings in Paper I, this may suggest that diffuse, unselective increases in tonic NE foster recurrent amplification in integrative processing among distributed regions. This aligns with theory regarding the non-specific effects of tonic gain on neural responsiveness (Aston-Jones & Cohen 2005; O'Callaghan et al 2021) and recent empirical findings of greater functional integration (i.e., weaker clustering) with increases in neural gain (Shine et al 2018).

If this representation is accurate, previous reports of stronger intra-network DMN connectivity preceding self-reported mind wandering (Kucyi & Davis 2014; Mittner et al 2014) and during periods of poor behavioral performance (Kucyi et al 2017a) may indicate the presence of task-disengagement that is not driven by the LC/NE tonic mode. In recent theoretical work, it was postulated that various levels of tonic NE govern qualitatively distinct attentional states (Mittner et al 2016). While the off-focus state depends on high tonic NE, both active mind wandering and task-focused attention rely on the phasic LC/NE mode to induce an optimal cortical gain milieu for facilitating the exploitation of ongoing goals, whether directed internally or toward the primary task. Consequently, the degree to which gain increases are temporally selective to task events is thought to maximally discriminate these two states at intermediate levels of tonic NE. In Paper II, the Bayesian model revealed that the relationship between phasic PD and probe-caught mind wandering was dependent on tonic PD, which could indicate evidence for dissociable states based on the underlying LC-modulated gain mode. Specifically, phasic dilatory responses to task events indicated enhanced external processing for task-focused attention and perceptual decoupling for mind wandering only during relatively large tonic pupil size. This relationship reversed when tonic pupil size was reduced, potentially indicating a separate mechanism of task-disengagement that was instead characterized by the amplification of external information processing. Together with previous work, the findings in this thesis suggests that LC/NE dynamics are involved in facilitating the global architectures that may relate to functionally heterogeneous attentional states.

However, pupillary dynamics are not likely an exclusive indicator for LC/NE activity but may relate to diverse neuromodulatory influences (Reimer et al 2016; De Gee et al 2017; Larsen & Waters 2018; Van Slooten et al 2018). In a recent paper, O'Callaghan et al (2021) proposed that specific concentrations of multiple neuromodulators are ultimately responsible for shaping the neural architecture that is conducive to mind wandering. They hypothesized that mind wandering occurs through distributed information processing during moderate arousal driven by heightened NE and low levels of acetylcholine and serotonin. Empirical evidence has linked cholinergic and dopaminergic

systems to spontaneous changes in the global brain signal (Turchi et al 2018) and exploration-exploitation tradeoffs (Cohen et al 2007; Frank et al 2009; Chakroun et al 2020). Intriguingly, we found in Paper II that periods of enlarged tonic PD correlated with increases in blood supply to a large brainstem and midbrain voxel-cluster that likely covered the LC as well as other neuromodulatory nuclei, including the ventral tegmental area (VTA), substantia nigra (SN), pedunculopontine nuclei (PPN), and raphe nuclei. Thus, the pupillary findings as described here may reflect an amalgamation of interacting neuromodulatory systems, rather than the isolated effects of NE on mind wandering. One proposed mechanism through which neuromodulatory tone elicits the onset of a mind wandering episode is a spontaneous signature of the HPC called the sharp-wave ripple that propagates to other functional systems such as the DMN (O'Callaghan et al 2021). Although we failed to demonstrate direct evidence for hippocampal activations preceding mind wandering reports, we showed that the right HPC significantly covaried with increases in tonic PD (Paper II), intrinsic activity in the bilateral HPC was moderately correlated with neuromodulatory nuclei (LC, SN, VTA, PPN; r=.47–.57), and functional subdivisions within the HPC echoed spontaneous signals from default, salience, and visual networks (Paper III). In conjunction with previous work, a tempting speculation based on these findings is that the HPC couples with various functional networks under the influence of neuromodulatory interactions to trigger the generation of spontaneous thought processes.

Besides the HPC, multiple well-described ICNs were represented in the thalamus and striatum, further substantiating their role as subcortical zones for network convergence and information integration. Consistent with prior work, both these structures displayed subregional connectivity profiles that overlapped with data-driven default, attention, salience, and control networks. The dorsomedial thalamus in particular has been strongly implicated in the DMN and self-generated thought (Alves et al 2019; Harrison et al 2022), and correspondingly showed evidence for signal echoes from the DMN in Paper III. Additionally, in agreement with the proposal of 'cognitive integration zone' (Greene et al 2020), functional topography of the striatum – particularly the caudate head and tail – was organized to support the convergence of default, control, and salience networks. Importantly, the right striatum was significantly activated preceding probe-caught mind wandering during the FT-RSGT in Paper II. One careful interpretation of these findings might be that the thalamus and striatum play a role in dynamic thought processes such as mind wandering, possibly through mediating the balance between thought continuity and state switching during high cognitive demand (e.g., Tang et al 2012; Christoff et al 2016; Chou et al 2017).

4.2   Methodological considerations

By capitalizing on established methodological frameworks combined with novel applications for multimodal data and the subcortex, the work in this thesis collectively entails a multidisciplinary approach to investigate the neural mechanisms of mind wandering. Whereas Paper I and II exploited more temporally resolved methods by means of single-trial state classification and trial-by-trial performance monitoring, respectively, Paper III took advantage of the fine-grained spatial resolution of ultra-high field fMRI. Notwithstanding, each study also presents several limitations. In Paper I, the fMRI analysis was restricted to a set of predefined anatomical ROIs within the DMN and ACN, preventing assessment of the functional contributions from regions beyond these networks, including the subcortex. The whole-brain analyses in Paper II revealed substantial neural activity outside the boundaries of the DMN and ACN that related to task performance and probe-caught mind wandering, among which the cerebellum, lingual gyrus, occipital cortex, and striatum, emphasizing the utility of whole-brain versus ROI-based analysis. Conversely, omitting assessment of dynamic FC and its relationship with behavior and self-reported experience is an eminent limitation of Paper II, especially given the results of Paper I. Finally, a disadvantage of Paper III concerns the absence of explicit online or retrospective measures for mind wandering that could be correlated with intrinsic neural architecture during resting-state. Consequently, no inferences on the functional significance of subcortical echoes for the spontaneous generation of mental content can be drawn.

Generally, fMRI data are confounded with numerous sources of noise and variability that can bias the results, including artifactual signals, individual variation in the BOLD response, and magnetic field distortions. For example, the temporal lobe includes important lateral and medial structures implicated in mind wandering, yet is prone to fMRI signal dropouts that may obscure its functioning. Indeed, we observed the lowest temporal SNR (tSNR) values in the anterior temporal cortex, resulting in an underrepresentation of temporal lobe networks in the analysis in Paper III. Similarly, the evidence for functional heterogeneity of the thalamus, striatum, claustrum, and hippocampus may have been confounded by their relatively large size and high tSNR compared to the other subcortical ROIs. In addition, regardless of structure size or position, the number of ICA components was fixed at 10. Given that the results were not validated against alternative model orders, the possibility of underfitting (i.e., not accounting for true independent signals) or overfitting (i.e., splitting true signal) in individual subcortical structures can not be fully excluded.

There are several obstacles more specific to mind wandering research, including its covert manifestation that creates challenges for reliable detection and the fact that spontaneous forms of cognition can not be consistently induced or prevented under experimental control. Contemporary research still relies mostly on subjective reports to derive underlying mental states such as mind wandering. Thought probes as implemented in Paper I and II inherently set constraints on the type of

experiences being reported. That is, by collapsing all thoughts in categories of 'on-task' and 'off-task', potential heterogeneity in task-unrelated states was reduced into a single quantification. Consequently, we could not discriminate thoughts that emerged involuntarily versus deliberately, were more coherent versus elusive, or were oriented to the past or future. Blending together these diverse aspects of mind wandering as if it were a uniform construct has likely contributed to mischaracterizations of its relationships with both behavior and the DMN and may explain some of the controversies in the field. Triangulation strategies that combine subjective and objective features are necessary to validate mind wandering derived from self-report.

The reported inconsistencies may be partially attributed to different dichotomization methods of ordinal probe responses (e.g., Christoff et al 2009; Mittner et al 2014). In Paper II, we attempted to negate response biases arising from individual differences in introspective ability and willingness based on the idea that the per-subject maximum would always reflect mind wandering while the per-subject minimum would always reflect task-focused attention. Through implementation of this customized algorithm, significant clusters of brain activity preceding mind wandering reports were observed that were otherwise absent using a standard, split-the-middle approach, revealing a vulnerability of probe categorization for neural analysis. Furthermore, it is not inconceivable that varying degrees of executive resource use may influence individuals' introspective abilities. For example, during moments of low meta-awareness or 'mind blanking', individuals may resort to evaluating their own performance when probed with a question about their internal state. Since we did not measure confidence ratings or self-caught mind wandering, we can not account for potential inconsistencies arising from varying degrees of meta-awareness.

Some of these limitations may be addressed with multidimensional experience sampling – i.e., probing for subtypes of self-generated thought with a series of questions that assess different temporal and phenomenological facets of the mental experience (e.g., Sormaz et al 2018; Wang et al 2018; Turnbull et al 2019a). Yet, even the most all-encompassing multidimensional thought probes are unable to describe how changes in attentional focus and thought content evolve moment-to-moment. As argued by Smallwood (2013), the factors that drive the initiation of a mind wandering episode (i.e., its *occurrence)* can therefore not be distinguished from those that are involved in its continuation (i.e., its *process)*. For example, a task-unrelated thought may arise involuntarily but develop into a coherent stream of thought that is more intentionally pursued once consciously detected. Instead, the evolution of a mind wandering episode and its shift to or from other internal and external states may be more accurately modeled with unsupervised learning algorithms. For example, Hidden Markov Models (HMM) estimate 'hidden' latent states and their transition probabilities from the temporal dynamics of the data (e.g., Bastian & Sackur 2013; Karapanagiotidis et al 2020; Zanesco 2020b). An exciting prospect is the combination of such models that capitalize on temporal dynamics in the data with fast-paced paradigms such as the FT-RSGT in order to more precisely estimate the onset and offsets of a

mind wandering episode. Theoretical and empirical work indicates that perpetuating self-generated cognition recruits various neural components in a sequential manner in order to support the dynamic aspects of the train of thought (Christoff et al 2016; Ellamil et al 2016). Indeed, organized patterns of functional activity are not invariant but have been shown to reconfigure over time and with changes in external demand (Leech et al 2012; Braga et al 2013; Schaefer et al 2014; Tian et al 2020; Gonzales-Castillo et al 2021). Therefore, capturing these fluctuations with time-varying methods likely provides more adequate neural representations of the cognitive mechanisms during mind wandering. While we included dynamic FC features in Paper I, the ICA-DR analysis in Paper III did not allow separation of stable configurations that may reflect correlates at trait-level from those dynamically transitioning – e.g., between segregated or integrated modes of processing – that may more accurately describe transient latent states.

Finally, it should be noted that the potential impact of interindividual variability in mind wandering propensity and interacting constructs such as working memory capacity and executive functioning was not accounted for in this thesis. Mittner et al (2014) reported high variance in Bayesian posterior distributions of a cognitive process model of the Stop-Signal task with experience sampling, indicating that the impact of mind wandering on behavioral outcomes varied across individuals. Similarly, pronounced individual differences in classification accuracy of mind wandering based on EEG (Jin et al 2019) and variations in the functional connectome using fMRI (e.g., Sylvester et al 2020; Greene et al 2020; Marek et al 2021) may have distorted our interpretation of the neural features of mind wandering phenomena at group level. An interesting future endeavor could thus be to map the facets of mind wandering that share variance at the population level versus those that vary within individuals, for example with precision functional mapping (Greene et al 2020; Marek et al 2021).

4.3   Implications

The omnipresence of mind wandering accentuates an integral, natural ability to generate multifarious cognitive content without perceptual input or guidance. Identification of the neurobiological mechanisms that control when mind wandering takes over our mental experience could reveal crucial insights into how and why our central nervous system is organized to make tradeoffs between internally driven cognition and meeting the demands of an external task. Mind wandering is thought to serve important adaptive functions, such as preparing for future events by simulating hypothetical scenarios and exploring creative solutions to solve problems (Smallwood & Schooler 2015; Shepard 2019). Simultaneously, mind wandering perseveres in situations when sustaining external attention is necessary to avoid errors with potential catastrophic consequences and cultivates in ways that can negatively impact psychological well-being (Smallwood et al 2007; Killingsworth & Gilbert 2010).

Both aspects of thought content and temporal flow have been related to psychological cost, such as profuse amounts of retrospective thinking (Smallwood & Schooler 2006). As such, identification of the neurobiological markers of undesirable thought patterns would be necessary to design specific therapeutic interventions while unharming the adaptive functions of mind wandering. For example, focal modulation of the neural system that is responsible for exerting constraints on the flow of thought may alleviate symptoms such as rumination and obsessive thought by releasing automatic constraints or improve thought stability and coherence for individuals with ADHD by reinforcing deliberate constraints (Christoff et al 2016). Although functional neuroimaging does not allow causal inferences between neural activity and cognitive processes, evidence for regional activation patterns and connectivity profiles can inform target selection for therapeutic non-invasive brain stimulation (NIBS) protocols. Understanding the neural mechanisms that underlie mind wandering might thus improve our knowledge of the neurobiological basis of cognitive dysfunction in several psychiatric diseases and facilitate a path toward effective interventions aimed at negating some of the negative consequences of mind wandering on sustained attention and psychological well-being.

4.4 Conclusions

The majority of past studies on mind wandering have focused on measurements within a single imaging modality, producing a vast amount of valuable yet isolated findings. Given the sustained uncertainty surrounding many neural and behavioral correlates, the contemporary literature does not converge on a mechanistic explanatory account. The work presented here emphasizes that a comprehensive understanding of the neurobiology that drives, maintains, and guides heterogeneous self-generated experiences requires the study of dynamic interactions between neuromodulatory systems, functional networks, and subcortical connectivity.

Mind wandering is a complex and heterogeneous construct that includes a wide variety of processes that are not exhaustively measured by experience sampling. The combination of direct and indirect measures at high spatial and temporal resolution holds promise for improving the detection of mind wandering among task-focused attention. While single-trial classification based on multimodal neuropsychological features shows comprehensive spatiotemporal neural signatures of self-reported attention, demanding cognitive tasks such as the FT-RSGT are paramount for disentangling ongoing interactions between mind wandering and highly controlled behavior governed by executive functions. Finally, recent advances in subcortical imaging and atlasing encourage the exploration of the extensive functional synergy between subcortical and cortical systems and its role in higher-level cognition.

The evidence in this thesis contributes to an increasingly complex mechanistic understanding of mind wandering and highlight several key features of its neurobiological underpinnings. Dynamic changes in the functional coupling and decoupling of regions within the DMN and frontal and salience networks seem to best capture the fleeting and transient nature of mind wandering above and beyond other neurophysiological domains. Global patterns of interregional clustering and segregation may be driven by shifts in exploration-exploitation tradeoffs governed by the LC/NE system, while transmodal hubs like the PCC and subcortical structures such as the thalamus and striatum are organized to integrate distributed information processing and may mediate transitions between attentional states. The diverging observations from direct and indirect markers and their interactions with situational factors furthermore underscore the non-unitary nature of mind wandering that can not be adequately described by an invariant system or feature, such as the DMN. Instead, charting the harmonics between the various neural systems provides a more realistic representation that will ultimately lead us to understand how we guide ourselves through a rich landscape of multifaceted internal experiences.

References

Alkemade A, Keuken MC, Forstmann BU (2013) A perspective on terra incognita: uncovering the neuroanatomy of the human subcortex. *Front Neuroanat,* 7:40.

Alkemade A, Mulder MJ, Groot JM, Isaacs BR, Van Berendonk N, Lute N, Isherwood SJS, Bazin P-L, Forstmann BU (2020) The Amsterdam ultra-high field adult lifespan database (AHEAD): A freely available multimodal 7 Tesla submillimeter magnetic resonance imaging database. *NeuroImage,* 221:117200.

Alves PN, Foulon C, Karolis V, Bzdok D, Margulies DS, Volle E, Thiebaut De Schotten M (2019) An improved neuroanatomical model of the default-mode network reconciles previous neuroimaging and neuropathological findings. *Commun Biol,* 2:370.

Anderson T, Petranker R, Lin H, Farb NAS (2020) The metronome response task for measuring mind wandering: Replication attempt and extension of three studies by Seli et al. *Atten Percept Psychophys,* 83:315-330.

Andrews-Hanna JR, Reidler JS, Huang C, Buckner RL (2010) Evidence for the default network's role in spontaneous cognition. *J Neurophysiol,* 104:322-335.

Andrews-Hanna JR (2012) The brain's default mode network and its adaptive role in internal mentation. *Neuroscientist,* 18:251-270.

Aston-Jones G, Rajkowski J, Cohen J (1999) Role of locus coeruleus in attention and behavioral flexibility. *Biol Psychiatry,* 46:1309-1320.

Aston-Jones G, Cohen JD (2005) An integrative theory of locus coeruleus-norepinephrine function: adaptive gain and optimal performance. *Annu Rev Neurosci,* 28:403-450.

Axelrod V, Rees G, Lavidor M, Bar M (2015) Increasing propensity to mind-wander with transcranial direct current stimulation. *PNAS,* 112:3314-3319.

Baddeley A, Emslie H, Kolodny J, Duncan J (1998) Random generation and the executive control of working memory. *Q J Exp Psychol A,* 51:819-852.

Baldwin CL, Roberts DM, Barragan D, Lee JD, Lerner N, Higgins JS (2017) Detecting and quantifying mind wandering during simulated driving. *Front Hum Neurosci,* 11:406.

Banks, JB, Welhaf MS, Hood AVB, Boals A, Tartar JL (2016) Examining the role of emotional valence of mind wandering: all mind wandering is not equal. *Conscious Cogn,* 43:167-176.

Bär K-J, De la Cruz F, Schumann A, Koehler S, Sauer H, Critchley H, Wagner G (2016) Functional connectivity and network analysis of midbrain and brainstem nuclei. *NeuroImage,* 134:53-63.

Barron E, Riby LM, Greer J, Smallwood J (2011) Absorbed in thought: the effect of mind wandering on the processing of relevant and irrelevant events. *Psychol Sci,* 22:596-601.

Bastian M, Sackur J (2013) Mind wandering at the fingertips: automatic parsing of subjective states based on response time variability. *Front Psychol,* 4:573.

Bazin P-L, Alkemade A, Mulder MJ, Henry AG, Forstmann BU (2020) Multi-contrast anatomical subcortical structures parcellation. *eLife,* 9:e59430.

Bell PT, Shine JM (2015) Estimating large-scale network convergence in the human functional connectome. *Brain Connect,* 5:565-574.

Bell PT, Shine JM (2016) Subcortical contributions to large-scale network convergence. *Neurosci Biobehav Rev,* 71:313-322.

Boayue NM, Csifcsák G, Kreis IV, Schmidt C, Finn I, Vollsund AEH, Mittner M (2020a) The interplay between executive control, behavioural variability and mind wandering: insights from a high-definition transcranial direct-current stimulation study. *Eur J Neurosci,* 00:1-19.

Boayue NM, Csifcsák G, Aslaksen P, Turi Z, Antal A, Groot J, Hawkins GE, Forstmann B, Opitz A, Thielscher A, Mittner M (2020b) Increasing propensity to mind-wander by transcranial direct current stimulation? A registered report. *Eur J Neurosci,* 51:755-780.

Bocharov AV, Knyazev GG, Savostyanov AN, Astakhova TN, Tamozhnikov SS (2019) EEG dynamics of spontaneous stimulus-independent thoughts. *Cogn Neurosci*, 10:77–87.

Bonelli RM, Cummings JL (2007) Frontal-subcortical circuitry and behavior. *Dialogues Clin Neurosci*, 9:141-151.

Bozhilova NS, Michelini G, Kuntsi J, Asherson P (2018) Mind wandering perspective on attention-deficit/hyperactivity disorder. *Neurosci Biobehav Rev,* 92:464-476.

Braga RM, Sharp DJ, Leeson C, Wise RJS, Leech R (2013) Echoes of the brain within default mode, association, and heteromodal cortices. *J Neurosci,* 33:14031-14039.

Britz J, Van De Ville D, Michel C (2010) Bold correlates of EEG topography reveal rapid resting-state network dynamics. *NeuroImage,* 52:1162-1170.

Buckner RL, Andrews-Hanna JR, Schacter DL (2008) The brain's default mode network: anatomy, function, and relevance to disease. *Ann NY Acad Sci,* 1124:1-38.

Buckner RL (2010) The role of the hippocampus in prediction and imagination. *Annu Rev Psychol*, 61:27-48.

Bullock M, Jackson GD, Abbott DF (2021) Artifact reduction in simultaneous EEG-fMRI: A systematic review of methods and contemporary usage. *Front Neurol*, 12:622719.

Callard F, Smallwood J, Golchert J, Margulies DS (2013) The era of the wandering mind? Twenty-first century research on self-generated mental activity. *Front Psychol,* 4:891.

Chakroun K, Mathar D, Wiehler A, Ganzer F, Peters J (2020) Dopaminergic modulation of the exploration/exploitation trade-off in human decision-making. *eLife,* 9:e51260.

Choi EY, Yeo BTT, Buckner RL (2012) The organization of the human striatum estimated by intrinsic functional connectivity. *J Neurophysiol,* 108:2242-2263.

Chou Y-H, Sundman M, Whitson HE, Gaur P, Chu M-L, Weingarten CP, Madden DJ, Wang L, Kirste I, Joliot M, Diaz MT, Li Y-J, Song AW, Chen N-K (2017) Maintenance and representation of mind wandering during resting-state fMRI. *Sci Rep,* 7:407222.

Christoff K, Gordon AM, Smallwood J, Smith R, Schooler JW (2009) Experience sampling during fMRI reveals default network and executive system contributions to mind wandering. *PNAS,* 106:8719-8724.

Christoff K (2012) Undirect thought: Neural determinants and correlates. *Brain Res,* 1428:51-59.

Christoff K, Irving ZC, Fox KCR, Spreng N, Andrews-Hanna JR (2016) Mind-wandering as spontaneous thought: a dynamic framework. *Nature Rev,* 17:718-731.

Christoff K, Mills C, Andrews-Hanna JR, Irving ZC, Thompson E, Fox KCR, Kam JWY (2018) Mind-wandering as a scientific concept: Cutting through the definitional haze. *Trends Cogn Sci,* 22:957-959.

Cohen JD, McClure SM, Yu AJ (2007) Should I stay or should I go? How the human brain manages the trade-off between exploitation and exploration. *Phil Trans R Soc,* 362:933-942.

Cole DM, Smith SM, Beckmann CF (2010) Advances and pitfalls in the analysis and interpretation of resting-state FMRI data. *Front Sys Neurosci*, 4:8.

Cole MW, Ito T, Bassett DS, Schultz DH (2016) Activity flow over resting-state networks shapes cognitive task activations. *Nature Neurosci,* 19:1718-1726.

Compton RJ, Gearinger D, Wild H (2019) The wandering mind oscillates: EEG alpha power is enhanced during moments of mind-wandering. *Cogn Affect Behav Neurosci,* 19:1184-1191.

Crittenden BM, Mitchell DJ, Duncan J (2015) Recruitment of the default mode network during a demanding act of executive control. *eLife,* 4:e06481.

Csifcsák G, Mittner M (2017) Linking brain networks and behavioral variability to different types of mind-wandering. *PNAS,* 114:6031-6032.

De Gee JW, Colizoli O, Kloosterman NA, Knapen T, Nieuwenhuis S, Donner TH (2017) Dynamic modulation of decision biases by brainstem arousal systems. *eLife,* 6:e23232.

De Hollander G, Keuken MC, Forstmann BU (2015) The subcortical cocktail problem; mixed signals from the subthalamic nucleus and substantia nigra. *PLoS One,* 10:e0120572.

De Hollander G, Keuken MC, Van der Zwaag W, Forstmann BU, Trampel R (2017) Comparing functional MRI protocols for small, iron-rich basal ganglia nuclei such as the subthalamic nucleus at 7T and 3T. *Hum Brain Mapp,* 38:3226-3248.

Deng Y-Q, Li S, Tang Y-Y (2012) The relationship between wandering mind, depression and mindfulness. *Mindfulness,* 5:124-128.

Dhindsa K, Acai A, Wagner N, Bosynak D, Kelly S, Bhandari M, Petrisor B, Sonnadara RR (2019) Individualized pattern recognition for detecting mind wandering from EEG during live lectures. *PLoS One,* 14:e0222276.

El Haj M, Antoine P, Moustafa AA, Roche J, Quaglino V, Gallouj K (2019) Off-track thoughts: Intentional and unintentional mind wandering in Alzheimer's disease. *Geriatr Gerontol Int,* 19:342-346.

Eldar E, Cohen JD, Niv Y (2013) The effects of neural gain on attention and learning. *Nature Neurosci,* 16:1146-1153.

Ellamil M, Fox KCR, Dixon ML, Pritchard S, Todd RM, Thompson E, Christoff K (2016) Dynamics of neural recruitment surrounding the spontaneous arising of thoughts in experienced mindfulness practitioners. *NeuroImage,* 136:186-196.

Esterman M, Noonan SK, Rosenberg M, Degutis J (2013) In the zone or zoning out? Tracking behavioral and neural fluctuations during sustained attention.*Cereb Cortex*, 23:2712–2723.

Faber M, Bixler R, D'Mello SK (2018) An automated behavioral measure of mind wandering during computerized reading. *Behav Res,* 50:134-150.

Ferguson KA, Cardin JA (2020) Mechanisms underlying gain modulation in the cortex. *Nature Rev,* 21:80-92.

Filmer HL, Griffin A, Dux PE (2019) For a minute there, I lost myself… dosage dependent increases in mind wandering via prefrontal tDCS. *Neuropsychologia,* 129:379384.

Forstmann BU, De Hollander G, Van Maanen L, Alkemade A, Keuken MC (2017) Towards a mechanistic understanding of the human subcortex. *Nature Rev,* 18:57-65.

Fox MD, Snyder AZ, Vincent JL, Corbetta M, Van Essen DC, Raichle ME (2005) The human brain is intrinsically organized into dynamic, anticorrelated functional networks. *PNAS,* 102:9673-9678.

Fox KCR, Spreng RN, Ellamil M, Andrews-Hanna JR, Christoff K (2015) The wandering brain: Meta-analysis of functional neuroimaging studies of mind-wandering and related spontaneous thought processes. *NeuroImage,* 111:611-621.

Frank MJ, Doll BB, Oas-Terpstra J, Moreno F (2009) Prefrontal and striatal dopaminergic genes predict individual differences in exploration and exploitation. *Nature Neurosci,* 12:1062-1068.

Franklin MS, Smallwood J, Schooler JW (2011) Catching the mind in flight: Using behavioral indices to detect mindless reading in real time. *Psycho Bull Rev,* 18:992–997.

Franklin MS, Mrazek MD, Broadway JM, Schooler JW (2013a) Disentangling decoupling: Comment on Smallwood (2013). *Psychol Bull,* 139:536-541.

Franklin MS, Broadway JM, Mrazek MD, Smallwood J, Schooler JW (2013b) Rapid communication window to the wandering mind: pupillometry of spontaneous thought while reading. *Q J Exp Psychol,* 66:2289-2294.

Gilzenrat MS, Nieuwenhuis S, Jepma M, Cohen JD (2010) Pupil diameter tracks changes in control state predicted by the adaptive gain theory of locus coeruleus function. *Cogn Affect Behav Neurosci,* 10:252-269.

Glover GH, Li TQ, Ress D (2000) Image-based method for retrospective correction of physiological motion effects in fMRI: RETROICOR. *Magn Reson Med,* 44:162-167.

Gonzales-Castillo J, Kam JWY, Hoy CW, Bandettini PA (2021) How to interpret resting-state fMRI: ask your participants. *J Neurosci,* 41:1130-1141.

Grandchamp R, Braboszcz C, Delorme A (2014) Oculometric variations during mind wandering. *Front Psychol,* 5:31.

Greene DJ, Marek S, Gordon EM, Siegel JS, Gratton C, Laumann TO, Gilmore AW, Berg JJ, Nguyen AL, Dierker D, Van AN, Ortega M, Newbold DJ, Hampton JM, Nielsen AN, McDermott KB, Roland JL, Norris SA, Nelson SM, Snyder AZ, Schlagger BL, Petersen SE, Dosenbach NUF (2020) Integrative and network-specific connectivity of the basal ganglia and thalamus defined in individuals. *Neuron,* 105:742-758.

Greicius MD, Menon V (2004). Default-mode activity during a passive sensory task: uncoupled from deactivation but impacting activation. *J Cogn Neurosci,* 16:1484-1492.

Handy TC, Kam JWY (2015) Mind wandering and selective attention to the external world. *Can J Exp Psychol,* 69:183-189.

Harrison BJ, Davey CG, Savage HS, Jamieson AJ, Leonards CA, Moffat BA, Glarin RK, Steward T (2022) Dynamic subcortical modulators of human default mode network function. *Cereb Cortex,* 32:4345-4355.

Hasenkamp W, Wilson-Mendenhall CD, Duncan E, Barsalou LW (2012) Mind wandering and attention during focused meditation: A fine-grained temporal analysis of fluctuating cognitive states. *NeuroImage,* 59:750-760.

Hawkins GE, Mittner M, Forstmann BU, Heathcote A (2019) Modeling distracted performance. *Cogn Psychol,* 112:48-80.

Hoeks B, Levelt WJM (1993) Pupillary dilation as a measure of attention: a quantitative system analysis. *Behav Res Methods,* 25:16-26.

Hu Y, Yang Z (2021) Impact of inter-individual variability on the estimation of default mode network in temporal concatenation group ICA. *NeuroImage,* 237:118114.

Hunyadi B, Woolrich MW, Quinn AJ, Vidaurre D, De Vos M (2019) A dynamic system of brain networks revealed by fast transient EEG fluctuations and their fMRI correlates. *NeuroImage,* 185:72-82.

Ingvar DH (1979) 'Hyperfrontal' distribution of the cerebral grey matter flow in resting wakefulness; on the functional anatomy of the conscious state. *Acta Neurol Scand,* 60:12-25.

Janacsek K, Evans TM, Kiss M, Shah L, Blumenfeld H, Ullman MT (2022) Subcortical cognition: The fruit below the rind. *Annu Rev Neurosci,* 45:361-386.

Jahanshahi M, Dirnberger G, Fuller R, Firth CD (2000) The role of the dorsolateral prefrontal cortex in random number generation: a study with positron emission tomography. *NeuroImage,*12:713-725.

Jarbo K, Verstynen T (2015) Converging structural and functional connectivity of orbitofrontal, dorsolateral prefrontal, and posterior parietal cortex in the human striatum. *J Neurosci,* 35:3865-3878.

Jepma M, Nieuwenhuis S (2011) Pupil diameter predicts changes in the exploration-exploitation trade-off: Evidence for the adaptive gain theory. *J Cogn Neurosci,* 23:1587-1596.

Ji JL, Spronk M, Kulkarni K, Repovs G, Anticevic A, Cole MW (2019) Mapping the human brain's cortico-subcortical functional network organization. *NeuroImage,* 185:35-57.

Jin CY, Borst JP, Van Vugt MK (2019) Predicting task-general mind-wandering with EEG. *Cogn Affect Beha. Neurosci*, 19:1059–1073.

Jin CY, Borst JP, Van Vugt MK (2020) Distinguishing vigilance decrement and low task demands from mind-wandering: a machine learning analysis of EEG. *Eur J Neurosci,* 00:1-18.

Johansen-Berg H (2013) Human connectomics – What will the future demand? *NeuroImage,* 80:541-544.

Joshi S, Li Y, Kalwani RM, Gold JI (2016) Relationships between pupil diameter and neuronal activity in the locus coeruleus, colliculi, and cingulate cortex. *Neuron,* 1:221-234.

Jubera-Garcia E,Gevers W, Van Opstal F (2019) Influence of content and intensity of thought on behavioral and pupil changes during active mind wandering, off-focus, and on-task states. *Atten Percept Psychophys,* 82:1125-1135.

Kam JWK, Handy TC (2013) The neurocognitive consequences of the wandering mind: a mechanistic account of sensory-motor decoupling. *Front Psychol,* 4:725.

Kam JWY, Dao E, Farley J, Fitzpatrick K, Smallwood J, Schooler JW, Handy TC (2011) Slow fluctuations in attentional control of sensory cortex. *J Cogn Neurosci,* 23:460-470.

Kam JWY, Xu J, Handy TC (2013) I don't feel your pain (asmuch): the desensitizing effect of mind wandering on the perception of others'discomfort. *Cogn Affect Behav Neurosci,* 14:286-296.

Kam JWY, Rahnuma T, Park YE, Hart CM (2022) Electrophysiological markers of mind wandering: A systematic review. *NeuroImage,* 258:119372.

Kane MJ, Brown LH, McVay JC, Silvia PJ, Myin-Germeys I, Kwapil TR (2007) For whom the mind wanders, and when: an experience-sampling study of working memory and executive control in daily life. *Psychol Sci,* 18:614-621.

Karapanagiotidis T, Vidaurre D, Quinn AJ, Vatansever D, Poerio GL, Turnbull A, Ho NSP, Leech R, Bernhardt BC, Jefferies E, Margulies DS, Nichols TE, Woolrich MW, Smallwood J (2020) The psychological correlates of distinct neural states occurring during wakeful rest. *Sci Rep,* 10:21121.

Keuken MC, Van Maanen L, Boswijk M, Forstmann BU, Steyvers M (2018a) Large scale structure-function mappings of the human subcortex. *Sci Rep,* 8:15854.

Keuken MC, Isaacs BR, Trampel R, Van der Zwaag W, Forstmann BU (2018a) Visualizing the human subcortex using ultra-high field magnetic resonance imaging. *Brain Topogr,* 31:513-545.

Kelly AM, Uddin LQ, Biswal BB, Castellanos FX, Milham MP (2008) Competition between functional brain networks mediates behavioral variability. *NeuroImage,* 39:527-537.

Killingsworth MA, Gilbert DT (2010) A wandering mind is an unhappy mind. *Science,* 330:932.

Klinger E (1971) Structure and functions of fantasy. New York: Wiley.

Klinger E, Cox WM (1987) Dimensions of thought flow in everyday life. *Imagin Cogn Pers,* 7:105-128.

Klinger E (2013) Goal commitments and the content of thoughts and dreams: basic principles. *Front Psychol,* 4:415.

Konishi M, Brown K, Battaglini L, Smallwood J (2017) When attention wanders: pupillometric signatures of fluctuations in external attention. *Cognition,* 168:16-26.

Krakow K, Allen PJ, Symms MR, Lemieux L, Josephs O, Fish DR (2000) EEG recording during fMRI experiments: Image quality. *Hum Brain Mapp*, 10:10-15.

Kristo G, Rutten GJ, Raemaekers M, de Gelder B, Rombouts SA, Ramsey NF (2014) Task and task-free FMRI reproducibility comparison for motor network identification. *Hum Brain Mapp,* 35:340-352.

Kucyi A (2018) Just a thought: how mind-wandering is represented in dynamic brain connectivity. *NeuroImage,* 180:505-514.

Kucyi A, Salomons TV, Davis KD (2013) Mind wandering away from pain dynamically engages antinociceptive and default mode brain networks. *PNAS,* 110:46.

Kucyi A, Davis KD (2014) Dynamic functional connectivity of the default mode network tracks daydreaming. *NeuroImage,* 100:471-480.

Kucyi A, Esterman M, Riley CS, Valera EM (2016) Spontaneous default network activity reflects behavioral variability independent of mind-wandering. *Proc Natl Acad Sci,* 113:13899-13904.

Kucyi A, Hove MJ, Esterman M, Hutchison RM, Valera EM (2017a) Dynamic brain network correlates of spontaneous fluctuations in attention. *Cereb Cortex,* 27:1831-1840.

Kucyi A, Esterman M, Valera EM (2017b) Fitting data to neural models of mind-wandering. *PNAS,* 114:e6033.

Larsen RS, Waters J (2018) Neuromodulatory correlates of pupil dilation. *Front Neural Circuits,* 12:21.

Lee S-H, Dan Y (2012) Neuromodulation of brain states. *Neuron,* 1:209-222.

Leech R, Kamourieh S, Beckmann CF, Sharp DJ (2011) Fractionating the default mode network: distinct contributions of the ventral and dorsal posterior cingulate cortex to cognitive control. *J Neurosci,* 31:3217-3224.

Leech R, Braga R, Sharp DJ (2012) Echoes of the brain within the posterior cingulate cortex. *J Neurosci,* 32:215-222.

Levinson DB, Smallwood J, Davidson RJ (2012) The persistence of thought: evidence for a role of working memory in the maintenance of task-unrelated thinking. *Psychol Sci,* 23:375-380.

Li J, Curley WH, Guerin B, Dougherty DD, Dalca AV, Fischl B, Horn A, Edlow BL (2021) Mapping the subcortical connectivity of the human default mode network. *NeuroImage,* 245:118758.

Liefgreen A, Dalton MA, Maguire EA (2020) Manipulating the temporal locus and content of mind-wandering. *Conscious Cogn,* 79:102885.

Liu KY, Marijatta F, Hämmerer D, Acosta-Cabronero J, Düzel E, Howard RJ (2017) Magnetic resonance imaging of the human locus coeruleus: A systematic review. *Neurosci Biobehav Rev,* 3:325-355.

Logothetis NK (2008) What we can do and what we cannot do with fMRI. *Nature,* 453:869-878.

Maillet M, Seli P, Schacter DL (2017) Mind-wandering and task stimuli: Stimulus-dependent thoughts influence performance on memory tasks and are more often past- versus future-oriented. *Conscious Cogn,* 52:55-67.

Marchetti I, Koster EHW, Klinger E, Alloy LB (2016) Spontaneous Thought and Vulnerability to Mood Disorders: The Dark Side of the Wandering Mind. *Clin Psychol Sci,* 4:835-857.

Marek S, Greene DJ (2021) Precision functional mapping of the subcortex and cerebellum. *Curr Opin Behav Sci,* 40:12-18.

Mathôt S (2018) Pupillometry: Psychology, physiology, and function. *J Cogn,* 1:16.

Margulies DS, Ghosh SS, Goulas A, Falkiewicz M, Huntenburg JM, Langs G, Bez-gin G, Eickhoff SB, Castellanos FX, Petrides M, Jefferies E, Smallwood J (2016) Situating the default-mode network along a principal gradient of macroscale cortical organization. *PNAS*, 113:12574-12579.

Marino M, Arcara G, Porcaro C, Mantini D (2019) Hemodynamic correlates of electrophysiological activity in the default mode network. *Front Neurosci,* 13:1060.

Mason MF, Norton MI, Van Horn JD, Wegner DM, Grafton ST, Macrae CN (2007) Wandering minds: the default network and stimulus-independent thought. *Science,* 315:393-395.

McKiernan KA, D'Angelo BR, Kaufman JN, Binder JR (2006) Interrupting the "stream of consciousness": an fMRI investigation. *NeuroImage,* 29:1185–1191.

McVay JC, Kane MJ (2009) Conducting the train of thought: working memory capacity, goal neglect, and mind wandering in an executive-control task. *J Exp Psychol: Learn Mem Cogn,* 35:196-204.

McVay JC, Kane MJ (2010) Does mind wandering reflect executive function or executive failure? Comment on Smallwood and Schooler (2006) and Watkins (2008). *Psychol Bull,* 136:188-207.

Merchant H, Grahn J, Trainor L, Rohrmeier M, Fitch WT (2015) Finding the beat: a neural perspective across humans and non-human primates. *Phil Trans R Soc B,* 370:20140093.

Miletić S, Bazin P-L, Isherwood SJS, Keuken MC, Alkemade A, Forstmann BU (2022) Charting human subcortical maturation across the adult lifespan with in vivo 7 T MRI. *NeuroImage,* 249:118872.

Miletić S, Bazin P-L, Weiskopf N, Van der Zwaag W, Forstmann BU, Trampel R (2020) fMRI protocol optimization for simultanously studying small subcortical and cortical areas at 7 T. *NeuroImage,* 219:116992.

Mittner M (2020) Pypillometry: a Python package for pupillometric analyses. *J Open Source Soft,* 5:2348.

Mittner M, Boekel W, Tucker AM, Turner BM, Heathcote A, Forstmann BU (2014) When the brain takes a break: a model-based analysis of mind wandering. *J Neurosci,* 34:16286-16295.

Mittner M, Hawkins GE, Boekel W, Forstmann BU (2016) A neural model of mind wandering. *Trends Cogn Sci*, 20:570-578.

Mooneyham BW, Schooler JW (2013) The costs and benefits of mind-wandering: A review. *Can J Exp Psychol,* 67:11-18.

Murphy PR, Robertsen IH, Balsters JH, O'Connell RG (2011) Pupillometry and P3 index the locus coeruleus-noradrenergic arousal function in humans. *Psychophysiol,* 48:1532-1543.

Neuner I, Arrubla J, Werner CJ, Hitz K, Boers F, Kawohl W, Shah NJ (2014) The default mode network and EEG regional spectral power: a simultaneous fMRI-EEG study. *PLoS One,* 9:88214.

O'Callaghan C, Walpola IC, Shine JM (2020) Neuromodulation of the mind-wandering brain state: The interaction between neuromodulatory tone, sharp wave-ripples and spontaneous thought. *Phil Trans Royal Soc,* 376:20190699.

O'Connell RG, Dockree PM, Robertson IH, Bellgrove MA, Foxe JJ, Kelly SP (2009) Uncovering the neural signature of lapsing attention: electrophysiological signals predict errors up to 20 s before they occur. *J Neurosci,* 29:8604-8611.

Paquette S, Fujii S, Li HC, Schlaug G (2017) The cerebellum's contribution to beat interval discrimination. *NeuroImage,* 163:177-182.

Pelagatti C, Binda P, Vannucci M (2018) Tracking the dynamics of mind wandering: Insights from pupillometry. *J Cogn,* 1:38.

Peters M, Giesbrecht T, Jelicic M, Merckelback H (2007) The random number generation task: psychometric properties and normative data on an executive function task in a mixed sample. *J Int Neuropsychol Soc,* 13:626-634.

Pincus S, Kalman RE (1997) Not all (possibly) "random" sequences are created equal. *PNAS,* 94:3513-3518.

Raichle ME, MacLeod AM, Snyder AZ, Powers WJ, Gusnard DA, Schulman GL (2001) A default mode of brain function. *PNAS,* 98:676-682.

Raichle ME (2010) Two views of brain function. *Trends Cogn Neurosci,* 14:180-190.

Rajkowski J, Kubiak P, Aston-Jones G (1993) Correlations between locus coeruleus (LC) neural activity, pupil diameter and behavior in monkey support a role of LC in attention. *Soc Neurosci Abstr,* 19:974.

Reimer J, McGinley MJ, Liu Y, Rodenkirch C, Wang Q, McCormick DA, Tolias AS (2016) Pupil fluctuations track rapid changes in adrenergic and cholinergic activity in cortex. *Nat Commun,* 7:13289.

Robertson H, Manly T, Andrade J, Baddeley BT, Yiend J (1997) 'Oops!': Performance correlates of everyday attentional failures in traumatic brain injured and normal subjects. *Neuropsychologia,* 35:747-758.

Robison MK, Unsworth N (2019) Pupillometry tracks fluctuations in working memory performance. *Attent Percept Psychophys,* 81:407-419.

Rummel J, Boywitt CD (2014) Controlling the stream of thought: Working memory capacity predicts adjustment of mindwandering to situational demands. *Psychon Bull Rev,* 21:1309-1315.

Schaefer A, Margulies DS, Lohmann G, Gorgolewski KJ, Smallwood J, Kiebel SJ, Villringer A (2014) Dynamic network participation of functional connectivity hubs assessed by resting-state fMRI. *Front Hum Neurosci,* 8:195.

Scheeringa R, Bastiaansen MCM, Petersson KM, Oostenveld R, Norris DG, Hagoort P (2008) Frontal theta EEG activity correlates negatively with the default mode network in resting state. *Int J Psychophys,* 67:242-251.

Schooler JW, Smallwood J, Christoff K, Handy TC, Reichle ED, Sayette MA (2011) Meta-awareness, perceptual decoupling and the wandering mind. *Trends Cogn Sci,* 15:319-326.

Seitzman BA, Gratton C, Marek S, Raut RV, Dosenbach NUF, Schlagger BL, Petersen SE, Greene DJ (2020) A set of functionally-defined brain regions with improved representation of the subcortex and cerebellum. *NeuroImage,* 206:116290.

Seli P, Cheyne JA, Smilek D (2013) Wandering minds and wavering rhyhtms: linking mind wandering and behavioral variability. *J Exp Psychol,* 39:1-15.

Seli P, Smallwood J, Cheyne JA, Smilek D (2015) On the relation of mind wandering and ADHD symptomatology. *Psychon Bull Rev,* 22:629-636.

Seli P, Risko EF, Purdon C, Smilek D (2017) Intrusive thoughts: linking spontaneous mind wandering and OCD symptomatology. *Psychol Res,* 81:392-398.

Seli P, Kane MJ, Smallwood J, Schacter DL, Maillet D, Schooler JW, Smilek D (2018a) Mind-wandering as a natural kind: A family-resemblences view. *Trends Cogn Sci,* 22:479-490.

Seli P, Beaty RE, Cheyne JA, Smilek D, Oakman J, Schacter DL (2018b) How pervasive is mind wandering, really? *Conscious Cogn,* 66:74-78.

Shamloo F, Helie S (2016) Changes in default mode network as automaticity develops in a categorization task. *Behav Brain Res,* 15:324-333.

Shepard J (2019) Why does the mind wander? *Neurosci Conscious,* 5:014.

Shine JM, Aburn MJ, Breakspear M, Poldrack RA (2018) The modulation of neural gain facilitates a transition between functional segregation and integration in the brain. *eLife,* 7:e31130.

Smallwood J (2011) Mind-wandering while reading: Attentional decoupling, mindless reading and the cascade model of inattention. *Linguist Lang Compass,* 5:63-77.

Smallwood J (2013) Distinguishing how from why the mind wanders: a process-occurrence framework for self-generated mental activity. *Psychol Bull,* 139:519-535.

Smallwood J, Davies JB, Heim D, Finnigan F, Sudberry M, O'Connor R, Obonsawin M (2004) Subjective experience and the attentional lapse: Task engagement and disengagement during sustained attention. *Conscious Cogn,* 13:657-690.

Smallwood J, Schooler JW (2006) The restless mind. *Psychol Bull,* 132:946-958.

Smallwood J, Schooler JW (2015) The science of mind wandering: empirically navigating the stream of consciousness. *Ann Rev Psychol,* 66:487-518.

Smallwood J, O'Connor RC, Sudbery MV, Obonsawin M (2007) Mind-wandering and dysphoria. *Cogn Emot,* 21:816-842.

Smallwood J, Beach E, Schooler JW, Handy TC (2008) Going AWOL in the brain: mind wandering reduces cortical analysis of external events. *J Cogn Neurosci,* 20:458-469.

Smallwood J, Brown KS, Tipper C, Giesbrecht B, Franklin MS, Mrazek MD, Carlson JM, Schooler JW (2011) Pupillometric evidence for the decoupling of attention from perceptual input during offline thought. *PLoS One,* 6:e18298.

Smallwood J, Brown K, Baird B, Schooler JW (2012a) Cooperation between the de- fault mode network and the frontal-parietal network in the production of an internal train of thought. *Brain Res,* 1428:60-70.

Smallwood J, Brown KS, Baird B, Mrazek MD, Franklin MS, Schooler JW (2012b) Insulation of daydreams: a role for tonic norepinephrine in the facilitation of internally guided thought. *PLoS One,* 7:33706.

Smallwood J, Andrews-Hanna J (2013) Not all minds that wander are lost: the importance of a balanced perspective on the mind-wandering state. *Front Psychol,* 4:441.

Smith SM, Fox PT, Miller KL, Glahn DC, Fox PM, Mackay CE, Filippini N, Watkins KE, Toro R, Laird AR, Beckmann CF (2009) Correspondence of the brain's functional architecture during activation and rest. *PNAS,* 106:13040-13045.

Smith V, Mitchell DJ, Duncan J (2018) Role of the Default Mode Network in Cognitive Transitions, *Cereb Cortex*, 28:3685-3696.

Smitha KA, Raja KA, Arun KM, Rajesh PG, Thomas B, Kapilamoorthy TR, Kesavadas C (2017) Resting state fMRI: A review on methods in resting state connectivity analysis and resting state networks. *Neuroradiol J,* 30:305-317.

Sormaz M, Murphy C, Wang H-T, Hymers M, Karapanagiotidis T, Poerio G, Margulies DS, Jefferies E, Smallwood J (2018) Default mode network can support the level of detail in experience during active task states. *PNAS,* 115:9318-9321.

Spreng RN, Mar RA, Kim ASN (2009) The common neural basis of autobiographical memory, prospection, navigation, theory of mind, and the default mode: a quantitative meta-analysis. *J Cogn Neurosci*, 21:489-510.

Spreng RN, Stevens WD, Chamberlain JP, Gilmore AW, Schacter DL (2010) Default network activity, coupled with the frontoparietal control network, supports goal-directed cognition. *NeuroImage* 53:303-317.

Stawarczyk D, Majerus S, Maj M, Van der Linden M, D'Argembeau A (2011a) Mind-wandering: phenomenology and function as assessed with a novel experience sampling method. *Acta Psychol,* 136:370-381.

Stawarczyk D, Majerus S, Maquet P, D'Argembeau A (2011b) Neural correlates of ongoing conscious experience: Both task-unrelatedness and stimulus-independence are related to default network activity. *PLoS One,* 6:e16997.

Sylvester CM, Yu Q, Srivastava AB, Marek S, Zheng A, Alexopoulos D, Smyser CD, Shimony JS, Ortega M, Dierker DL, Patel GH, Nelson SM, Gilmore AW, McDermott KB, Berg JJ, Drysdale AT, Perino MT, Snyder AZ, Raut RV, Laumann TO, Gordon EM, Barch DM, Rogers CE, Greene DJ, Raichle ME, Dosenbach NUF (2020) Individual-specific functional connectivity of the amygdala: A substrate for precision psychiatry. *PNAS,* 117:3808-3818.

Tang Y-Y, Rothbart MK, Posner MI (2012) Neural correlates of establishing, maintaining, and switching brain states. *Trends Cogn Sci,* 16:330-337.

Teasdale JD, Dritschel BH, Taylor MJ, Proctor L, Lloyd CA, Nimmo-Smith I, Baddeley AD (1995) Stimulus-independent thought depends on central executive resources. *Mem Cogn,* 23:551-559.

Thompson GJ, Magnuson ME, Merritt MD, Schwarb H, Pan W-J, McKinley A, Tripp LD, Schumacher EH, Keilholz SD (2013) Short-time windows of correlation between large-scale functional brain networks predict vigilance intraindividually and interindividually. *Hum Brain Mapp,* 34:3280-3298.

Tian Y, Margulies DS, Breakspear M, Zalesky A (2020) Topographic organization of the human subcortex unveiled with functional connectivity gradients. *Nature Neurosci,* 23:1421-1432.

Tona K-D, Keuken MC, De Rover M, Lakke E, Forstmann BU, Nieuwenhuis S, Van Osch MJP (2017) In vivo visualization of the locus coeruleus in humans: quantifying the test-retest reliability. *Brain Struct Funct,* 222:4203-4217.

Turchi J, Chang C, Ye FQ, Russ BE, Yu DK, Cortes CR, Monosov IE, Duyn JH, Leopold DA (2018) The basal forebrain regulates global resting-state fMRI fluctuations. *Neuron,* 97:940-952.

Turnbull A, Wang H-T, Schooler JW, Jefferies E, Margulies DS, Smallwood J (2019a) The ebb and flow of attention: between-subject variation in intrinsic connectivity and cognition associated with the dynamics of ongoing experience. *NeuroImage,* 185:286-299.

Turnbull A, Wang H-T, Murphy C, Ho NSP, Wang X, Sormaz M, Karapanagiotidis T, Leech RM, Bernhardt B, Margulies DS, Vatansever D, Jefferies E, Smallwood J (2019b) Left dorsolateral prefrontal cortex supports context-dependent prioritisation of off-task thought. *Nat Commun,* 10:3816.

Unsworth N, Robison MK (2016) Pupillary correlates of lapses of sustained attention. *Cogn Affect Behav Neurosci,* 16:601-615.

Unsworth N, Robison MK (2018) Tracking arousal state and mind wandering with pupillometry. *Cogn Affect Behav Neurosci,* 18:638-664.

Van Calster L, D'Argembeau A, Salmon E, Peters F, Majerus S (2017) Fluctuations of attentional networks and default mode network during the resting state reflect variations in cognitive states: evidence from a novel resting-state experience sampling method. *J Cogn Neurosci,* 29:95-113.

Van den Brink RL, Murphy PR, Nieuwenhuis S (2016) Pupil diameter tracks lapses of attention. *PLoS One,* 11:e0165274.

Van der Meer JN, Pampel A, Van Someren EJW, Ramautar JR, Van der Werf YD, Gomez-Herrero G, Lepsien J, Hellrung L, Hinrichs H, Möller HE, Walter M (2016) Carbon-wire loop based artifact correction outperforms post-processing EEG/fMRI corrections – A validation of a real-time simultaneous EEG/fMRI correction method. *NeuroImage,* 125:880-894.

Van Slooten JC, Jahfari S, Knapen T, Theeuwes J (2018) How pupil responses track value-based decision-making during and after reinforcement learning. *PLoS Comput Biol,* 14:e1006632.

Varoquaux G, Sadaghiani S, Pinel P, Kleinschmidt A, Poline JB, Thirion B (2010) A group model for stable multi-subject ICA on fMRI datasets. *NeuroImage,* 51:288-299.

Wang X, Xu M, Song Y, Li X, Zhen Z, Yang Z, Liu J (2014)The network property of the thalamus in the default mode network is correlated with trait mindfulness. *Neurosci,* 278:91-301.

Wang H-T, Poerio G, Murhpy C, Bzdok D, Jefferies E, Smallwood J (2018) Dimensions of experience: Exploring the heterogeneity of the wandering mind. *Psychol Sci,* 29:56-71.

Weinstein Y (2018) Mind-wandering, how do I measure three with probes? Let me count the ways. *Behav Res Methods,* 50:642-661.

Weissman DH, Roberts KC, Visscher KM, Woldorff MG (2006) The neural bases of momentary lapses in attention. *Nature Neurosci,* 9:971.

James W (1890) The principles of psychology. New York: Henry Holt.

Ye R, Rua C, O'Callaghan C, Jones PS, Hezemans FH, Kaalund SS, Tsvetanov KA, Rodgers CT, Williams G, Passamonti L, Rowe JB (2021) An in vivo probabilistic atlas of the human locus coeruleus at ultra-high field. *NeuroImage,* 225:117487.

Yeo BTT, Krienen FM, Sepulcre J, Sabuncu MR, Lashkari D, Hollinshead M, Roffman JL, Smoller JW, Zöllei L, Polimeni JR, Fischl B, Liu H, Buckner RL (2011) The organization of the human cerebral cortex estimated by intrinsic functional connectivity. *J Neurophysiol,* 106:1125-1165.

Zanesco AP, Denkova E, Jha AP (2020a) Self-reported mind wandering and response time variability differentiate prestimulus electroencephalogram microstate dynamics during a sustained attention task. *J Cogn Neurosci,* 33:28-45.

Zanesco AP, Denkova E, Witkin JE, Jha AP (2020b) Experience sampling of the degree of mind wandering distinguishes hidden attentional states. *Cognition,* 205:104380.

Paper I

Probing the neural signature of mind wandering with simultaneous fMRI-EEG and pupillometry

Josephine Maria Groot, Nya Menhwolo Boayue, Gábor Csifcsák, Wouter Boekel, Rene Huster, Birte U

Forstmann, Matthias Mittner
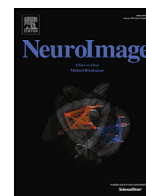
Probing the neural signature of mind wandering with simultaneous fMRI-EEG and pupillometry

Josephine M Groot [a,b], Nya M Boayue [a], Gábor Csifcsák [a], Wouter Boekel [c], René Huster [d], Birte U Forstmann [b], Matthias Mittner [a,*]

[a] *Department of Psychology, UiT – The Arctic University of Norway, 9037 Tromsø, Norway*
[b] *Department of Psychology, University of Amsterdam, 1001 NK Amsterdam, The Netherlands*
[c] *Institute of Psychology, Leiden University, 2333 AK Leiden, The Netherlands*
[d] *Department of Psychology, University of Oslo, 0317 Oslo, Norway*

ABSTRACT

Mind wandering reflects the shift in attentional focus from task-related cognition driven by external stimuli toward self-generated and internally-oriented thought processes. Although such task-unrelated thoughts (TUTs) are pervasive and detrimental to task performance, their underlying neural mechanisms are only modestly understood. To investigate TUTs with high spatial and temporal precision, we simultaneously measured fMRI, EEG, and pupillometry in healthy adults while they performed a sustained attention task with experience sampling probes. Features of interest were extracted from each modality at the single-trial level and fed to a support vector machine that was trained on the probe responses. Compared to task-focused attention, the neural signature of TUTs was characterized by weaker activity in the default mode network but elevated activity in its anticorrelated network, stronger functional coupling between these networks, widespread increase in alpha, theta, delta, but not beta, frequency power, predominantly reduced amplitudes of late, but not early, event-related potentials, and larger baseline pupil size. Particularly, information contained in dynamic interactions between large-scale cortical networks was predictive of transient changes in attentional focus above other modalities. Together, our results provide insight into the spatiotemporal dynamics of TUTs and the neural markers that may facilitate their detection.

1. Introduction

Humans pervasively engage in shifting attentional focus from demands in the environment toward self-generated, task-unrelated trains of thought (TUTs), leading to performance errors during tasks that require sustained vigilance (Smallwood and Schooler, 2015). Although this phenomenon, also termed mind wandering, has been of increasing interest in the past decades, its underlying neural signature remains a question of interest.

Converging evidence from functional magnetic resonance imaging (fMRI) studies indicates an association between activity in areas in the default mode network (DMN) and mind wandering (Mason et al., 2007; Christoff et al., 2009). These areas behave antagonistically with a task-positive, or anticorrelated network (ACN) that generally constitutes regions of frontoparietal control (FPCN) and dorsal attention (DAN) networks (Fox et al., 2005; Mittner et al., 2014). Although these findings support a major role for the DMN in internal mentation, more

recent accounts argue that its transmodal architecture allows flexible coupling with other networks in order to support a variety of task-relevant cognitive functions (Elton and Gao, 2015; Margulies et al., 2016; Sormaz et al., 2018). Furthermore, observations of coincidental activity in FPCN/DAN regions suggest recruitment of networks beyond the DMN during mind wandering (Christoff et al., 2009; Fox et al., 2015). In a recent study, Turnbull et al. (2019a) demonstrated the involvement of DAN and ventral attention network (VAN) systems in regulating TUTs, whereas activity in the posterior cingulate cortex (PCC), a central node of the DMN, was related to detailed ongoing thought during working memory performance. Together, these findings highlight the complexity of neural patterns during mind wandering and negate the notion of a single task-negative system represented by the DMN.

Accordingly, recent findings emphasize the importance of dynamic changes in cortical functional connectivity (FC) to support transient cognitive processes (Kucyi, 2018; Kucyi et al., 2018; Maillet et al., 2019). Although the DMN and ACN are intrinsic connectivity networks

---

(ICNs) that demonstrate a stable functional organization across individuals and mental states when measured statically (Gratton et al., 2018), studies investigating the dynamic FC (at a temporal resolution of seconds) between them have described opposite associations with behavior, with greater DMN/ACN anticorrelation during vigilant attention (Thompson et al., 2013) as well as during periods of mind wandering (Mittner et al., 2014).

Cortical dynamics during internal states have also been examined with more temporally precise measures including electroencephalography (EEG). A robust finding from these studies concerns the decrease in amplitude of event-related potentials (ERPs) prior to performance errors and self-reported TUTs (Smallwood et al., 2008; Kam et al., 2011), supporting the idea that attention is perceptually detached from external input during mind wandering episodes (Schooler et al., 2011). Since the attenuation of sensory processing may arise from concurrent increases in alpha power that have been observed over widespread cortical areas, alpha-band activity may serve as a reliable electrophysiological correlate of mind wandering (O'Connell et al., 2009; Compton et al., 2019; Jin et al., 2019).

New lines of research suggest that fluctuations in attention are modulated through the locus coeruleus/norepinephrinergic (LC/NE) system (Aston-Jones and Cohen, 2005; Mittner et al., 2016). Specifically, changes in tonic and phasic NE levels are proposed to facilitate transitions between exploratory and exploitative states in order to optimize behavior. These dynamics have been derived from changes in pupil size at baseline and in response to stimuli (Gilzenrat et al., 2010). Whereas (phasic) pupil responses seem consistently smaller during TUTs, changes in (tonic) baseline pupil size have yielded different results across experiments (Smallwood et al., 2012a; Grandchamp et al., 2014; Mittner et al., 2014; Konishi et al., 2017). This suggests that there are distinct forms of mind wandering characterized by varying levels of tonic arousal and neural gain (Mittner et al., 2016; Unsworth and Robison, 2016, 2018).

The possibility to detect the occurrence of mind wandering episodes has been examined with machine learning techniques using neural markers from different imaging modalities. For example, non-linear support vector machines (SVM) built for EEG data were trained on mind wandering probes during SART and visual search tasks (Jin et al., 2019, 2020) and live lectures (Dhindsa et al., 2019). These studies demonstrate that EEG markers can be used to predict TUTs, and that this predictive ability can be generalized across tasks and settings. In another classification study, Mittner et al. (2014) successfully predicted self-reported TUTs across subjects with a non-linear SVM based on single-trial fMRI activity, functional connectivity, as well as pupillometric measures. Rather than excluding all measures that cannot be directly related to a self-reported attentional state, machine learning allows examination of data that is not interrupted by thought probing and offers a powerful tool for single-trial detection of latent cognitive processes. However, the predictive power of classifiers based on multimodal imaging datasets remains unexplored.

The interplay between temporally well-defined neural responses and spatially-localized functional networks can be assessed by multimodal neuroimaging. Although studies have been conducted combining EEG with resting-state MRI to determine the electrophysiological correlates of the DMN (Neuner et al., 2014; Bowman et al., 2017; Marino et al., 2019), to our knowledge none exist that investigate the neural substrate of TUTs during a cognitive task. We expected that the complementary contributions of neural modalities offers unique spatial and temporal information for detecting TUT episodes. Therefore, we present the first study of mind wandering that utilizes simultaneous fMRI-EEG and pupillometry measures during task performance. By combining multimodal neural information with machine learning, we aimed to explore the markers sensitive to the fluctuations in attention that underlie mind wandering to ultimately gain a better understanding of its neural mechanisms. Specifically, we aimed to replicate the methods previously employed by Mittner et al. (2014) with addition of exploring more temporally refined features from EEG.

2. Materials and methods

2.1. Overview

Simultaneous fMRI-EEG, and pupillometry data were collected during performance of a sustained attention task with probe-caught experience sampling. Features of interest were selected based on prior findings and extracted from each modality after preprocessing. We aimed to extend the single-trial analysis approach introduced by Mittner et al. (2014) by exploring activity and synchronicity within and between ICNs as well as changes in EEG markers and pupil size in relation to fluctuations in attentional focus. To this end, we employed a supervised learning algorithm trained to classify single trials as either 'on-task' or 'off-task' states. We then analyzed and compared the spatiotemporal signatures of respective states. Additionally, we performed recursive feature elimination procedures across different combinations of modalities to assess the relative importance of individual features in distinguishing between on and off-task states. Data and code are publicly available and can be found at https://osf.io/43dp5.

2.2. Participants

Ethical approval was obtained from the ethics review board of the University of Amsterdam. Thirty healthy adult volunteers (25 female, aged 21 ± 2.51 years) were recruited and screened for MRI compatibility with a standard safety questionnaire. Participants were eligible when none of the following exclusion criteria were met: having a (record of) neurological or psychiatric disease, impaired vision, or any contraindication for MRI such as certain medical implants or prostheses. Written informed consent was obtained prior to the experiment. Participation was compensated with a €20,- reward for a total duration of approximately 1.5 h. Two participants were excluded due to ending the experiment prematurely. Therefore, we performed data analysis on 28 datasets of which two were incomplete (one without EEG and another without eye-tracking) due to technical issues.

2.3. Sustained attention to response task

Participants performed a fast-paced sustained attention to response task (SART) that consisted of a series of non-target and target digits at an average 9:1 ratio. Stimuli were presented on a 32 inch BOLD screen using the Presentation software (Neurobehavioral Systems, Inc., Berkeley, CA). The SART was divided into two runs of 700 trials each, with a 1.4 s trial duration. At the start of each trial, a centered fixation cross was presented on a gray background for 400 ms before it was replaced by a random stimulus (digits 1 to 9) for 400 ms. Participants were instructed to respond to every digit with a button press using their right index finger unless the target stimulus appeared (digit 3). The train of stimuli was occasionally interrupted by a thought probe to track ongoing fluctuations in attentional focus, which was formulated as the following question: "Where was your attention during the previous trials?". To respond to the probe, participants had to use left and right response buttons to move an arrow above a 4-point slidebar ranging from 1 (off-task) to 4 (on-task). After a fixed duration of 6 s, the location at which the arrow was positioned was registered as the response to the probe and the task continued. Participants were instructed to respond with 'off-task' when their attention was not primarily focused on the task or environmental distractions but on internal processes such as memories or personally relevant thoughts.

An online iterative algorithm was implemented to optimize the onsets of thought probes in order to maximize the probability of capturing off-task thought episodes throughout the task. To achieve this, the reaction time coefficient of variability (RT_{CV}) was tracked as a continuous index of attentional focus based on previous findings relating mind wandering to increases in RT_{CV} (Bastian and Sackur, 2013). For every trial that returned an RT, the RT_{CV} was computed over the previous eight

trials (RT_{SD} / RT_{mean}). When a threshold was crossed of either above 80% or below 20% of the entire RT_{CV} history, the algorithm searched for a peak or trough, respectively, in the previous RT_{CV} values. Specifically, a peak was identified if the RT_{CV} of the second last trial (T–2) was higher than that of the third last trial (T–3) and the last trial (T–1), and the RT_{CV} of T–1 was also higher than that of the current trial (T). Similarly, a trough was identified if the RT_{CV} of T–2 was lower than that of T–3 and T–1, and the RT_{CV} of T–1 was also lower than that of T. If such a pattern was detected, a probe onset was triggered. The algorithm was not activated when the current trial did not return an RT or when the RT_{CV} did not cross the initial threshold. Thought probe onsets were constrained to have no less than 15 trials (21 s) and no more than 45 trials (63 s) between them. Thus, a probe onset was omitted if one had occurred within the past 15 trials but forced if one had not occurred for 45 trials, regardless of whether the current trial's RT_{CV} reached threshold. On average, 22 thought probes (min = 19, max = 25) were presented per SART run. A short practice run of the task was completed prior to the experiment to ensure participants understood all task instructions.

2.4. Behavioral analysis

Thought probe responses were dichotomized by collapsing response options 1 and 2 into 'off-task' and response options 3 and 4 into 'on-task'. Behavioral indices of mind wandering were calculated for windows spanning 10 pre-probe trials (14 s) separately for off-task and on-task thought probes and included: (i) RT coefficient of variability ($RT_{CV} = RT_{SD}$ / RT_{mean}); (ii) omission error rate (failure to respond to non-targets); and (iii) commission error rate (failure to withhold a response to targets). We selected a 10-trial window *a priori* based on the assumption that mind wandering occurs in slowly fluctuating episodes spanning multiple seconds and to include sufficient data for detecting differences in error rates, which are relatively low in this experimental paradigm.

2.5. Functional neuroimaging

2.5.1. Acquisition

Participants were scanned with a 3 Tesla Philips Achieva MRI system with a 32-channel head coil. T_1-weighted (T_1w) images were acquired with a turbo field-echo (TFE) sequence in 220 transverse slices with 1 mm slice thickness (FOV = 240 × 220 × 188 mm, TR = 8192 ms, TE = 3760 ms, voxel size = 1 mm isotropic). Whole-brain functional images were acquired with a fast-echo (FE) echo-planar imaging (EPI) sequence in 38 transverse slices with 2.5 mm thickness and a 0.25 mm slice gap (FOV = 200 × 104 × 200 mm, TR = 2250 ms, TE = 29.94 ms, flip-angle = 80^0, voxel size = 2.5 mm isotropic).

2.5.2. Preprocessing

Standard image preprocessing was performed in FSL (v6.0; Jenkinson et al., 2012) with custom Python scripts (v2.7.15; Van Rossum and Drake, 2011) using the Nipype framework (v1.1.8; Gorgolewski et al., 2011). Each of the two functional BOLD runs was spatially smoothed with a 6 mm full-width half-maximum Gaussian kernel using SUSAN (Smith and Brady, 1997), motion-corrected with MCFLIRT (Jenkinson et al., 2002) and slice-time corrected with slicetimer. The signal was then high-pass filtered at 1/44 Hz to remove slow fluctuating noise such as scanner drift. The brain was extracted from T_1w images with BET (Smith, 2002) and segmented into gray matter (GM), white matter (WM), and cerebrospinal fluid (CSF) with FAST (Zhang et al., 2001). To investigate task-unrelated patterns of brain activity, a general linear model (GLM) was constructed using FEAT (Woolrich et al., 2001) and included: (i) task regressors that were prepared by convolving stimulus, thought probe, and response onsets with a standard hemodynamic response function to model task-dependent BOLD signal; and (ii) nuisance regressors including six motion (direction and amplitude) parameters as well as mean time courses in WM and CSF masks. The modeled data were obtained via ordinary least-squares linear regression and subtracted from the preprocessed signal. The residual time-series were then merged across the two runs for each subject, normalized, and used for further analyses.

2.5.3. Feature extraction

We followed the procedure described by Mittner et al. (2014) to determine regions of interest (ROIs) by performing a seed-based correlation analysis with a prior mask of the posterior cingulate cortex (PCC; Van Maanen et al., 2011) as seed-region. First, the mask was transformed to native space using FLIRT (Jenkinson and Smith, 2001) and the mean time course of voxels within the mask was correlated with all other voxels in the brain, yielding a connectivity map for each subject. Next, individual connectivity maps were registered with FLIRT to MNI space, Fisher z-transformed, and averaged to create a group-level connectivity map. The group-level map was then thresholded to locate the voxels with the 5% strongest positive and 5% strongest negative correlations with the PCC to determine the DMN and ACN, respectively (Fig. 1). Automated segmentation of the group-level thresholded maps into spatial clusters resulted in seven nodes for the DMN (posterior cingulate cortex/precuneus [PCC/PCUN], medial prefrontal cortex [mPFC], bilateral angular gyri [AG], bilateral superior frontal gyri [SFG], and left middle temporal gyrus [MTG]) and six nodes for the ACN (supplementary motor area [SMA], right supramarginal gyrus [SMG], bilateral insular cortex [INS], and bilateral dorsolateral prefrontal cortex [DLPFC]). The thresholded ROI maps were projected back to native space in order to extract the mean time-series from a 3 × 3 × 3 cube centered around the peak-correlation voxel of each ROI for each subject. These individual time-series were linearly interpolated to find the signal at stimulus onset at every trial, resulting in 13 single-trial node-activity features per subject. Additionally, the mean time-series of every ROI was correlated with that of every other ROI using sliding-window correlations of 45 s, resulting in another 78 single-trial node-connectivity features per subject (i.e., 21 pairs for intra-DMN connectivity, 15 pairs for intra-ACN connectivity, and 42 pairs for inter-network connectivity).

2.6. Electroencephalography

2.6.1. Acquisition

Continuous EEG data were concurrently acquired with an MRI-compatible, 64-channel HydroCel Geodesic Sensor system and Net Amps 300 amplifier (Electrical Geodesics, Inc., Eugene, OR, USA) and processed with Net Station (v4.5.2; Eugene, OR, USA). The cap was fitted with carbon-wire loops sensitive to movement-induced variations in the magnetic field, serving as a reference for cardioballistic artifacts (Van der Meer et al., 2016). The signal was collected at a sampling rate of 1000 Hz, online high-pass filtered at 0.1 Hz, and referenced to the Cz electrode. Electrooculography (EOG) was recorded from four electrodes positioned above and below and outer canthi of the eyes.

2.6.2. Preprocessing

Data were analyzed in EEGLAB (v14.1.2; Delorme and Makeig, 2004) using MATLAB (R2018b; Mathworks, Natick, MA, United States) and BrainVision Analyzer (v2.1.2; Brain Products GmbH, Gilching, Germany). First, data were filtered with a fourth-order zero phase-shift Butterworth filter (24 dB/oct) with a low cut-off of 0.33 Hz followed by a high cut-off of 125 Hz. Next, average artifact subtraction (AAS; Allen et al., 2000) with a sliding window of 21 artifacts was used to correct for MR gradient artifacts. In addition, cardioballistic artifacts were removed with the regression-based method described by Van der Meer et al. (2016) and artifacts related to eye-movement were removed with independent component analysis (ICA). Bad EEG channels were interpolated before re-referencing data to the average reference. Subsequently, data were high-pass and low-pass filtered at 1 Hz and 30 Hz, respectively, segmented into epochs from −1000 ms to 600 ms post-stimulus, and DC trends were removed.

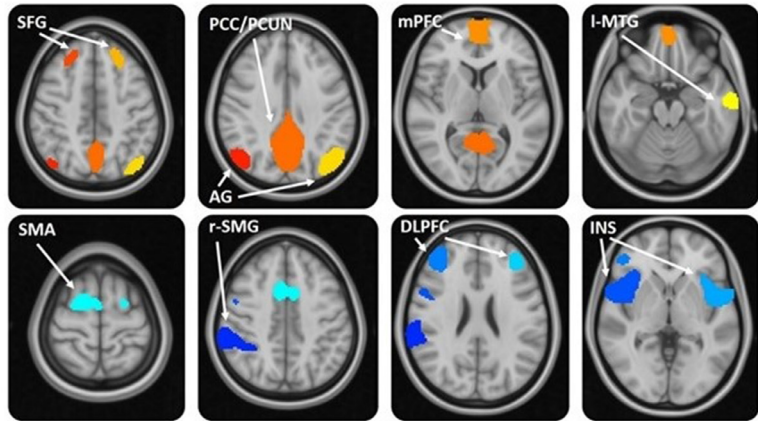| Region of interest	Peak coordinates			N_{vox}
	MNI_x	MNI_y	MNI_z	
Default Mode Network				
PCC/PCUN	-1	-57	26	5561
mPFC	-1	59	2	2537
right-AG	48	-66	31	1024
left-AG	-45	-69	31	1712
right-SFG	24	33	45	170
left-SFG	-22	34	45	267
left-MTG	-61	-12	-21	287
Anti-Correlated Network				
SMA	7	4	53	1630
right-SMG	56	-38	38	2142
right-INS	48	10	3	2093
left-INS	-47	6	-0	1406
right-DLPFC	40	42	19	1074
left-DLPFC	-37	41	22	347

Fig. 1. Seed-based network parcellation of residual time-series. (*Nvox = number of voxels; PCC/PCUN = posterior cingulate cortex/precuneus; mPFC = medial prefrontal cortex; AG = angular gyrus; SFG = superior frontal gyrus; MTG = middle temporal gyrus; SMA = supplementary motor area; SMG = supramarginal gyrus; INS = insular cortex; DLPFC = dorsolateral prefrontal cortex*). Note: the color index does not refer to specific labels but serves to aid the visual distinction of region borders.

2.6.3. Feature extraction

Based on previous findings, we were interested in local changes in prestimulus oscillatory power across multiple frequency bands. To extract prestimulus frequency power, data were first baseline corrected (1000 ms prestimulus) and pooled into four channel clusters centered above frontal, bilateral parietal, and occipital scalp locations (Supplementary Figure A.1A). These clusters were selected to provide both sufficient coverage of widespread cortical areas and allow inferences on local changes with respect to the underlying functional anatomy and comparison to other studies. Data were then re-epoched from −1000 ms to 0 ms post-stimulus and processed with Fast Fourier Transform (FFT) with a Hanning window of 10%, resulting in a frequency resolution of 0.977 Hz. The sum of the power values was then extracted for four frequency bands (delta [1–4 Hz], theta [4–8 Hz], alpha [8–12 Hz], and beta [12–30 Hz]) at each channel cluster, yielding 16 single-trial prestimulus frequency power features per subject.

Furthermore, we were interested in differences in amplitudes of event-related EEG signals across midline occipital (MidOcc), occipitotemporal (OccTem), midline parietal (MidPar), and midline frontal (MidFro) channel clusters, roughly corresponding to the scalp distributions of P1, N1, P300, and associated frontal ERPs, respectively (Supplementary Figure A.1B). Where the posterior P1 and N1 are believed to signal early perceptual processes in the visual domain, the later P300 component is thought to index working memory and related cognitive processes (Shendan and Lucia, 2010). We used an offset of 8 ms to correct for the delay from the anti-aliasing filter of the Net Amps 300 amplifier. Data were baseline corrected (100 ms prestimulus) and pooled into aforementioned ERP clusters. Semi-automatic artifact correction was performed (gradient threshold 50 μV/ms, amplitude criteria ±100 μV, and low activity criterion 0.5 μV/100 ms) and applied to the full epoch after visual verification. The 0 to 600 ms post-stimulus time window was then subdivided into 24 bins of 25 ms and the mean of raw amplitudes was extracted for each bin at each ERP channel cluster, which generated 96 single-trial ERP features per subject.

2.7. Pupillometry

2.7.1. Acquisition

Pupil diameter (PD) of the left eye was continuously recorded with EyeLink 1000 and EyeLink 1000 Plus tracking systems (SR Research, Ottawa, Canada) at a sampling rate of 1000 Hz.

2.7.2. Preprocessing

Blinks were identified using EyeLink's built-in online saccade and blink detection algorithm and linearly interpolated using the start-saccade and end-saccade markers as start and end points of each blink, respectively. Visual inspection showed that blink offset was registered prematurely across the majority of blinks and a correctional buffer of 70 ms was added to the end-saccade markers. If blink duration exceeded 1500 ms, data between the start-saccade and end-saccade markers were removed. Remaining artifacts were identified by thresholding single-trial PD ranges (−400 ms to 1000 ms post-stimulus) at the 95th percentile. Most of these extreme PD ranges were caused by large eye movements or technical issues with pupil tracking rather than physiological changes in pupil size. Trials containing such artifacts or with more than 40% missing data were excluded from further analysis (12.7% of trials across all subjects).

2.7.3. Feature extraction

Due to the tempo at which stimuli were presented, we found that baseline pupil fluctuations were contaminated by evoked dilations from preceding trials, preventing selection of single-trial time windows for determining baseline PD. We therefore developed a novel method for modeling pupillometric changes for fast-paced task designs, which is documented in detail in the recently developed package Pypillometry (Mittner, 2020). First, the preprocessed signal was low-pass filtered with a zero-phase shift second-order Butterworth filter, preserving signal fluctuations slower than 2 Hz. The lower peaks in the signal were then identified based on their prominence and connected through cubic spline interpolation. This resulted in a lower-peak envelope that was used as an estimation of the tonic, baseline fluctuations on which the phasic, pupil responses are superimposed. Consequently, single-trial baseline pupil diameter (BPD) was featured as the value of the lower peak-envelope at stimulus onset for each trial. To determine evoked pupil diameter (EPD), single-trial regressors with a delta-peak at each stimulus and response onset (if any) were prepared and convolved with an Erlang gamma function: $h = s \times t^n \times e^{-n/t_{max}}$, where $s = 1/10^{24}$ equals a scaling constant and $n = 10$ and $t_{max} = 930$ are empirically determined constants (Hoeks and Levelt, 1993). After subtraction of the baseline signal, the data were fitted with a linear regression model. Since pupil diameter cannot physiologically reach a value below zero, the beta coefficients of the model were constrained to be positive with a non-negative least-squares solver as implemented in scipy.optimize.nnls() by using the for-

mula: $\text{argmin}_b||Xb-y||_2$ for $b \geq 0$ (Lawson and Hanson, 1987). Single-trial estimators for EPD were then defined as the estimated b coefficients at each trial.

2.8. Supervised machine learning

Following previous machine learning studies of mind wandering (e.g., Mittner et al., 2014; Jin et al., 2019), we used a non-linear support vector machine (SVM) with radial basis functions (RBF) as kernel to classify single trials into on-task or off-task attentional states with scikit-learn.svm (Pedregosa et al., 2011). SVM classifiers attempt to separate classes with a hyperplane that is optimized by maximizing its margin. Besides generally being well understood and effective in high dimensionality, SVM's do not require a linear relationship between target labels and predictor variables and were shown to outperform (linear) logistic regression analysis when predicting mind wandering with EEG (Jin et al., 2019). The SVM-RBF was trained on a dataset containing the three trials (4.2 s) preceding each thought probe, resulting in $n = 3655$ trials that were assigned the dichotomized probe responses as target labels. Training was based on a total of 205 single-trial features that could be grouped in five modalities: (i) activation in seven DMN and six ACN nodes; (ii) intra-network and inter-network dynamic functional connectivity ([DMN × DMN], [ACN × ACN], [DMN × ACN]); (iii) prestimulus frequency power in four bands [delta, theta, alpha, beta] at four channel clusters [frontal, bilateral parietal, occipital]; (iv) ERP amplitudes at four channel clusters [MidFro, MidPar, OccTemp, MidOcc] in 24 time windows; and (v) baseline and evoked PD. Features in the fMRI and pupil modalities were standardized (z-scored) within each subject, whereas the frequency power features were standardized within subjects and channel clusters. The ERP features were first baseline corrected by subtracting the mean at stimulus onset at each trial for each ERP within subjects and then standardized by dividing by the standard deviation across trials for each subject.

First, tuning parameters for the SVM-RBF were optimized through grid-search over a large range of values (2^{-1} to 2^{15} for soft-margin C and 2^{-20} to 2^0 for kernel-width γ) and leave-one-subject-out cross-validation (LOSOCV), using the F1 metric as objective function. In this procedure, the classifier was trained on all possible combinations of datasets of size $n - 1$ in order to predict the one dataset that was left out. Classification performance was measured as the accuracy, recall, and precision averaged across all folds, where recall (sensitivity) reflects the ability to detect positive cases and precision (positive predictive value) is the proportion of positive cases that were correctly identified. Second, the most optimal set of features was evaluated with recursive feature elimination (RFE), in which all possible combinations of feature sets of size $n - 1$ were evaluated with LOSOCV. The feature set with the highest cross-validated (CV) mean F1 score was then selected, resulting in the elimination of one feature at every iteration. This process was repeated until the size of the feature set was $n = 1$. The feature set that produced the highest mean CV accuracy across all iterations was then selected as the final set and used to classify the remaining, unlabeled data.

Additionally, we performed a cross-modality RFE procedure for each of the five modalities separately (node activity, functional connectivity, frequency power, ERP amplitudes, and pupil diameter), for each combination of modalities (all doubles, triples, and quadruples), as well as for the full five-modality classifier decribed above. This resulted in a total of 31 independent classifiers that allowed assessment of the pattern of feature elimination across different combinations of modalities. The proportion of times a feature survived elimination in a classifier relative to the number of times the modality was represented was used to indicate a feature's importance (0 being always eliminated and 1 being never eliminated), or the amount of predictive information as perceived by the classifier with respect to distinguishing off-task from on-task trials.
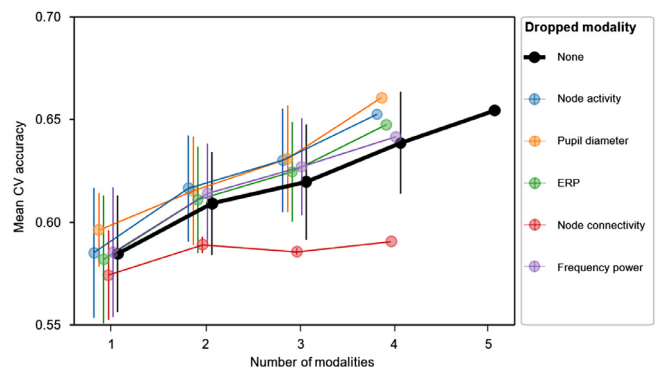

Fig. 2. The effect of dropping modalities from support vector machines on cross-validated (CV) classification performance. Averages and error bars (SE) are calculated across all 31 fits from the cross-modality RFE procedure. Classification performance increases as a function of the number of modalities added to the classifier. Note that exclusion of dynamic functional connectivity features (red) results in the lowest accuracy scores, suggesting that classification of attentional state was mostly driven by information contained in this modality.

3. Results

3.1. Behavioral performance is impaired during mind wandering

During the SART, participants indicated on 42.6% of total thought probes that their attention was focused on internal trains of thought rather than on the task or external distractions. In line with our expectations, behavioral performance was significantly worse preceding off-task reports, with higher RT_{CV} (ms) ($M_{\text{OFF}} = 236$, $M_{\text{ON}} = 184$, $t(27) = 4.00$, $p < 0.001$), proportion of omission errors ($M_{\text{OFF}} = 0.046$, $M_{\text{ON}} = 0.014$, $t(27) = 2.91$, $p < 0.01$), and proportion of commission errors ($M_{\text{OFF}} = 0.064$, $M_{\text{ON}} = 0.025$, $t(27) = 5.48$, $p < 0.0001$). Mean RT (ms) was slightly but significantly shorter preceding off-task reports ($M_{\text{OFF}} = 373$, $M_{\text{ON}} = 386$, $t(27) = -2.36$, $p < 0.05$).

3.2. Modalities contribute to the prediction of mind wandering episodes

The optimized SVM-RBF performed single-trial classification with a mean accuracy of 65% (F1 = 0.51, 57% recall and 54% precision) based on a set of 74 features (36.1% of total), indicating an above chance-level ability to predict the incidence of TUT episodes. The cross-modality RFE procedure furthermore revealed a linear increase in accuracy with increasing number of modalities added to the classifier, suggesting that features from each modality contribute unique spatial and temporal information that improves the prediction of TUTs (Fig. 2). Collectively, intra-network and inter-network functional connectivity features carried most of this predictive information, as all classifiers performed worse when this modality was excluded. Individual feature importance scores from the cross-modality RFE procedure are presented in Supplementary Figure A.2.

3.3. The multimodal neural signatures of mind wandering

After supervised classification learning, all features were standardized and averaged separately for all trials classified as either off-task or on-task (Fig. 3). Whether a feature survived the elimination procedure of the optimized five-modality SVM-RBF was interpreted as an indication of that feature's significance in predicting TUT episodes. Contrary to expectations, all nodes of the DMN showed a stronger mean signal in on-task trials compared to off-task trials. In contrast, all nodes of the ACN were more active during off-task, with the exception of the right-SMG (Fig. 3A). Whereas most nodes were selected in the optimized classifier, the PCC and right-SFG (DMN) and right-DLPFC (ACN) did not survive
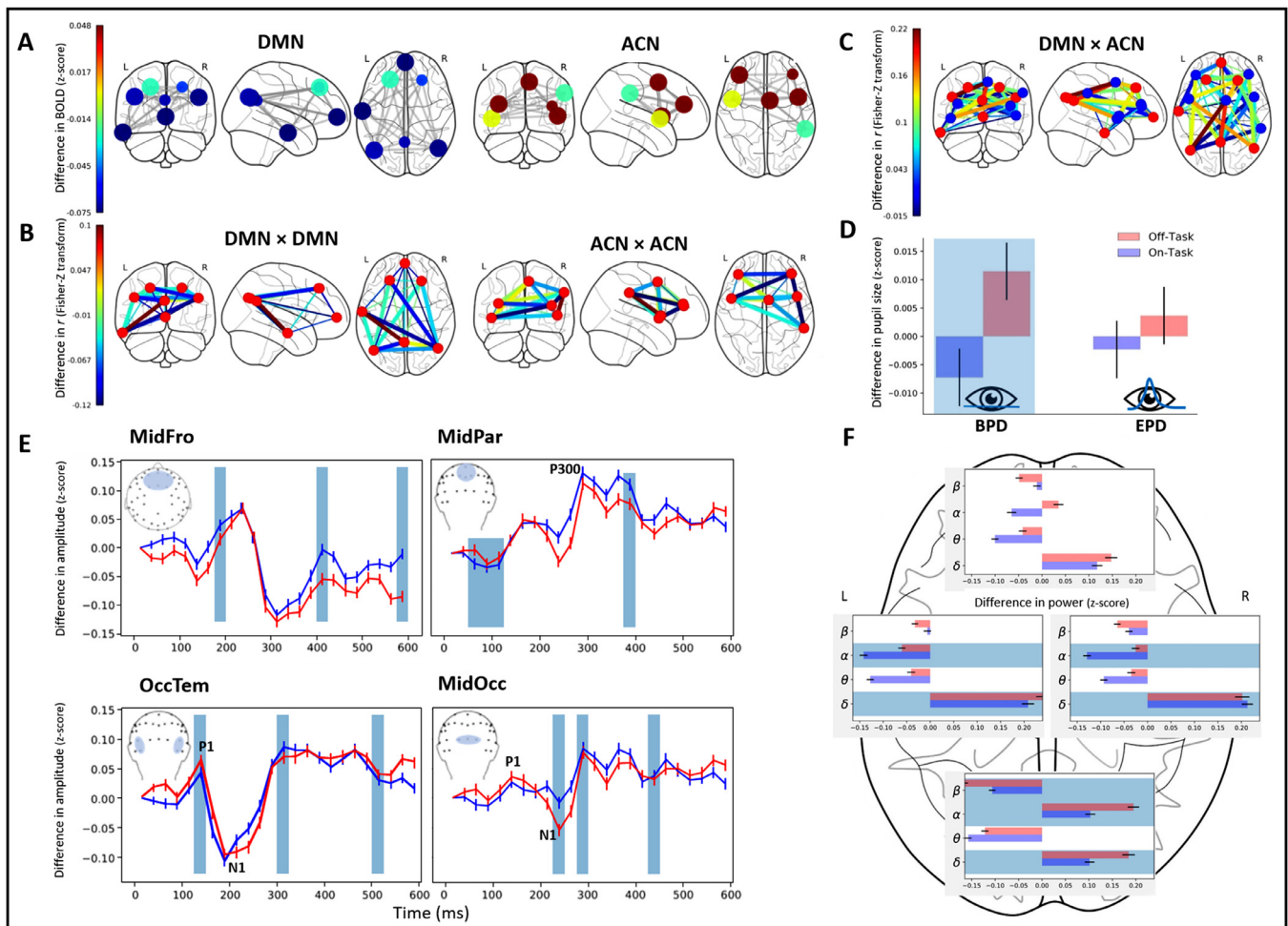
Fig. 3. Standardized feature activation across all trials after supervised classification learning. **(A)** Average difference (off-task minus on-task) in DMN (left) and ACN (right) node activity, where positive values indicate stronger activity during off-task and negative values stronger activity during on-task. **(B)** Average difference in intra-DMN and intra-ACN node-pair connectivity, where positive values indicate stronger positive correlation (less anticorrelation) during off-task and negative values stronger positive correlation during on-task. **(C)** Average difference in inter-network node-pair connectivity. **(D)** Average baseline and evoked PD separately for off-task (red) and on-task (blue). **(E)** Average amplitudes in bins of 25 ms (0–600 ms post-stimulus) per ERP channel cluster separately for off-task and on-task. **(F)** Average prestimulus beta (β), alpha (α), theta (θ), and delta (δ) frequency power per channel cluster separately for off-task and on-task, where more positive (less negative) values indicate more power. Features that survived elimination are indicated by larger (vs. smaller) nodes, thicker (vs. thinner) edges, or lightblue colored backgrounds (*DMN = default mode network; ACN = anticorrelated network; PD = pupil diameter; MidFro = midline frontal; MidPar = midline parietal; OccTem = occipitotemporal; MidOcc = midline occipital*).

feature elimination, suggesting that signal fluctuations within these regions were not predictive of TUT episodes.

For both networks, nodes were more often positively correlated with each other during on-task trials compared to off-task trials (28 of 36 node-pairs; Fig. 3B). Interestingly, four of five intra-DMN connections that were positively correlated during off-task were connected to the PCC, including: left-MTG, right-AG, and bilateral SFG. From these, the PCC to left-MTG connection was the strongest, whereas the connections with the SFG and the remaining connection (right-SFG to left-MTG) were weakest and did not survive feature elimination. For the ACN, all three node-pairs that were positively correlated in off-task trials were selected by the optimized SVM-RBF (from strongest to weakest: right-SMG to right-INS, left-INS to SMA, and right-SMG to left-DLPFC [visible in the coronal view of the ACNxACN plot in Fig. 3B]).

Whereas most of the intra-network connections were positively correlated during on-task, the majority of inter-network node-pairs were positively correlated during off-task (38 of 42 node-pairs; Fig. 3C). The positive connections that were not eliminated often included the SMA (from strongest to weakest: left-AG, PCC, right-SFG), PCC (SMA, left-INS, right-DLPFC), left-INS (right-AG, right-SFG, PCC), left-DLPFC

(left-AG, right-SFG, mPFC), and right-SFG (SMA, left-INS, right-SMG). Thus, whereas information in the PCC and right-SFG themselves did not distinguish between on-task and off-task states, their functional interregional connections seem important for predicting TUT episodes. Similar roles for the SMA and left-INS are unsurprising given their high anatomical and functional heterogeneity and their involvement in domain-general cognitive processes (Uddin et al., 2017; Cona and Semenza, 2017; Ruan et al., 2018).

With respect to the pupil features, BPD was selected in the optimized SVM-RBF and indicated more dilation in off-task compared to on-task trials, indicating higher levels of tonic NE (Fig. 3D). Pupillary response, however, did not seem to differentiate between the two states and was eliminated. Similarly, we observed that early positive and negative peaks reflecting P1 and N1 components, respectively, were more pronounced in off-task states, indicating the absence of attenuated early perceptual processing (Fig. 3E). However, decreased amplitudes at especially the midline frontal and parietal clusters from 250 to 300 ms onward implicate reduced information processing during off-task states at later latencies. Although several early bins did survive feature elimination, the majority of retained features occurred after the 200 ms post-

stimulus mark (8 of 13 bins), suggesting that late rather than early event-related signals were predictive of mind wandering.

The frequency power analysis revealed a global increase in prestimulus alpha, theta, and delta power during mind wandering, with the exception of delta power over the right parietal cortex (Fig. 3F). In contrast, beta power was consistently reduced in off-task compared to on-task trials across the scalp. Although bilateral parietal alpha and beta features also survived elimination, the greatest changes in power were observed over the occipital cortex. None of the theta features were selected in the optimized SVM-RBF, suggesting that theta power itself did not contribute to classification and that the predictive information contained in theta fluctuations was instead carried by other features.

4. Discussion

The detection of ongoing covert cognitive processes in humans has been a problem facing significant methodological challenges. The present study provides new insights into the neural markers that reflect the attentional shift from externally-oriented cognition toward self-generated trains of thought. By integrating single-trial features across multiple neural modalities in a classification learning algorithm, we showed that specific patterns of fMRI activity and connectivity, EEG markers, and baseline pupil size were predictive of TUTs. Although each neural modality provided unique information that improved classification performance, the greatest predictive power encompassed dynamic interactions within and between intrinsic connectivity networks (ICNs), including the DMN and ACN.

Our results indicate recruitment of ACN nodes during TUTs. This finding is not surprising given the growing body of evidence advocating a role for these regions in spontaneous thought processes (Christoff et al., 2009; Fox et al., 2015; Dixon et al., 2018). Specifically, their recruitment has been suggested to reflect a mechanism in which top-down control systems exert deliberate constraints on the stream of internally-oriented thoughts in order to guide them toward motivationally relevant or rewarding goals (Christoff et al., 2016; Shepard, 2019). According to this view, mind wandering may be characterized by the redistribution of executive and attentional resources toward the internal environment driven by the prioritization of relevant information (Turnbull et al., 2019b).

In line with this, it has been argued that attentional decoupling in the form of suppression of sensory inputs may serve adaptive functions by insulating the stream of thought from external interference (Kam and Handy, 2013; Smallwood, 2013). Although we did not find evidence for deficits in early sensory processing, our results may be interpreted as cognitive disengagement from task-relevant information as reflected in reduced amplitudes of P300 and midfrontal ERPs prior to self-reported TUTs. Correspondingly, task performance was significantly affected as indexed by increased RT variability and error rates. This corroborates an earlier finding (O'Connell et al., 2009) and may imply that the shallow processing of visual information remains relatively unimpaired during mind wandering, whereas later cognitive and decision-making processes involved in assimilating the deeper meaning of stimuli needed to accurately perform the task are disrupted.

Contrary to expectations, we did not observe any increase in DMN activity during mind wandering. Although this finding seems counterintuitive, previous studies have reported a similar association between the recruitment of DMN regions and optimized behavior ("in-the-zone"), whereas suboptimal behavioral performance ("out-the-zone") was instead associated with DAN activation (Esterman et al., 2014; Kucyi et al., 2017; Yamashita et al., 2020). Although speculative, together these findings may point to DMN activity during task-focused attention as representing a weaker engagement in goal-directed behavior or attentional stability needed to accurately perform the task. Indeed, it is generally assumed that habitual response tendencies are developed early during repetitive tasks such as the SART and thus stable performance may rely

more heavily on automatic processes (Hawkins et al., 2019). As previous work has suggested a role for the DMN in automated cognition as opposed to mindful, focused attention (Shamloo and Helie, 2016; Vatansever et al., 2017; Scheibner et al., 2017), our findings may be tentatively interpreted as a lesser engagement of top-down resources during the (more automated) task-focused state compared to the (more goal-directed) mind wandering state (Christoff et al., 2016; Seli et al., 2016).

An alternative explanation may be that parts of the DMN, specifically its core nodes (PCC and mPFC), are not directly involved in mind wandering but rather function as a "global workspace" by tailoring their activity to the temporal dynamics of other ICNs (Mittner et al., 2016). Thus, when attention is focused either externally (oriented to the task) or internally (mind wandering), functionally specific networks are recruited to support goal-directed behavior whereas converging network activity is lowered, resulting in deactivation of the PCC and mPFC. While we did not observe that single-trial activity in the PCC itself was predictive of TUTs, our results indicate high importance of the dynamic coupling between the PCC and other nodes of the DMN and ACN during both task-related and task-unrelated thought. Together with previous work (Leech et al., 2012; Kucyi and Davis, 2014; Lin et al., 2016; Zhou et al., 2019), this finding supports the intriguing possibility that the PCC is involved in the coordination of network interactions to regulate shifts in attentional focus by maintaining or suppressing ongoing trains of thought.

Importantly, previous work has demonstrated the significance of context for the role that different networks play in ongoing thought. Activity in both the DMN and ACN has been associated with task-related as well as task-unrelated cognitive operations, depending on task difficulty (Turnbull et al., 2019a, 2019b; Konu et al., 2020). These findings align with the context-regulation hypothesis, which states that mind wandering instances are adaptively regulated depending on environmental demands in order to minimize the negative impact on maintaining task performance (Smallwood and Andrews-Hanna, 2013). Thus, to better understand how complex large-scale network activity gives rise to mind wandering, specific task effects need to be considered. One such task characteristic that varies among studies is pacing of trials. Compared to previous studies showing a link between the DMN and mind wandering, the SART design in the current study was faster paced (stop-signal paradigm; Mittner et al., 2014) and contained a lower proportion of target trials and was overall shorter in duration (SART; Christoff et al., 2009). Therefore, the role that the DMN plays in mind wandering during a sustained task may depend heavily on such effects.

Previous work indicates that the interactions within and between ICNs dynamically reconfigure to transient changes in ongoing cognitive processes such as mind wandering (Thompson et al., 2013; Mittner et al., 2014). Accordingly, we observed high importance of information contained in functional connectivity compared to other modalities. Specifically, our results indicate that mind wandering is associated with overall decreased connectivity within and increased connectivity between the DMN and ACN. Thus, whereas these networks are intrinsically anticorrelated at rest (Fox et al., 2005), the dynamic coupling between them during sustained attentional demands may support spontaneous fluctuations in ongoing internal trains of thought (Smallwood et al., 2012b; Dixon et al., 2018).

The electrophysiological origin of this coupling may concern theta-band oscillations (Kam et al., 2019), which is in line with our observation of a widespread increase in theta power during TUTs, even though theta power itself was not found to be predictive of mind wandering. We also replicated increases in alpha power and reduced beta power across the cortex (Jin et al., 2019; Compton et al., 2019; Van Son et al., 2019). Although the functional significance of alpha oscillations remains ambiguous, our data imply a role in active mind wandering that may involve inhibition of irrelevant representations and top-down interference (Palva and Palva, 2011; Benedek et al., 2011). In addition, the increase in synchronized delta-band activity over frontal, left parietal, and occip-

ital areas may have been involved in the maintenance of ongoing trains of thought by inhibiting interfering information (Harmony, 2013).

Similarly, our findings indicate increases in baseline pupil size during mind wandering compared to task-focused attention, which may reflect higher levels of tonic NE and has been proposed to underlie the reduced sensitivity to external interference favoring mental exploration (Murphy et al., 2011; Smallwood et al., 2012a). Consequently, as exploitation of task-relevant information is no longer prioritized, the cognitive capacity for pursuing alternative goals that are motivationally salient is enhanced (Bouret and Richmond, 2015). Possibly, the low incentive of the SART may warrant the adaptive redistribution of intrinsic motivation, regardless of its detrimental effect on performance. Together with our observations in other modalities, this implies that TUTs in our study were characterized by effortful and guided cognition rather than a state of low alertness or arousal. Although previous work also suggests a linear relationship between phasic NE and task performance, we did not observe any contributions from evoked pupil responses in differentiating attentional state.

One continuing challenge concerns the differences in measuring mind wandering, complicating the comparison of findings across studies. Research has shown that mind wandering is a non-uniform construct that varies along dimensions of intentionality (Seli et al., 2016), meta-awareness (Christoff et al., 2009), temporal locus (Liefgreen et al., 2020), emotional valence (Banks et al., 2016), self-relevance (Bocharov et al., 2019), and arousal (Unsworth and Robison, 2018), which likely contributes to the divergent patterns of neural activation. The current study is likewise limited by the use of uni-dimensional experience sampling followed by a coarse dichotomy of attentional state. Therefore, our attempt to capture the spatiotemporal dynamics of TUTs within one signature based on a single task may compromise the generalizability of our results. Although the SART is an attractive and widely used paradigm to study mind wandering, more complex designs are necessary to disentangle the effect of TUTs on other cognitive processes and behavior (Boayue et al., 2020).

The low complexity of the paradigm combined with individual biases in self-report due to variation in meta-awareness or thought content may have negatively influenced classification performance. Although we achieved above chance-level detection of attentional state with 65% accuracy across subjects, a previous study reported 79% accuracy based on fMRI and pupil measures alone (Mittner et al., 2014). However, other EEG classifiers showed similar detection levels of TUTs (Dhindsa et al., 2019; Jin et al., 2019) which substantially improved when models were fitted to individual datasets, suggesting that high inter-individual variability in EEG markers can affect cross-subject classification.

5. Conclusion

Although proven to be detrimental to maintaining attention to task-relevant events, the capability to engage in internal trains of thought is integral to human neurocognitive functioning. More accurate detection of mind wandering episodes will lead to a more profound understanding of its effect on other cognitive processes. However, such detection is complicated as cognition evolves dynamically in complex spatiotemporal patterns. Multimodal classification enabling single-trial analyses may provide effective means to gain mechanistic insights into the neural basis of attentional fluctuations. We hope that our findings will motivate future studies to consider an agnostic, whole-brain approach to better entangle the respective contributions of dynamic interactions. Furthermore, employing paradigms that allow continuous tracking of attentional intensity combined with neuroimaging are better suited to investigate the evolution of task-unrelated trains of thought with higher temporal precision.

Declaration of Competing Interest

None.

CRediT authorship contribution statement

Josephine M Groot: Formal analysis, Methodology, Data curation, Visualization, Writing - original draft. **Nya M Boayue:** Formal analysis, Writing - review & editing. **Gábor Csifcsák:** Formal analysis, Writing - review & editing. **Wouter Boekel:** Methodology, Investigation, Writing - review & editing. **René Huster:** Formal analysis, Writing - review & editing. **Birte U Forstmann:** Conceptualization, Methodology, Writing - review & editing, Supervision, Funding acquisition. **Matthias Mittner:** Conceptualization, Methodology, Software, Formal analysis, Writing - review & editing, Supervision, Funding acquisition.

Supplementary materials

Supplementary material associated with this article can be found, in the online version, at doi:10.1016/j.neuroimage.2020.117412.

References

Allen, P.J., Josephs, O., Turner, R., 2000. A method for removing imaging artifact from continuous EEG recorded during functional MRI. Neuroimage 12, 230–239.

Aston-Jones, G., Cohen, J.D., 2005. An integrative theory of locus coeruleus-norepinephrine function: adaptive gain and optimal performance. Ann. Rev. Neurosci. 28, 403–450.

Banks, J.B., Welhaf, M.S., Hood, A.V.B., Boals, A., Tartar, J.L., 2016. Examining the role of emotional valence of mind wandering: all mind wandering is not equal. Conscious. Cogn. 43, 167–176.

Bastian, M., Sackur, J., 2013. Mind wandering at the fingertips: automatic parsing of subjective states based on response time variability. Front. Psychol. 4, 573.

Benedek, M., Bergner, S., Könen, T., Fink, A., Neubauer, A.C., 2011. EEG alpha synchronization is related to top-down processing in convergent and divergent thinking. Neuropsychologia 49, 3505–3511.

Boayue, N.M., Csifcsák, G., Kreis, I.V., Schmidt, C., Finn, I., Vollsund, A.E.H., Mittner, M., 2020. The interplay between cognitive control, behavioral variability and mind wandering: insights from a HD-tDCS study. PsyArXiv doi:10.31234/osf.io/d9ngb.

Bocharov, A.V., Knyazev, G.G., Savostyanov, A.N., Astakhova, T.N., Tamozhnikov, S.S., 2019. EEG dynamics of spontaneous stimulus-independent thoughts. Cogn. Neurosci. 10, 77–87.

Bouret, S., Richmond, B.J., 2015. Sensitivity of locus ceruleus neurons to reward value for goal-directed actions. J. Neurosci. 35, 4005–4014.

Bowman, A.D., Griffis, J.C., Visscher, K.M., Dobbins, A.C., Gawne, T.J., DiFrancesco, M.W., Szaflarski, J.P., 2017. Relationship between alpha rhythm and the default mode network: an EEG-fMRI study. J. Clin. Neurophysiol. 34, 527–533.

Christoff, K., Gordon, A.M., Smallwood, J., Smith, R., Schooler, J.W., 2009. Experience sampling during fMRI reveals default network and executive system contributions to mind wandering. Proc. Natl Acad. Sci. USA 106, 8719–8724.

Christoff, K., Irving, Z.C., Fox, K.C.R., Spreng, N., Andrews-Hanna, J.R., 2016. Mind-wandering as spontaneous thought: a dynamic framework. Nat. Rev. Neurosci. 17, 718–731.

Compton, R.J., Gearinger, D., Wild, H., 2019. The wandering mind oscillates: EEG alpha power is enhanced during moments of mind-wandering. Cogn. Affect. Behav. Neurosci. 19, 1184–1191.

Cona, G., Semenza, C., 2017. Supplementary motor area as key structure for domain-general sequence processing: a unified account. Neurosci. Biobehav. Rev. 72, 28–42.

Delorme, A., Makeig, S., 2004. EEGLAB: an open source toolbox for analysis of single-trial EEG dynamics including independent component analysis. J. Neurosci. Methods 134, 9–21.

Dhindsa, K., Acai, A., Wagner, N., Bosynak, D., Kelly, S., Bhandari, M., Petrisor, B., Sonnadara, R.R., 2019. Individualized pattern recognition for detecting mind wandering from EEG during live lectures. PLoS One 14, 0222276.

Dixon, M.L., De La Vega, A., Mills, C., Andrews-Hanna, J., Spreng, R.N., Cole, M.W., Christoff, K., 2018. Heterogeneity within the frontoparietal control network and its relationship to the default and dorsal attention networks. Proc. Natl Acad. Sci. USA 115, 1598–1607.

Elton, A., Gao, W., 2015. Task-positive functional connectivity of the default mode network transcends task domain. J. Cogn. Neurosci. 27, 2369–2391.

Esterman, M., Rosenberg, M.D., Noonan, S.K., 2014. Intrinsic fluctuations in sustained attention and distractor processing. J. Neurosci. 34, 1724–1730.

Fox, K.C.R., Spreng, R.N., Ellamil, M., Andrews-Hanna, J.R., Christoff, K., 2015. The wandering brain: meta-analysis of functional neuroimaging studies of mind-wandering and related spontaneous thought processes. Neuroimage 111, 611–621.

Fox, M.D., Snyder, A.Z., Vincent, J.L., Corbetta, M., Van Essen, D.C., Raichle, M.E., 2005. The human brain is intrinsically organized into dynamic, anticorrelated functional networks. Proc. Natl Acad. Sci. USA 102, 9673–9678.

Gilzenrat, M.S., Nieuwenhuis, S., Jepma, M., Cohen, J.D., 2010. Pupil diameter tracks changes in control state predicted by the adaptive gain theory of locus coeruleus function. Cogn. Affect. Behav. Neurosci. 10, 252–269.

Gorgolewski, K., Burns, C.D., Madison, C., Clark, D., Halchenko, Y.O., Waskom, M.L., Ghosh, S.S., 2011. Nipype: a flexible, lightweight and extensible neuroimaging data processing framework in python. Front. Neuroinform. 5, 13.

Grandchamp, R., Braboszcz, C., Delorme, A., 2014. Oculometric variations during mind wandering. Front. Psychol. 5, 31.

Gratton, C., Laumann, T.O., Nielsen, A.N., Greene, D.J., Gordon, E.M., Gilmore, A.W., Nelson, S.M., Coalson, R.S., Snyder, A.Z., Schlagger, B.L., Dosenbach, N.U.F., Petersen, S.E., 2018. Functional brain networks are dominated by stable group and individual factors, not cognitive or daily variation. Neuron 98, 439–452.

Harmony, T., 2013. The functional significance of delta oscillations in cognitive processing. Front. Integr. Neurosci. 7, 83.

Hawkins, G.E., Mittner, M., Forstmann, B.U., Heathcote, A., 2019. Modeling distracted performance. Cogn. Psychol. 112, 48–80.

Hoeks, B., Levelt, W.J.M., 1993. Pupillary dilation as a measure of attention: a quantitative system analysis. Behav. Res. Methods 25, 16–26.

Jenkinson, M., Bannister, P., Brady, J.M., Smith, S.M., 2002. Improved optimisation for the robust and accurate linear registration and motion correction of brain images. Neuroimage 17, 825–841.

Jenkinson, M., Beckmann, C.F., Behrens, T.E.J., Woolrich, M.W., Smith, S.M., 2012. FSL. Neuroimage 62, 782–790.

Jenkinson, M., Smith, S.M., 2001. A global optimisation method for robust affine registration of brain images. Med. Image Anal. 5, 143–156.

Jin, C.Y., Borst, J.P., Van Vugt, M.K., 2019. Predicting task-general mind-wandering with EEG. Cogn. Affect. Behav. Neurosci. 19, 1059–1073.

Jin, C.Y., Borst, J.P., Van Vugt, M.K., 2020. Distinguishing vigilance decrement and low task demands from mind-wandering: a machine learning analysis of EEG. Eur. J. Neurosci. 00, 1–18.

Kam, J.W.Y., Dao, E., Farley, J., Fitzpatrick, K., Smallwood, J., Schooler, J.W., Handy, T.C., 2011. Slow fluctuations in attentional control of sensory cortex. J. Cogn. Neurosci. 23, 460–570.

Kam, J.W.Y., Handy, T.C., 2013. The neurocognitive consequences of the wandering mind: a mechanistic account of sensory-motor decoupling. Front. Psychol. 4, 725.

Kam, J.W.Y., Lin, J.J., Solbakk, A.-K., Endestad, T., Larsson, P.G., Knight, R.T., 2019. Default network and frontoparietal control network theta connectivity supports internal attention. Nat. Hum. Behav. 3, 1263–1270.

Konishi, M., Brown, K., Battaglini, L., Smallwood, J., 2017. When attention wanders: pupillometric signatures of fluctuations in external attention. Cognition 168, 16–26.

Konu, D., Turnbull, A., Karapanagiotidis, T., Wang, H.-T., Brown, L.R., Jefferies, E., Smallwood, J., 2020. A role for the ventromedial prefrontal cortex in self-generated episodic social cognition. Neuroimage 218, 116977.

Kucyi, A., Davis, K.D., 2014. Dynamic functional connectivity of the default mode network tracks daydreaming. Neuroimage 100, 471–480.

Kucyi, A., Hove, M.J., Esterman, M., Hutchison, R.M., Valera, E.M., 2017. Dynamic brain network correlates of spontaneous fluctuations in attention. Cereb. Cortex 27, 1831–1840.

Kucyi, A., 2018. Just a thought: how mind-wandering is represented in dynamic brain connectivity. Neuroimage 180, 505–514.

Kucyi, A., Tambini, A., Sadaghiani, S., Keilholz, S., Cohen, J.R., 2018. Spontaneous cognitive processes and the behavioral validation of time-varying brain connectivity. Network Neurosci. 2, 397–417.

Lawson, C., Hanson, R.J., 1987. Solving Least Squares Problems. SIAM, Philadelphia, PA.

Leech, R., Braga, R., Sharp, D.J., 2012. Echoes of the brain within the posterior cingulate cortex. J. Neurosci. 32, 215–222.

Liefgreen, A., Dalton, M.A., Maguire, E.A., 2020. Manipulating the temporal locus and content of mind-wandering. Conscious. Cogn. 79, 102885.

Lin, P., Yang, Y., Jovicich, J., De Pisapia, N., Wang, X., Zuo, C.S., Levit, J.J., 2016. Static and dynamic posterior cingulate cortex nodal topology of default mode network predicts attention task performance. Brain Imaging Behav 10, 212–225.

Maillet, D., Beaty, R.E., Kucyi, A., Schacter, D.L., 2019. Large-scale network interactions involved in dividing attention between the external environment and internal thoughts to pursue two distinct goals. Neuroimage 197, 49–59.

Margulies, D.S., Ghosh, S.S., Goulas, A., Falkiewicz, M., Huntenburg, J.M., Langs, G., Bezgin, G., Eickhoff, S.B., Castellanos, F.X., Petrides, M., Jefferies, E., Smallwood, J., 2016. Situating the default-mode network along a principal gradient of macroscale cortical organization. Proc. Natl Acad. Sci. USA 113, 12574–12579.

Marino, M., Arcara, G., Porcaro, C., Mantini, D., 2019. Hemodynamic correlates of electrophysiological activity in the default mode network. Front. Neurosci. 13, 1060.

Mason, M.F., Norton, M.I., Van Horn, J.D., Wegner, D.M., Grafton, S.T., Macrae, C.N., 2007. Wandering minds: the default mode network and stimulus-independent thought. Science 315, 393–395.

Mittner, M., Boekel, W., Tucker, A.M., Turner, B.M., Heathcote, A., Forstmann, B.U., 2014. When the brain takes a break: a model-based analysis of mind wandering. J. Neurosci. 34, 16286–16295.

Mittner, M., Hawkins, G.E., Boekel, W., Forstmann, B.U., 2016. A neural model of mind wandering. Trends Cogn. Sci. 20, 570–578.

Mittner, M., 2020. Pypillometry: a Python package for pupillometric analyses. J. Open Source Soft. 5, 2348.

Murphy, P.R., Robertsen, I.H., Balsters, J.H., O'Connell, R.G., 2011. Pupillometry and P3 index the locus coeruleus-noradrenergic arousal function in humans. Psychophysiology 48, 1532–1543.

Neuner, I., Arrubla, J., Werner, C.J., Hitz, K., Boers, F., Kawohl, W., Shah, N.J., 2014. The default mode network and EEG regional spectral power: a simultaneous fMRI-EEG study. PLoS One 9, 88214.

O'Connell, R.G., Dockree, P.M., Robertson, I.H., Bellgrove, M.A., Foxe, J.J., Kelly, S.P., 2009. Uncovering the neural signature of lapsing attention: electrophysiological signals predict errors up to **20 s** before they occur. J. Neurosci. 29, 8604–8611.

Palva, S., Palva, J.M., 2011. Functional roles of alpha-band phase synchronization in local and large-scale cortical networks. Front. Psychol. 2, 204.

Pedregosa, F., Varoquaux, G., Gramfort, A., Michel, V., Thirion, B., Grisel, O., Blondel, M., Prettenhofer, P., Weiss, R., Dubourg, V., Vanderplas, J., Passos, A., Cournapeau, D., Brucher, M., Perrot, M., Duchesnay, E., 2011. Scikit-learn: machine learning in python. J. Mach. Learn. Res. 12, 2825–2830.

Ruan, J., Bludau, S., Palomero-Gallagher, N., Caspers, S., Mohlberg, H., Eickhoff, S.B., Seitz, R.J., Amunts, K., 2018. Cytoarchitecture, probability maps, and functions of the human supplementary and pre-supplementary motor areas. Brain Struct. Funct. 223, 4169–4186.

Scheibner, H.J., Bogler, C., Gleich, T., Haynes, J.-D., Bermpohl, F., 2017. Internal and external attention and the default mode network. Neuroimage 148, 381–389.

Schooler, J.W., Smallwood, J., Christoff, K., Handy, T.C., Reichle, E.D., Sayette, M.A., 2011. Meta-awareness, perceptual decoupling and the wandering mind. Trends Cogn. Sci. 15, 319–326.

Seli, P., Risko, E.F., Smilek, D., 2016. On the necessity of distinguishing between unintentional and intentional mind wandering. Psychol. Sci. 27, 685–691.

Shamloo, F., Helie, S., 2016. Changes in default mode network as automaticity develops in a categorization task. Behav. Brain Res. 313, 324–333.

Shendan, H.E., Lucia, L.C., 2010. Object-sensitive activity reflects earlier perceptual and later cognitive processing of visual objects between 95 and 500 ms. Brain Res. 1329, 124–141.

Shepard, J., 2019. Why does the mind wander? Neurosci. Conscious 5, 014.

Smallwood, J., Beach, E., Schooler, J.W., Handy, T.C., 2008. Going AWOL in the brain: mind wandering reduces cortical analysis of external events. J. Cogn. Neurosci. 20, 458–469.

Smallwood, J., Brown, K.S., Baird, B., Mrazek, M.D., Franklin, M.S., Schooler, J.W., 2012a. Insulation of daydreams: a role for tonic norepinephrine in the facilitation of internally guided thought. PLoS One 7, 33706.

Smallwood, J., Brown, K., Baird, B., Schooler, J.W., 2012b. Cooperation between the default mode network and the frontal-parietal network in the production of an internal train of thought. Brain Res. 1428, 60–70.

Smallwood, J., 2013. Distinguishing how from why the mind wanders: a process-occurrence framework for self-generated mental activity. Psychol. Bull. 139, 519–535.

Smallwood, J., Schooler, J.W., 2015. The science of mind wandering: empirically navigating the stream of consciousness. Ann. Rev. Psychol. 66, 487–518.

Smith, S.M., 2002. Fast robust automated brain extraction. Hum. Brain Mapp. 17, 143–155.

Smith, S.M., Brady, J.M., 1997. SUSAN – a new approach to low level image processing. Int. J. Comput. Vis. 23, 45–78.

Sormaz, M., Murphy, C., Wang, H.-T., Hymers, M., Karapanagiotidis, T., Poerio, G., Margulies, D.S., Jefferies, E., Smallwood, J., 2018. Default mode network can support the level of detail in experience during active task states. Proc. Natl Acad. Sci. USA 115, 9318–9321.

Thompson, G.J., Magnuson, M.E., Merritt, M.D., Schwarb, H., Pan, W.-J., McKinley, A., Tripp, L.D., Schumacher, E.H., Keilholz, S.D., 2013. Short-time windows of correlation between large-scale functional brain networks predict vigilance intraindividually and interindividually. Hum. Brain Mapp. 34, 3280–3298.

Turnbull, A., Wang, H.-T., Schooler, J.W., Jefferies, E., Margulies, D.S., Smallwood, J., 2019a. The ebb and flow of attention: between-subject variation in intrinsic connectivity and cognition associated with the dynamics of ongoing experience. Neuroimage 185, 286–299.

Turnbull, A., Wang, H.-T., Murphy, C., Ho, N.S.P., Wang, X., Sormaz, M., Karapanagiotidis, T., Leech, R.M., Bernhardt, B., Margulies, D.S., Vatansever, D., Jefferies, E., Smallwood, J., 2019b. Left dorsolateral prefrontal cortex supports context-dependent prioritisation of off-task thought. Nat. Commun. 10, 3816.

Uddin, L.Q., Nomi, J.S., Hebert-Seropian, B., Ghaziri, J., Boucher, O., 2017. Structure and function of the human insula. J. Clin. Neurophysiol. 34, 300–306.

Unsworth, N., Robison, M.K., 2016. Pupillary correlates of lapses of sustained attention. Cogn. Affect. Behav. Neurosci. 16, 601–615.

Unsworth, N., Robison, M.K., 2018. Tracking arousal state and mind wandering with pupillometry. Cogn. Affect. Behav. Neurosci. 18, 638–664.

Van der Meer, J.N., Pampel, A., Van Someren, E.J.W., Ramautar, J.R., Van der Werf, Y.D., Gomez-Herrero, G., Lepsien, J., Hellrung, L., Hinrichs, H., Möller, H.E., Walter, M., 2016. Carbon-wire loop based artifact correction outperforms post-processing EEG/fMRI corrections – A validation of a real-time simultaneous EEG/fMRI correction method. Neuroimage 125, 880–894.

Van Maanen, L., Brown, S.D., Eichele, T., Wagenmakers, E.J., Ho, T., Serences, J., Forstmann, B.U., 2011. Neural correlates of trial-to-trial fluctuations in response caution. J. Neurosci. 31, 17488–17495.

Van Rossum, G., Drake, F., 2011. The Python Language Reference Manual. Network Theory, Bristol, UK.

Van Son, D., De Blasio, F.M., Fogarty, J.S., Angelidis, A., Barry, R.J., Putman, P., 2019. Frontal EEG theta/beta ratio during mind wandering episodes. Biol. Psychol. 140, 19–27.

Vatansever, D., Menon, D.K., Stamatakis, E.A., 2017. Default mode contributions to automated information processing. Proc. Natl Acad. Sci. USA 114, 12821–12826.

Woolrich, M.W., Ripley, B.D., Brady, M., Smith, S.M., 2001. Temporal autocorrelation in univariate linear modeling of FMRI data. Neuroimage 14, 1370–1386.

Yamashita, A., Rothlein, D., Kucyi, A., Valera, E.M., Esterman, M., 2020. Two dominant brain states reflect optimal and suboptimal attention. BioRxiv 2020.01.31.928523.

Zhang, Y., Brady, M., Smith, S., 2001. Segmentation of brain MR images through a hidden markov random field model and the expectation-maximization algorithm. IEEE Trans. Med. Imag. 20, 45–57.

Zhou, Z.-W., Lan, X.-Q., Fang, Y.-T., Gong, Y., Zang, Y.-F., Luo, H., Zhang, H., 2019. The inter-regional connectivity within the default mode network during the attentional process of internal focus and external focus: an fMRI study of continuous finger force feedback. Front. Psychol. 10, 2198.

Paper II

Catching wandering minds with tapping fingers: Neural and behavioral insights into task-unrelated cognition

Josephine Maria Groot, Gábor Csifcsák, Sven Wientjes, Birte U Forstmann, Matthias Mittner

OXFORD

Catching Wandering Minds with Tapping Fingers: Neural and Behavioral Insights into Task-unrelated Cognition

Josephine M. Groot [ID] [1,2], Gábor Csifcsák[1], Sven Wientjes[3], Birte U. Forstmann[2] and Matthias Mittner[1]

[1]Department of Psychology, UiT – The Arctic University of Norway, Tromsø 9037 , Norway
[2]Integrative Model-Based Cognitive Neuroscience Research Unit, University of Amsterdam, Amsterdam 1018 WB , The Netherlands
[3]Department of Experimental Psychology, University of Ghent, Ghent 9000 , Belgium
Address correspondence to Matthias Mittner, Department of Psychology, UiT – The Arctic University of Norway, Huginbakken 32, 9037 Tromsø, Norway. Email: matthias.mittner@uit.no

Abstract

When the human mind wanders, it engages in episodes during which attention is focused on self-generated thoughts rather than on external task demands. Although the sustained attention to response task is commonly used to examine relationships between mind wandering and executive functions, limited executive resources are required for optimal task performance. In the current study, we aimed to investigate the relationship between mind wandering and executive functions more closely by employing a recently developed finger-tapping task to monitor fluctuations in attention and executive control through task performance and periodical experience sampling during concurrent functional magnetic resonance imaging (fMRI) and pupillometry. Our results show that mind wandering was preceded by increases in finger-tapping variability, which was correlated with activity in dorsal and ventral attention networks. The entropy of random finger-tapping sequences was related to activity in frontoparietal regions associated with executive control, demonstrating the suitability of this paradigm for studying executive functioning. The neural correlates of behavioral performance, pupillary dynamics, and self-reported attentional state diverged, thus indicating a dissociation between direct and indirect markers of mind wandering. Together, the investigation of these relationships at both the behavioral and neural level provided novel insights into the identification of underlying mechanisms of mind wandering.

Keywords: approximate entropy, executive function, fMRI, mind wandering, pupillometry

Introduction

The phenomenon of mind wandering in humans can be described as the spontaneous stream of consciousness that comprises thoughts, emotions, and memories (Smallwood and Schooler 2015) that are often related to personal goals and concerns (Shepard 2019) and pervasively occur during daily life and experimental tasks (Killingsworth and Gilbert 2010; Seli, Beaty, et al. 2018). Unsurprisingly given this broad definition, mind wandering has been studied in a wide range of settings and under different labels, for example, stimulus-independent, spontaneous, and task-unrelated thought (Callard et al. 2013). Researchers have identified important dimensions of mind wandering, including intentionality (Seli et al. 2016), emotional valence (Banks et al. 2016), temporality (Maillet et al. 2017), and meta-awareness (Schooler et al. 2011). Here, we define mind wandering as self-generated thoughts that arise independently from external sensory input and pertain to any content that is unrelated to the task at hand.

Notwithstanding the diversity of contexts in which mind wandering has been previously investigated,

researchers continue in their pursuit to further unravel its underlying neural mechanisms and its effect on other cognitive processes and behavior. In particular, although there is little debate regarding the involvement of executive functions in mind wandering in general, there is no consensus on exactly how mind wandering interacts with executive control systems and whether it is better characterized as executive function use (Teasdale et al. 1995; Smallwood and Schooler 2006) or as the result of executive failure (McVay and Kane 2010; Kane and McVay 2012). Whereas some behavioral research has associated mind wandering with failures of executive control processes (Smallwood et al. 2004; McVay and Kane 2009), converging evidence from neuroimaging studies suggest that mind wandering recruits widespread cortical networks involved in goal-directed behavior, including the frontoparietal control network (FPCN) and dorsal and ventral attention networks (Christoff et al. 2009; Fox et al. 2015; Dixon et al. 2018; Turnbull et al. 2019). Interestingly, there are even reports of associations between task-related attention, as opposed to mind wandering, and greater activation of

the default mode network (DMN; Esterman et al. 2014; Kucyi et al. 2017; Groot, Boayue, et al. 2021), a network previously considered to mainly engage during resting-state and self-referential processing (Raichle 2015). Furthermore, a recent resting-state fMRI study with experience sampling demonstrated that activity in the DMN was associated with self-generated thoughts that were not independent from the external environment whereas activity in the dorsal attention network (DAN) related specifically to increases in perceived control over spontaneous thought (Van Calster et al. 2017). Together, these findings undermine the assumption that task-related and task-unrelated states of mind can be independently partitioned into specific functional networks and warrant the development of sensitive behavioral paradigms that disentangle the complex interplay between executive functions and forms of spontaneous thought.

The majority of mind wandering research reports data from self-reports through periodical thought probing and performance errors, usually during a sustained attention to response Task (SART; Christoff et al. 2009; Christoff 2012; Hawkins et al. 2019; Boayue et al. 2019). However, the SART is often slow paced and target stimuli are presented infrequently, preventing more fine-grained tracking of ongoing fluctuations in both attention and executive control. Arguably, a more suitable paradigm to investigate executive functioning is the random number generation task (RNGT; Baddeley et al. 1998) as it is assumed that the generation of random sequences of numbers or letters requires highly controlled executive processes that strategically monitor and inhibit habitual tendencies in order to avoid repetition of response patterns (Jahanshahi et al. 2000; Joppich et al. 2004; Jahanshahi et al. 2006; Peters et al. 2007). Indeed, competing processes such as mind wandering or dual task performance result in the reduced ability to produce such random behavior (Teasdale et al. 1995; Boayue et al. 2020). Thus, investigation of the relationships between the degree of sequence randomness and the occurrence of mind wandering episodes has the potential to provide insights into how the mental processes supporting departures from a task-focused state compete with the cognitive resources needed for executive task performance.

Besides monitoring executive function use, findings from several studies suggest trial-to-trial response time variability as a promising and sensitive marker for fluctuations in attentional focus (Bastian and Sackur 2013; Jubera-Garcia et al. 2019; Zanesco et al. 2020), especially when combined with a monotone and simplistic finger-tapping task that facilitates mind wandering (Seli et al. 2013; Kucyi et al. 2017). Building on these findings, Boayue et al. (2020) recently developed a fast-paced paradigm that combines both these aspects of behavior into a finger-tapping random-sequence generation task (FT-RSGT), allowing ongoing assessment of the degree of self-generated randomness as well as behavioral variability at high temporal resolution. In a series of

experiments, it was demonstrated that both measures were consistently related to mind wandering in opposite ways: variability in finger-tapping increased whereas sequence randomness decreased prior to self-reports of mind wandering throughout the task.

Similarly, several studies have attempted to identify psychophysiological markers reliably related to an individual's attentional state. In particular, a growing body of evidence suggests that spontaneous changes in pupil size are linked to dynamic fluctuations between internal versus external attention and awareness (Laeng et al. 2012; Schneider et al. 2016; DiNuzzo et al. 2019). Changes in slowly fluctuating baseline pupil size as well as fast evoked pupillary responses are thought to be modulated by the locus coeruleus–norepinephrinergic system (LC/NE; Aston-Jones and Cohen 2005; Joshi et al. 2016) and have introduced new opportunities to objectively monitor mind wandering and arousal state (Mittner et al. 2014; Unsworth and Robison 2016). However, research on the relationship between mind wandering and tonic pupil size has yielded more inconsistent results as both larger and smaller tonic pupils have been associated with mind wandering (Smallwood et al. 2012; Grandchamp et al. 2014; Konishi et al. 2017; Jubera-Garcia et al. 2019). This is possibly due to differences in task demands and thereby the required levels of vigilance (Unsworth and Robison 2018) or, as proposed in a recent theoretical model, variations in tonic pupil size may reflect qualitatively distinct task-unrelated states (Mittner et al. 2016).

In summary, the DMN, attention and executive control networks, and the LC/NE-system are all implicated in mind wandering but empirical evidence into how these neural systems interact to give rise to mind wandering is at present incomplete. Building on previous findings, we aimed to address this by employing an fMRI version of the FT-RSGT that combines experience sampling with objectively defined measures interpreted as indirect makers for changes in ongoing attentional state, including sensitive behavioral indices and pupillometric measures. Following Boayue et al. (2020), we expected increases in the variability of finger-tapping and decreases in the degree of randomness of the tapping-sequence preceding self-reported mind wandering episodes. Furthermore, we aimed to validate that performance of the FT-RSGT indeed relies on executive control processes that are known to be recruited during the original RNGT. To this end, we contrasted brain activation during the generation of random tapping-sequences with a simple alternating finger-tapping task and expected to observe greater activation in frontoparietal regions involved in executive control during random finger-tapping.

Additionally, we explored the pattern of neural activation in relation to both direct and indirect markers of mind wandering by directly assessing the patterns of network-wide activity in the periods preceding experience sampling probes as well as the brain regions that correlated with behavioral performance. In line with a previous finger-tapping study, we expected to observe

recruitment of ventral and dorsal attention networks and cerebellum when variability in finger-tapping was high and DMN activation when finger-tapping was more stabilized (Kucyi et al. 2017). The degree of sequence randomness was expected to correlate with activity in frontoparietal and sensorimotor areas associated with executive control and self-determined action (Schubert et al. 1998; Jahanshahi et al. 2000). Direct predictions regarding network activation preceding self-reports of mind wandering are less evident considering the contradictory findings in the literature (Christoff et al. 2009; Mittner et al. 2014; Groot, Boayue, et al. 2021), but similar patterns of neural recruitment are expected for direct (self-report) and indirect (objective task performance and pupil dynamics) measures of mind wandering given that these relationships are replicated on the behavioral level. Finally, dynamic changes in tonic and phasic pupil size were assessed and related to self-reported mind wandering throughout the task. Whereas phasic pupil responses to task-related events are generally expected to be smaller during mind wandering due to perceptual decoupling (Smallwood et al. 2011; Unsworth and Robison 2018), the exact relationship with tonic pupil size is less clear. We therefore also investigated the neural substrates of both pupillary components to explore whether the brain regions correlating with changes in tonic and phasic pupil size would demonstrate similarity to the pattern of neural activity associated with mind wandering.

Materials and Methods
Participants

The study was approved by the Ethics Review Board of the Faculty of Social and Behavioral Sciences at the University of Amsterdam. Participants were 27 healthy adult volunteers aged 20–45 years (15 male, mean age = 27.5, SD = 7.2 years) who were recruited from the Amsterdam ultra-high field adult lifespan database (AHEAD; Alkemade et al. 2020). Participants had normal or corrected-to-normal vision, no self-reported (history of) psychiatric or neurological illness, and no contraindications for MRI as assessed with a standard safety questionnaire. To avoid biases in task performance related to individual differences in rhythmic abilities and finger tapping, experienced and (semi-)professional musicians were excluded from the study. Written informed consent was obtained prior to the experiment and participation was compensated with a standard monetary reward of €15 for a total duration of 90 min. All materials, anonymized data, and code are publicly available in an Open Science Framework (OSF) repository (Groot, Csifcsák, et al. 2021).

Finger-Tapping Random-Sequence Generation Task

Participants completed 18 experimental and 9 control blocks of the finger-tapping random-sequence generation task (FT-RSGT, Boayue et al. 2020; Fig. 1) in a pseudorandomized order. Stimuli were presented on a 32 inch BOLD screen using PsychoPy (Peirce 2007). At the start of each block, instructions appeared for 4000 ms at the center of the screen to indicate whether it was an experimental ("RANDOM") or control ("ALTERNATING") block. In the alternating task, participants were instructed to simply press the response buttons with their left and right index fingers in an alternating sequence (L-R-L-R-L-R-etc.). In the random task, they were asked to generate a sequence of left and right button presses with maximum unpredictability, or randomness (e.g., L-R-L-L-L-R-etc.). Hence, the two tasks were identical with respect to stimulus presentation and execution of motor responses but differed in the randomness criterion and thus, in the extent to which executive control processes were necessary to maintain performance. The concept of randomness was explained with a coin flip analogy: Similar to flipping a coin, a left versus right button press should occur at equal probability and be independent from past or future button presses. To ensure that participants understood these instructions, they performed a short practice run of the task and answered quiz-questions about the concept of randomness (e.g., "If there have been three right presses, must there always be a left press?"). If mistakes were made, further instructions and practice were provided until the task was mastered.

Throughout the experiment, participants had to synchronize their finger-tapping with an ongoing metronome that was presented as an auditory stimulus (440 Hz pitch for 75 ms) every 750 ms. Previous experiments determined that this pace is optimal for engaging in generating random sequences compared to slower and faster metronomes (Boayue et al. 2020). During finger-tapping, participants fixated on a centered fixation cross that was presented on a gray background while attending to the stimuli through MR-compatible headphones. Every block consisted of 80 stimuli on average (range = 74–87) and ended with a thought probe so that the onsets of thought probes were pseudorandomized to occur between 55.5 and 65.3 s (60 s on average). Thought probes were presented for 6000 ms plus a random jitter between 0 and 1000 ms, formulated as: "Where was your attention (i.e., your thoughts) focused just before this question?". Responses to the thought probes were ordered on a six-point Likert scale with the following annotations: "clearly on-task," "partly on-task," "slightly on-task," "slightly off-task," "partly off-task," and "clearly off-task". To indicate their answer, participants pressed left and right response buttons to navigate an arrow pointing at the categories. The starting point of the arrow on either extreme end of the Likert scale was randomized across thought probes. Participants were explicitly instructed that "off-task" included all thoughts unrelated to the task, for example, daydreaming, personal memories, or future plans whereas "on-task" referred to task-related thoughts, such as thinking about which button to press
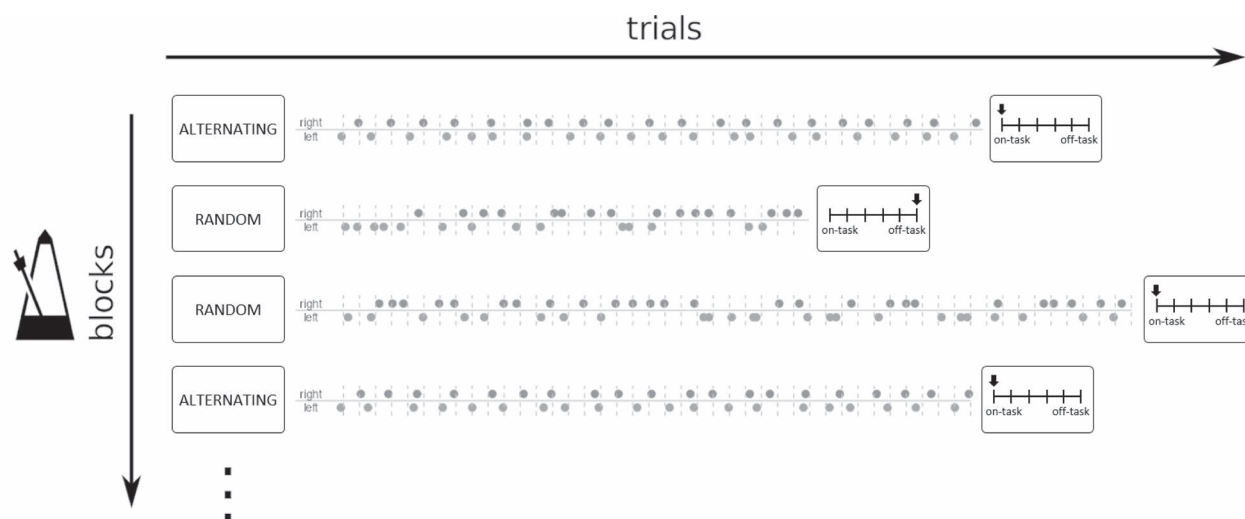
Figure 1. Schematic of the finger-tapping random-sequence generation task (FT-RSGT). Participants produced either alternating sequences of left versus right finger-tapping (alternating blocks) or generated sequences trying to maximize their randomness (random blocks). The rhythm of finger-tapping was continuously indicated by an auditory stimulus paced at 750 ms (metronome). At the end of each block, participants were probed to report to what degree their thoughts were unrelated to the task on a six-point Likert scale (reproduced from Groot, Csifcsák, et al. 2021).

next or focusing the rhythm of the metronome. The total duration of the task was ∼30 min.

Acquisition and Preprocessing
Behavior
Two aspects of FT-RSGT performance were assessed. First, behavioral variability (BV) was calculated as the standard deviation of the intertap intervals (ITIs) of the 25 finger-taps preceding each thought probe. No filtering or preprocessing was performed so that missing or double taps per trial were included in the calculation. The raw standard deviations were log-transformed to approximate a normal distribution. Second, the degree of randomness in the self-generated sequence of left and right finger-taps was measured with the approximate entropy (AE) metric (Pincus and Kalman 1997). As the generated sequences during alternating blocks were completely predictable (i.e., AE = 0), AE was calculated only for the random task condition. Specifically, AE quantifies the regularity in a sequence by evaluating the conditional probability that subsequences of length m that are similar remain similar for subsequences augmented by one position (more details on the calculation of AE are in Supplementary Material A). A previous study showed that AE ($m = 2$) measured in the FT-RSGT correlated with the entropy measure in a keyboard version of the original RNGT, validating its use as an index for executive control (Boayue et al. 2020). AE was calculated for every thought probe across the same preceding 25-tap window and transformed as $-\ln(\ln2 - AE)$. Both BV and AE were then standardized (Z-scored) across subjects (i.e., the grand mean and standard deviations were used for standardization). The choice of the 25-tap window was decided a priori based on the assumption that mind wandering occurs in slowly fluctuating episodes spanning multiple seconds as well as for ensuring that sufficient data was gathered for

reliable calculations of BV and AE. Additionally, previous experiments revealed that BV and AE based on this window size had the strongest relationship with self-reported mind wandering compared to shorter windows (Boayue et al. 2020).

Pupillometry
The pupil area of the left eye was concurrently recorded during the fMRI session at a sampling rate of 1000 Hz with the Eyelink 1000 Plus tracking system (SR Research). The pypillometry package (Mittner 2020) was used to determine subject-specific velocity profiles for blink detection based on the algorithms described by Mathôt (2013). Additional parameters were fine-tuned based on visual inspection of individual datasets, including the margin around blink onset and offset for linear interpolation and maximum distance in time between consecutive blinks for merging. Data were then filtered with a zero-phase shift Butterworth low-pass filter at 5 Hz that was set at 3 Hz for 12 datasets and at 2 Hz for three datasets as visual inspection revealed the presence of abundant high-frequency noise in the pupil signal. These steps ensure rigorous and optimized preprocessing of the pupil signal, circumventing artifacts associated with the high inter-individual variability in blinking transients and frequency. However, due to excessive blinking or technical issues with pupil tracking, the quality of six datasets remained inadequate and these subjects were therefore excluded from all further pupillometric analyses.

Selecting specific windows for extracting the mean pupil signal or peak amplitude is complicated in fast-paced task designs due to the build-up of evoked pupil responses that resemble increases in baseline pupil size and therefore contaminate the baseline estimates of subsequent trials. Therefore, to produce more valid estimates of single-trial tonic (baseline) and phasic

(evoked) pupillary dynamics, a recently developed deconvolution-based approach was applied (Mittner 2020). First, the data were downsampled to 250 Hz. Tonic fluctuations were estimated using B-spline basis functions constrained to pass through high prominence troughs in the pupil signal. A second iteration of this estimation, following subtraction of the first tonic estimate as well as modeled pupil–response functions (PRF; Hoeks and Levelt 1993) located at known task events, ensured that the final tonic estimate constituted a smooth curve that remained below the signal on which the phasic pupil responses are superimposed. Single-trial tonic pupil size was then calculated at every stimulus onset. To model phasic pupil responses to task-related events, regressors for every stimulus and tap onset were convolved with the pupil-response function (PRF; $h = t^n e^{-n/t_{max}}$, where $n = 10$ and $t_{max} = 900$; Hoeks and Levelt 1993) and fitted with a nonnegative least-squares solver (Lawson and Hanson 1987) to recover the amplitude of phasic responses as estimated b coefficients. However, predictor multicollinearity was observed as stimulus and tap onsets occurred close in time. Therefore, the final single-trial phasic pupil responses were calculated as the sum of b coefficients from all events located within the 200-ms window before and after each stimulus onset. Finally, single-trial tonic and phasic pupil responses were standardized (Z-scored) within subjects to remove incidental differences in absolute pupil size across subjects. More details on the deconvolution-based pupil analysis are described by Mittner (2021), and an implementation is provided in the pupillometry package (Mittner 2020).

Functional Neuroimaging

Participants were scanned with a 3Tesla Philips Achieva MRI system with a 32-channel head coil. T_1-weighted (T_1w) images were acquired with a turbo field-echo (TFE) sequence in 257 sagittal slices (FOV = 256 × 240 × 180 mm [F-H × A-P × R-L], TR = 11 ms, TE = 5.1 ms, acquired voxel size = 0.7 × 0.76 × 0.7 mm, reconstructed voxel size = 0.67 × 0.67 × 0.7 mm). Whole-brain functional images were acquired in a single fMRI run with single-shot fast field-echo (FFE) echo-planar imaging (EPI), collecting 56 transverse slices per volume with 0.2 mm slice gap (FOV = 224 × 224 × 123 mm, TR = 1800 ms, TE = 30 ms, flip angle = 70°, voxel size = 2 mm isotropic). An additional EPI field map with opposite phase-encoding direction was acquired to measure and correct for field distortions.

Imaging data were preprocessed with fMRIPrep v1.1.7 (Esteban et al. 2018) using Nipype v1.1.3 (Gorgolewski et al. 2011). Structural (T_1w) images were corrected for intensity non-uniformity with N4BiasFieldCorrection (ANTs v2.2.0; Tustison et al. 2010), skull-stripped with antsBrainExtraction using the OASIS target template, and spatially normalized to the ICBM 152 Nonlinear Asymmetrical template version 2009c (MNI152Nlin2009cAsym; Fonov et al. 2009) using the nonlinear registration tool in antsRegistration (Avants et al. 2008). Brain tissue was segmented in cerebrospinal fluid (CSF), white matter (WM), and gray matter (GM) using FAST (FSL v5.0.9; Zhang et al. 2001). The functional images were corrected for susceptibility distortion with 3dQwarp (AFNI; Cox and Hyde 1997), using a deformation field estimated from the two EPI references with opposing phase-encoding directions. The unwarped BOLD reference based on the estimated susceptibility distortion was then co-registered to the T_1w reference with FLIRT (FSL v5.0.9; Jenkinson and Smith 2001) using the boundary-based registration cost-function (Greve and Fischl 2009) and 9 degrees of freedom to account for remaining BOLD distortions. Head-motion parameters (rotation and translation) were estimated with MCFLIRT (FSL v5.0.9; Jenkinson et al. 2002). The preprocessed data were resampled back to native space as well as to standard space (MNI152Nlin2009cAsym template) and smoothed with a 6 mm full-width half-maximum Gaussian kernel using SUSAN (Smith and Brady 1997). All subsequent fMRI analyses were performed on the smoothed preprocessed timeseries in standard space.

Data Analysis

Bayesian Hierarchical Ordered Probit Regression Models

The relationships between self-reported mind wandering, behavioral performance, and pupillary dynamics were assessed with regression models using the thought probe responses from the experimental blocks (random task) of the FT-RSGT as dependent variable. Treating the ordinal probe responses as continuous introduces a range of statistical problems, including poor model fitting, low power, increasing the risk for type I and II errors, and spurious interaction effects (Liddell and Kruschke 2018). To circumvent these issues, we applied Bayesian hierarchical ordered probit regression (Boayue et al. 2019, 2020; Bürkner and Vuorre 2019; Alexandersen et al. 2021) using the brms package (Bayesian Regression Models using Stan; Bürkner 2017). This method models the probability of each discrete point rather than relying on the assumption that the probe responses are normally distributed. In addition, within-subject variability in mind wandering can be taken into account with subject-level random intercepts. As a consequence, probit models are more suitable and sensitive to detect effects in Likert-scale data. For each regression coefficient, we report the posterior mean, its 95% highest-density interval (HDI), and the evidence ratio in favor of a positive (ER$_+$) or negative (ER$_-$) effect. The ER is calculated as the ratio between the probability of the effect being positive divided by the inverse probability of the effect being zero or negative (ER$_+$) or the inverse of that ratio (ER$_-$) and can be interpreted as an odds-ratio. We consider an effect as reliable when the area under the marginal posterior distribution that is larger than zero (for ER$_+$) or smaller than zero (for ER$_-$) is >0.95 (corresponding to an ER of 19 and the 95% HDI excluding zero). The models were fitted with four Hamiltonian Monte Carlo (HMC) chains, each with 1000 warm-up and 4000 post warm-up samples.

In the first probit model, the effects of time (probe number), BV, AE, and the BV × AE interaction on 486 thought probe responses (27 subjects × 18 blocks) were modeled. In accordance with our hypotheses, for time, BV, and BV × AE, we evaluated the evidence for the effect to be larger than zero (ER_+) and for AE to be smaller than zero (ER_-). Similarly, the effects of tonic and phasic pupillary dynamics as well as the tonic × phasic interaction were assessed in addition to time in a second regression model using the 18 random blocks from the 21 subjects with complete pupil datasets. For every thought probe, the extracted single-trial tonic and phasic features were averaged across the preceding 25 trials (18.75 s), ignoring trials with more than 40% missing pupil data. This criterion resulted in exclusion of six thought probes, therefore the model was fitted on 372 thought probe responses in total. The evidence for effects larger than zero (ER_+) for tonic pupil size and the tonic phasic interaction and smaller than zero (ER_-) for phasic pupil responses was evaluated.

fMRI Analysis: General Linear Models

Whole-brain general linear models (GLM) were fitted to the fMRIPrep-preprocessed time series using FSL FEAT (Woolrich et al. 2001) to explore differences in brain activity between the two task conditions and to investigate the role of brain regions involved in mind wandering using 1) experience sampling probes, 2) task performance, and 3) pupillary dynamics. All first-level GLMs included four task-related regressors (left and right finger-taps, metronome stimuli, and thought probe onsets) that were convolved with a double-gamma hemodynamic response function (HRF). In addition, fMRIPrep-derived nuisance regressors calculated for every volume were added, including mean time courses in CSF and WM masks, framewise displacement (FD), six rotation and translation parameters, and discrete-cosine transform (DCT) basis functions to model low-frequency scanner drifts. The modeled data were obtained via ordinary least-squares linear regression. Second-level analyses were performed with FLAME (Beckmann et al. 2003) to obtain group-level parametric contrast maps. Statistical significance of brain areas was evaluated with cluster z-thresholding (Friston et al. 1994). First, a primary voxel-level threshold of $z > 2.3$ defined clusters of above-threshold voxel activations. Second, a cluster-level threshold of $P < 0.05$ was applied to eliminate non-significant clusters.

First, we explored the hypothesis that random-sequence generation recruits more widespread executive and attentional networks compared to alternating finger-tapping. In addition to the task-related and nuisance regressors, the occurrence of random and alternating blocks was modeled by two boxcar functions convolved with a double-gamma HRF. In a second model, patterns of brain activity associated with episodes of mind wandering compared to on-task thoughts were investigated by convolving boxcar functions that modeled the 10s intervals preceding off-task versus on-task thought probes (Christoff et al. 2009). To account for individual differences in response tendencies, the six probe response categories were dichotomized using an algorithm that determined subject-specific boundaries, where the split-point for each subject was chosen to set the proportion of off-task versus on-task probes as close to 50% as possible. This approach allowed us to identify potential episodes of mind wandering in subjects that selected only a very narrow range of response categories to reflect their current attentional state, possibly due to some degree of satisficing, primacy, and social desirability biases (Weinstein 2018; Weinstein et al. 2018). For example, if a subject exclusively answered with "clearly on-task" and "partly on-task," responses in the latter category were labeled as off-task in the analysis. The total proportion of off-task reports was 49% using the split-point algorithm whereas this proportion was 36% when collapsing the first three categories into on-task and the other three into off-task. With the latter approach no significant brain activations preceding off-task reports could be observed. Since the two task conditions were presumed to differ in terms of executive resources necessary for performance and may therefore interact differently with mind wandering, probe regressor functions were created separately for random and alternating blocks.

Third, regressors for task performance were modeled to evaluate brain activity corresponding to increases and decreases in BV and AE. Starting at the 25th trial (metronome onset) per block, BV and AE (random blocks only) were calculated for every single trial based on the preceding 25 finger-taps. To create parametric regressors, single-trial BV and AE were transformed and standardized across subjects before nearest-neighbor interpolation and resampling to the resolution of the fMRI timeseries (Fig. 2). The use of 25-tap sliding windows resulted in smooth and time-lagged regressor functions that did not require additional convolution with a canonical HRF. Our window size of 25 taps was determined a priori based on previous studies on the latency of mind wandering and on-task episodes (Bastian and Sackur 2013; Pelagatti et al. 2020), in order to ensure comparable measures for BV and AE to the behavioral analysis, and considering the slow nature of the physiological BOLD response. In the final GLM, we explored changes in brain activity associated with increases and decreases in tonic and phasic pupillary dynamics. The single-trial tonic and phasic pupil features were interpolated with nearest-neighbor interpolation and resampled to the resolution of the fMRI timeseries (TR). Whereas tonic pupil was already modeled as a smooth and slowly fluctuating signal, phasic responses were convolved with a double-gamma HRF.

For every resulting group-level statistical map we calculated the overlap with the 7- network parcellation (Yeo et al. 2011), the Harvard-Oxford subcortical structural atlas (Harvard Center for Morphometric Analysis),
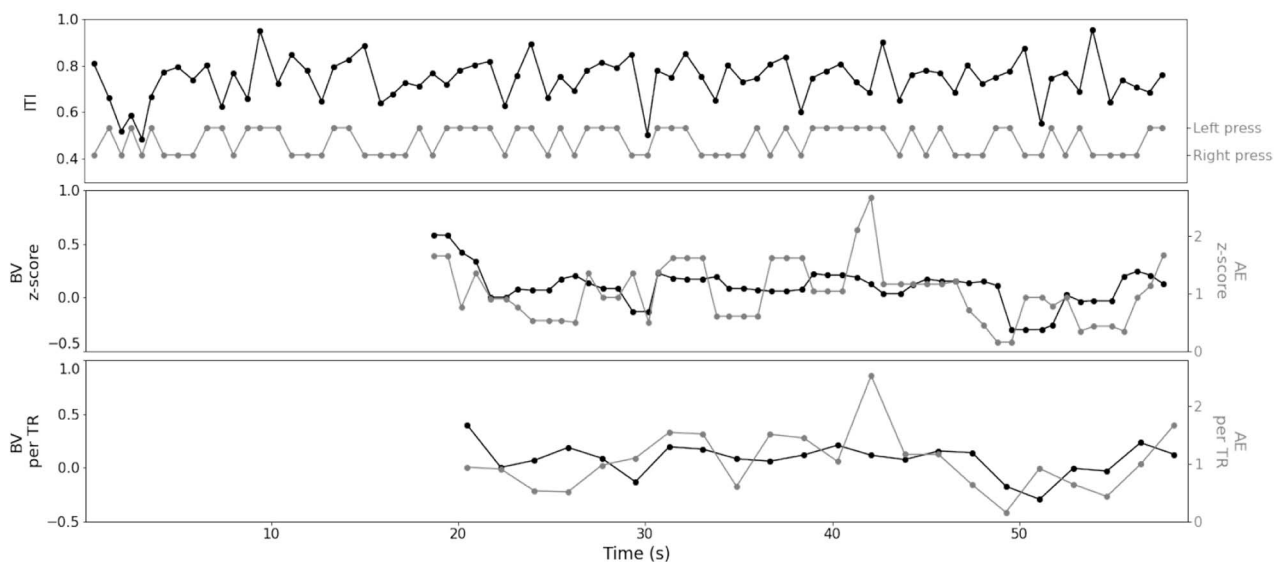
Figure 2. Behavioral performance during a random task block from a single subject (80 stimuli), showing inter-tap intervals (ITI) and left versus right button presses (*top*), used to calculate behavioral variability (BV) and approximate entropy (AE) starting at the 25th stimulus per block (*middle*), which were then linearly interpolated and resampled to the resolution of the fMRI timeseries for the GLM analysis (*bottom*) (reproduced from Groot, Csifcsák, et al. 2021).

and the probabilistic cerebellar atlas (Diedrichsen et al. 2009) in standard MNI152 space. The cortical network parcellation included visual (VIS), somatomotor (SOM), dorsal attention (DAN), salience/ventral attention (VAN), limbic (LIM), control (CON), and default mode (DMN) networks. The subcortical parcellation consisted of thalamic nuclei, striatum, pallidum, hippocampus, amygdala, nucleus accumbens, and brainstem and were combined into a general subcortical mask for calculating the total percentage overlap and illustration purposes. All three atlases were resampled to the resolution of the functional timeseries using nearest-neighbor interpolation and binarized. The percentage of voxels in the statistical contrast maps that overlapped with each of the binarized atlases was then calculated, ignoring above-threshold voxel clusters that were located in cerebral white matter. Therefore, regardless of the size of significant clusters, every contrast map was always fully accounted for by the parcellation.

Results
Effects of Task Condition on Mind Wandering Reports and Performance

In total, 36% of probe responses were in one of the three off-task categories. The mean probe response given by participants was 2.89 ($SD = 1.46$, median = 3) on the six-point Likert-scale, demonstrating that participants reported that their thoughts were more often focused on performing the task rather than being engaged in mind wandering. Indeed, five subjects never reported that their thoughts were in any of the three off-task categories. There was no significant difference in mind wandering propensity between the random ($M = 2.86$, $SD = 0.95$) and alternating task conditions

($M = 2.93$, $SD = 1.14$, $t(26) = -0.53$, $P = 0.602$). Mean behavioral variability was, however, significantly higher during random ($M = 0.11$, $SD = 0.57$) compared to alternating finger-tapping ($M = -0.07$, $SD = 0.53$, $t(26) = 3.30$, $P < 0.01$) suggesting that the additional task of generating random sequences interfered with maintaining synchronized motor responses to the externally cued rhythm.

Task Performance and Pupil Dynamics Relate to Mind Wandering Reports

The unadjusted Bayesian R^2 for the first probit model was 0.56 [0.52, 0.59]. In line with expectations, the coefficients for time ($b = 0.09$ [0.07, 0.11], $ER_+ = \infty$), BV ($b = 0.33$ [0.21, 0.45], $ER_+ = \infty$), and BV × AE ($b = 0.07$ [−0.05, 0.17], $ER_+ = 7.18$) were positive whereas the coefficient for AE ($b = -0.09$ [−0.20, 0.02], $ER_- = 18.61$) was negative. Thus, mind wandering self-reports were more frequent as the task progressed and were preceded by increases in tapping variability and decreases in self-generated sequence randomness although the HDI of the latter coefficient did not exclude zero. The direction of the BV × AE interaction suggests that the relationship between BV and mind wandering was stronger at high levels of AE and weaker (but still positive) at low levels of AE. However, the HDI of this effect included zero, warranting a cautious interpretation of this result. Since BV was significantly higher in the random task, we assessed whether task condition modulated the relationship between BV and mind wandering. We performed a probit model with a BV × task interaction ($b = -0.04$ [−0.21, 0.14], $ER_- = 1.98$), which indicated that the observed positive relationship between BV and mind wandering was independent from task condition.

For the probit model including pupil regressors, the unadjusted Bayesian R^2 was 0.53 [0.47, 0.57]. The positive
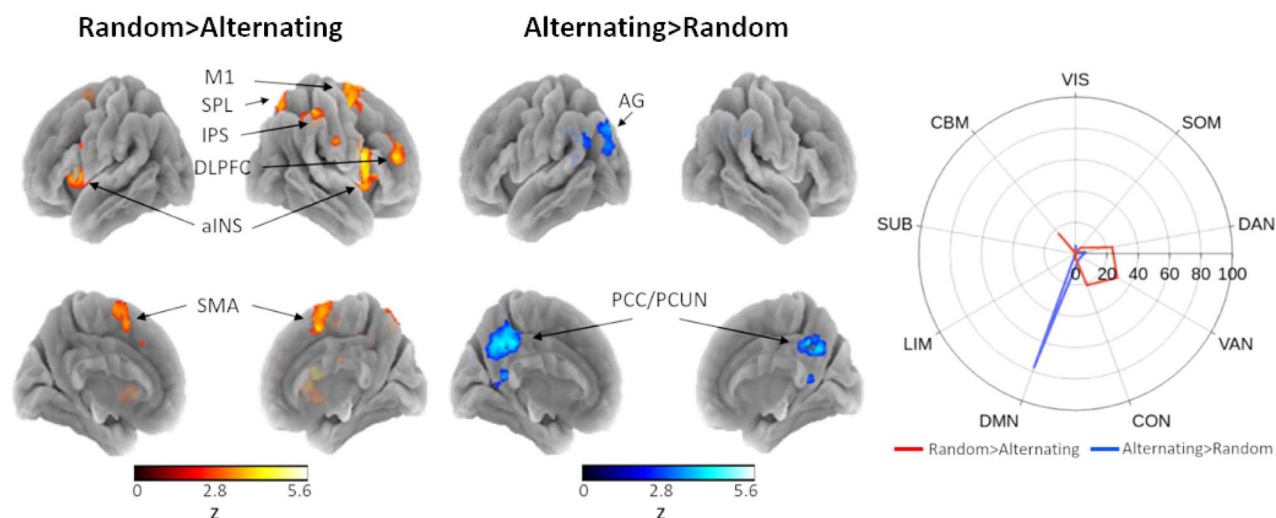
Figure 3. Activations during random-sequence generation contrasted with alternating finger-tapping (*left*) and vice versa (*middle*) and percentage of contrast maps that overlap with a 7-network cortical, subcortical, and cerebellar parcellation (*right*). M1 = primary motor cortex; SPL = superior parietal lobe; IPS = intraparietal sulcus; DLPFC = dorsolateral prefrontal cortex; aINS = anterior insula; SMA = supplementary motor area; AG = angular gyrus; PCC/PCUN = posterior cingulate cortex/precuneus; SUB = subcortex; CBM = cerebellum (reproduced from Groot, Csifcsák, et al. 2021).

effect of time on mind wandering was replicated ($b = 0.08$ [0.06, 0.11], $ER_+ = \infty$). Although phasic pupil responses related to mind wandering in the expected direction ($b = -0.13$ [−0.39, 0.13], $ER_- = 5.39$), tonic pupil size decreased as self-reports of mind wandering increased ($b = -0.12$ [−0.28, 0.04], $ER_+ = 0.08$). However, both effects can be considered inconclusive as the HDIs did not exclude zero. Instead, the tonic × phasic interaction ($b = -0.36$ [−0.65, −0.07], $ER_+ = 159$) provided evidence of a negative interaction effect. This finding suggests that the relationship between phasic responses and mind wandering is dependent on fluctuations in tonic pupil size. Specifically, the negative relationship between phasic pupil responses and mind wandering, as would be expected due to perceptual coupling, only exists when tonic pupil size is high.

Random Sequence Generation Recruits Executive and Attentional Networks

When contrasted with random-sequence generation, we observed that alternating finger-tapping was associated with localized activity in the posterior cingulate cortex/precuneus and left angular gyrus, both regions that are core nodes of the DMN. In line with our hypothesis, the generation of random tapping sequences instead revealed widespread recruitment of cortical areas generally attributed to attention and executive control networks, including the superior parietal lobe, intraparietal sulcus, primary motor cortex, and dorsolateral prefrontal cortex of the right hemisphere as well as bilateral anterior insula, bilateral medial supplementary motor areas, and bilateral anterior and posterior parts of the cerebellum (Fig. 3, Supplementary Material B). Together, these results provide evidence that the two tasks are qualitatively different regarding the cognitive resources necessary for performance and that random-sequence

generation during the FT-RSGT requires the recruitment of brain regions associated with executive functioning.

Mind Wandering Signatures Diverge for Direct versus Indirect Markers

Contrary to previous findings, brain activations directly preceding self-reports of mind wandering when contrasted with on-task reports could not be localized to the known cortical nodes of either the DMN or FPCN/DAN. Instead, we observed clusters of brain activation associated with mind wandering in visual, cerebellar, and subcortical areas that could be distinguished between the two task conditions. Specifically, mind wandering in the alternating task was preceded by activity in the left inferior occipital gyrus, temporal subgyral white matter (not plotted on the surface mesh), and parts of the bilateral anterior and posterior cerebellum, whereas mind wandering during the random task was associated with greater activity in the right striatum (Fig. 4A, Supplementary Material B). To test whether these results were influenced by the selection of the selected data window, the same analysis was performed using 18 s preprobe intervals which resulted in similar activation patterns. In addition, the analysis was repeated combining both task conditions to assess whether separation of the tasks influenced the observed neural correlates of mind wandering. Across tasks, we observed significant activation mainly in the right striatum preceding mind wandering reports when contrasted to on-task reports (Supplementary Material C), showing high overlap (Dice similarity coefficient = 0.68) with the activations preceding mind wandering in the random task condition.

Next, we assessed patterns of neural activity corresponding to variability in finger-tapping (Fig. 4B, Supplementary Material B) and obtained strikingly similar results as reported in a previous rhythmic finger-tapping
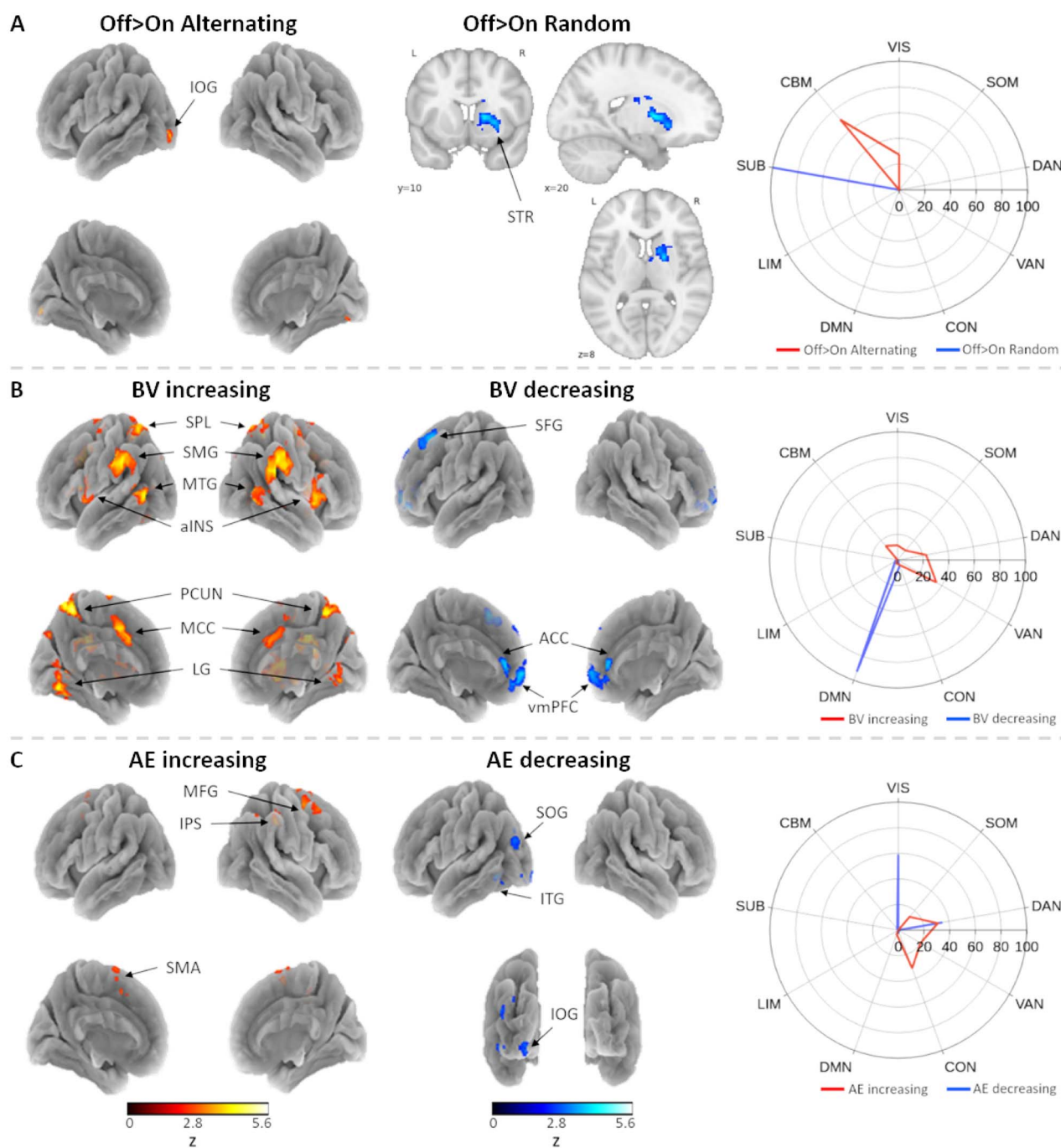
Figure 4. (A) Active brain regions preceding mind wandering reports during the alternating (*left*) and random (*middle*) task conditions. (B) Regions correlating with increases (*left*) and decreases (*middle*) in behavioral variability. (C) Regions correlating with increases (*left*) and decreases (*middle*) in approximate entropy. (*right*) Percentage of contrast maps that overlap with a 7-network cortical, subcortical, and cerebellar parcellation. IOG = inferior occipital gyrus; STR = striatum; SPL = superior parietal lobe; SMG = supramarginal gyrus; MTG = middle temporal gyrus; aINS = anterior insula; SFG = superior frontal gyrus; ACC = anterior cingulate cortex; vmPFC = ventromedial prefrontal cortex; MFG = middle frontal gyrus; IPS = intraparietal sulcus; SOG = superior occipital gyrus; ITG = inferior temporal gyrus; SMA = supplementary motor area; SUB = subcortex; CBM = cerebellum (reproduced from Groot, Csifcsák, et al. 2021).

study (Kucyi et al. 2017). Increases in finger-tapping variability were correlated with activity in dorsal and ventral attention networks, including the superior parietal lobes, supramarginal gyri, posterior middle temporal gyri, anterior insula, midcingulate cortices, precuneus, lingual gyri of both hemispheres, and bilateral anterior cerebellum. Furthermore, less variable finger-tapping and thus more

optimized task performance was associated with greater activity in left superior frontal gyrus, bilateral anterior cingulate cortex, and bilateral ventromedial prefrontal cortex, thereby mostly mapping to the DMN.

Similarly, we observed correlated neural activity in the expected frontoparietal regions for increases in the degree of randomness in the tapping-sequence as

quantified with AE, namely within the right intraparietal sulcus, right posterior middle frontal gyrus, and left medial supplementary motor area, thus showing a similar pattern of neural network recruitment as observed for the random task condition in general. Decreases in AE, signaling decrements in task performance, were instead associated with the left inferior temporal sulcus (poorly visible on the plotted surface mesh) and the superior and inferior occipital gyri of the left hemisphere (Fig. 4C). Similar results were obtained when the analyses were performed using 20-tap and 10-tap sliding windows for BV and AE regressor calculation, indicating that the observed patterns of neural activation are robust against changes in this analysis parameter.

Pupillary Dynamics Map to Subcortical and Visual Cortical Areas

Positive correlations with tonic pupil size were observed almost exclusively in subcortical and cerebellar areas, including the thalamus, internal capsule, and intracalcarine cortex of both hemispheres as well as the right hippocampus. In addition, a large brainstem cluster covered the locus coeruleus, substantia nigra, and subthalamic and ventral tegmental nuclei. Furthermore, widespread cerebellar activation was observed in the anterior and posterior lobes and dentate nuclei. Interestingly, brain regions that negatively correlated with tonic pupil size largely overlapped with visual and somatomotor cortical network parcellations, including the primary somatosensory cortices, superior frontal gyri, medial primary motor cortices, lateral occipital cortices, superior temporal gyri, hippocampal areas, and cuneal cortices of both hemispheres in addition to the left middle temporal gyrus and right fusiform gyrus (Fig. 5A, Supplementary Material B). In contrast, activity in brain regions that corresponded with changes in phasic pupil responses to task-related events was less and extensive and more posteriorly localized. Specifically, larger phasic pupil responses were associated with greater activity in the left lingual gyrus, whereas smaller phasic pupil responses were associated with activation of the left superior temporal gyrus (poorly visible on the surface mesh), right inferior occipital gyrus, and bilateral superior occipital gyri (Fig. 5B).

Discussion

To disentangle the complex interplay between mind wandering, executive functions, and behavior, we employed an fMRI version of a recently developed finger-tapping random-sequence generation task (FT-RSGT). This novel paradigm allows assessment of ongoing fluctuations in task-related and task-unrelated attentional states through self-reports and sensitive indices of task performance at high temporal resolution. Concurrent fMRI and pupillometric measures were used to investigate the neural substrates of direct and indirect markers of mind wandering.

Participants completed interleaved blocks of two different finger-tapping tasks, one where they performed alternating sequences and one that required randomized responding, that were otherwise identical in terms of stimulus presentation, task pacing, and thought probe frequency. We therefore hypothesized that the difference in neural recruitment between the two tasks should be mainly reflected in the activation of brain regions associated with executive functioning. Indeed, our results demonstrate greater involvement of attention and executive control networks during the generation of random sequences compared to alternating finger-tapping. Specifically, activation was localized in brain regions previously implicated in random number generation, including the right superior parietal lobe and intraparietal sulcus, primary and supplementary motor areas, right dorsolateral prefrontal cortex (DLPFC), anterior insula, and cerebellum (Mattay et al. 1998; Jahanshahi et al. 2000; Gountouna et al. 2010). The DLPFC has been proposed to play an especially important role in the suppression of repetition in response patterns (Jahanshahi et al. 1998; Jahanshahi et al. 2000; Joppich et al. 2004; Capone et al. 2014) and is a major node in the frontoparietal control network (FPCN) that is typically associated with strategic planning and goal-directed cognition. Thus, the coordinated activity of the DLPFC together with somatomotor areas, insula, and cerebellum likely orchestrates the complex behavior required for this task, including the evaluation and selection of spatiotemporal motor actions, suppression of sequence reiterations, and synchronization of responses to an externally-cued rhythm.

In addition, we observed a similar pattern of frontoparietal cortical activation associated with increases in sequence randomness, including the right intraparietal sulcus, right posterior middle frontal gyrus, and left medial supplementary motor area. This is consistent with an early study employing a finger-tapping task combined with random sequence generation (Schubert et al. 1998) and suggests that these regions are especially important for self-determined action planning and execution. In particular, the intraparietal sulcus has been argued to serve important integrative functions of sensorimotor information required to monitor the ongoing movement sequence and adapt new movements according to the randomness criterion (Schubert et al. 1998; Tanabe et al. 2005). However, the absence of correlated activity in the DLPFC with sequence randomness was surprising given previous findings (Jahanshahi et al. 2000; Joppich et al. 2004). Interestingly, a recent study reported a similar dissociation as anodal tDCS of the left DLPFC failed to modulate sequence randomness as measured with approximate entropy (Boayue et al. 2020). Since we did not find evidence for a difference in mind wandering propensity between the two tasks, it is possible that the DLPFC is not necessary for the optimization of sequence entropy but is rather involved in the task-specific coordination and distribution of executive control processes
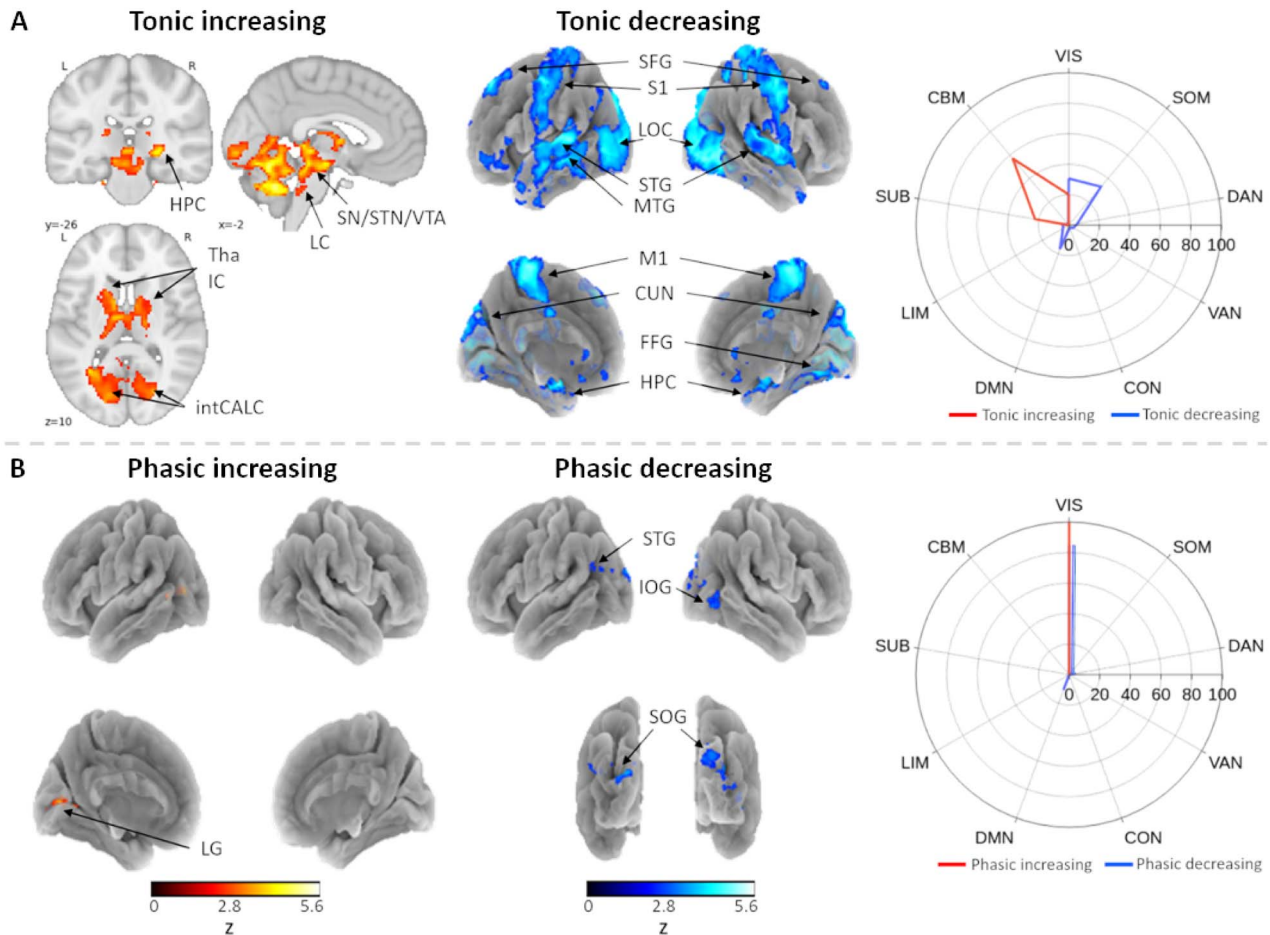
Figure 5. (A) Active brain regions with increasing (*left*) and decreasing (*middle*) tonic pupil size. (B) Regions correlating with increasing (*left*) and decreasing (*middle*) phasic pupil responses to task-related events. (*Right*) Percentage of contrast maps that overlap with a 7-network cortical, subcortical, and cerebellar parcellation. HPC = hippocampus; LC = locus coeruleus; SN = substantia nigra; STN = subthalamic nucleus; VTA = ventral tegmental area; Tha = thalamus; IC = internal capsule; intCALC = intracalcarine cortex; SFG = superior frontal gyrus; S1 = primary somatosensory cortex; LOC = lateral occipital cortex; STG = superior temporal gyrus; MTG = middle temporal gyrus; M1 = primary motor cortex; CUN = cuneal cortex; FFG = fusiform gyrus; HPC = hippocampus; LG = lingual gyrus; IOG = inferior occipital gyrus; SOG = superior occipital gyrus. SUB = subcortex; CBM = cerebellum (reproduced from Groot, Csifcsák, et al. 2021).

that may also periodically engage in task-unrelated processes such as mind wandering. This interpretation is in line with the proposed role of the DLPFC in context regulation (Turnbull et al. 2019) and conforms to the observation that anodal tDCS of the DLPFC reduced involuntary shifts in task-unrelated attention (Boayue et al. 2020).

Decreases in randomness, as would be expected to occur when thoughts drift away from the task as subjects engage in mind wandering, were instead associated with activity in the left inferior temporal sulcus and left superior and inferior occipital gyri. Although these regions are not typically associated with decrements in task performance, a large-scale meta-analysis (Spreng et al. 2002) reported that the left inferior temporal sulcus is often associated with autobiographical memory retrieval and default mode functions. However, the ordinal regression analysis did not reveal a clear relationship between approximate entropy of the tapping-sequence and mind wandering, suggesting that mind wandering was less detrimental to this aspect of task performance compared

to the maintenance of synchronized finger-tapping to the metronome as reflected in the strong relationship with behavioral variability. As we also observed generally higher tapping variability during the random task, participants were possibly more strongly engaged in maintaining task performance by optimizing sequence randomness, leading to the deterioration of tapping rhythmicity.

When executive task demands were low and participants were required to simply produce an alternating finger-tapping sequence, greater activity was observed in the core nodes of the DMN, namely the posterior cingulate cortex/precuneus and left angular gyrus. Given the context-regulation hypothesis, which states that the propensity to mind wander is adaptively adjusted to environmental demands (Smallwood and Andrews-Hanna 2013), it is conceivable that the less effortful alternating finger-tapping task, as opposed to random sequence-generation, was more facilitative of mind wandering as reflected in greater DMN activation (Mason et al. 2007). However, as we failed to observe activation of the DMN

directly preceding self-reports of mind wandering, or any difference in mind wandering propensity between the two tasks, an alternative explanation may be that DMN recruitment rather indicated a greater reliance on automated behavior (Shamloo and Helie 2016; Scheibner et al. 2017; Vatansever et al. 2017). This explanation is in line with our observation of correlated activity in the DMN (ventromedial prefrontal cortex and left superior frontal gyrus) when the rhythm of finger-tapping was more synchronized with the metronome, which is in agreement with previous findings characterizing stable or "in-the-zone" behavior (Esterman et al. 2013, 2014; Kucyi et al. 2016; Kucyi et al. 2017; Yamashita et al. 2020). Together, these results suggest that automatic and repetitive behavior that is considered less effortful might be governed by the DMN and fluctuations in behavioral variability may provide a sensitive marker for changes in attention as reflected in neural correlates of attention rather than sensorimotor networks. Furthermore, increases in finger-tapping variability were predictive of self-reported mind wandering episodes throughout the task, highlighting the robustness of this relationship across different tasks and studies (Bastian and Sackur 2013; Hawkins et al. 2019; Boayue et al. 2020) and additionally substantiating behavioral variability as a sensitive marker for departures from task-focused attention.

We did not observe a difference in mind wandering propensity between the two task conditions, which is surprising given previous studies demonstrating an effect of task difficulty on mind wandering (Seli, Konishi, et al. 2018; Brosowsky et al. 2021). One possible explanation as to why levels of mind wandering during the less demanding alternating finger-tapping task were similar to those during the random task is that exposure to the former, easier task was limited. Specifically, alternating blocks composed only one-third of the experiment and were pseudo-randomized, making it unlikely for two alternating blocks to occur sequentially. Therefore, occasional periods of 1-min lasting alternating finger-tapping were possibly not long enough to induce significantly more mind wandering, resulting in comparable levels of mind wandering between the two tasks.

Contrary to expectations, the patterns of neural recruitment directly preceding mind wandering self-reports and during periods of increased tapping variability did not converge. However, the observed divergence in our study is less surprising given the results of a previous study employing a continuous performance task (Kucyi et al. 2016), in which the authors demonstrated greater activation of the DMN in relation to self-reported mind wandering as well as stable performance even though mind wandering was preceded by increases in response variability. Combined with our results, these findings suggest a certain level of independence in the relationships between the DMN and mind wandering on the one hand, and between the DMN and behavioral variability on the other. Although the authors of that study report DMN activation prior to mind wandering,

our results failed to show such a relationship. Instead, we observed that mind wandering self-reports were preceded by local activation of the left inferior occipital gyrus and cerebellum during the alternating task and the right striatum during the random task. Regardless of the discrepancy with the neural recruitment during task performance, these results are puzzling on their own as they strongly deviate from the neural regions typically associated with mind wandering and spontaneous thought (Christoff et al. 2009; Fox et al. 2015). However, several studies indicate that cerebellar regions are functionally connected to cortical intrinsic connectivity networks, including the DMN (Habas et al. 2009; Buckner et al. 2011; Vatansever et al. 2015; Habas 2021), revealing a role for the cerebellum in cognition. In addition, earlier findings are suggestive of a role for the striatum in brain state maintenance through connections with the insula in order to sustain mind wandering episodes (Tang et al. 2012; Chou et al. 2017) and a recent study reported the thalamus and basal forebrain as subcortical nodes of the DMN (Alves et al. 2019). Furthermore, a recent study analyzing the dynamics within and between large-scale networks observed that mind wandering interacted with changes in the segregation and integration of visual and subcortical networks (Zuberer et al. 2021). Specifically, mind wandering was associated with higher levels of integration of the visual network compared to optimal sustained attention, whereas the subcortical network showed stronger segregation, suggesting that visual and subcortical system dynamics are sensitive to perturbations from mind wandering. Hence, although the role of cerebellar and subcortical regions and cortico-subcortical network interactions in mind wandering is currently understudied, these findings warrant consideration for future research.

It should be noted that there exists a large heterogeneity in the design and the direct or indirect measurement of mind wandering across previous studies and different forms of mind wandering or spontaneous thought can be discerned based on their neural correlates (Fox et al. 2015). In addition, some researchers have proposed a distinction between stimulus-independent versus stimulus-oriented mind wandering (Gilbert et al. 2007; Maillet et al. 2017), a dimension that cannot be directly investigated in most continuous performance and sustained attention tasks that implement ongoing stimulus delivery. Instead, the FT-RSGT can be considered mostly a stimulus-independent paradigm and thus task performance in general relies more prominently on internal representations. An intriguing speculation arising from these considerations is that network configurations supporting such representations might be similar for task-related and task-unrelated processes, which would explain the absence in neural contrast. Alternatively, the divergence in brain activation identified through direct (self-report) versus indirect (objective) measures may arise from the difference in how they relate to its heterogeneous phenomenological aspects. For example,

experience sampling may capture a wide variety of types of spontaneous thought, including episodes that are brief versus prolonged, aware versus unaware, and deliberate versus involuntary. Indeed, there is evidence that the spontaneous generation of mind wandering and its subjective experience are separable components (Smallwood et al. 2007) that can also be distinguished on the neural level (Christoff et al. 2009). In contrast, indices of objective performance may consistently "catch" a distinct and uniform aspect of mind wandering, such as its depth or intensity. As there is evidence that mind wandering without meta-awareness is more disruptive of task performance (Smallwood et al. 2007, 2008), increases in behavioral variability may especially reflect deep and unaware episodes of task disengagement. Future studies are necessary to further investigate these hypotheses.

Finally, we investigated the neural correlates of changes in slowly-fluctuating pupil dilations and constrictions as well as changes in the amplitude of evoked transient responses to task-related events as derivatives of tonic and phasic LC/NE dynamics, respectively (Aston-Jones and Cohen 2005). In agreement with previous reports, spontaneous tonic pupil dilations were correlated with activity in occipito-temporal regions, thalamus, brainstem, and cerebellum, whereas negative correlations were observed within widespread visual and somatomotor cortical areas (Murphy et al. 2014; Yellin et al. 2015; Schneider et al. 2016; DiNuzzo et al. 2019). Especially, the involvement of the LC and thalamus is unsurprising given their known role as drivers of cortical arousal and neural gain that is necessary for optimized task performance (Aston-Jones et al. 1991; Aston-Jones and Cohen 2005; Saper et al. 2005) as well as the proposed role of the thalamus in orchestrating attentional switches between internally versus externally-directed awareness (Wang et al. 2014; Cunningham et al. 2016; Sweeney-Reed et al. 2017) and directing attention to episodic memories (Leszczynski and Staudigl 2016). In addition, the somatosensory cortices have been previously associated with spontaneous thought (Fox et al. 2015) as well as visual imagery and thoughts relating to body-centered information during mind wandering (Delamillieure et al. 2010; Fox et al. 2013). As tonic pupil size was negatively related to self-reported mind wandering, the observed activation of somatosensory cortices in association with tonic pupil constriction could therefore reflect involvement in mind wandering episodes.

Interestingly, occipital activation was frequently either directly or indirectly associated with mind wandering, including when sequence randomness decreased (left superior and inferior occipital gyri), during tonic (lateral occipital cortices) and phasic (right inferior and bilateral superior occipital gyri) pupil constriction, and preceding mind wandering reports in the alternating task (left inferior occipital gyrus), possibly suggesting similar underlying cognitive states. It has been argued that through cortical feedback mechanisms, the occipital cortex may play

a role in cognition independent from perceptual input, such as internal visual representations that transpire during mental imagery and mind wandering (Kosslyn et al. 2001; Petro et al. 2016). Together with previous work, these findings provide important insights into how tonic and phasic pupil dynamics may operate as indicators of task-unrelated mental states such as mind wandering (Mittner et al. 2016; Konishi et al. 2017; Unsworth and Robison 2018; Groot, Boayue, et al. 2021). The ordinal regression analysis furthermore revealed a significant interaction between the two pupil components, suggesting that phasic responses only demonstrate a negative relationship with mind wandering when tonic pupil size is increased. This is in line with a recently proposed model of mind wandering based on the adaptive gain theory (Mittner et al. 2016), which poses that two distinct task-unrelated states ("active mind wandering" and "off-focus") are distinguishable based the level of tonic NE. Specifically, active mind wandering is characterized by similar tonic levels as the on-task state reflecting optimal neural gain and arousal, whereas the off-focus state represents an exploratory mode during which brain networks reconfigure to select relevant behavioral goals. If we assume that participants had generally low levels of arousal and vigilance during the FT-RSGT, the observed high levels of tonic pupil size could possibly reflect optimal levels of tonic NE, during which the amplitude of phasic responses maximally discriminate between active mind wandering (low phasic responses indicate task disengagement and perceptual decoupling) and on-task (high phasic responses reflect task-focused attention).

In summary, we demonstrated that the FT-RSGT relies on the recruitment of attentional and executive control networks, providing evidence for our hypothesis that the generation of random as opposed to alternating finger-tapping sequences requires the use of executive resources. Secondly, we observed positive significant relationships between self-reported episodes of mind wandering and time-on-task as well as behavioral variability, replicating earlier findings and validating the use of this task as an fMRI paradigm (Boayue et al. 2020). Finally, we replicated at least partially the neural correlates of indirect markers of mind wandering and arousal state using sensitive indices of behavioral performance and pupillometric measures as derivatives for LC/NE functioning. In contrast, neither the previously reported cortical networks underlying mind wandering, nor the activation patterns associated with task performance could be observed in the neural contrasts preceding thought probes, suggesting a dissociation between indirect and direct (subjective) measures that may underline the vulnerability of thought probing for disentangling the neural underpinning of this heterogeneous mental state. Together, our results add to the growing body of work to better understand the mechanisms of ongoing fluctuations in attention and how various markers of mind wandering

relate to each other at both the behavioral and neural level.

Supplementary Material

Funding

Notes

References

Alexandersen A, Csifcsák G, Mittner M. 2021. The effect of transcranial direct current stimulation on the interplay between executive control, behavioral variability, and mind wandering: a registered report. *PsyArXiv* Preprints. https://doi.org/10.31234/osf.io/qfcm9.

Alkemade A, Mulder MJ, Groot JM, Isaacs BR, Van Berendonk N, Lute N, Isherwood SJS, Bazin P-L, Forstmann BU. 2020. The Amsterdam ultra-high field adult lifespan database (AHEAD): a freely available multimodal 7 tesla submillimeter magnetic resonance imaging database. *NeuroImage*. 221:117200.

Alves PN, Foulon C, Karolis V, Bzdok D, Margulies DS, Volle E, De Schotten MT. 2019. An improved neuroanatomical model of the default-mode network reconciles previous neuroimaging and neuropathological findings. *Commun Biol*. 2:370.

Aston-Jones G, Cohen JD. 2005. An integrative theory of locus coeruleus-norepinephrine function: adaptive gain and optimal performance. *Ann Rev Neurosci*. 28:403–450.

Aston-Jones G, Chiang C, Alexinsky T. 1991. Discharge of noradrenergic locus coeruleus neurons in behaving rats and monkeys suggests a role in vigilance. *Prog Brain Res*. 88:501–520.

Avants B, Epstein C, Grossman M, Gee J. 2008. Symmetric diffeomorphic image registration with cross-correlation: evaluating automated labeling of elderly and neurodegenerative brain. *Med Image Anal*. 12:26–41.

Baddeley A, Emslie H, Kolodny J, Duncan J. 1998. Random generation and the executive control of working memory. *Q J Exp Psychol A*. 51:819–852.

Banks JB, Welhaf MS, Hood AVB, Boals A, Tartar JL. 2016. Examining the role of emotional valence of mind wandering: all mind wandering is not equal. *Conscious Cogn*. 43:167–176.

Bastian M, Sackur J. 2013. Mind wandering at the fingertips: automatic parsing of subjective states based on response time variability. *Front Psychol*. 4:573.

Beckmann CF, Jenkinson M, Smith SM. 2003. General multilevel linear modeling for group analysis in FMRI. *NeuroImage*. 20: 1052–1063.

Boayue NM, Csifcsák G, Aslaksen P, Turi Z, Antal A, Groot J, Hawkins GE, Forstmann B, Opitz A, Thielscher A, et al. 2019. Increasing propensity to mind-wander by transcranial direct current stimulation? A registered report. *Eur J Neurosci*. 1–19.

Boayue NM, Csifcsák G, Kreis IV, Schmidt C, Finn I, Vollsund AEH, Mittner M. 2020. The interplay between executive control, behavioral variability and mind wandering: insights from a high-definition transcranial direct-current stimulation study. *Eur J Neurosci*. 53:1498–1516.

Brosowsky NP, Murray S, Schooler JW, Seli P. 2021. Thought dynamics under task demands: evaluating the influence of task difficulty on unconstrained thought. *J Exp Psychol*. 47:1298–1312.

Buckner RL, Krienen FM, Castellanos A, Diaz JC, Yeo BTT. 2011. The organization of the human cerebellum estimated by intrinsic functional connectivity. *J Neurophysiol*. 106:2322–2345.

Bürkner P-C. 2017. Brms: an R package for Bayesian multilevel models using Stan. *J Stat Softw*. 80:1–28.

Bürkner P-C, Vuorre M. 2019. *Ordinal regression models in psychology: a tutorial Adv Meth Pract Psychol Sci*. 2:77–101.

Callard F, Smallwood J, Golchert J, Margulies DS. 2013. The era of the wandering mind? Twenty-first century research on self-generated mental activity. *Front Psychol*. 4:891.

Capone F, Capone G, Ranieri F, Di Pino G, Oricchio G, Di Lazzaro V. 2014. The effect of practice on random number generation task: a transcranial direct current stimulation study. *Neurobiol Learn Mem*. 114:51–57.

Chou Y-H, Sundman M, Whitson HE, Gaur P, Chu M-L, Weingarten CP, Madden DJ, Wang L, Kirste I, Joliot M, et al. 2017. Maintenance and representation of mind wandering during resting-state fMRI. *Sci Rep*. 7:40722.

Christoff K. 2012. Undirect thought: neural determinants and correlates. *Brain Res*. 1428:51–59.

Christoff K, Gordon AM, Smallwood J, Smith R, Schooler JW. 2009. Experience sampling during fMRI reveals default network and executive system contributions to mind wandering. *Proc Natl Acad Sci U S A*. 106:8719–8724.

Cox RW, Hyde JS. 1997. Software tools for analysis and visualization of fMRI data. *NMR Biomed*. 10:171–178.

Cunningham SI, Tomasi D, Volkow ND. 2016. Structural and functional connectivity of the precuneus and thalamus to the default mode network. *Hum Brain Mapp*. 38:938–956.

Delamillieure P, Doucet G, Mazoyer B, Turbelin MR, Delcroix N, Mellet E, Zago L, Crivello F, Petit L, Tzourio-Mazoyer N, et al. 2010. The resting state questionnaire: an introspective questionnaire for evaluation of inner experience during the conscious resting state. *Brain Res Bull*. 81:565–573.

Diedrichsen J, Balsters JH, Flavell J, Cussans E, Ramnani N. 2009. A probabilistic MR atlas of the human cerebellum. *NeuroImage*. 46: 39–46.

DiNuzzo M, Mascali D, Moraschi M, Bussu G, Maugeri L, Mangini F, Fratini M, Giove F. 2019. Brain networks underlying eye's pupil dynamics. *Front Neurosci*. 13:965.

Dixon ML, De La Vega A, Mills C, Andrews-Hanna J, Spreng RN, Cole MW, Christoff K. 2018. Heterogeneity within the frontoparietal control network and its relationship to the default and dorsal attention networks. *Proc Natl Acad Sci U S A*. 115:1598–1607.

Esteban O, Markiewicz CJ, Blair RW, Moodie CA, Isik AI, Erramuzpe A, Kent JD, Goncalves M, DuPre E, Snyder M, et al. 2018. fMRIPrep: a robust preprocessing pipeline for functional MRI. *Nat Methods*. 16:111–116.

Esterman M, Noonan SK, Rosenberg M, Degutis J. 2013. In the zone or zoning out? Tracking behavioral and neural fluctuations during sustained attention. *Cereb Cortex*. 23:2712–2723.

Esterman M, Rosenburg MD, Noonan SK. 2014. Intrinsic fluctuations in sustained attention and distractor processing. *J Neurosci*. 34: 1724–1730.

Fonov VS, Evans AC, McKinstry RC, Almli CR, Collins DL. 2009. Unbiased nonlinear average age-appropriate brain templates from birth to adulthood. *NeuroImage*. 47:102.

Fox KCR, Nijeboer S, Solomonova E, Domhoff GW, Christoff K. 2013. Dreaming as mind wandering: evidence from functional neuroimaging and first-person content reports. *Front Hum Neurosci*. 7:412.

Fox KCR, Spreng RN, Ellamil M, Andrews-Hanna JR, Christoff K. 2015. The wandering brain: meta-analysis of functional neuroimaging studies of mind-wandering and related spontaneous thought processes. *NeuroImage*. 111:611–621.

Friston KJ, Worsley KJ, Frackowiak RS, Mazziotta JC, Evans AC. 1994. Assessing the significance of focal activations using their spatial extent. *Hum Brain Mapp*. 1:210–220.

Gilbert SJ, Dumontheil I, Simons JS, Frith CD, Burgess PW. 2007. Comment on "wandering minds: the default mode network and stimulus-independent thought". *Science*. 317:43.

Gorgolewski K, Burns CD, Madison C, Clark D, Halchenko YO, Waskom ML, Ghosh SS. 2011. Nipype: a flexible, lightweight and extensible neuroimaging data processing framework in python. *Front Neuroinform*. 5:13.

Gountouna V-E, Job DE, McIntosh AM, Moorhead TWJ, Lymer GKL, Whalley HC, Hall J, Waiter GD, Brennan D, McGonigle DJ, et al. 2010. Functional magnetic resonance imaging (fMRI) reproducibility and variance components across visits and scanning sites with a finger tapping task. *NeuroImage*. 49:552–560.

Grandchamp R, Braboszcz C, Delorme A. 2014. Oculometric variations during mind wandering. *Front Psychol*. 5:31.

Greve DN, Fischl B. 2009. Accurate and robust brain image alignment using boundary-based registration. *NeuroImage*. 48:63–72.

Groot JM, Boayue NM, Csifcsák G, Boekel W, Huster R, Forstmann BU, Mittner M. 2021. Probing the neural signature of mind wandering with simultaneous fMRI-EEG and pupillometry. *NeuroImage*. 224:117412.

Groot JM, Csifcsák G, Wientjes S, Forstmann BU, Mittner M. 2021. Materials for "catching wandering minds with tapping fingers: neural and behavioral insights into task-unrelated cognition". *Open Science Framework*. https://doi.org/10.17605/OSF.IO/56FCX

Habas C. 2021. Functional connectivity of the cognitive cerebellum. *Front Sys Neurosci*. 15:642225.

Habas C, Kamdar N, Nguyen D, Prater K, Beckmann CF, Menon V, Greicius MD. 2009. Distinct cerebellar contributions to intrinsic connectivity networks. *J Neurosci*. 29:8586–8594.

Hawkins GE, Mittner M, Forstmann BU, Heathcote A. 2019. Modeling distracted performance. *Cogn Psychol*. 112:48–80.

Hoeks B, Levelt WJM. 1993. Pupillary dilation as a measure of attention: a quantitative system analysis. *Behav Res Methods*. 25:16–26.

Jahanshahi M, Profice P, Brown RG, Ridding MC, Dirnberger G, Rothwell JC. 1998. The effects of transcranial magnetic stimulation over the dorsolateral prefrontal cortex on suppression of habitual counting during random number generation. *Brain*. 121:1533–1544.

Jahanshahi M, Dirnberger G, Fuller R, Firth CD. 2000. The role of the dorsolateral prefrontal cortex in random number generation: a study with positron emission tomography. *NeuroImage*. 12:713–725.

Jahanshahi M, Saleem T, Ho AK, Dirnberger G, Fuller R. 2006. Random number generation as an index of controlled processing. *Neuropsychology*. 20:391–399.

Jenkinson M, Smith SM. 2001. A global optimisation method for robust affine registration of brain images. *Med Image Anal*. 5:143–156.

Jenkinson M, Bannister P, Brady JM, Smith SM. 2002. Improved optimisation for the robust and accurate linear registration and motion correction of brain images. *NeuroImage*. 17:825–841.

Joppich G, Däuper J, Dengler R, Johannes S, Rodriguez-Fornells A, Münte TF. 2004. Brain potentials index executive functions during random number generation. *Neurosci Res*. 49:157–164.

Joshi S, Li Y, Kalwani RM, Gold JI. 2016. Relationship between pupil diameter and neuronal activity in the locus coeruleus, colliculi, and cingulate cortex. *Neuron*. 89:221–234.

Jubera-Garcia E, Gevers W, Van Opstal F. 2019. Influence of content and intensity of thought on behavioral and pupil changes during active mind wandering, off-focus, and on-task states. *Atten Percept Psychophys*. 82:1125–1135.

Kane MJ, McVay JC. 2012. What mind wandering reveals about executive-control abilities and failures. *Curr Dir Psychol Sci*. 21:348–354.

Killingsworth MA, Gilbert DT. 2010. A wandering mind is an unhappy mind. *Science*. 330:932.

Konishi M, Brown K, Battaglini L, Smallwood J. 2017. When attention wanders: pupillometric signatures of fluctuations in external attention. *Cognition*. 168:16–26.

Kosslyn SM, Ganis G, Thompson WL. 2001. Neural foundations of imagery. *Nat Rev Neurosci*. 2:635–642.

Kucyi A, Esterman M, Riley CS, Valera EM. 2016. Spontaneous default network activity reflects behavioral variability independent of mind-wandering. *Proc Natl Acad Sci*. 113:13899–13904.

Kucyi A, Hove MJ, Esterman M, Hutchison RM, Valera EM. 2017. Dynamic brain network correlates of spontaneous fluctuations in attention. *Cereb Cortex*. 27:1831–1840.

Laeng B, Sirois S, Gredebäck G. 2012. Pupillometry: a window to the preconscious? *Perspect Psychol Sci*. 7:18–27.

Lawson C, Hanson RJ. 1987. *Solving least squares problems*. Philadelphia (PA): SIAM.

Leszczynski M, Staudigl T. 2016. Memory-guided attention in the anterior thalamus. *Neurosci Biobehav Rev*. 66:163–165.

Liddell TM, Kruschke JK. 2018. Analyzing ordinal data with metric models: what could possibly go wrong? *J Exp Soc Psychol*. 79:328–348.

Maillet D, Seli P, Schacter DL. 2017. Mind-wandering and task stimuli: stimulus-dependent thoughts influence performance on memory tasks and are more often past- versus future-oriented. *Conscious Cogn*. 52:55–67.

Mason MF, Norton MI, Van Horn JD, Wegner DM, Grafton ST, Macrae CN. 2007. Wandering minds: the default mode network and stimulus-independent thought. *Science*. 315:393–395.

Mathôt S. 2013. A simple way to reconstruct pupil size during eye blinks. https://doi.org/10.6084/m9.figshare.688001.

Mattay VS, Callicott JH, Bertolino A, Santha AKS, Van Horn JD, Tallent KA, Frank JA, Weinberger DR. 1998. Hemispheric control of motor function: a whole brain echo planar fMRI study. *Psychiatry Res Neuroimaging*. 83:7–22.

McVay JC, Kane MJ. 2009. Conducting the train of thought: working memory capacity, goal neglect, and mind wandering in an executive-control task. *J Exp Psychol Learn Mem Cogn*. 35:196–204.

McVay JC, Kane MJ. 2010. Does mind wandering reflect executive function or executive failure? Comment on Smallwood and Schooler (2006) and Watkins (2008). *Psychol Bull*. 136:188–207.

Mittner M. 2020. Pypillometry: a python package for pupillometric analyses. *J Open Source Soft*. 5:2348.

Mittner M. 2021. Estimation of tonic and phasic pupillometric signals. *Figshare*. https://doi.org/10.6084/m9.figshare.17022104.v2.

Mittner M, Boekel W, Tucker AM, Turner BM, Heathcote A, Forstmann BU. 2014. When the brain takes a break: a model-based analysis of mind wandering. *J Neurosci*. 34:16286–16295.

Mittner M, Hawkins GE, Boekel W, Forstmann BU. 2016. A neural model of mind wandering. *Trends Cogn Sci*. 20:570–578.

Murphy PR, O'Connell RG, O'Sullivan M, Robertson IH, Balsters JH. 2014. Pupil diameter covaries with BOLD activity in human locus coeruleus. *Hum Brain Mapp*. 35:4140–4154.

Peirce JW. 2007. PsychoPy - psychophysics software in python. *J Neurosci Methods*. 162:8–13.

Pelagatti C, Binda P, Vannucci M. 2020. A closer look at the time-course of mind wandering: pupillary response and behavior. *PLoS One*. 15:0226792.

Peters M, Giesbrecht T, Jelicic M, Merckelback H. 2007. The random number generation task: psychometric properties and normative data on an executive function task in a mixed sample. *J Int Neuropsychol Soc*. 13:626–634.

Petro LS, Paton AT, Muckli L. 2016. Contextual modulation of primary visual cortex by auditory signals. *Phil Trans R Soc B*. 372:20160104.

Pincus S, Kalman RE. 1997. Not all (possibly) "random" sequences are created equal. *Proc Natl Acad Sci U S A*. 94:3513–3518.

Raichle ME. 2015. The brain's default mode network. *Annu Rev Neurosci*. 38:433–447.

Saper CB, Scammel TE, Lu J. 2005. Hypothalamic regulation of sleep and circadian rhythms. *Nature*. 437:1257–1263.

Scheibner HJ, Bogler C, Gleich T, Haynes JD, Bermpohl F. 2017. Internal and external attention and the default mode network. *NeuroImage*. 148:381–389.

Schneider M, Hathway P, Leuchs L, Sämann PG, Czisch M, Spoormaker VI. 2016. Spontaneous pupil dilations during resting state are associated with activation of the salience network. *NeuroImage*. 139:189–201.

Schooler JW, Smallwood J, Christoff K, Handy TC, Reichle ED, Sayette MA. 2011. Meta-awareness, perceptual decoupling and the wandering mind. *Trends Cogn Sci*. 15:319–326.

Schubert T, von Cramon DY, Niendorf T, Pollman S, Bublak P. 1998. Cortical areas and the control of self-determined finger movements. *Neuroreport*. 9:3171–3176.

Seli P, Cheyne JA, Smilek D. 2013. Wandering minds and wavering rhythms: linking mind wandering and behavioral variability. *J Exp Psychol*. 39:1–15.

Seli P, Risko EF, Smilek D. 2016. On the necessity of distinguishing between unintentional and intentional mind wandering. *Psychol Sci*. 27:685–691.

Seli P, Beaty RE, Cheyne JA, Smilek D, Oakman J, Schacter DL. 2018. How pervasive is mind wandering, really? *Conscious Cogn*. 66: 74–78.

Seli P, Konishi M, Risko EF, Smilek D. 2018. The role of task difficulty in theoretical accounts of mind wandering. *Conscious Cogn*. 65: 255–262.

Shamloo F, Helie S. 2016. Changes in default mode network as automaticity develops in a categorization task. *Behav Brain Res*. 313:324–333.

Shepard J. 2019. Why does the mind wander? *Neurosci Conscious*. 5:014.

Smallwood J, Andrews-Hanna J. 2013. Not all minds that wander are lost: the importance of a balanced perspective on the mind-wandering state. *Front Psychol*. 4:441.

Smallwood J, Schooler JW. 2006. The restless mind. *Psychol Bull*. 132: 946–958.

Smallwood J, Schooler JW. 2015. The science of mind wandering: empirically navigating the stream of consciousness. *Ann Rev Psychol*. 66:487–518.

Smallwood J, Davies JB, Heim D, Finnigan F, Sudberry M, O'Connor R, Obonsawin M. 2004. Subjective experience and the attentional lapse: task engagement and disengagement during sustained attention. *Conscious Cogn*. 13:657–690.

Smallwood J, McSpadden M, Schooler JW. 2007. The lights are on but no one's home: meta-awareness and the decoupling of attention when the mind wanders. *Psychon Bull Rev*. 14:527–533.

Smallwood J, McSpadden M, Luus B, Schooler J. 2008. Segmenting the stream of consciousness: the psychological correlates of temporal structures in the time series data of a continuous performance task. *Brain Cogn*. 66:50–56.

Smallwood J, Brown KS, Tipper C, Giesbrecht B, Franklin MS, Mrazek MD, Carlson JM, Schooler JW. 2011. Pupillometric evidence for the decoupling of attention from perceptual input during offline thought. *PLoS One*. 6:18298.

Smallwood J, Brown KS, Baird B, Mrazek MD, Franklin MS, Schooler JW. 2012. Insulation for daydreams: a role for tonic norepinephrine in the facilitation of internally guided thoughts. *PLoS One*. 7:33706.

Smith SM, Brady JM. 1997. SUSAN – a new approach to low level image processing. *Int J Comput Vis*. 23:45–78.

Spreng NR, Mar RA, Kim ASN. 2002. The common neural basis of autobiographical memory, prospection, navigation, theory of mind, and the default mode: a quantitative meta-analysis. *J Cogn Neurosci*. 21:489–510.

Sweeney-Reed CM, Zaehle T, Voges J, Schmitt FC, Buentjen L, Borchardt V, Walter M, Hinrichs H, Heinze H-J, Rugg MD, et al. 2017. Anterior thalamic high frequency band activity is coupled with theta oscillations at rest. *Front Hum Neurosci*. 11:358.

Tanabe C, Kato M, Miyauchi S, Hayashi S, Yanagida T. 2005. The sensorimotor transformation of cross-modal spatial information in the anterior intraparietal sulcus as revealed by functional MRI. *Cogn Brain Res*. 22:385–396.

Tang YY, Rothbart MK, Posner MI. 2012. Neural correlates of establishing, maintaining, and switching brain states. *Trends Cogn Sci*. 16:330–337.

Teasdale JD, Dritschel BH, Taylor MJ, Proctor L, Lloyd CA, Nimmo-Smith I, Baddeley AD. 1995. Stimulus-independent thought depends on central executive resources. *Mem Cogn*. 23: 551–559.

Turnbull A, Wang H-T, Murphy C, Ho NSP, Wang X, Sormaz M, Karapanagiotidis T, Leech RM, Bernhardt B, Margulies DS, et al. 2019. Left dorsolateral prefrontal cortex supports context-dependent prioritisation of off-task thought. *Nat Commun*. 10:3816.

Tustison NJ, Avants BB, Cook PA, Zheng Y, Egan A, Yushkevich PA. 2010. N4ITK: improved N3 bias correction. *IEEE Trans Med Imaging*. 29:1310–1320.

Unsworth N, Robison MK. 2016. Pupillary correlates of lapses of sustained attention. *Cogn Affect Behav Neurosci*. 16:601–615.

Unsworth N, Robison MK. 2018. Tracking arousal state and mind wandering with pupillometry. *Cogn Affect Behav Neurosci*. 18: 638–664.

Van Calster L, D'Argembeau A, Salmon E, Peters F, Majerus S. 2017. Fluctuations of attentional networks and default mode network during the resting state reflect variations in cognitive states: evidence from a novel resting-state experience sampling method. *J Cogn Neurosci*. 29:95–113.

Vatansever D, Menon DK, Manktelow AE, Sahakian BJ, Stamatakis EA. 2015. Default mode network connectivity during task execution. *NeuroImage*. 122:96–104.

Vatansever D, Menon DK, Stamatakis EA. 2017. Default mode contributions to automated information processing. *Proc Natl Acad Sci U S A*. 114:12821–12826.

Wang X, Xu M, Song Y, Li X, Zhen Z, Yang Z, Liu J. 2014. The network property of the thalamus in the default mode network is correlated with trait mindfulness. *Neuroscience*. 278: 91–301.

Weinstein Y. 2018. Mind-wandering, how do I measure three with probes? Let me count the ways. *Behav Res Methods*. 50:642–661.

Weinstein Y, De Lima HJ, Van Der Zee T. 2018. Are you mind-wandering, or is your mind on task? The effect of probe framing on mind-wandering reports. *Psychon Bull Rev*. 25: 754–760.

Woolrich MW, Ripley BD, Brady M, Smith SM. 2001. Temporal auto-correlation in univariate linear modeling of FMRI data. *NeuroImage*. 14:1370–1386.

Yamashita A, Rothlein D, Kucyi A, Valera EM, Esterman M. 2021. Brain state-based detection of attentional fluctuations and their modulation. *NeuroImage*. 236:118072.

Yellin D, Berkovich-Ohana A, Malach R. 2015. Coupling between pupil fluctuations and resting-state fMRI uncovers a slow build-up of antagonistic responses in the human cortex. *NeuroImage*. 106: 414–427.

Yeo BTT, Krienen FM, Sepulcre J, Sabuncu MR, Lashkari D, Hollinshead M, Roffman JL, Smoller JW, Zöllei L, Polimeni JR, et al. 2011. The organization of the human cerebral cortex estimated by intrinsic functional connectivity. *J Neurophysiol*. 106:1125–1165.

Zanesco AP, Denkova E, Jha AP. 2020. Self-reported mind wandering and response time variability differentiate prestimulus electroencephalography microstate dynamics during a sustained attention task. *J Cogn Neurosci*. 33:28–45.

Zhang Y, Brady M, Smith S. 2001. Segmentation of brain MR images through a hidden markov random field model and the expectation-maximization algorithm. *IEEE Trans Med Imag*. 20: 45–57.

Zuberer A, Kucyi A, Yamashita A, Wu CM, Walter M, Valera EM, Esterman M. 2021. Integration and segregation across large-scale intrinsic brain networks as a marker of sustained attention and task-unrelated thought. *NeuroImage*. 229:117610.

Paper III

Echoes from intrinsic connectivity networks in the subcortex

Josephine Maria Groot, Steven Miletić, Scott JS Isherwood, Desmond HY Tse, Sarah Habli, Asta K Håberg, Birte U Forstmann, Pierre-Louis Bazin, Matthias Mittner

Echoes from intrinsic connectivity networks in the subcortex

Josephine M Groot[1,2], Steven Miletic[2], Scott JS Isherwood[2], Desmond HY Tse[3], Sarah Habli[4], Asta K Håberg[5,6], Birte U Forstmann[2], Pierre-Louis Bazin[1,7]*, Matthias Mittner[1]*

*Authors contributed equally
[1] Department of Psychology, UiT – The Arctic University of Norway, Tromsø, Norway
[2] Integrative Model-based Cognitive Neuroscience research unit, University of Amsterdam, Amsterdam, The Netherlands
[3] Department of Neuropsychology and Psychopharmacology, Maastricht University, Maastricht, The Netherlands
[4] Department of Psychology, Norwegian University of Science and Technology, Trondheim, Norway
[5] Department of Neuromedicine and Movement Science, Norwegian University of Science and Technology, Trondheim, Norway
[6] Department of Radiology and Nuclear Medicine, St. Olavs Hospital, Trondheim, Norway
[7] Departments of Neurophysics and Neurology, Max Planck Institute for Human Cognitive and Brain Sciences, Leipzig, Germany

Abstract

Decades of research have greatly improved our understanding of human brain organization in terms of intrinsic connectivity networks and the transmodal hubs within the cortex at which they converge. However, subcortical substrates of multi-network integration remain mostly uncharted. In this study, we exploited recent advances in subcortical imaging and atlasing by combining state-of-the-art subcortical parcellations with ultra-high field imaging optimized for the subcortex to investigate the functional architecture of a large set of subcortical nuclei using a data-driven, multivariate analysis approach. We revealed an intricate system of signal repetitions, or echoes, from multiple intrinsic connectivity networks that indicates a functionally heterogeneous organization supportive of large-scale network convergence within various subcortical structures. Diversified network affiliations were especially prominent within the thalamus, striatum, claustrum, and hippocampus. Whereas subsignals within the globus pallidus externa, subsantia nigra, and ventral tegmental area also correlated with widely distributed functional networks, other structures including the subthalamic nucleus, red nucleus, and locus coeruleus demonstrated a stronger local connectivity profile indicative of more segregated functional processing. With these results, we present new evidence for the subcortical contributions to systems-level information integration, emphasizing the importance of regions beyond associative cortex for global brain communication.

Keywords: resting-state, 7 Tesla, functional connectivity, dual regression, network integration

Introduction

A large body of neuroscientific research in the past decades has focused on the description of the macroscopic organization of the human brain in terms of intrinsic functional connectivity and its role in orchestrating cognitive processes and behavior (Damoiseaux et al 2006; Liégeois et al 2019; Lee et al 2019). The integration of distributed, functionally specialized networks is thought to be essential, especially for higher-level cognition and consciousness (Senden et al 2014; Bell and Shine 2016). Using a variety of methods, specific sites for large-scale network convergence were identified in the posterior cingulate cortex/precuneus (PCC), anterior cingulate cortex (ACC), temporo-parietal junction (TPJ), and the posterior parietal and superior frontal cortices (Tomasi and Volkow 2011; Bell and Shine 2015; Lyu et al 2021), revealing an ensemble, or 'rich-club' of transmodal cortical regions that enable efficient global communication (Van der Heuvel and Sporns 2011; Grayson et al 2014).

Braga and Leech (2015) argued that brain regions facilitating cross-network information integration should feature signal repetitions or 'echoes' of multiple networks within its local, subregional functional architecture. Using resting-state functional magnetic resonance imaging (rs-fMRI), they performed a data-driven multivariate analysis for separating the mixture of neural signals within a predefined region (Leech et al 2012; Braga et al 2013). Importantly, by controlling for the multiple subsignals when estimating their whole-brain functional connectivity (FC), they uncovered a more subtle subregional topography beyond the region's global connectivity profile. For example, Leech et al (2012) observed echoes of different functional networks within separate, but spatially overlapping subregions of the PCC that were concealed by its principal connection with the default mode network in a univariate FC analysis. Furthermore, this characteristic was specific to the PCC and other transmodal cortical areas (Braga et al 2013), demonstrating sensitivity of this method to detect varying degrees of functional heterogeneity.

Although previous work has provided important insights into the mechanisms of network integration, the vast majority of studies have followed a corticocentric view and neglected the potential prominent role that subcortical structures may have in whole-brain communication (Bell and Shine 2016: Forstmann et al 2017; Ji et al 2019; Tian et al 2020). The subcortex contains highly diverse and densely packed grey matter nuclei that are challenging to visualize with conventional MRI due to their small size, varied magnetic tissue properties (due to e.g., iron or neuromelanin content), and generally weaker signal-to-noise ratio (SNR) compared to the cortex (De Hollander et al 2017; Keuken et al 2018a). As a result, many subcortical structures remain underrepresented in functional imaging studies of human cognitive phenomena, reflecting a knowledge gap in brain structure-function mappings (Keuken et al 2018b).

69   Intriguingly, the subcortex is anatomically well-positioned to support information convergence

70   through widely distributed cortical projections and extensive reciprocal connections embedded in

71   cortico-subcortical circuit loops (Haber 2003), and several rs-fMRI studies have observed intrinsic FC

72   between thalamic, midbrain, and basal ganglia nodes and the default mode network (e.g., Lee et al

73   2018; Ji et al 2019; Li et al 2021). The thalamus and striatum are larger subcortical structures that are

74   centrally located within a macrocircuitry linking neuromodulatory systems with sensorimotor, limbic,

75   and associative information. Consequently, they have received a comparatively high amount of

76   attention across different studies, leading to their recognition as subcortical hubs (e.g., Jarbo and

77   Verstynen 2015; Bell and Shine 2016; Keuken et al 2018b; Seitzman et al 2020; Greene et al 2020). For

78   example, using co-clustering connectional topography, Cheng and Liu (2021) showed an optimal

79   partitioning of the thalamus into five subdivisions, each with connections to well-established brain

80   networks. In another study, graph theory analyses indicated properties of thalamic nuclei that

81   supported integration of diverse functional networks and multimodal cognitive processing (Hwang et

82   al 2017). Similarly, consistent with anatomical tracing studies, distinct cortical zones were identified

83   within the striatum using rs-fMRI (Choi et al 2012).

84   In addition, there is evidence that other structures outside the neocortex, including the

85   hippocampus, amygdala, claustrum, and cerebellum, are affiliated with multiple functional networks,

86   suggesting involvement in systems-level communication beyond local functional couplings within

87   more segregated communities (Tomasi and Volkow 2011; Van der Heuvel and Sporns 2011; Bell and

88   Shine 2015; Blessing et al 2016; Krimmel et al 2019; Sylvester et al 2020). Intrinsic connectivity was

89   also observed between midbrain and brainstem nuclei and widespread functional networks, including

90   the default mode and executive control networks (Bär et al 2016), implying the involvement of

91   structures driving the main dopaminergic and noradrenergic modulatory systems in integrative

92   processing and cognition (Liu et al 2017; De Gee 2017; Zhang et al 2016).

93   Together, these results are promising and advance the field toward a better understanding of

94   subcortical functional architecture. However, direct empirical evidence for the role of many subcortical

95   structures in large-scale network integration is scarce and not all preliminary findings converge. For

96   example, Bär et al (2016) showed that locus coeruleus (LC) connectivity to the default mode network

97   disappeared when controlling for adjacent neural signals and that hub-like features of midbrain nuclei

98   were not supported by a graph theory analysis. Furthermore, the majority of human imaging studies

99   were performed with 3 Tesla fMRI, limiting the resolution needed to resolve small subcortical

100   structures (Forstmann et al 2017). In addition, data are often subjected to spatial smoothing (5-8mm

101   smoothing kernels), further limiting the spatial resolution and increasing the risk of signal blurring and

102   misattribution of signals to nearby areas, especially in the subcortex (De Hollander et al 2015). Due to

103   these shortcomings, the precise architecture of systems-level integration across distributed and

104   functionally diverse cortico-subcortical brain networks remains poorly understood. Charting the

105   pattern of large-scale network echoes within the subcortex may provide a compelling approach to

106   accomplish new insights into the subcortical contributions to whole-brain communication and higher-

107   level cognition. Furthermore, comprehensive knowledge of subcortical functional architecture may be

108   vital for improving disease models given that dysfunction of subcortical structures is heavily implicated

109   in a wide range of neurological and psychiatric diseases. For example, deep brain stimulation (DBS) of

110   subcortical nuclei has variable clinical outcomes and frequent side-effects (Odekerken et al 2013;

111   Zarzycki and Domitrz 2020), which are likely to improve with optimized target selection based on more

112   precise information regarding subregional functional sites within the subcortex.

113   In this study, we aim to investigate the functional heterogeneity of a wide range of subcortical

114   structures by quantifying the existence of signal echoes from distributed functional networks, using a

115   data-driven, multivariate analysis approach (Braga et al 2013). Specifically, we aim to assess the

116   independent connectivity profiles of functional subdivisions within subcortical regions that are likely

117   hidden in previous univariate analyses. We expect that subcortical structures involved in multi-

118   network integration show a complex connectivity pattern reflected by affiliations with different

119   intrinsic connectivity networks. We address this research question with an rs-fMRI protocol at 7T

120   tailored to subcortical imaging and parcellations of fourteen regions of interest, including the

121   thalamus, striatum, globus pallidus externa, globus pallidus interna, subthalamic nucleus, claustrum,

122   hippocampus, amygdala, substantia nigra, red nucleus, ventral tegmental area, locus coeruleus,

123   periaqueductal grey, and pedunculopontine nucleus. To validate our novel results for the subcortex,

124   we additionally assessed if we could reproduce the previously reported pattern of network echoes

125   within the PCC, medial prefrontal cortex (mPFC), and visual cortex (Braga et al 2013). Filling the

126   persistent subcortical knowledge gap in large-scale network dynamics, we draw on recent advances in

127   sensitive functional neuroimaging at ultra-high resolution (Miletic et al 2020) and automated

128   parcellation algorithms for the subcortex (Bazin et al 2020), making the current study both timely and

129   warranted.

Methods

Overview

Figure 1 provides an overview of our 'echo' analysis, extending the approach of Leech et al (2012) and Braga et al (2013) to the subcortex. This analysis approach allowed us to identify regions in the subcortex that have the potential to facilitate functional network integration. Forty healthy adults underwent two 15-minute runs of whole-brain resting-state fMRI at 7T with a spatial resolution of 1.5mm isotropic. Resting-state data were pre-processed with fMRIPrep, smoothed with a Gaussian kernel with a full-width half maximum of 1.5mm, denoised in a general linear model with a series of nuisance regressors, and registered to standard MNI2009c space. Fourteen subcortical regions of interest (ROIs) were defined using open-source atlases (Table 1, Figure 2a). Multivariate decomposition using canonical independent component analysis (canICA) was performed to separate the mixture of neural signals and obtain 10 spatiotemporal independent subregions within each ROI. The whole-brain FC of each subregion was then assessed with dual regression, by estimating the unique contribution of each subregion's timecourse while controlling for the variance in the remaining timecourses. To quantify the presence of signal echoes from distributed resting-state networks within subregions, the 10 FC maps for each ROI were spatially correlated with 16 data-driven reference networks extracted from a whole-brain canICA on the resting-state timeseries. All unthresholded group-level spatial maps from the canICA and dual regression analyses are available in an Open Science Framework repository at: https://osf.io/wt3uc.

Participants

The study was approved by the Ethics Review Board of the University of Amsterdam and the Regional Committees for Medical and Health Research Ethics in Norway. Forty healthy adults between 19 and 39 years old (21 female, mean age=26.5, *SD*=5.5 years) were recruited from the general population in Norway and screened for MRI compatibility as part of a multi-session 7T study. Exclusion criteria were self-reported (history of) neurological or psychiatric disease, impaired vision, or any contra-indications for MRI at 7T such as metal implants. Written informed consent was obtained prior to data collection. The resting-state data used in this study were collected together with anatomical scans during the first session, lasting approximately 60 minutes in total. Materials and code used in this study are publicly available at an Open Science Framework repository at https://osf.io/wt3uc.
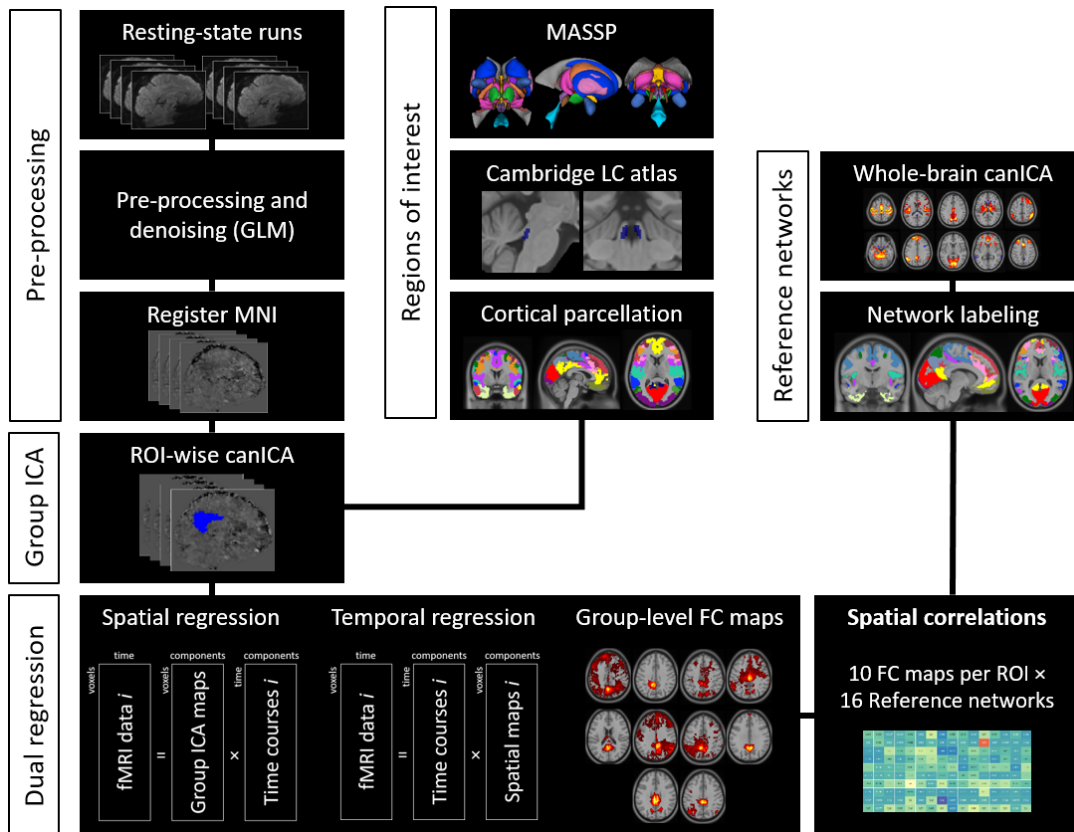
Figure 1. Overview of the data analysis.

Table 1. Parcellation details for regions of interest.

Region of interest		*N* voxels	Mean (SD) tSNR	Source*
Forebrain				
Thalamus	Tha	6 130	47.94 (6.31)	MASSP
Striatum	Str	8 552	52.17 (8.11)	MASSP
Globus pallidus externa	GPe	1 241	35.44 (5.58)	MASSP
Globus pallidus interna	GPi	453	34.18 (4.39)	MASSP
Subthalamic nucleus	STN	93	32.30 (4.25)	MASSP
Claustrum	Cl	683	59.12 (4.71)	MASSP
Hippocampus	HPC	2 894	37.84 (10.44)	17-network cortical parcellation
Amygdala	Amg	1 063	39.89 (7.22)	MASSP
Midbrain				
Substantia nigra	SN	481	31.51 (5.32)	MASSP
Red nucleus	RN	232	33.75 (3.05)	MASSP
Ventral tegmental area	VTA	220	37.68 (3.05)	MASSP
Periaqueductal grey	PAG	198	32.37 (10.56)	MASSP
Brainstem				
Locus coeruleus	LC	98	39.01 (7.31)	7T Probabilistic LC Atlas
Pedunculopontine nucleus	PPN	135	40.00 (3.29)	MASSP

Number of voxels (*N* voxels) are in functional space (1.5mm voxel resolution).
* MASSP (Multi-contrast Anatomical Subcortical Parcellation; Bazin et al 2020), 17-network cortical parcellation (Yeo et al 2011), 7T Probabilistic LC Atlas (Ye et al 2021).

6

Data acquisition and preprocessing

Neuroimaging data were collected with a Siemens MAGNETOM Terra 7Tesla system with a 32-channel phased-array head coil. Structural images were obtained with a MP2RAGE sequence (Marques et al 2010) in 224 sagittal slices at 0.75mm isotropic voxel resolution (TR=4300ms; $TI_{1,2}$=840, 2370ms; flip-angles$_{1,2}$=5, 6°; TE=1.99ms; FOV=240×240×168mm). Functional images were acquired during two runs of 15 minutes eyes-open wakeful rest (fixation on centered cross) using a gradient echo echo-planar imaging (EPI) sequence with a voxel resolution of 1.5mm isotropic (82 transverse slices per volume; TR=1380ms; TE=14ms; flip-angle=60°; in-plane acceleration factor (GRAPPA)=3; multiband acceleration factor=2; partial Fourier=6/8). An additional EPI sequence with opposite phase-encoding direction was performed for susceptibility distortion correction purposes. Heart rate and respiratory data were acquired with a fingerclip and waistband, respectively, to correct for physiological noise, which is especially prominent in the subcortex.

MR images were preprocessed with fMRIPrep (v20.2.6; Esteban et al 2018) in the Nipype framework (Gorgolewski et al 2011). The structural (T1-weighted) scan was corrected for intensity non-uniformity with N4BiasFieldCorrection (ANTs v2.3.3; Tustison et al 2010) and skull-stripped with antsBrainExtraction using the OASIS30ANTs target template. Brain tissue segmentation of cerebrospinal fluid (CSF), white matter (WM), and gray matter (GM) was performed with FAST (FSL v5.0.9; Zhang et al 2001). For each of the two resting-state runs, a reference volume and its skull-stripped version were generated. A fieldmap based on the EPI references with opposing phase-encoding directions was calculated with 3dQwarp (AFNI; Cox 1996) and susceptibility distortion correction was applied to the EPI reference prior to co-registration to the T1-weighted reference using the boundary-based registration cost-function in bbregister with 6 degrees of freedom (FreeSurfer; Greve and Fischl 2009). Head-motion parameters (rotation and translation) were estimated with MCFLIRT (FSL v5.0.9; Jenkinson et al 2002) and slice-time correction to half of the acquisition range (0.674s) was performed with AFNI's 3dTshift. Following fMRIPrep, data were spatially smoothed with a full-width half-maximum Gaussian kernel of 1.5mm using SUSAN (Smith and Brady 1997) and denoised with a first-level general linear model in FEAT (Woolrich et al 2001) that included fMRIPrep-derived confound regressors, including: mean signal in CSF and WM, framewise displacement (FD), six rotation and translation parameters, and discrete-cosine transform (DCT) basis functions to model low-frequency scanner drifts. In addition, cardiac and respiratory sources of nuisance were based on acquired physiological data and modeled with RETROICOR (Glover et al 2000) using the Matlab PhysIO toolbox (Kasper et al 2017) in TAPAS (Frässle et al 2021). For one subject with missing physiological data, the same number of fMRIPRrep's anatomical component-based noise correction (aCompCor; Behzadi et al 2007) regressors were entered in the model instead. The modeled data were obtained

204 via linear regression and normalized. Finally, the two residual runs were concatenated and registered
205 to the ICBM 152 Nonlinear Assymetrical template version 2009c (MNI152Nlin2009cAsym; Fonov et al
206 2009) using the nonlinear registration tool in antsRegistration (Avants et al 2008) with the
207 transformation parameters provided by fMRIPrep.

208
209 **Defining regions of interest**

210 Anatomical ROI masks were computed with the Multi-contrast Anatomical Subcortical Parcellation
211 algorithm (MASSP; Bazin et al 2020) based on quantitative MRI data from 105 healthy adults (ages 18-
212 80) part of the 7Tesla Amsterdam ultra-high field adult lifespan database (AHEAD; Alkemade et al 2020)
213 in high-resolution MNI space (MNI152Nlin2009bAsym; Fonov et al 2009). The MASSP parcellations
214 include the thalamus (Tha), striatum (Str), claustrum (Cl), globus pallidus externa (GPe), globus pallidus
215 interna (GPi), substantia nigra (SN), subthalamic nucleus (STN), ventral tegmental area (VTA), red
216 nucleus (RN), amygdala (Amg), periaqueductal grey (PAG), and pedunculopontine nucleus (PPN). The
217 locus coeruleus (LC) was defined with the 7T Probabilistic LC Atlas based on 53 healthy adults aged 52-
218 84 years (Ye et al 2021). In addition, the 17-network cortical parcellation (Yeo et al 2011) was used for
219 extracting masks of the hippocampus (HPC), which was taken from the Default C network, the posterior
220 cingulate cortex (PCC) and medial prefrontal cortex (mPFC) from the Default A network, as well as the
221 Visual Central network which consists of striate and extrastriate cortex. For bilateral ROIs, left and right
222 hemispheres were combined into a single binary mask and all masks were resampled to the resolution
223 of the functional data with FLIRT using nearest-neighbor interpolation (v6.0; Jenkinson and Smith
224 2001). The probabilistic LC mask was thresholded liberally so that voxels that overlapped 1% or more
225 were included in the resampled mask.

226
227 **Multivariate functional connectivity analysis**
228 The pre-processed resting-state timeseries were masked with each of the ROIs and decomposed
229 into 10 spatiotemporal independent subregions with a spatially-restricted group canonical
230 independent component analysis (canICA) as implemented in Nilearn. Although the temporal
231 concatenation ICA approach is a popular technique in combination with dual regression, biases in the
232 estimation of group-level networks may arise with varying degrees of inter-individual variability (Hu
233 and Yang 2021). Instead, canICA applies a hierarchical approach in which individual data is decomposed
234 prior to canonical correlation analysis to identify group commonalities (Varoquaux et al 2010).
235 Although the precise dimensionality of regions may vary, we followed previous approaches and
236 restricted the canICA to 10 components in order to examine interregional differences in the degree of
237 network echoes.

238   Following the ROI-wise canICA, a back-reconstruction to estimate subject-specific contributions to

239   the group-level components was performed using dual regression (Beckmann et al 2009; Zuo et al

240   2010). First, the 10 spatial maps from the ROI-wise canICA were regressed onto every individual's

241   whole-brain resting-state data in order to estimate the subject-specific timecourse for each

242   independent component. Because the spatial maps were simultaneously entered as design matrix, the

243   timecourses for each component were estimated while statistically controlling for the variance

244   explained by the other components. Second, the 10 estimated subject-specific independent

245   timecourses were regressed onto the subject's resting-state data to obtain corresponding subject-

246   specific spatial maps, providing a measure of whole-brain voxel-wise FC for each subregion while

247   statistically controlling for the other subregional timecourses. The subject-level FC maps were then

248   combined in a group-level analysis using 5000 permutations of non-parametric random permutation

249   testing with threshold-free cluster enhancement (TFCE). This resulted in a *t*-statistical map for each

250   subregion within each ROI that was thresholded at family-wise error (FWE) corrected $p<.05$ to

251   represent the significant whole-brain FC at group-level.

252   To assess the dominant connectivity pattern for each ROI in a control analysis, we performed a

253   standard, univariate seed-based approach by correlating the mean timeseries of voxels underneath

254   the mask of each ROI with all other voxels in the brain for each subject. These individual seed-based

255   connectivity maps were then Fisher z-transformed and averaged to yield a group-level FC map per ROI,

256   which was thresholded to retain voxels with the 5% strongest positive correlations before calculating

257   spatial correlations with each of the reference networks (Supplement E).

258

Quantifying echoes of intrinsic connectivity networks

260   To identify resting-state reference networks in a data-driven manner, the pre-processed resting-

261   state data were spatiotemporally decomposed with a whole-brain canICA restricted to 20 independent

262   components. Based on visual inspection and low spatial Pearson product-moment correlation

263   coefficients with an existing 17-network cortical parcellation (Yeo et al 2011), four components (r=.05,

264   r=.04, r=.13, r=.04) were identified as artifactual and removed from further analysis. Because we aimed

265   to quantify echoes from cortical intrinsic connectivity networks, we removed any remaining voxels

266   located outside cortical grey matter (e.g., cerebral white matter, subcortex, CSF) by masking the

267   remaining 16 spatial maps with the 17-network cortical parcellation. Together, the reference networks

268   covered 66% of cortical grey matter defined in this parcellation. The strongest deviation with the

269   cortical parcellation was observed in the anterior temporal cortex, which was not remedied by

270   increasing model order (40 or 100 independent components) or a cortically-restricted ICA. To assess

271   whether this observation was associated with variations in temporal signal-to-noise ratio (tSNR), we

272   calculated voxel-wise tSNR values as the ratio of the mean and standard deviation of the resting-state
273   timeseries after temporal high-pass filtering (1/128s). Individual tSNR maps (*n*=40) were registered to
274   standard MNI space with before voxel-wise tSNR values were averaged across subjects and runs to
275   create a group-level map (Supplement F). We observed reduced tSNR in the temporal lobe compared
276   to other cortical areas, and as a consequence, temporal networks were underrepresented in our
277   results.

278   To identify traces of intrinsic connectivity network echoes within subregions of subcortical
279   structures, the 10 thresholded subregion-FC maps for each ROI were then spatially correlated with the
280   unthresholded, cortically-masked spatial maps of the remaining 16 reference networks.

Results

Data-driven networks correspond to existing cortical network parcellations

The 16 data-driven reference networks were labeled automatically according to their maximum spatial correlation with a well-established 17-network cortical parcellation (Yeo et al 2011; Figure 2b), that is based on rs-fMRI data from 1000 individuals. Despite large methodological differences in field strength, data resolution, and network parcellation, we found Pearson product-moment correlation coefficients ranging from 0.21 to 0.67 (mean $r=.44$, $SD=.14$), generally indicating moderate to good spatial overlap with their reference network counterparts (Figure 2b, lower right): Somatomotor A ($r=.66$), Somatomotor B ($r=.30$), Control A ($r=.46$), Control B ($r=.51$), Control C ($r=.57$), Salience/Ventral Attention A ($r=.34$), Salience/Ventral Attention B ($r=.54$), Temporal Parietal ($r=.21$), Dorsal Attention A ($r=.46$), Dorsal Attention B ($r=.25$), Default A ($r=.42$), Default B ($r=.47$), Limbic A ($r=.30$), Limbic B ($r=.41$), Visual Central ($r=.49$), and Visual Peripheral ($r=.67$). The data-driven Temporal Parietal network also partially overlapped with the Control A network parcellation ($r=.15$).
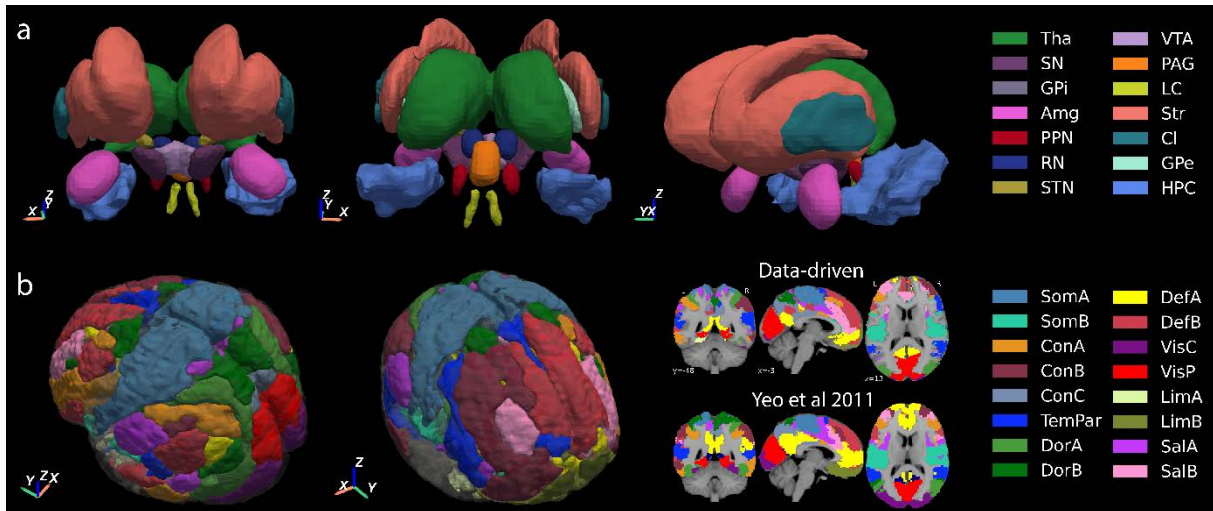

Figure 2. Parcellations of subcortical regions of interest and reference networks. (a) Subcortical regions of interest defined with open-source atlases and **(b)** data-driven reference networks from a whole-brain canonical ICA on the resting-state timeseries, labeled according to their maximum spatial correlation with a 17-network cortical parcellation. *Labels: thalamus (Tha), striatum (Str), globus pallidus externa (GPe), globus pallidus interna (GPi), claustrum (Cl), hippocampus (HPC), amygdala (Amg), substantia nigra (SN), subthalamic nucleus (STN), ventral tegmental area (VTA), red nucleus (RN), periaqueductal grey (PAG), pedunculopontine nucleus (PPN), locus coeruleus (LC), Somatomotor A (SomA), Somatomotor B (SomB), Control A (ConA), Control B (ConB), Control C (ConC), Temporal Parietal (TemPar), Dorsal Attention A (DorA), Dorsal Attention B (DorB), Default A (DefA), Default B (DefB), Visual Central (VisC), Visual Peripheral (VisP), Limbic A (LimA), Limbic B (LimB), Salience/Ventral Attention A (SalA), Salience/Ventral Attention B (SalB).*

Subcortical structures echo signals from different resting-state networks

The 10 thresholded FC maps for each ROI, representing the unique whole-brain FC of each subregion at the group-level, were spatially correlated with the 16 unthresholded spatial maps of the data-driven reference networks. Figure 3a summarizes the degree of network echoes for the nine ROIs that demonstrated at least one spatial correlation with any reference network above a threshold that was arbitrarily set at the 97th percentile of all spatial correlations (r=0.16). Echoes were quantified by counting above-threshold spatial correlations in terms of (1) the number of reference networks represented in each ROI and (2) the number of subregions that echoed a reference network. For example, six distinct striatal subregions displayed FC profiles that spatially correlated above-threshold with in total 10 different resting-state networks. Figure 3b presents the actual maximum spatial correlations between each ROI and each reference network, independent of subregion. The reference network that was represented most often was the Salience B network, correlating above-threshold with seven ROIs, followed by Default A, Control C, and Visual Peripheral, each with at least one above-threshold spatial correlation with six different ROIs.

Seven subcortical ROIs echoed signals from more than one network, including: the thalamus (Tha), striatum (Str), hippocampus (HPC), claustrum (Cl), globus pallidus externa (GPe), substantia nigra (SN), and ventral tegmental area (VTA). The former four ROIs furthermore showed that the echoes from different reference networks were distributed among multiple subregions, indicating evidence for a heterogeneous functional organization. In contrast, both the amygdala (Amg) and pedunculopontine nucleus (PPN) showed medium and small spatial correlations, respectively, with only one reference network (Amg: r=.37 [DefA]; PPN: r=.19 [SalB]). The globus pallidus interna (GPi), subthalamic nucleus (STN), red nucleus (RN), periaqueductal grey (PAG), and locus coeruleus (LC) failed to show evidence of echoes as none of their subregions demonstrated a functional connectivity pattern that resembled the pattern of an intrinsic connectivity network.

The FC maps of each subregion were also spatially correlated with the 17-network cortical parcellation (Yeo et al 2011), which yielded generally lower spatial correlations but a qualitatively similar pattern of results (Supplement A). To validate these novel results for the subcortex, we repeated the analyses for three cortical regions that were previously investigated. Results for the PCC, mPFC, and visual cortex are presented in Supplement B and are largely consistent with previous findings (Leech et al 2012; Braga et al 2013).
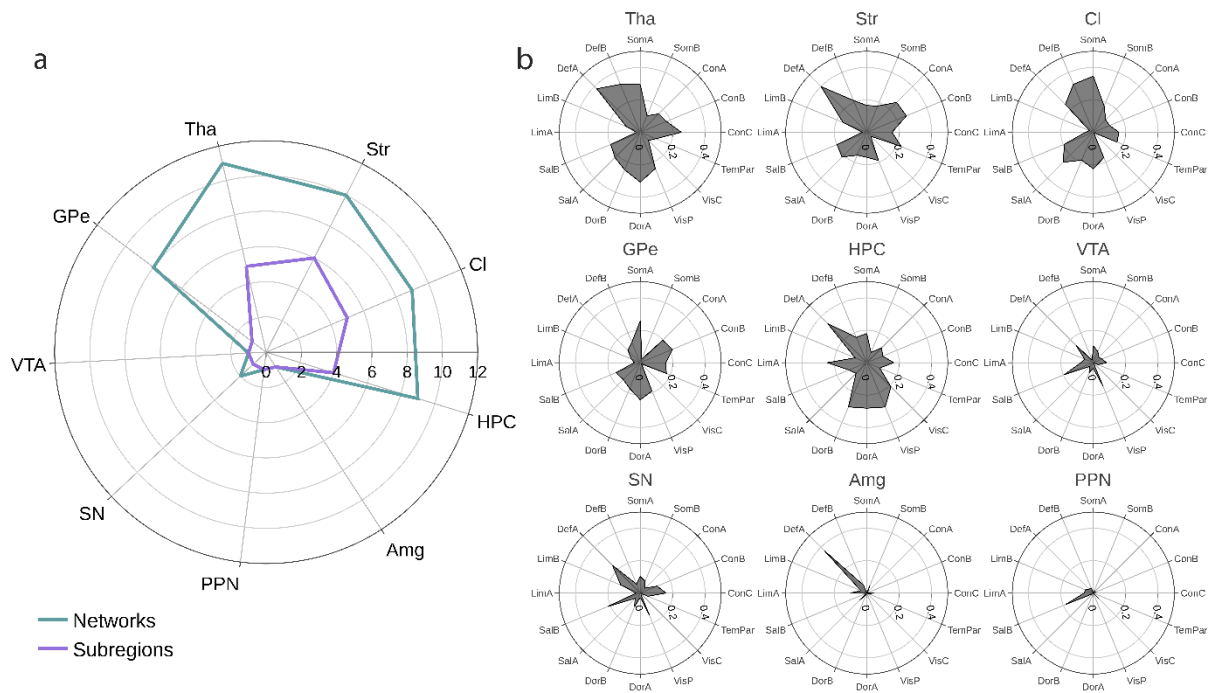
Figure 3. Echoes of intrinsic connectivity networks in the subcortex. (a) The number of distinct subregions within a ROI with a functional connectivity profile that resembled a reference network ('Subregions') and the number of different reference networks that were echoed within a region ('Networks') both defined by counting above-threshold spatial correlations. **(b)** The maximum spatial correlation between each ROI and each reference network, independent of subregion, for nine ROIs that demonstrated at least one above-threshold spatial correlation to any reference network. *Labels: thalamus (Tha), striatum (Str), globus pallidus externa (GPe), claustrum (Cl), hippocampus (HPC), amygdala (Amg), substantia nigra (SN), ventral tegmental area (VTA), pedunculopontine nucleus (PPN), Somatomotor A (SomA), Somatomotor B (SomB), Control A (ConA), Control B (ConB), Control C (ConC), Temporal Parietal (TemPar), Dorsal Attention A (DorA), Dorsal Attention B (DorB), Default A (DefA), Default B (DefB), Visual Central (VisC), Visual Peripheral (VisP), Limbic A (LimA), Limbic B (LimB), Salience/Ventral Attention A (SalA), Salience/Ventral Attention B (SalB).*

Topographic organization of functionally heterogeneous subcortical structures

Figure 4 shows the topographic pattern of network echoes in the subregions of the seven ROIs with more than one above-threshold spatial correlation. Subregions are color coded according to the reference network they echoed most strongly, whereas subregions with a maximum spatial correlation below threshold (*r*<0.16) are translucent. For every ROI, there were several subregions that did not mirror the activity in any intrinsic connectivity network, because they were predominantly functionally connected to other subcortical structures (Supplement C) or because their signal largely reflected noise upon visual inspection. In some cases, a subregion's functional connectivity profile was widespread and shared spatial similarity with more than one reference network. Supplement D presents a few FC maps to illustrate the diversity and similarity in connectivity profiles to different reference networks across a subset of subcortical structures.

Five thalamic subregions echoed signals from various reference networks, demonstrating a heterogeneous organization that was mostly symmetrically distributed in bilateral subdivisions. Left and right ventromedial subregions were both most strongly correlated to the Somatomotor A network

13

363   (left: *r*=.26, right: *r*=.20), although the right subregion's connectivity profile also spatially overlapped

364   with Salience B (*r*=.20). A more dorsomedial bilateral subregion displayed a connectivity pattern that

365   correlated with the pattern of multiple reference networks, including Default A (*r*=.38), Default B

366   (*r*=.32), and Control A (*r*=.25). Another bilateral subregion, more dorsolaterally located, correlated

367   most strongly with the Dorsal Attention A network (*r*=.31), although there was also spatial overlap with

368   Somatomotor A (*r*=.29), Dorsal Attention B (*r*=.25), and Visual Peripheral (*r*=.24) networks. Finally, the

369   Default B network was represented in the posterior part of the left-sided thalamus (*r*=.22).

370   Within the striatum, there were six different subregions that echoed one or more reference

371   networks, located mostly within the caudate nucleus. A subregion primarily in the left tail of the

372   caudate nucleus spatially correlated with the Default B network (*r*=.21), whereas a subregion covering

373   more of the right tail of caudate nucleus most strongly echoed Control B (*r*=.26), although its

374   widespread connectivity pattern also overlapped with Temporal Parietal (*r*=.23) and Salience A (*r*=.22)

375   networks. A bilateral subregion covering the nucleus accumbens correlated most strongly with Default

376   A (*r*=.40), whereas another bilateral subregion in the mediodorsal part of the caudate head was

377   functionally connected with Control A (*r*=.26) and Default B (*r*=.21) networks. Subregions that most

378   strongly echoed the Salience A network included a division in the posterior parts of the left caudate

379   tail and left putamen (*r*=.20) as well as a bilateral region in the lateral nucleus accumbens (*r*=.19).

380   For the hippocampus, we observed that different intrinsic connectivity networks were echoed

381   within four different subregions. In the left hemisphere, a posterior dorsal subregion correlated most

382   strongly with Default A (*r*=.34), whereas a more ventrally located subregion correlated exclusively with

383   the Limbic A network (*r*=.24). A bilateral anteromedial subregion was functionally connected to the

384   Visual Central network (*r*=.21), whereas a posterior dorsal subregion in the right hemisphere echoed

385   the Visual Peripheral (*r*=.30) as well as the Dorsal Attention networks (DorA: *r*=.28, DorB: *r*=.30).

386   Five subregions of the claustrum showed an FC profile that correlated with different reference

387   networks. A small, bilateral subregion in the ventral claustrum had a widespread cortical connectivity

388   that had the strongest spatial similarity with Dorsal Attention A (*r*=.23), but also Somatomotor A

389   (*r*=.20), Dorsal attention B (*r*=.19), and Salience B (*r*=.19) networks. Left and right subdivisions in the

390   posterior part both echoed the Salience A network (*r*=.26 and *r*=.21, respectively). In addition, an

391   exclusive functional connection with the Default B network was observed in an anterior subregion of

392   the left claustrum (*r*=.32) and with the Somatomotor A network in a more posterior subregion of the

393   right claustrum (*r*=.35).

394   The GPe and SN each had one subregion with a widespread connectivity profile comprising seven

395   and three reference networks, respectively (Figure 3b). In the GPe, a bilateral dorsolateral subdivision

396   most strongly echoed the Somatomotor A network (*r*=.26), but its signal also correlated with activity

397   in Dorsal Attention A (*r*=.23) and Control networks A and B (*r*=.20 and *r*=.22, respectively). The most

398 pronounced network echo within the SN was from Default A (*r*=.24) and came from a bilateral
399 subregion in the medial anterior SN. The same subregion also showed traces from Salience B (*r*=.22)
400 and Control C (*r*=.16) networks. For the VTA, a large inferomedial subdivision in the right hemisphere
401 was most strongly connected to Salience B (*r*=.19) and just below threshold to Visual Peripheral (*r*=.15)
402 networks. Echoes from the Default A network were furthermore present in two other subregions of
403 the VTA, but spatial correlations were weaker (*r*=.15 and *r*=.13).

404

405

406
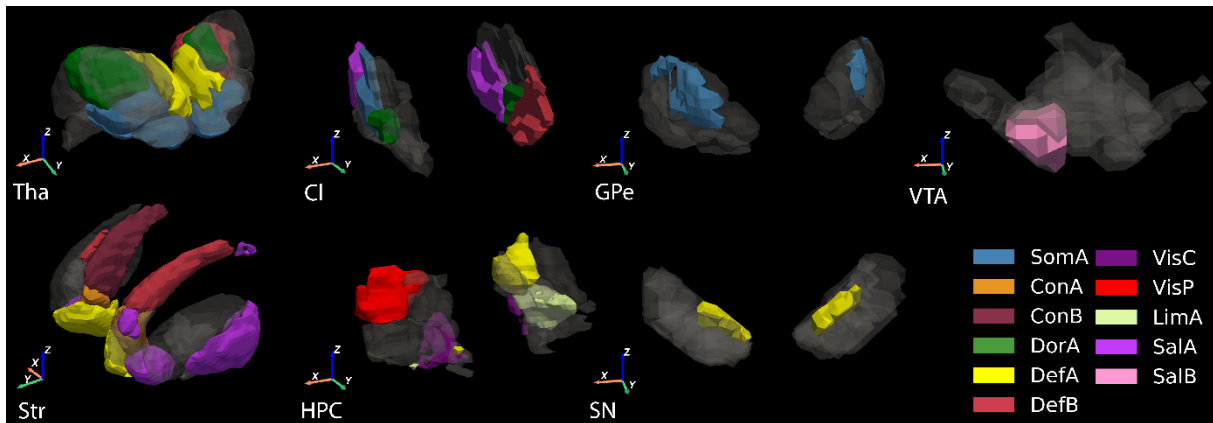
407

408 **Figure 4. Topography of network echoes within heteromodal subcortical structures.** Spatiotemporal decomposition of
409 subcortical structures into independent subregions, color coded according to their strongest network echo or made
410 translucent if their maximum spatial correlation with any reference network did not reach threshold. *Labels: thalamus (Tha),*
411 *striatum (Str), globus pallidus externa (GPe), claustrum (Cl), hippocampus (HPC), substantia nigra (SN), ventral tegmental area (VTA),*
412 *Somatomotor A (SomA), Somatomotor B (SomB), Control A (ConA), Control B (ConB), Control C (ConC), Temporal Parietal (TemPar), Dorsal*
413 *Attention A (DorA), Dorsal Attention B (DorB), Default A (DefA), Default B (DefB), Visual Central (VisC), Visual Peripheral (VisP), Limbic A*
414 *(LimA), Limbic B (LimB), Salience/Ventral Attention A (SalA), Salience/Ventral Attention B (SalB).*

Discussion

Despite accumulating insights into the underlying mechanisms of systems-level integration within the cortex, subcortical substrates of global brain communication are largely unexplored. However, the subcortex is embedded within an extensive cortico-subcortical architecture through dense projections and circuit loops that are thought to serve integrative rather than purely segregated functions (Haber 2003). In this study, we aimed to more closely investigate the functional organization of subcortical nuclei in terms of their unique subregional connectivity to large-scale intrinsic connectivity networks. By revealing a diversified and complex pattern of network echoes within the subcortex, we provide new insights into the subcortical contributions to multi-network integration.

Our results emcompass a number of key observations. Firstly, consistent with our expectations and the idea proposed by Braga and Leech (2015), we show that subcortical nuclei contain a composite of neural signals that can be decomposed into independent activity traces that mirror the pattern of large-scale intrinsic network activity. In their study, Braga et al (2013) showed that information from distributed functional networks converges at specific transmodal regions of the cortex, reflected in a mixture of dissociable subsignals that partially correlate with their input networks, indicating a mechanism for cross-network information integration. We now demonstrate that this property is present in various subcortical structures as well. Specifically, compared to other subcortical nuclei, our findings provide the strongest evidence for functional heterogeneity within the thalamus, striatum, claustrum, and hippocampus. Within each of these structures, we observed a complex pattern of subregional whole-brain connectivity that mirrored the activity in different intrinsic connectivity networks. Consistent with prior work, topographic maps showed a largely symmetrical bilateral organization, where subregions in left and right hemispheres had similar spatiotemporal signatures that echoed the same functional networks (Cheng and Liu 2021).

Unsurprisingly, the thalamus and striatum are the most commonly represented non-cortical structures in studies of global brain connectivity, providing support for their putative role as transmodal hub regions (Bell and Shine 2015, 2016; Van der Heuvel and Sporns 2011). Whereas several studies report an amalgamation of primarily sensory information within thalamic subregions consistent with its gating function (Tomasi and Volkow 2011; Ji et al 2019), we observed traces of somatomotor as well as default mode and dorsal attention networks. The somatomotor subdivisions also spatially overlapped with cingulo-opercular regions of the salience network, in agreement with findings of a 'motor integration zone' within ventral thalamic nuclei (Greene et al 2020). Additionally, we observed that dorsal attention, somatomotor, and visual networks converged in a dorsolateral subregion, similar although less posterior to the 'visual integration zone' in the pulvinar nucleus reported by Greene et al (2020). Intriguingly, these organizational similarities were detectable despite

449   large differences in methodology, where the results from Greene et al (2020) were based on voxel-

450   wise mapping of highly-sampled individuals, contrary to our more coarse description of subregional

451   topography at the group-level.

452   Furthermore, Greene et al (2020) reported a 'cognitive integration zone' for converging attention

453   and control networks within the head of caudate and putamen. In another study, the caudate head

454   was associated with the default mode network and the caudate tail with the frontoparietal control

455   network (Seitzman et al 2020). Similarly, Choi et al (2012) found that most of the striatum was

456   functionally connected to frontoparietal control and default mode networks. These findings are

457   consistent with our observation of signal echoes from default mode, control, and salience networks

458   predominantly within the caudate head and left tail, right tail, and left putamen, respectively.

459   Together, this supports the evidence for thalamic and striatal roles in integrative processing, possibly

460   indicating the underlying mechanism for their association with higher-level cognitive functions (Haber,

461   2003; Hwang et al 2017).

462   Although these coarse descriptions of subregional topography may broadly concur, the precise

463   functional boundaries and network associations diverge across studies. For example, the subdivisions

464   and network echoes identified in our study partially deviate from a co-partitioning based on data-

465   driven connectional topography (Cheng and Liu 2021) and a voxel-wise winner-take-all approach

466   (Seitzman et al 2020) for the thalamus, as well as the from the striatal topography presented in Choi

467   et al (2012). Whereas most studies acknowledge a functional connection between the thalamus and

468   default mode network, there are notable discrepancies in the exact topographic mapping of this

469   connection. Such inconsistencies are evident for the hippocampus as well, for which we observe

470   echoes from visual and dorsal attention networks predominantly in the right hippocampus, and default

471   mode and limbic networks in the left hippocampus. These inter-hemispheric differences in functional

472   organization are inconsistent with earlier studies, in which lateralized divisions along the anterior-

473   posterior axis are often reported, as well as variations in the exact origin of the default mode network

474   connection along this axis (Blessing et al 2016; Cheng et al 2020; Ezama et al 2021). Thus, it remains

475   an open question what parts of the thalamus and hippocampus preferentially connect with the default

476   mode network.

477   As differences in connectivity with surrounding entorhinal and parahippocampal cortex have been

478   observed (Qin et al 2016; Seoane et al 2018), it is possible that the extent of hippocampal and

479   surrounding voxels included in the analysis explains some of the discrepancies across studies, which

480   might be further exacerbated by the effects of spatial smoothing. Another plausible explanation for

481   the divergence in topographic mapping across studies is the degree of inter-individual variability in the

482   subcortex (De Hollander et al 2015; Marek and Greene 2021). Substantial individual variation in

483   functional architecture has been reported for the amygdala, striatum, and hippocampus (Sylvester et

484 al 2020; Greene et al 2020; Tian et al 2020). Therefore, group-level analyses may distort or

485 underestimate aspects of the functional connectome in the subcortex.

486 Secondly, similar to previous findings for the cortex (Braga et al 2013), we demonstrate that

487 transmodal characteristics are specific to certain structures and not ubiquitously present throughout

488 the subcortex. For several subcortical structures, only one subregion mirrored large-scale network

489 activity, including the GPe, SN, and VTA. One subregion within the dorsolateral GPe preferentially

490 connected with the somatomotor network, although its widespread connectivity profile also spatially

491 overlapped with dorsal attention and control networks, indicating an integrative site that may support

492 its known role in voluntary, planned movement. Both the SN and VTA displayed a pattern of converging

493 signals from default mode and salience networks, although this pattern was less pronounced within

494 the VTA. Whereas associations of these structures with the default mode network have been

495 previously reported (Bär et al 2016; Edlow 2021; Zhang et al 2016; Li et al 2021), the functional

496 connection with the salience network is less consistent, and may indicate involvement in attentional

497 control and spontaneous thought (O'Callaghan et al 2020).

498 In contrast, we found no clear evidence of integrative processing properties within the amygdala

499 and PPN. Whereas the PPN is known to primarily connect to a more segregated community of other

500 subcortical structures involved in arousal and locomotion (Martinez-Gonzales et al 2011; Bennarroch

501 2013), the amygdala has been proposed as a hub structure (Tomasi and Volkow 2011). Functional

502 connectivity profiles from separate nuclei within the amygdala were previously differentiated,

503 although all subregions showed a global connection with the ventrolateral prefrontal cortex (Kerestes

504 et al 2017). This dominant connection with the default mode network is supported by other studies

505 (Sylvester et al 2020; Harrison et al 2021) and aligns with our finding, though our results were not

506 consistent with the notion of the amygdala as a site for functional network convergence.

507 For several subcortical structures, we failed to observe any traces of large-scale cortical network

508 activity, including the GPi, STN, RN, PAG, and LC. None of these regions revealed unique whole-brain

509 connectivity profiles that mirrored the activity in intrinsic connectivity networks, but rather showed

510 evidence for stronger, local connectivity to other subcortical nuclei, consistent with prior work (Singh

511 et al 2022). Although univariate (seed-based) FC studies have indicated correlations with widespread

512 cortical activity patterns for some of these structures (Zhang et al 2016; Anteraper et al 2018), our

513 multivariate analysis showed that partialing out adjacent subsignals does not result in a clear group-

514 level pattern of cortical connectivity. Thus, these regions are likely predominantly supportive of

515 segregated functions within local, subcortical circuits rather than integrating information from

516 widespread functional networks.

517 In summary, we observed variations in subcortical nuclei regarding the degree to which their

518 functional architecture supports information integration across intrinsic connectivity networks. This

519 characteristic seems to be expressed along a gradient, where structures adjacent to the cortex are

520 more likely to participate in large-scale network dynamics compared to deep grey matter nuclei in the

521 midbrain and brainstem. Possible confounding effects here are that the deeper structures are

522 evidently also generally smaller and have weaker SNR, as well as that structures near the cortex are

523 more susceptible to signal bleeding from adjacent cortical voxels, to which they are also reciprocally

524 connected. For example, Choi et al (2012) reported that regressing out signals from the insular cortex

525 altered the connectivity pattern within the posterior putamen from ventral attention to the

526 somatomotor network. In our study, this issue might be especially prominent in the claustrum, which

527 is a thin sheet-like structure situated directly between the striatum and insula. However, using a novel

528 regression technique on similar high-resolution rs-fMRI (1.5mm voxels), Krimmel et al (2019) isolated

529 signal within the claustrum from nearby cortical and striatal voxels and found that widespread

530 functional connectivity with cortical networks involved in attention and cognitive control was

531 preserved. Thus, although we did not correct for potential signal bleeding beyond limiting the amount

532 of spatial smoothing, our observation of echoes from dorsal attention, salience, default mode, and

533 somatomotor networks within distinct subdivision of the claustrum coincide with Krimmel et al (2019)

534 and the claustrum's postulated role higher-level cognition, salience processing, and attention (Bell and

535 Shine 2015; Smith et al 2020).

536 Finally, one noteworthy limitation of our and other studies investigating intrinsic connectivity is that

537 spatial patterns of functional networks are not invariant attributes but rather dynamically reconfigure

538 over time. Several studies have shown both subtle and pronounced reorganizations in subcortical

539 functional architecture in response to changes in task demands (Leech et al 2012; Braga et al 2013;

540 Tian et al 2020). Therefore, although we can detect robust, large-scale spatiotemporal patterns with

541 static methods, capturing fluctuations in the functional connectome may more accurately describe

542 mechanisms of integration and segregation within the subcortex, and may improve consensus in

543 topographic mapping across individuals and studies.

544 Despite these limitations, our study demonstrates that various subcortical nuclei are functionally

545 heterogeneous and organized in topographic maps that relate to the spatial pattern of neural activity

546 in large-scale intrinsic connectivity networks. Although the precise functional significance of these

547 network echoes for cognition and behavior is not resolved, our findings strengthen the evidence that

548 the subcortex contains a rich functional architecture through which it participates in systems-level

549 information integration. Henceforth, our results may ignite new intriguing hypotheses on the neural

550 mechanisms of more elusive, dynamic cognitive states such as mind wandering (Mittner et al 2016;

551 Zuberer et al 2021). Previous work has shown that episodes of mind wandering inconsistently correlate

552 with activation of the default mode and frontoparietal control networks as well as the subcortex

553 (Mittner et al 2014; Kucyi et al 2017; Groot et al 2022). Therefore, investigations of how changes in

554   cognitive demands perturb the complex pattern of network echoes within the subcortex may provide

555   novel mechanistic insights into the underlying factors driving the fluctuations in external and internal

556   attention. Thus, mechanisms of large-scale network convergence within the subcortex may hold

557   insights that are crucial for understanding the functional connectome that underlies higher-level

558   cognitive functions and that are necessary to eventually close the subcortical knowledge gap.

References

Alkemade A, Mulder MJ, Groot JM, Isaacs BR, Van Berendonk N, Lute N, Isherwood SJS, Bazin P-L, Forstmann BU (2020) The Amsterdam Ultra-high field adult lifespan database (AHEAD): A freely available multimodal 7 Tesla submillimeter magnetic resonance imaging database. *NeuroImage, 221*:117200. doi: 10.1016/j.neuroimage.2020.117200

Anteraper SA, Guell X, Whitfield-Gabrieli S, Triantafyllou C, Mattfeld AT, Gabrieli JD, Geddes MR (2018) Resting-state functional connectivity of the subthalamic nucleus to limbic, associative, and motor networks. *Brain Connectivity, 8:*22-32. doi: 10.1089/brain.2017.0535

Avants B, Tustison NJ, Song G (2008). Advanced normalization tools (ANTS). *Insight Journal,* 1-35. doi: 10.54294/uvnhin.

Bär K-J, De la Cruz F, Schumann A, Koehler S, Sauer H, Critchley H, Wagner G (2016) Functional connectivity and network analysis of midbrain and brainstem nuclei. *NeuroImage, 134:*53-63. doi: 10.1016/j.neuroimage.2016.03.071

Bazin P-L, Alkemade A, Mulder MJ, Henry AG, Forstmann BU (2020) Multi-contrast anatomical subcortical structures parcellation. *eLife, 9:*e59430. doi: 10.7554/eLife.59430

Beckmann CF, Mackay CE, Filippini N, Smith SM (2009) Group comparison of resting-state fMRI data using multi-subject ICA and dual regression. *NeuroImage, 47(Suppl 1):*S148. doi: 10.1016/S1053-8119(09)71511-3

Behzadi Y, Restom K, Liau J, Liu TT (2007) A component based noise correction method (CompCor) for BOLD and perfusion based fMRI. *NeuroImage, 37:*90-101. doi: 10.1016/j.neuroimage.2007.04.042

Bell PT, Shine JM (2015) Estimating large-scale network convergence in the human functional connectome. *Brain Connectivity, 5:*565-574. doi: 10.1089/brain.2015.0348

Bell PT, Shine JM (2016) Subcortical contributions to large-scale network communication. *Neuroscience and Biobehavioral Reviews, 71:*313-322. doi: 10.1016/j.neubiorev.2016.08.036

Bennarroch EE (2013) Pedunculopontine nucleus: Functional organization and clinical implications. *Clinical Implications of Neuroscience Research, 80:*1148-1155. doi: 10.1212/WNL.0b013e3182886a76

Blessing EM, Beissner F, Schumann A, Brünner F, Bär K-J (2016) A data-driven approach to mapping cortical and subcortical intrinsic functional connectivity along the longitudinal hippocampal axis. *Human Brain Mapping, 37:*462-476. doi: 10.1002/hbm.23042

593 Braga RM, Sharp DJ, Leeson C, Wise RJS, Leech R (2013) Echoes of the brain within default mode,
594   association, and heteromodal cortices. *Journal of Neuroscience,* 28:14031-14039. doi:
595   10.1523/JNEUROSCI.0570-13.2013

596 Braga RM, Leech R (2015) Echoes of the brain: Local-scale representation of whole-brain functional
597   networks   within   transmodal   cortex.   *The   Neuroscientist,   21:*540-551.   doi:
598   10.1177/1073858415585730

599 Cheng H, Zhu H, Zheng Q, Liu J, He G (2020) Functional parcellation of the hippocampus by semi-
600   supervised clustering of resting state fMRI data. *Scientific Reports, 10:*16402. doi: 10.1038/s41598-
601   020-73328-1

602 Cheng H, Liu J (2021) Concurrent brain parcellation and connectivity estimation via co-clustering of
603   resting state fMRI: A novel approach. *Human Brain Mapping, 42:*2477-2489. doi:
604   10.1002/hbm.25381

605 Choi EY, Yeo BTT, Buckner RL (2012) The organization of the human striatum estimated by intrinsic
606   functional connectivity. *Journal of Neurophysiology, 108:*2242-2263. doi: 10.1152/jn.00270.2012.

607 Cox RW (1996) AFNI: software for analysis and visualization of functional magnetic resonance
608   neuroimages. *Comput Biomed Res*, 29:162-73. doi: 10.1006/cbmr.1996.0014

609 Damoiseaux JS, Rombouts SARB, Barkhof F, Scheltens P, Stam CJ, Smith SM, Beckmann CF (2006)
610   Consistent   resting-state   networks   across   healthy   subjects.   *PNAS,   103:*13848-13853.   doi:
611   10.1073/pnas.0601417103

612 De Gee JW, Colizoli O, Kloosterman NA, Knapen T, Nieuwenhuis S, Donner TH (2017) Dynamic
613   modulation of decision biases by brainstem arousal systems. *eLife, 6*:e23232. doi:
614   10.7554/elife.23232

615 De Hollander G, Keuken MC, Forstmann BU (2015) The subcortical cocktail problem: Mixed signals
616   from the subthalamic nucleus and substantia nigra. *PLoS One, 10:*e0120572. doi:
617   10.1371/journal.pone.0120572

618 De Hollander G, Keuken MC, Van der Zwaag W, Forstmann BU, Trampel R (2017) Comparing functional
619   MRI protocols for small, iron-rich basal ganglia nuclei such as the subthalamic nucleus at 7 T and 3
620   T. *Human Brain Mapping, 38:*3226-3248. doi: 10.1002/hbm.23586

621 Edlow BL (2021) Dopaminergic modulation of human consciousness via default mode network
622   connectivity. *PNAS, 118:*e2111268118. doi: 10.1073/pnas.2111268118.

623 Esteban O, Markiewicz CJ, Blair RW, Moodie CA, Isik AI, Erramuzpe A, Kent JD, Goncalves M, DuPre E,
624   Snyder M, Oya H, Ghosh SS, Wright J, Durnez J, Poldrack RA, Gorgolewski KJ (2018) fMRIPrep: a
625   robust preprocessing pipeline for functional MRI. *Nature Methods*, 16:111-116. doi:
626   10.1038/s41592-018-0235-4

627 Ezama L, Hernández-Cabrera JA, Seoane S, Pereda E, Janssen N (2021) Functional connectivity of the
628   hippocampus and its subfields in resting-state networks. *European Journal of Neuroscience,*
629   *53:*3378-3393. doi: 10.1111/ejn.15213

630   Fonov VS, Evans AC, McKinstry RC, Almli CR, Collins DL (2009) Unbiased nonlinear average age-
631   appropriate brain templates from birth to adulthood. *NeuroImage, 47:*102. doi: 10.1016/S1053-
632   8119(09)70884-5

633   Forstmann BU, De Hollander G, Van Maanen L, Alkemade A, Keuken MC (2017) Towards a mechanistic
634   understanding of the human subcortex. *Nature Reviews, 18:*57-65. doi: 10.1038/nrn.2016.163

635   Frässle S, Aponte EA, Bollmann S, Brodersen KH, Do CT, Harrison OK, Harrison SJ, Heinzle J, Iglesias S,
636   Kasper L, Lokamina EI, Mathys C, Müller-Schrader M, Pereira I, Petzschner FH, Raman S, Schöbi D,
637   Toussaint B, Weber LA, Yao Y, Stephan KE (2021) TAPAS: an open-source software package for
638   Translational Neuromodeling and Computational Psychiatry. *Frontiers in Psychiatry, 12:*680811.
639   doi: 103389/fpsyt.2021.680811

640   Glover GH, Li TQ, Ress D (2000) Image-based method for retrospective correction of physiological
641   motion effects in fMRI: RETROICOR. *Magnetic Resonance in Medicine, 44:*162-167.

642   Gorgolewski K, Burns CD, Madison C, Clark D, Halchenko YO, Waskom ML, Ghosh SS (2011) Nipype: a
643   flexible, lightweight and extensible neuroimaging data processing framework in Python. *Frontiers
644   in Neuroinformatics*, 5:13. doi: 10.3389/fninf.2011.00013

645   Grayson DS, Ray S, Carpenter S, Iyer S, Costa Dias TG, Stevens C, Nigg JT, Fair DA (2014) Structural and
646   functional rich club organization of the brain in children and adults. *PloS One, 9:*e88297. Doi:
647   10.1371/journal.pone.0088297

648   Greene DJ, Marek S, Gordon EM, Siegel JS, Gratton C, Laumann TO, Gilmore AW, Berg JJ, Nguyen AL,
649   Dierker D, Van AN, Ortega M, Newbold DJ, Hampton JM, Nielsen AN, McDermott KB, Roland JL,
650   Norris SA, Nelson SM, Snyder AZ, Schlagger BL, Petersen SE, Dosenbach NUF (2020) Integrative and
651   network-specific connectivity of the basal ganglia and thalamus defined in individuals. *Neuron,
652   105:*742-758. doi: 10.1016/j.neuron.2019.11.012

653   Greve DN, Fischl B (2009) Accurate and robust brain image alignment using boundary-based
654   registration. *NeuroImage, 48:*63-72. doi: 10.1016/j.neuroimage.2009.06.060

655   Groot JM, Csifcsák G, Wientjes S, Forstmann BU, Mittner M (2022) Catching wandering minds with
656   tapping fingers: Neural and behavioral insights into task-unrelated cognition. *Cerebral Cortex,* doi:
657   10.1093/cercor/bhab494

658   Haber SN (2003) The primate basal ganglia: Parallel and integrative networks. *Journal of Chemical
659   Neuroanatomy, 26:*317-330. doi: 10.1016/j.jchemneu.2003.10.003

660   Harrison OK, Guell X, Klein-Flügge MC, Barry RL (2021) Structural and resting state functional
661   connectivity beyond the cortex. *NeuroImage, 240:*118379. doi: 10.1016/j.neuroimage.2021.118379

662   Hu Y, Yang Z (2021) Impact of inter-individual variability on the estimation of default mode network in
663   temporal   concatenation   group   ICA.   *NeuroImage,   237:*118114.   doi:
664   10.1016/j.neuroimage.2021.118114

665   Hwang K, Bertolero MA, Liu WB, D'Esposito M (2017) The human thalamus is an integrative hub for
666   functional brain networks. *J Neurosci, 37:*5594-5607

667 Jarbo K, Verstynen TD (2015) Converging structural and functional connectivity of orbitofrontal,
668   dorsolateral, prefrontal, and posterior parietal cortex in the human striatum. *J Neurosci, 35:*3865-
669   3878. doi: 10.1523/JNEUROSCI.2636-14.2015

670 Jenkinson M, Bannister P, Brady JM, Smith SM (2002) Improved optimisation for the robust and
671   accurate linear registration and motion correction of brain images. *NeuroImage*, 17:825-841. doi:
672   10.1016/s1053-8119(02)91132-8

673 Jenkinson M, Smith SM (2001) A global optimisation method for robust affine registration of brain
674   images. *Medical Image Analysis*, 5:143-156. doi: 10.1016/s1361-8415(01)00036-6

675 Ji JL, Spronk M, Kulkarni K, Repovs G, Anticevic A, Cole MW (2019) Mapping the human brain's cortical-
676   subcortical functional network organization. *NeuroImage, 185:*35-57. doi:
677   10.1016/j.neuroimage.2018.10.006

678 Kasper L, Bollmann S, Diaconescu AO, Hutton C, Heinzle J, Iglesias S, Hauser TU, Sebold M, Manjaly Z-
679   M, Pruessmann KP, Stephan KE (2017) The PhysIO Toolbox for modeling physiological noise in fMRI
680   data. *Journal of Neuroscience Methods, 276*: 56-72. doi: 10.1016/j.jneumeth.2016.10.019

681 Kerestes R, Chase HW, Philips ML, Ladouceur CD, Eickhoff SB (2017) Multimodal evaluation of the
682   amygdala's functional connectivity. *NeuroImage, 148:*219-229. doi:
683   10.1016/j.neuroimage.2016.12.023

684 Keuken MC, Isaacs BR, Trampel R, Van der Zwaag W, Forstmann BU (2018a) Visualizing the human
685   subcortex using ultra-high field magnetic resonance imaging. *Brain Topography, 31:*513-545. doi:
686   10.1007/s10548-018-0638-7

687 Keuken MC, Van Maanen L, Boswijk M, Forstmann BU, Steyvers M (2018b) Large scale structure-
688   function mappings of the human subcortex. *Scientific Reports, 8:*15854. doi: 10.1038/s41598-018-
689   33796-y

690 Krimmel SR, White MG, Panicker MH, Barrett FS, Mathur BN, Seminowicz DA (2019) Resting state
691   functional connectivity and cognitive task-related activation of the human claustrum. *NeuroImage,*
692   *196:*59-67. doi: 10.1016/j.neuroimage.2019.03.075

693 Lee T-W, Xue S-W (2018) Functional connectivity maps based on hippocampal and thalamic dynamics
694   may account for the default-mode network. *European Journal of Neuroscience, 47:*388-398. doi:
695   10.1111/ejn.13828

696 Lee WH, Moser DA, Ing A, Doucet GE, Frangou S (2019) Behavioral and health correlates of resting-
697   state metastability in the Human Connectome Project. *Brain Topography, 32:*80-86. doi:
698   10.1007/s10548-018-0672-5

699 Leech R, Braga R, Sharp DJ (2012) Echoes of the brain within the posterior cingulate cortex. *Journal of*
700   *Neuroscience, 32:*215-222. doi: 10.1523/JNEUROSCI.3689-11.2012

701 Li J, Curley WH, Guerin B, Dougherty DD, Dalca AV, Fischl B, Horn A, Edlow BL (2021) Mapping the
702   subcortical connectivity of the human default mode network. *NeuroImage, 245*:118758. doi:
703   10.1016/j.neuroimage.2021.118758

704 Liégeois R, Li J, Kong R, Orban C, Van de Ville D, Ge T, Sabuncu MR, Yeo T (2019) Resting brain dynamics
705   at different timescales capture distinct aspects of human behavior. *Nature Communications,*
706   *10:*2317. doi: 10.1038/s41467-019-10317-7

707 Liu KY, Marijatta F, Hämmerer D, Acosta-Cabronero J, Düzel E, Howard RJ (2017) Magnetic resonance
708   imaging of the human locus coeruleus: A systematic review. *Neuroscience and Biobehavioral*
709   *Reviews, 83:*325-355. doi: 10.1016/j.neubiorev.2017.10.023

710 Lyu D, Pappas I, Menon DK, Stamatakis EA (2021) A precuneal causal loop mediates external and
711   internal information integration in the human brain. *Journal of Neuroscience, 41:*9944-9956. doi:
712   10.1523/JNEUROSCI.0647-21.2021

713 Marek S, Greene DJ (2021) Precision functional mapping of the subcortex and cerebellum. *Current*
714   *Opinion in Behavioral Sciences, 40:*12-18. doi: 10.1016/j.cobeha.2020.12.011

715 Martinez-Gonzales C, Bolam JP, Mena-Segovia J (2011) Topographical organization of the
716   pedunculopontine nucleus. *Frontiers in Neuroanatomy, 5:*22. doi: 10.3389/fnana.2011.00022

717 Marques JP, Kober T, Krueger G, Van der Zwaag W, Van de Moortele PF, Gruetter R (2010) MP2RAGE,
718   a self bias-field corrected sequence for improved segmentation and T1-mapping at high field.
719   *NeuroImage, 15*:1271-81. doi: 10.1016/j.neuroimage.2009.10.002

720 Miletic S, Bazin P-L, Weiskopf N, Van der Zwaag W, Forstmann BU, Trampel R (2020) fMRI protocol
721   optimization for simultanously studying small subcortical and cortical areas at 7 T. *NeuroImage,*
722   *219:*116992. doi: 10.1016/j.neuroimage.2020.116992

723 Mittner M, Hawkins GE, Boekel W, Forstmann BU (2016) A neural model of mind wandering. *Trends in*
724   *Cognitive Sciences*, 20:570-578. doi: 10.1016/j.tics.2016.06.004

725 O'Callaghan C, Walpola IC, Shine JM (2020) Neuromodulation of the mind-wandering brain state: The
726   interaction between neuromodulatory tone, sharp wave-ripples and spontaneous thought.
727   *Philosophical Transactions of the Royal Society, 376:*20190699. doi: 10.1098/rstb.2019.0699

728 Odekerken VJJ, Van Laar T, Staal MJ, Mosch A, Hoffmann CFE, Nijssen PCG, Beute GN, Van Vugt JPP,
729   Lenders MWPM, Contarino MF, Mink MSJ, Bour LJ, Van den Munckhof P, Schmand BA, De   Haan
730   RJ, Schuurman PR, De Bie RMA (2013) Subthalamic nucleus versus globus pallidus   bilateral deep
731   brain stimulation for advanced Parkinson's disease (NSTAPS study): A randomised controlled trial.
732   *The Lancet Neurology, 12:*37-44. https://doi.org/10.1016/S1474-4422(12)70264-8

733 Qin S, Duan X, Supekar K, Chen H, Chen T, Menon V (2016) Large-scale intrinsic functional network
734   organization along the long axis of the human medial temporal lobe. *Brain Structure and Function,*
735   *221:*3237-3258. doi: 10.1007/s00429-015-1098-4

736 Seitzman BA, Gratton C, Marek S, Raut RV, Dosenbach NUF, Schlagger BL, Petersen SE, Greene DJ
737   (2020) A set of functionally-defined brain regions with improved representation of the subcortex
738   and cerebellum. *NeuroImage, 206:*116290. doi: 10.1016/j.neuroimage.2019.116290

739 Senden M, Deco G, De Reus MA, Goebel R, Van den Heuvel MP (2014) Rich club organization supports
740   a diverse set of functional network configurations. *NeuroImage, 96:*174-182. doi:
741   10.1016/j.neuroimage.2014.03.066

742 Seoane S, Modroño C, Gonzáles-Mora J, Janssen N (2022) Medial temporal lobe contributions to
743   resting-state networks. *Brain Structure and Function, 227:*995-1012. doi: 10.1007/s00429-021-
744   02442-1

745 Singh K, Cuazzo S, García-Gomar MG, Stauder M, Vanello N, Passino C, Bianciardi M (2022) Functional
746   connectome of arousal and motor brainstem nuclei in living humans by 7 Tesla resting-state fMRI.
747   *NeuroImage, 249:*118865. doi: 10.1016/j.neuroimage.2021.118865

748 Smith JB, Lee AK, Jackson J (2020) The claustrum. *Current Biology, 30:*1401-1406. doi:
749   10.1016/j.cub.2020.09.069

750 Smith SM, Brady JM (1997) SUSAN – a new approach to low level image processing. *Int J Comput Vis*,
751   23:45-78. doi: 10.1023/A:1007963824710

752 Sylvester CM, Yu Q, Srivastava AB, Marek S, Zheng A, Alexopoulos D, Smyser CD, Shimony JS, Ortega
753   M, Dierker DL, Patel GH, Nelson SM, Gilmore AW, McDermott KB, Berg JJ, Drysdale AT, Perino MT,
754   Snyder AZ, Raut RV, Laumann TO, Gordon EM, Barch DM, Rogers CE, Greene DJ, Raichle ME,
755   Dosenbach NUF (2020) Individual-specific functional connectivity of the amygdala: A substrate for
756   precision psychiatry. *PNAS, 117:*3808-3818. doi: 10.1073/pnas.1910842117

757 Tian Y, Margulies DS, Breakspear M, Zalesky A (2020) Topographic organization of the human subcortex
758   unveiled with functional connectivity gradients. *Nature Neuroscience, 23:*1421-1432. doi:
759   10.1038/s41593-020-00711-6

760 Tomasi D, Volkow ND (2011) Association between functional connectivity hubs and brain networks.
761   *Cerebral Cortex, 21:*2003-2013. doi: 10.1093/cercor/bhq268

762 Tustison NJ, Avants BB, Cook PA, Zheng Y, Egan A, Yushkevich PA (2010) N4ITK: improved N3 bias
763   correction. *IEEE Trans Med Imaging*, 29:1310-1320. doi: 10.1109/TMI.2010.2046908

764 Van der Heuvel MP, Sporns O (2011) Rich-club organization of the human connectome. *Journal of
765   Neuroscience, 31:*15775-15786. doi: 10.1523/JNEUROSCI.3539-11.2011

766 Varoquaux G, Sadaghiani S, Pinel P, Kleinschmidt A, Poline JB, Thirion B (2010) A group model for stable
767   multi-subject ICA from fMRI datasets. *NeuroImage, 51:*288-299. doi:
768   10.1016/j.neuroimage.2010.02.010

769 Woolrich MW, Ripley BD, Brady M, Smith SM (2001) Temporal autocorrelation in univariate linear
770   modeling of FMRI data. *NeuroImage,* 14:1370-1386. doi: 10.1006/nimg.2001.0931

771 Ye R, Rua C, O'Callaghan C, Jones PS, Hezemans FH, Kaalund SS, Tsvetanov KA, Rodgers CT, Williams G,
772   Passamonti L, Rowe JB (2021) An *in vivo* probabilistic atlas of the human locus coeruleus at ultra-
773   high field. *NeuroImage, 225:*117487. doi: 10.1016/j.neuroimage.2020.117487

774 Yeo BTT, Krienen FM, Sepulcre J, Sabuncu MR, Lashkari D, Hollinshead M, Roffman JL, Smoller JW, Zöllei
775   L, Polimeni JR, Fischl B, Liu H, Buckner RL (2011) The organization of the human cerebral cortex
776   estimated by intrinsic functional connectivity. *Journal of Neurophysiology*, 106:1125-1165. doi:
777   10.1152/jn.00338.2011

778 Zarzycki MZ, Domitrz I (2020) Stimulation-induced side effects after deep brain stimulation – a
779   systematic review. *Acta Neuropsychiatrica, 32:*57–64. doi: 10.1017/neu.2019.35

780   Zhang Y, Brady M, Smith S (2001) Segmentation of brain MR images through a hidden markov random
781   field model and the expectation-maximization algorithm. *IEEE Trans Med Imag*, 20:45-57. doi:
782   10.1109/42.906.424

783   Zhang S, Hu S, Chao HH, Li C-SR (2016) Resting-state functional connectivity of the locus coeruleus in
784   humans: In comparison with the ventral tegmental area/substantia nigra pars compacta and the
785   effects of age. *Cerebral Cortex, 26:*3413-3427. doi: 10.1093/cercor/bhv172

786   Zuberer A, Kucyi A, Yamashita A, Wu CM, Walter M, Valera EM, Esterman M (2021) Integration and
787   segregation across large-scale intrinsic brain networks as a marker of sustained attention and task-
788   unrelated thought. *NeuroImage*, 229:117610. doi: 10.1016/j.neuroimage.2020.117610

789   Zuo X-N, Kelly C, Adelstein JS, Klein DF, Castellanos FX, Milham MP (2010) Reliable intrinsic connectivity
790   networks: Test-retest evaluation using ICA and dual regression approach. *NeuroImage, 49:*2163-
791   2177. doi: 10.1016/j.neuroimage.2009.10.080